Bone marrow regeneration in the mouse by using bone marrow derived stem cells

Thesis submitted to Jawaharlal Nehru University
for the award of the degree of

DOCTOR OF PHILOSOPHY

NASEEM AHAMAD

School of Life Sciences
Jawaharlal Nehru University
New Delhi-110067
INDIA

July 2017

School of Life Sciences

Jawaharlal Nehru University

New Delhi-110067

INDIA

CERTIFICATE

The research work included in this thesis entitled **"Bone marrow regeneration in the mouse by using bone marrow derived stem cells"** has been carried out by **Mr. Naseem Ahamad** in the School of Life Sciences, Jawaharlal Nehru University, New Delhi. This research work is original and has not been submitted so far in part or full for any other degree or diploma of any other university.

Naseem Ahamad
(Candidate)

PCRath 21/7/17

Prof. Pramod C. Rath
(Supervisor)

Prof. Pramod C. Rath
Molecular Biology Laboratory
School of Life Sciences
Jawaharlal Nehru University
New Delhi - 110067

for PCRath 21/7/17

Prof. S.K. Goswami
(Dean)

Dedicated to the Almighty God,
Dearest Ammi, Papa,
Family Members
And
Friends

My Inspiration

AQRA! BISM RABBIK ALLADHI KHALAQ

Translation: Read in the name of thy Lord who creates

THE NOBLE **QUR'AN**

ACKNOWLEDGEMENTS

I would like to start with the name of God, the Most Beneficent, the Most Gracious and the Most Merciful. I want to say my sincere thanks with sincere belief to Almighty Allah for giving me life and all that I have. My parents are the first blessing to me that Allah gave me. I am very grateful to Allah that gives me the understanding and sense of taking up this fascinating research study.

The research work performed in this thesis would not have been accomplished without love, care and support of many people. I would take this moment to state my genuine gratitude and appreciation to all those who made this Ph.D. thesis work possible.

First and foremost, I would like to express my sincere thanks to my Ph.D. supervisor Prof. Pramod C. Rath for supporting me throughout my research by his valuable, essential and honest suggestions, which would support my whole life. He has been very supportive and has given me liberty to do research without any doubt. He was instrumental in encouraging me to complete this research. I would like to say without his support and scientific management this research work would not have been achieved.

I am very thankful to my Doctoral Committee members, Prof. Alok Bhattacharya (Chairperson), Prof. Pramod C. Rath (my supervisor), Prof. Shweta Saran (member), Prof. Niti Puri (member) and Prof. Devinder Sehgal (external member, NII, New Delhi) for their advice and remarks to improve my research and for giving shape and direction to my research through progress report presentation.

My particular thanks should also go to the former Deans of the School of Life Sciences including Prof. N. B. Sarin, Prof. B. N. Mallick, Prof. B. C. Tripathy and present Dean Prof. S.K. Goswami for providing access to the very well organized and functional Central Instrumentation Facility (CIF) of the School for research.

I would also like to appreciate Prof. Ajay Kumar Saxena, Prof. Alok Bhattacharya, Prof. Ashis K Nandi, Dr. Ashu Bhan Tiku, Prof. Ashwani Pareek, Prof. Atul Kumar Johri, Prof. B.C. Tripathy, Prof. B.N. Mallick, Prof. Deepak Sharma, Prof. K. Natarajan, Prof. N.B. Sarin, Dr. Neelima Mondal, Dr. Nirala Ramchiary, Dr. Niti Puri, Prof. P.C. Rath, Prof. P.K. Yadava, Prof. R. Madhubala, Prof. R.K. Kale, Prof. R.N.K. Bamezai, Prof. Rana P. Singh, Dr. Rohini Muthuswami, Prof. S. Chakraborty, Prof. S.K. Goswami, Prof. Samudrala Gourinath, Prof. Shweta Saran, Dr. Sneh Lata Panwar, Prof. Sneha Sudha Komath, Dr. Sushil K Jha for their teaching throughout the one year duration “M.Phil. Course work” from July, 2011 to July, 2012.

I would also like to thank Prof. Shweta Saran (Microscopy In Charge), Dr. Niti Puri (FACS In Charge), Prof. Jaishree Paul, Dr. Ashu Bhan Tiku (Animal Tissue Culture Laboratory In

Charge) for providing continuous and well functional respective facilities and for 24x7 access and freedom to work without any objection.

Other faculty members, including Dr. Rajendra Prasad, Prof. Alok Kumar Mondal, Dr. Nirala Ramchiary, and Dr. Soumya Prasad are also thanked and honestly appreciated for their important ideas, suggestions, and guidance during several educational talks and presentations.

I considerably acknowledge the excellent technical staff of the Central Instrumentation Facility (CIF), Shri S. K. Mishra (Radiation Safety Officer, J.N.U.), Mr. Rajendra and Technical Assistant Mrs. Sarika Gupta (FACS facility), Mrs. Tripti and Ms. Poonam (Microscopy Facility) as well as the associated temporary staff for always being so kind and friendly. People here are genuinely friendly and responsible for assuring the smooth functioning of the numerous instruments and other central facilities. They always want to support you, and I'm glad to have been associated with them.

I would also like to appreciate the Veterinary Officer Dr. D. K. Yadav, Person-in-Charge Mr. Pandey Ji and general staff at the Animal House Facility, J.N.U., for proper maintenance of the experimental animals and sterile environment throughout the year.

I would also like to thank the Institutional Animal Ethics Committee members Prof. Deepak Sharma (Chairperson), Dr. R. Gopinath (CPCSEA Nominee), Dr. D. K. Yadav (Member Secretary), Dr. Shikha Yadav (Scientist from outside the Institute), Mr. Hans Raj Punhani (Socially-aware member), Prof. P. C. Rath (Member), Dr. Shushil Kumar Jha (Member) for helping me to understand the ethical concerns and matters related to experimental animal research.

I heartily thank the Office Staff of the School, especially Mrs. Sunita madam and Mrs. Shiny Madam for their constant cooperation and support in the Office and document-related matters. My thanks goes to Mr. Ram Kripal, In Charge of the Store for making available general chemicals to us on short notice.

I am very thankful to my seniors and colleagues in the laboratory, Dr. Manish Gupta (very helpful and supportive), Dr. Deepak K. Singh (very sincere), Dr. Kumar Sandeep (very friendly), Dr. Jeetendra Kumar Chaudhary (very rational, logical, intelligent and smart in research) and Dr. Sukhleen Kour, Mr. Vineet Sharma, Ms. Veena Sharma, Ms. Harpreet Kaur and Mr. Pankaj Kesari for providing assistance, support, and friendly scientific atmosphere in the laboratory, which helped me a lot in carrying out my work efficiently and happily. My appreciation also extends to Mr. Bittu for his contributing hand in many ways. I am grateful to Dr. Jeetendra Kumar Chaudhary, my senior for his guidance in the experiment design during my research work. This help is a great gift for me.

I am also thankful to Prof. Seyed E. Hasnain, Dr. K. K. Mohanty, Dr. Ankush Gupta, Dr. Arttatrarna Pal, and Dr. Rasmi Mishra for encouraging me and offering me help anytime in research work.

I would like to acknowledge all of my Ph. D. batchmates, seniors and juniors particularly Dr. Neeraj, Dr. Vandana, Prajapati, Dr. Anwar Alam, Dr. Rafia Shaikh, Dr. Zeeshan Ahamad Dr. Rajrani Ruhel, Ms. Isha Nagpal, Ms. Isha Goel, Ms. Ishani Majumdar, Mr. Om Prakash, Mr. Gopinath, Mr. Manjeet Kumar, Mr. Subhash Chandra, Mr. Rakesh Kapoor, Ms. Ranjna Maurya, Ms. Deep Jyoti, Ms. Shazia, Ms. Abhilasha Ghabriya, Ms. Aliya Sharma, Ms. Suchhanda, Ms. Gowri, Ms. Ruby for providing the constant cooperation, support and companionship that I required.

I would also like to appreciate my M. Sc. friends Mr. Ronaq Ali, Mrs. Madhu Singh, Mr. Mohit Gupta, Mr. Mohit Nagpal, Mr. Zeeshan Khan, Mr. Himanshu Malhotra, Mr. Prashant Arya, Mrs. Hina Jain, Mr. Madhav Aggarwal, Dr. Gaurav Sharma and Mr. Shabaz for their friendliness and real cooperation. These friends have been very precious, enlightening and inspiring at different stages of my educational career.

I take this opportunity to acknowledge the Council of Scientific & Industrial Research (CSIR) for providing fellowship (as JRF/SRF), and University Grants Commission-Research Network Resource Centre (UGC-RNRC) for financial assistance for carrying out my research work.

I bestow my deep sense of honor and appreciation to my best friend Motu urf Laddoo for strong and precious guidance and support during this study period. I'll never ignore the many excellent lunches, dinner, journey and fun movements that we've done collectively. The greatest consequence of these past few years is finding my best friend. I received the best personality out there for me. Motu is the only person who can recognize my quirkiness and sense of humor. There are no words to convey how much I love her. Motu has been a faithful and noble supporter and has unconditionally loved me throughout my good and bad times. She has been non-judgemental of me and contributory in imparting confidence. She has trust in me and my understanding. These preceding many years have not been a comfortable ride, both academically and personally. I sincerely praise Motu for adhering by my side, even when I was annoyed and depressed.

I would take this opportunity to express my deep sense of honor for my Ammi, Papa, brothers, sisters, family members, and relatives for all the love, appreciation, encouragement and affection. My hard-working parents have sacrificed their lives for us and gave unconditional love and care and taught me good things that matter in life. Their real love, care, and support have always been my strength. I understand, I would always have my family to depend when time is rough. I would not have gone this far without them. I love them so much.

NASEEM AHAMAD

ABBREVIATIONS

-/-	Knockout
AD	Alzheimer's Disease
Aβ	Amyloid β/Beta amyloid
ADSCs	Adipose tissue-derived stem cells/ Adipose tissue stem cells
bp	Base Pair
BM	Bone marrow
BMCs	Bone marrow cells
BM-MSCs	Bone marrow mesenchymal stem cells/ Bone marrow-derived Mesenchymal stem cells
CD	Cluster of differentiation
G/M/GM/M	Macrophage-Erythroid
CFU-F	Colony forming unit-fibroblast
COX-2	Cyclooxygenase-2
CO^{60}	Cobalt-60, radioactive element
CV	Crystal violet
DBD	DNA binding domain
DCs	Dendritic cells
DEPC	Diethylpyrocarbonate
DMEM-HG	Dulbecco's Modified Eagle Medium with high glucose
DNA	Deoxyribonucleic acid
dsRNA	Double stranded ribonucleic acid
EDTA	Ethylene diamine tetra acetic acid
ECs	Endothelial cells
ESCs	Embryonic stem cells

ERK	Extracellular-signal regulated kinase
FACS	Fluorescence-activated cell sorting
FBS	Fetal bovine serum
FSC	Forward scatter
FFA	Free fatty acid
FL2-A	Filter 2-area
FL2-W	Filter 2-width
g	Gram
GAPDH	Glyceraldehyde-3-phosphate dehydrogenase
GM-CSF	Granulocyte macrophage-colony-stimulating factor
H_2O_2	Hydrogen peroxide
hMSCs	Human mesenchymal stem cells
HPCs	Hematopoietic Progenitor Cells
ICSBP	Interferon Consensus Sequence-Binding Protein
IFN	Interferon
IL	Interleukin
iNOS	inducible nitric oxide synthase
iPSCs	Induced-pluripotent stem cells
IRF	Interferon regulatory factor
IRF-E	Interferon regulatory factor-Element
ISGF3	Interferon stimulated gene factor-3
ISRE	Interferon stimulated response element
Kb	Kilo base
kDa	Kilo Dalton
LIF	Leukaemia inhibitory factor

LPS	Lipopolysaccharide
M	Molar
MAPK	Mitogen activated protein kinase
MDS	Myelodysplastic syndrome
mg	Milligram
min	Minute
MAPCs	Multipotent Adult Progenitor Cells
MAPK	Mitogen activated protein kinase
mRNA	messenger RNA
MSCs	Mesenchymal Stem Cells
mM	Millimolar
MyD 88	Myeloid differentiation 88
N	Normal
NF-κB	Nuclear factor-Kappa B
NK cells	Natural Killar cells
ng	Nanogram
nt	Nucleotide
O/N	Overnight
PAMPs	Pathogen-associated molecular patterns
PBS	Phosphate buffered saline
PCR	Polymerase Chain Reaction
PD	Parkinson's Disease
PI3K	Phosphoinositide 3-kinase
RNA	Ribonucleic Acid
ROS	Reactive oxygen species

RT	Room temperature
RT-PCR	Reverse Transcription-Polymerase Chain Reaction
Sec	Second
SP	Side population
SSC	Side scatter
STAT 3	Signal Transducer and Activators of Transcription 3
TBI	Total body irradiation
TGF-β	Transforming growth factor-β
TLR	Toll Like Receptor
TNF α	Tumour Necrosis Factor-alpha
U	Unit
UV	Ultraviolet
VCAM-1	Vascular cell adhesion molecule-1
VEGF	Vascular endothelial growth factor
v/v	Volume/volume
WBI	Whole body irradiation
Wnt	Wingless and int homolog
w/v	Weight/volume
wt	Wild type
µg	Microgram
µl	Microliter
µM	Micromolar

CONTENTS

1 SUMMARY

Background

Bone marrow, a dynamic organ of a mammalian body, carries fundamentally of water, protein, and fat. These ingredients vary from person to person and within the same individual over time [1]. Bone marrow is a delicate, jellied, and powerful tissue which serves as an organ of the immune system. It is restrained in the center and the epiphysis of long bones like femora, tibia, humeri, ribs, pelvis, vertebrae, and skull of the body [2]. Bone marrow holds cellular component and soluble component. The cellular component comprises stem cells such as hematopoietic stem cells (HSCs), mesenchymal stem cells (MSCs), multipotent adult progenitor cells (MAPCs) and stroma cells of bone marrow such as endothelial cells (ECs), osteoclasts, osteoblasts, fibroblasts, tissue macrophages, and adipocytes, and the soluble component constitutes of cytokines, chemokines, growth factors, and hormones [3]. Bone marrow comprises two cellular components, parenchyma or hematopoietic component which includes HSCs and hematopoietic progenitor cells (HPCs) and stoma or vascular component bears non-hematopoietic progenitor cells such as endothelial cells (ECs), osteoclasts, osteoblasts, fibroblasts, tissue macrophages, adipocytes, MSCs and MAPCs [3-4]. Bone marrow is a considerable reservoir of pluripotent stem cells such as HSCs [5], MSCs [3, 6], MAPCs [7] and very small embryonic-like stem cells (VSELs) [8]. Stem cells have a unique capability to proliferate and differentiate into an undefined lineage of cells of the body. Each cell of bone marrow performs its appropriate function and preserves bone marrow structure and its purpose [3]. Bone marrow stem cells limit the immune rejection, a significant factor for the therapy of degenerative disorders [9]. There are various kinds of stem cells in the bone marrow. Hematopoietic stem cells (HSCs) restricted in both endosteal niche and vascular niche, generate all sort of blood cells [5, 10]. Mesenchymal stem cells (MSCs) detected in all tissues essentially vascularised tissues of the body, possessing trophic capabilities and immunomodulatory characteristics [6, 11]. Multipotent adult progenitor cells (MAPCs) that can differentiate into MSCs and hematopoietic lineage [7, 12]. The final one is very small embryonic-like stem cells (VSELs) can differentiate into all three embryonic germ layers.

They maintain homeostasis and get mobilized under several disease situations and regenerate the tissue [8]. The cellular components and soluble components constitute the microenvironment which is named as "bone marrow microenvironment or niche." Bone marrow microenvironment produces cell signals (intrinsic and extrinsic signals) and controls bone marrow (BM)-derived stem cells and progenitor cells, its functions comprises survival, migration, proliferation, mobilization, differentiation, and self-renewal of the cells [13].

The soluble component is essential for the precise functioning of bone marrow. The soluble component comprises cytokines, growth factors, hormones, calcium, and chemokines. The stem cells and their progeny cells produce soluble factors. For example, MSCs, ECs, osteoblasts and CAR cells secrete stromal cell derived factor-1 (SDF-1, also known as CXC12), which is an important chemokine participating in HSCs maintenance and HSCs homing within HSC niche [3]. SDF-1-/- Mice's HSCs have colonization defect, and reinforced expression of SDF-1 in bone marrow vascular endothelial cells improves colonization property of bone marrow by stem cells. Hence, bone marrow endothelial cells secreted SDF-1 is essential for hematopoietic colonization of bone marrow. SDF-1 also provokes expression of VCAM-1 on ECs and very late antigen (VLA)-4 on megakaryocyte [14]. Niche cells also deliver SCF and TGF-β which are related to regulation and HSCs maintenance. TGF-β secretion is associated with osteoblastic differentiation of MSCs [3].

Bone marrow (BM) is a repository of hematopoietic stem cells (HSCs). HSCs are not scattered everywhere in the body but are organized and confined in both the endosteal niche and vascular niche. HSCs generate all kinds of mature blood cells [10]. Bone marrow is the prime site of hematopoiesis, which is a continuously progressive process of generation and destruction of all terminally differentiated blood cells to serve various roles throughout a lifetime [15-16]. HSCs hold capabilities of self-renewal potential and reconstitution capacity of hematopoiesis, differentiated into lineage-committed and multi-potential progenitor cells [3]. HSCs capabilities or activities depend on Reactive oxygen species (ROS), particularly hydrogen peroxide (H_2O_2), generated by NADPH oxidase and mitochondria. Higher H_2O_2 level within HSCs or their niche favors migration, survival differentiation, the proliferation of HSCs or progenitor cells, while a low level of H_2O_2 in quiescent hematopoietic stem cells (HSCs) promotes and support "stemness," of HSCs [13]. HSCs and progenitor cells are not

randomly scattered; rather they are shielded and remained in a highly organized bone marrow microenvironment or bone marrow niche [3]. HSCs are first stem cells of bone marrow, and capable of producing all hematopoietic lineages [17].

It is assumed that MSCs are equipotent and ubiquitous. MSCs are tissue-specific stem cells and are not a lineage. MSCs do not contain a common embryonic origin. These cells are not identical and exhibit distinct differentiation capabilities based on their tissue origin. However, MSCs share their fibroblastic nature and cell surface markers expression [18]. A primary source of MSCs is bone marrow. Other studies confirm that the other prime reservoirs of mesenchymal stem cells are the umbilical cord, endometrial polyps, menses blood, adipose tissue, placenta, cruciate ligament and fallopian tubes, etc. [19]. MSCs are significantly connected with tissue homeostasis and formation of bone marrow niche structure and organization. MSCs support immunomodulation properties and proficient of suppressing and improve the immune system. Since MSCs are not immune cells but they control both innate immunity and adaptive immunity. Therefore, to emphasizing their position in modulating the immune response, MSCs are titled as "coordinators of the immune system." MSCs are a critical component of stem cell niche. MSCs manage differentiation; preservation and self-renewal of HSCs. MSCs release survival signals, helpful in stemness, and proliferation of HSCs and their progenitor cells. MSCs also protect HSCs from the chemotherapeutic agent and cytotoxic effect [3, 19].

MSCs possess characteristic properties which includes: Fibroblast cells like spindle-shaped morphology; plastic adherent property in culture; positive for MSCs-positive marker such as CD29, CD44, CD73, CD90, CD105 and Sca-1 and negative for MSCs-negative markers such as CD11b, CD34, CD45, and CD14; and differentiation into mesenchymal lineage such as chondrocytes, adipocytes, and osteocytes [3, 16, 18, 20-23]. MSCs are the heterogeneous mixture of a subpopulation of cells may or may not fulfill the specified stem cell criteria. MSCs, those satisfy the criteria term as "mesenchymal SCs," and those do not have term "multipotent mesenchymal stromal cells" [3].

Multipotent adult progenitor cells (MAPCs) from rat and mouse bone marrow was isolated by Catherine Verfaillie group, in 2002. Bone marrow derived MAPCs are adult stem cells and capable for insert trophic effect and immunomodulatory properties. Also, MAPCs are utilized

for tissue regeneration. Although new and originally isolated MAPCs exhibit robust differentiation towards neuro-dermal lineage and produce neuron-like cells [21]. However, MAPCs can differentiate into cells of all three germ layers such as mesodermal (e.g. endothelial cells, adipocytes, chondrocytes, and osteocytes), endo-dermal (e.g. hepatocytes), and ecto-dermal (e.g. astrocytes and neurons) [7]. MAPCs display robust endothelial expression as compared to MSCs [21]. Previous research showed that bone marrow-derived multipotent adult progenitor cells (MAPCs) are non-immunogenic and secrete large quantities of angiogenic growth factors after implantation and promote engraftment and survival [24]. Moreover, the previous report showed that similar to MSCs, rodent MAPCs also comprise immunomodulatory property. Mouse MAPCs can repress in vivo GVHD and T-cell alloresponse [25].

In addition to HSCs, MSCs, and MAPCs, Ratajczak's group has been revealed that several adult tissues such as bone marrow, cord blood, pancreas, testes, ovaries, and uterus contain very small embryonic-like stem cells (VSELs). VSELs show some specific traits like a rare occurrence, small size (2-6 μm), high nucleo-cytoplasmic ratio, spherical shape and quiescent in nature. VSELs exhibit a phenotypic profile of $LIN^{-}/CD45^{-}/SCA\text{-}1^{+}$ in mice and also express primordial germ cells (PGCs) and pluripotent surface markers. Similar to MSCs, VSELs differentiate into all three germ layers in mice as well as human and generate tissue committed progenitors cells and maintain homeostasis. VSELs mobilized following severe disease conditions and reconstructed the body tissue [8].

The certification of all types of stem cells is the capability of differentiation and self-renew. This property is called "stemness." The regeneration capacity of stem cells fundamentally explained by the following: Cellular signaling pathways preferentially expressed in the stem cells [26]; such as Wnt /beta-catenin which play a crucial role in self-renewal and differentiation mechanism of several types of stem cells. Also, Wnt /beta-catenin also involve in controlling of various functions such as growth, and death of stem cells. Stem cells require beta-catenin for maintenance and pluripotent state during embryogenesis. Signaling pathway of Wnt /beta-catenin manages the stability of the beta-catenin. Stabilized beta-catenin translocates and forming a beta-catenin-TCF/LEF complex in the nucleus controlling the transcription of precise target genes. Wnt signaling maintains stem cells. Impair Wnt /beta-

catenin signaling have shown close linked with several malignant stem cells and human cancers. Only controlled Wnt signaling allows the enhancement of stem cells and progenitor cell activity during regeneration [27]. Moreover, Wnt signaling regulates and communicates with Notch signaling. Hence, inhibition of the Wnt signaling influences HSC destiny. It is considered that the two pathways, Wnt signaling, and Notch signaling regulate a network of administrative circuits managing the HSC pool [10].

Chromatin regulatory pathways such as DNA/gene hypomethylation and histone and transcription factor modification also associated with pluripotency of stem cells [28]; Chromatin regulatory mechanisms, which involve DNA methylation (covalent modification of cytosine in CpG dinucleotides [29]), ATP-dependent chromatin remodeling, and covalent histone modification activate some genes and deactivate other genes to maintain the pluripotency and specific functions. For instance, at the time of differentiation, subsets of lineage-specific genes are switched on, whereas stem-cell-specific genes are switched off. Various researchers propose that DNA methylation may play an essential role in pluripotency, cell fate determination and regulate stem cells functions e.g. DNA methylation is claimed to assist hemopoietic stem cell self-renewal but not differentiation. Interestingly, recent genome-wide studies showed that stem cells have very little DNA methylation at CpG-rich sequences. In mouse ES, DNA methylation enzymes such as DNA methyl transferases (Dnmts) methylate the promoters of pluripotency genes such as Oct3/4 and Nanog. Hypermethylation of Oct3/4 promoter region in differentiating cells promote silencing, whereas hypomethylation is sufficient for high levels of Oct3/4 expression in cells, thus preserving them in a pluripotent state. These investigations collectively suggest that DNA methylation is associated with shutting down the pluripotency program upon lineage specification. However, how DNA methylation accurately operates in pluripotent, committed and differentiated cells is not well understood [30]. Moreover, The previous report reveals that demethylation of H3K4me2/3, H3K27me2/3, or H3k9me2/3 marks perform essential functions in supporting ES cell self-renewal, pluripotency, and differentiation [30].

Expression of transcription factors, such as Oct3/4, Sox-2, Nanog, Olig, Klf4, c-Myc, SALL4, etc., which are responsible for specifying the gene expression programs in the stem cells [28, 31-32]; The essential transcription factors, which regulate a central core regulatory systems

that sustain the pluripotent state of stem cells are Oct3/4, Sox-2, and Nanog. Oct3/4 (POU family transcription factor) encoded by Pou5f1 is a central regulator of pluripotency. Oct3/4 cellular concentration is very critical for pluripotency state of cells. Overexpression of Oct3/4 in ES cells favors differentiation into mesoderm lineages and primitive endoderm, whereas its deficiency begins the differentiation of the ICM and ES cells into trophectoderm and following cell death [30, 33]. Another component of the core pluripotency network is Sox-2 (SRY-related HMG-box transcription factor), needed for the maintenance of pluripotency. Sox-2-null embryos die immediately. However, in contrast to Oct3/4 and Nanog, the Sox-2 expression is not limited to pluripotent cells [30, 33]. Furthermore, next component of the core pluripotency network is Nanog (NK2-class homeobox transcription factor). Nanog expression is restricted to pluripotent cells and required for the maintenance of pluripotency in both the ICM and ES cells. It is not vital for the development of ES cells. However, Nanog deficiency in ES cells automatically differentiates into the primitive endoderm lineage, whereas overexpression can neglect the necessity of leukemia inhibitory factor (LIF) in controlling pluripotency in culture [30, 33]. Oct3/4, Sox-2, and Nanog biochemically communicate with each other and monitor the expression of many transcriptional target genes including histone modification genes and preserve genomic plasticity and pluripotency of stem cells [30, 33]. In addition to Oct3/4, Sox-2, and Nanog transcription factors, MYC (basic helix–loop–helix leucine-zipper (bHLH-LZ) family of TFs) also required for maintenance of cell reprogramming and pluripotency of stem cells. MYC modulates and integrates multiple mechanisms and act as a central hub in reprogramming and pluripotency state of stem cell. *MYC* knock-out embryos exhibit aberrations in a visceral organ such as heart, liver, lungs, stomach; and limb bud, and die between E10.5 and E12.5. Moreover, MYC also controls PSC-specific noncoding RNAs and control pluripotency [34].

Finally, more recently, the engagement of regulatory RNAs, such as the micro-RNAs (miRNAs) and long noncoding RNAs (lncRNAs), that control various function including growth, gene expression, epigenetic and differentiation of the bone marrow stem cells [35-37]. MicroRNAs (miRNAs), a type of small noncoding RNAs, are necessary for pluripotency. Previous researches showed that miRNAs are correlated with pluripotency network program. For instance, miR-290 and miR-302 are ESC-specific miRNAs clusters which inhibit somatic differentiation and support self-renewal [33]. Long noncoding RNAs (lncRNAs), more than

200 nt in length, has essential functions in the circuitry regulating ES cell and muscle differentiation. For instance, previously published reports showed that HOTAIRM1, a lncRNA, is associated with the differentiation of the myeloid cell line [38]. Moreover, it has been revealed that long noncoding, RNA H19, inhibits mesenchymal stem cells differentiation toward adipocyte [39]. Long noncoding RNAs (lncRNAs) also required in self-renewal, embryonic stem cell (ESC) pluripotency, lineage differentiation of the stem cells, such as HOTAIRM1 and EGO regulate the granulocyte differentiation, control hematopoietic stem cell function and cancer development [40]. Genome-wide study of mapping of transcriptional networks exhibits that many endogenous noncoding RNA molecules have potential roles in pluripotency. For instance, Long noncoding RNAs (lncRNAs), AK028326 and AK141205 perform in regulating the pluripotent nature. AK028326 maintain and increase the Oct4 mRNA level, and AK141205 repressed Nanog and control the pluripotent nature and the developmental state of mESCs [41].

Bone marrow is extremely unsafe to cytotoxicity caused by environmental factors, certain chemotherapeutic agents and accidental or deliberate exposure to a moderate or high dose of total body irradiation (TBI) resulting bone marrow (BM) suppression [42]. Radiation produces reactive oxygen species and free radicals, which damage important cellular targets such as membranes and DNA of stem cells. The microenvironment in the bone marrow includes stromal cells containing osteoclasts and osteoblasts for stem cell self-renewal and differentiation. These cells were diluted after irradiation [43]. It is well documented that ionizing radiation is one of the first causes of unrepaired genotoxic damage, stem cell pool depletion, impairing lineage functionality, cell death and accelerating aging, resulting in hematopoietic syndrome, one of the most dangerous radiation effects [44] Moreover, ionizing radiation induces a decline in the bone marrow cellularity and hematopoietic dysfunction, resulting in higher risk of bone marrow failure [45]. The previous literature revealed that total body irradiation provoked a quantitative and qualitative reduction of HSCs. In addition, long-term effects of radiation exposure initiate senescence and impairment of HSC self-renewal via activation pathways including p16/Rb and p53/p21. Radiation exposure also accelerates HSC aging, increasing spontaneous mutation, phenotypic changes, impaired reconstitution, increased apoptosis and accumulated DNA damage [44]. Previous studies revealed that exposure to total body irradiation (TBI) induces long-term or residual bone marrow (BM)

injury which includes decreased long-term repopulating capacity, permanent damage to hematopoietic stem cells (HSCs), myeloid skewing, and impaired self-renewal. These HSC injuries were related to significant increases in a generation of reactive oxygen species (ROS) due to radiation [46]. In addition to HSCs experience senescence after radiation which is linked to a defect in self-renewal of HSCs and decline of HSCs frequencies qualitatively and quantitatively [47]. Other investigations revealed that a most of the hematopoietic cells of bone marrow died by apoptosis after exposure to IR in vitro and those survived after IR damage failed their clonogenic function and showed an enhanced SA-β-gal activity, a biomarker for senescent cells [42, 47-48].

The previous studies have demonstrated that allogeneic bone marrow transplantation (BMT) is recommended treatment for both systemic and organ-specific autoimmune diseases associated with stem cell [49]. Moreover, bone marrow transplantation, approved therapy for bone marrow failure, is practiced for the treatment of many diseases such as non-malignant, malignant blood diseases [50]. Thus, transplanted bone marrow may be an excellent help under such conditions.

Bone microenvironment generates IFN-gamma, a pleotropic cytokine, identified to perform a significant role in bone remodeling. pINF-gamma injected mice exhibited enhanced discharge of pro-inflammatory cytokine by bone marrow cells; the interrupted cortical and trabecular bone microarchitecture, a pathologic bone marrow phenotype and bone marrow morphological alterations. Moreover, a redistribution and decline of CXCL12 cells and impaired mesenchymal stem cells' (MSCs) commitment to osteoblast have been detected [51]. The interferon regulatory factor (IRF) proteins form a nine-member family of the transcription factor known as IRF family that regulates the interferon (IFN)-α/β gene. Interferon regulatory factors perform a variety of function because of its posttranslational modification such as phosphorylation and interaction with other transcription factors resulting activate and deactivate various cellular functions [52-53]. The previous studies have shown that variety of agent like cytokines, double-stranded RNA (dsRNA), type I interferons, viral infection, etc. regulate the expression of both IRF-1 and IRF-2 [54-55]. Interferon regulatory factors are transcriptional activators. They stimulate a variety of genes that perform central roles in the regulation of innate and adaptive immunity during bone marrow recovery. IRF-1, serve as a

tumor suppressor, the expression is correlated with growth inhibition and anti-proliferation [56]. Whereas IRF-2 (having oncogenic property) arouses VCAM-1, TLR-9 and histone gene that regulate cell cycle and associated with various cancers [52, 55, 57]. IRF-1 and IRF-2 play very significant roles in the cells including, apoptosis of cells, regulation of NK cell development in the bone marrow, differentiation regulation of Th1 and Th2 cells, and controlling macrophage function. They also required in the regulation of T cells, B cells and dendritic cells development and their duties [52-53, 55, 58]. Moreover, irregularities in an expression of IRF-1 and IRF-2 create several diseases including cancer and bone marrow related disease such as myelodysplastic syndromes (MDS) [59].

Objectives

Based on the above background, following objectives were studied.

1. Isolation and culture of bone marrow (BM) cells and enrichment, isolation, culture, and propagation of mesenchymal stem cells (MSCs) from the C57Bl6J mouse as well as their morphological and immunophenotypic characterization.

2. Transplantation of BM cells and MSCs into irradiated mouse and study of bone marrow regeneration by: (a) cell cycle analysis by FACS, (b) CFU-F assay, (c) gene expression analysis by RT-PCR and (d) functional assay by measuring secretory factors.

3. Role of IRF-1 and IRF-2 transcription factors in this mouse model of bone marrow regeneration by (a) immunofluorescence, protein expression/ localization, (b) gene expression (RT-PCR) and (c) expression of IRF-1 and IRF-2-regulated genes by RT-PCR

Experiments

The aim of the present study is isolation, culture, and propagation of the mouse bone marrow cells (BMCs) and isolation, culture, enrichment and propagation of the mouse bone marrow-derived mesenchymal stem cells (passage-1) (MS-P1cells). The characterization of BMCs and MS-P1 cells was carried out by morphological features, immunophenotyping of the cell surface markers (positive and negative) and expression of pluripotency associated factors according to the minimum characterizing criteria for MSCs generated during the meeting of International Society for Cellular Therapy (ISCT)-2006. BMCs were transplanted into mouse

after exposure to radiation and regeneration of the bone marrow was studied. IRF-1 and IRF-2 expression was studied during bone marrow regeneration.

To address the above objectives, following experiments were carried out.

1. Isolation of bone marrow cells from C57/BL6 mouse bone marrow, (b) culture and expansion of mesenchymal stem cells (MSC) of passage 0 (P0) and passage 1 (P1) were conducted by intrinsic adherence property of MSCs, (c) culture and development of MSC-P1 cells were carried out by fundamental adherence property of MSCs, (d) cell cycle status of bone marrow cells and (e) Stem cell potential of bone marrow by CFU-F assay.

2. Characterization of MSCs by: (a) morphological features by microscopy (fibroblast-like spindle-shaped morphology), (b) immunophenotypic characterization by cell surface markers, e.g., (MSC-positive: CD29, CD44, Sca-1) and (MSC-negative: CD34, CD45 and CD11b) by FACS.

3. Generation of the irradiated mouse model and transplantation of BM cells into irradiated mouse. Mice of 8 weeks of age were exposed to the 4 Gy radiation and then BMCs ($10x10^6$ cells) were transplanted four hours post-radiation through tail vein injection. Post 24 hours-radiation mice (control, irradiated and transplanted) were sacrificed and analyzed.

4. Investigation of bone marrow regeneration by (a) cell cycle analysis by FACS, (b) CFU-F assay and (c) histological study of the bone from control, irradiated and transplanted mice

5. Examine the role of IRF-1 and IRF-2 transcription factors in this mouse model of bone marrow regeneration by (a) gene expression by real-time RT-PCR, (b) protein expression/ localization by immunofluorescence & confocal microscopy.

6. Study IRF-1 and IRF-2 transcription factors in bone marrow derived MSC-P1 cells by immunofluorescence and confocal microscopy for protein expression/ localization.

7. Study of pluripotency-associated transcription factors (Oct3/4 and Sox-2) in bone marrow cells and bone marrow derived MSC-P1 cells by immunofluorescence and confocal microscopy for protein expression/ localization.

An irradiated mouse model for bone marrow regeneration study was developed. The mouse was irradiated with sub-lethal dose, and BMCs were transplanted by tail vein injection. Cell cycle analysis, CFU-F assay and histological study were carried out to study bone marrow regeneration in this irradiated mouse model. Radiation-induced bone marrow damage was observed. The bone marrow recovery due to transplantation of bone marrow cells (24 hours) was up to 35% in this study.

Interestingly, it was observed that interferon regulatory factors (IRF-1 and IRF-2), the two important transcription factors, were expressed in BMCs and MSC-P1 cells. The study of IRF-1 and IRF-2 during bone marrow regeneration revealed that expression of IRF-1 and IRF-2 genes at both mRNA and protein levels are radiation-sensitive and responsive in the bone marrow. These two transcription factors are associated with several fundamental cellular processes such as cell growth, maturation, proliferation, and differentiation.

Moreover, BMCs and MSC-P1 cells expressed the stemness-related pluripotency associated transcription factors, such as Oct3/4 and Sox-2 at protein levels.

Results and Discussion

Mouse bone marrow contains mesenchymal stem cells, which proliferate and propagate up to passage-1 during *in vitro* culture. Cultured MSC-P1cells (33 days cultured) have plastic adherence properties and spindle-shaped morphology like fibroblasts. Mouse BMCs showed expression of MSC-positive markers such as Sca-1 (21.39 ± 5.54 %), CD44 (79.39 ± 4.47 %), CD29 (68.54 ± 5.45 %) and MSC-negative markers, which includes CD11b (54.61 ± 2.35 %), CD34 (21.12 ± 6.75 %), CD45 (71.34 ± 4.67 %). Immunophenotypic characterization of MSC-P1 cells (33 days cultured) showed that MSC-P1 cells expressed CD29 (96.90 %), CD44 (39.86 %), Sca-1 (32.70 %) as MSC-positive markers and expressed low levels of CD11b (28.28 %), CD34 (22.63 %) and CD45 (2.47 %) as MSC negative markers.

To study the bone marrow regeneration in a radiation-induced damage mouse model, cell cycle analysis, CFU-F assay and histological analysis were carried out in the bone marrow transplanted mouse.

Cell cycle status of bone marrow cells isolated from control, irradiated and transplanted mice showed that G1 phase cells (activated cells' potential) was significantly declined from 62.50 ± 4.18 % in control to 38.74 ± 3.43 % in irradiated mice. There was up to 38.01% damage in the G1 phase cells due to radiation. In transplanted mice, G1 phase cells increased from 38.74 ± 3.43 % in irradiated mice to 48.04 ± 2.70 % in transplanted mice, i.e. there was about 24 % recovery of the G1 phase cells 24 hours after transplantation. Cell cycle results showed that the bone marrow regeneration potential by transplantation was about 24 % within this time frame.

The damage to bone marrow potential due to radiation was 86.34 %, 79.39 %, and 54.77 % and the recovery of bone marrow potential due to transplantation was 34.53 %, 32.16 % and 8.71 % in the one, two and four million cells seeded for CFU-F assay, respectively.

Analysis of bone marrow cellularity from the histological images of control, irradiated and transplanted mice bones showed that 4 Gy radiation caused 43.44 % decrease in the cellularity of the bone marrow of irradiated mice compared to control. The declined cellularity was restored by transplantation of 10 million BMCs to the irradiated mice by the tail-vein-injection method, which increased the cellularity up to 28.45% after 24 hours. Thus histological analysis showed that regeneration was up to 28.45% within 24 hours after transplantation.

IRF-1 mRNA expression was significantly higher in irradiated (4.34x fold) and transplanted mice (3.85x fold) as compared to control mice. Similarly, IRF-2 mRNA expression was significantly higher in irradiated (3.87x fold) and transplanted (3.46x fold) as compared to control mice. Moreover, IRF-1 mRNA exhibited higher expression level compared to IRF-2 mRNA in the BMCs of irradiated (1.12x fold) and irradiated+transplanted (1.11x fold) mice.

Immunofluorescence for IRF-1 protein expression was cytoplasmic. IRF-1 protein showed significantly higher expression in BMCs of irradiated (2.12x fold) and transplanted (1.73x fold) as compared to control mice. Similar to IRF-1, immunofluorescence for IRF-2 expression was also cytoplasmic, which was more in BMCs of irradiated (1.71x fold) and transplanted (1.21x fold) as compared to control mice. Thus IRF-1 and IRF-2 are radiation responsive genes in the BMCs, and they may be involved in the bone marrow regeneration.

BMCs and MSC-P1 cells expressed IRF-1 and IRF-2. BMCs showed cytoplasmic expression. Comparative analysis of intensities of IRF-1 and IRF-2 of MS-P1 cells demonstrated that IRF-1 was 3.11x fold expressed in the cytoplasm compared to its nuclear expression and IRF-2 showed 4.19x fold more expressed in the nucleus compared to its cytoplasmic expression in MSC-P1 cells. Moreover, IRF-1 showed 1.57x fold higher than IRF-2 in the cytoplasmic expression, whereas IRF-2 showed 13.09x fold higher than IRF-1 in the nuclear expression in MSC-P1 cells. This may be linked to the immunomodulatory function(s) of MSCs.

The pluripotency associated transcription factor, Oct3/4 showed the cytoplasmic expression, but its localization was preferentially more peripheral in the BMCs as well as in the MSC-P1 cells. Whereas, another pluripotency associated transcription factor, Sox-2 showed stable expression, i.e. uniformly expressed in the nucleus and cytoplasm of the BMCs and MSC-P1 cells. This sub-cellular localization specific expression of Oct3/4 and Sox-2 may be important for the stem cell specific function(s) of MSCs.

Conclusion

Experimental methods for isolation, culture, characterization and propagation of mouse bone marrow cells and bone marrow derived mesenchymal stem cells (passage 1) were optimized. A method for radiation-induced bone marrow damage in mouse was optimized and bone marrow regeneration (24%) was achieved up to 24 hours after the damage by transplantation of bone marrow stem cells through tail-vein injection in the mouse. Bone marrow cells and bone marrow derived mesenchymal stem cells showed expression of the transcription factors: interferon regulatory factor-1 (IRF-1) and IRF-2, which was sensitive and responsive to radiation-induced damage and bone marrow regeneration. This experimental mouse model system for stem cell therapy can be used for studying many human diseases related to the bone marrow.

2 INTRODUCTION

Mammalian bone marrow (BM) is a very flexible, elastic and viscous tissue. BM is supposed one of the largest semi-solid organs in the human body, forming approximately 4%-5% of the total human body weight, 3% of adult body weight in rats and 2% of adult body weight in dogs. It is formed by a mixture of loose connective tissues, hematopoietic and non-hematopoietic cells. Bone marrow remains in the core and the epiphysis of long bones like femora, tibia, humeri, ribs, pelvis, vertebrae, and skull. Bone marrow is a fundamental element of the lymphoid system, providing the lymphocytes erythrocytes, granulocytes, monocytes, lymphocytes, platelets and related blood and immune cells that support the body's immune system [2]. Bone marrow comprises two elements. One is parenchyma or hematopoietic component which includes highly organized hematopoietic stem cells (HSCs) and hematopoietic progenitor cells (HPCs). And other is stroma, or vascular component contains non-hematopoietic progenitor cells [4] such as mesenchymal stem cells and several mesenchymal stem cell types such as perivascular cells, megakaryocytes, macrophages, Schwann cells, osteoclasts, osteoblasts and endothelial cells. Stromal cells promote hematopoiesis and monitor HSCs roles and act such as mobilization and quiescence [60]. Bone marrow changes over the time i.e. from beginning to old age marrow. Bone marrow converts red marrow (at birth) to yellow marrow (old age bone marrow). Red marrow or hematopoietic marrow holds greater cellularity and efficient in hematopoiesis because of greater self-renewal capacity and reconstitution potential. Yellow marrow (fatty marrow) containing numerous adipocytes and revealing insignificant hematopoietic activity due to limited self-renewal ability and reconstitution potential and myeloid-biased differentiation potential [26, 61].

Bone marrow stem cells limit the immune rejection, a significant factor for the therapy of degenerative disorders [9]. There are three main kinds of stem cells in the bone marrow. Hematopoietic stem cells (HSCs) restricted in both endosteal niche and vascular niche, generate all sort of blood cells [5, 10]. Moreover, HSCs and progenitors supporting bone marrow homeostasis after various abuses and challenges, including exsanguinations, inflammation, and infection. HSCs contain the extraordinary capacity to reconstitute the whole hematopoietic system of an organism after transplantation and recover ablated

hematopoietic system [62]. The next major stem cell population in bone marrow is bone marrow derived mesenchymal stem cells (BM-MSC). They are used for therapeutic organ treatment because they can be comparatively easy isolated from a mouse. BM-MSCs have high potential to differentiate into different types of cells of connective tissues such as adipose tissue, bones, cartilage, skeletal muscles and supporting stroma [63]. Mesenchymal stem cells (MSCs) detected in all tissues essentially vascularised tissues of the body, possessing trophic capabilities and immunomodulatory characteristics [6, 11]. Though, bone marrow is the primary source of MSCs. However, Other significant origins of mesenchymal stem cells are the umbilical cord, endometrial polyps, menses blood, adipose tissue, placenta, cruciate ligament and fallopian tubes, etc. [19]. MSCs possess characteristic properties which includes: Fibroblast cells like spindle-shaped morphology; plastic adherent property in culture; positive for MSCs-positive marker such as CD29, CD44, CD73, CD90, CD105 and Sca-1 and negative for MSCs-negative markers such as CD11b, CD34, CD45, and CD14; and differentiation into mesenchymal lineage such as chondrocytes, adipocytes, and osteocytes [3, 16, 20-23]. Bone marrow-derived multipotent adult progenitor cells (MAPCs) possess a high capability to differentiate into ectoderm, mesoderm, and endoderm (all three germinal layers). The source of MAPCs within bone marrow is still unexplained. However, MAPCs are supposed to produce from the bone marrow stroma compartment [7, 12]. The final one is very small embryonic-like stem cells (VSELs) similar to primordial germ cells (PGCs). VSELs migrate and survive in the gonads and many other organs and serve as a reserve pool for the tissue-committed stem cells. VSELs can differentiate into all three embryonic germ layers in both human and mice. They maintain homeostasis and mobilized under several disease situations and regenerated the tissue [8].

The regenerative, differentiation and self-renewal capacity of stem cells includes chromatin regulatory [28] and cellular signaling pathways [64], regulatory RNAs [36-37] and cellular concentration of pluripotent-associated transcription factors [28, 32].

Bone marrow and bone marrow native cells experience a continuous decline, degeneration, and deterioration as a result of different bone marrow associated disorders and outside factors, such as exposure to a fatal dose of radiation and other external physical, chemical and biological insults. Exposure of the whole body to a high dose of ionizing radiations, including

gamma (γ-ray) and X-rays drives chromosomal aberrations, such as double-strand breaks in chromosomal DNA, paracentric inversion, pericentric inversions, and intra-arm deletions [65]. Moreover, radiation also stimulates the formation of reactive oxygen species (ROS), which further harm the major biomolecules including DNA, RNA, Proteins, and lipids of hematopoietic stem and progenitor cells [48]. Moreover, ionizing radiation may lead to decline in hematopoietic precursors that may cause a reduction in bone marrow cellularity, hematopoietic dysfunction, degrade bone mineralization and a higher risk of bone marrow failure [45].

The field of bone marrow study is extremely dependent on in vivo experimentation because in vitro techniques do not simulate the complication of in vivo investigations. Whole-body irradiation is used as the most popular weapons for myeloablation of the recipient's bone marrow. Previous studies showed that bone marrow transplantation (BMT) is the therapy of opportunity for many diseases such as solid tumors, leukemias and radiation induce insults [45]. Stem cell transplantation studies recorded that inherited bone marrow failure syndromes (IBMFS) such as Fanconi anemia and dyskeratosis congenita can cure after hematopoietic stem cell transplantation (HSCT), practicing as essential conditioning regimen for achieving long-term survival rate in these patients [66]. In addition, allogeneic bone marrow transplantation has a capability to destroying leukemia and contributes to a role in controlling human cancers. This efficacy of allogeneic bone marrow transplantation proposes future directions to enhance leukemia treatment [67].

The interferon regulatory factor (IRF) proteins form a nine-member family of the transcription factor known as IRF family that regulates the interferon (IFN)-α/β gene. Interferon regulatory factors perform a variety of function because of its posttranslational modification such as phosphorylation and interaction with other transcription factors resulting activate and deactivate various cellular functions [52-53]. The previous studies have shown that variety of agent like cytokines, double-stranded RNA (dsRNA), type I interferons, viral infection, etc. regulate the expression of both IRF-1 and IRF-2 [54-55]. Interferon regulatory factors are transcriptional activators. They stimulate a variety of genes that perform central roles in the regulation of innate and adaptive immunity during bone marrow recovery. IRF-1, serve as a tumor suppressor, the expression is correlated with growth inhibition and anti-proliferation

[56]. Whereas IRF-2 (having oncogenic property) arouses VCAM-1, TLR-9 and histone gene that regulate cell cycle and associated with various cancers [52, 55, 57]. IRF-1 and IRF-2 play very significant roles in the cells including, apoptosis of cells, regulation of NK cell development in the bone marrow, differentiation regulation of Th1 and Th2 cells, and controlling macrophage function. They also required in the regulation of T cells, B cells and dendritic cells development and their duties [52-53, 55, 58]. Previous studies have confirmed that IRF-1 acts as a modulator of T regulatory (Treg) cells by suppressing Foxp3 on mice and aberrations in interferon regulatory factor-1 (IRF-1) expression is correlated with the development of myelodysplastic syndromes (MDS) [59].

3 REVIEW OF LITERATURE

3.1 Bone marrow

Bone marrow is a soft, gelatinous, and dynamic tissue which serves as an organ of the immune system. Its amount fluctuates from person to person and within the same individual over the time i.e. hematopoietic marrow comprising higher cellularity and efficient in hematopoiesis at childhood change to adulthood yellow or fatty marrow holding more adipocytes and having insignificant hematopoietic [1]. Therefore, bone marrow can be classified into the red bone marrow having active hematopoiesis and yellow bone marrow contain very less hematopoiesis activity [26]. Bone marrow (BM) and blood are considered as one of the great organs in the body and develop nearly 5% of the body weight in human. BM is confined in the medullary cavities of long bones such as humerus and femur [2]. BM is a primary lymphoid organ and the major hematopoietic organ which is efficient for the generation of all blood cells and immune cells during entire life. BM is supposed to provide approximately 500 billion cells per day. Bone marrow, 2600 g, is distributed within the about 206 bones of the adult human serving as a semi-autonomous organ. It is expected that 1,400 g out of 2600 g is actively engaged in blood cell production [68].

3.1.1 Bone marrow architecture

Bone marrow presented in the central cavity and protected or surrounded by bone. Bone is parted into an outer part which is composed of compact bone or cortical bone, formed by osteon unit. Osteon comprises bone cells or osteocytes and extracellular matrix, while the inner portion is constituted of cancellous bone or spongy bone near to bone marrow. Spongy bone contains trabeculae which are made up of osteoblast, osteoclast, and osteocytes [68-69]. Bone cells such as osteoblast are generated from stroma stem cells, while osteoclasts originated from HSCs's monocytes and macrophage lineage. In addition, bone marrow cells deliver some bone regulatory factors. Osteoblast and osteoclasts provide secretary factors and sustain and maintain the microenvironment or bone marrow niche for the particular functioning of stem cells. Although bones and bone marrows are two different and separate tissues or systems, they function complementary and act as a single functional unit [69].

Outer cellular stroma or vascular component holds vascular system including nutritive vessels, a very complex sinusoidal system receiving newly developed cells and discharge them into the venous side of the peripheral blood, a reticular network of cells as well as the central sinusoid managing recently formed cells of the sinusoidal system. In addition, cellular stroma also includes both myelinated as well as unmyelinated nerve fibers. Moreover, the vascular component receives non-hematopoietic progenitor cells such as MSCs and MAPCs. As far as the inner "parenchyma" or hematopoietic component is concerned, it certainly is constituted of HSCs; hematopoietic progenitor cells (HPCs) and all the different mature and immature blood cell progenitors [4, 68].

Bone marrow is a large reservoir of pluripotent stem cells, having unique ability to proliferate and differentiate into an unspecified lineage of cells of the body, such as hematopoietic stem cells (HSCs) [5], mesenchymal stem cells (MSCs) [3, 6], and multipotent adult progenitor cells (MAPCs) [7].

Bone marrow possesses cellular component and soluble component **(Figure I)**. The cellular component encompasses stem cells such as HSCs, MSCs, MAPCs and bone marrow stroma cells such as endothelial cells (ECs), osteoclasts, osteoblasts, fibroblasts, tissue macrophages, and adipocytes whereas soluble component constitutes of cytokines, chemokines, growth factors, and hormones [3]. Hormones also transform bone marrow cells. Elimination of gonad from male and female rats declines and increments the circulating erythrocyte, respectively and their effect abolished by administration of respective hormone [70]. Moreover, each cell of bone marrow (stem cells and supportive cells) performs its particular function and maintains bone marrow structure and functions. The most significant role of stem cells is movement and transport purposes to sites of local damages or tissue injury to promote appropriate cell and tissue renewal to reconstruct the damaged areas, which are extremely valuable for clinical utilization, especially in regenerative medicine [71] **(Table 1)**.

3.1.2 Bone marrow microenvironment or bone marrow nice and functions

Bone marrow stem cells are not randomly located within the bone marrow. HSCs and hematopoietic progenitor cells (HPCs) are localized in extremely organized a specialized area such as endosteum of bone and around blood vessels. Additionally, undifferentiated cells localized in endosteum area while mature and differentiated cells reside toward bone marrow

cavity [14]. Bone marrow niche is extremely designed and supportive microenvironment within the bone marrow. Bone marrow microenvironment constitutes of cellular component, contains stroma cells and accessory cells, and a soluble component that secreted by niche cells themselves. Bone marrow stroma cells include fibroblasts, bone marrow macrophage, endothelial cells (ECs), osteoblasts, osteoclasts, adipocytes, and MSCs. Accessory cells comprise myeloid originated cells such as dendritic cells, circulating macrophage, and lymphoid originated cells such as Natural killer cells, B-cells, and T-regulatory cells. Stem cell niche of bone marrow supports the growth and differentiation of stem cells where they confined. Niche also protects stem cells from damage and provides cytokines, stimulatory factors for accurate functioning. Almost all stroma cells originate from MSCs or HSCs or Progenitor cells [3].

According to the current concept of bone marrow niche, there are several types of niches within the bone marrow including **endosteal niche, vascular sinusoidal niches, perivascular arteriolar niche and sinusoidal megakaryocytic niche**. **Endosteal niche**, also known as **osteoblastic niche** or **osteo-hematopoietic niche** includes HSCs and osteoblast cell population. The osteoblastic cell population is spindle-shaped, cadherin-positive and located at the lining of the bone surface. Therefore, these cells also termed as spindle-shaped N-cadherin^{+} osteoblastic (SNO) cells. **Endosteal niche** favors HSC quiescence. Moreover, early lymphoid progenitors cells of mice predominantly found in an endosteal niche. **Vascular niche** or **vascular sinusoidal niche** or **sinusoidal reticular niche** includes the majority of HSCs and SMA^{+}CD146 pericytes. Additionally, Leptin-receptor^{+} cells, CAR (CXCL12 abundant reticular) are found predominantly in vascular niche and firmly associated with ECs and HSCs [3]. Thus, Endosteal niche favor HSCs maintenance and quiescence, and vascular niche provide a signal for differentiation of HSCs [14]. Hematopoietic stem and progenitor cells (HSPCs), nestin^{+} cells, Leptin-receptor^{+} cells, pericytes and CAR cells make up the **perivascular niche** or **perivascular arteriolar niche** or **pericytic arteriolar niche**. Mice HSCs and early myeloid progenitors cells predominantly located in perivascular niche. **Sinusoidal megakaryocytic niche** composes of HPSCs and megakaryocytes that secrete CXCL4 and involved in HSC quiescence and maintenance [3]. Translocation of megakaryocyte progenitors toward sinusoidal megakaryocytic niche induces platelet production and megakaryocyte maturation [14] **(Table 1)**. It remains to disclose how each

niche communicates with other, their way of working, as they function as a single unit or work together? Are they really separated niche? and how they respond toward disease or aging?

3.2 Cellular components of Bone marrow

3.2.1 Bone marrow stem cells and function

3.2.1.1 Hematopoietic stem cells (HSCs) and functions

HSCs are primary stem cells of bone marrow, and capable of producing all hematopoietic lineages. HSCs exhibit certain surface markers such as murine HSCs express Sca-1 and c-kit while human HSCs showed CD133. HSCs exhibit a lack of lineage-specific markers.

HSCs exhibit expression of surface markers such as CD34 which is the first differentiation and most commonly used marker for isolation and enrichment of primitive human HSCs. CD133 is another surface marker for h-HSCs selection. A more recently selection maker for h-HSCs is CDCP1 (Cub domain containing protein). Selection markers of h-HSCs include c-Kit for hematopoietic growth factors that control cell proliferation and survival; VEGFR-1 (vascular endothelial growth factor receptor-2), involved in HSC cycling; and VEGFR-2, also known as KDR, maintain HSC viability. Further research required to explore the exact surface markers selection for isolation and characterization of h-HSCs. Similar to human, mouse HSCs (m-HSCs) express c-Kit, Sca-1, Thy-1. Also, m-HSCs express CD34, which depends on activation status and developmental stage of cells, FGFR (fibroblast growth factor (FGF) receptor) marker used for HSCs which show a low level of Sca-1 marker. Highly purified m-HSCS express CD201 or EPCR (endothelial protein C receptor) and endothelial cells also positive for CD201. CD201 marker also expresses by h-HSCs. Also, m-HSCs surface marker expression list includes CD105, also known as endoglin, which involved in transforming growth factor (TGF) receptor (TGFR) signaling [17] **(Table 2)**.

Bone marrow is the primary site of hematopoiesis, which is a continuously dynamic process of production and consumption of all terminally differentiated blood cells to operate various functions throughout a lifetime [16]. HSCs, having self-renewal capacity and reconstitution ability of hematopoiesis following transplantation, differentiated into lineage-committed and multipotential progenitor cells. HSCs and progenitor cells are not randomly scattered; rather

they are protected and resided in a highly organized bone marrow microenvironment or bone marrow niche [3]. In the steady state, Hematopoietic progenitor cells (HPCs) which manage daily hematopoiesis. HPCs are of two types, lymphoid progenitor cells (LPCs) differentiate into lymphocytes and plasma cells; and myeloid progenitor cells (MPCs) which differentiate into granulocytes, monocytes, erythrocytes, and platelets, while HSCs are mostly quiescent [16].

Recent studies have classified HSC subtypes such as platelet-biased HSCs (PB-HSCs), balanced HSCs (B-HSCs), myeloid-biased HSCs (MB-HSCs) and lymphoid-biased HSCs (LB-HSCs). PB-HSCs can make MB-HSCs and LB-HSCs, and MB-HSCs can generate B-HSCs and LB-HSCs. Biased HSCs hold different lineage differentiation potential. For instance, MB-HSCs ($CD150^{high}CD34^{-}LKS$) contain greater self-renewal potential than B-HSCs and LB-HSCs which favor myelopoiesis over lymphopoiesis. As a result, MB-HSCs substitute all types of HSC population in the HSC hierarchy in the bone marrow during the age. LB-HSCs create more lymphoid lineage than myeloid lineage cells [16].

3.2.1.2 Mesenchymal stem cells and function

A primary source of MSCs is bone marrow. Other important sources of MSCs are adipose tissue, umbilical cord, umbilical cord blood, amniotic fluid, dental pulp, periodontal ligament, skin, fetal tissues, and placenta. MSCs are significantly involved in tissue homeostasis and formation of bone marrow niche structure and organization. MSCs maintain immunomodulation properties and capable of suppressing and regulate the immune system. Since MSCs are not immune cells but they control both innate immunity and adaptive immunity. Therefore, to emphasizing their role in modulating the immune response, MSCs are termed as “coordinators of the immune system.” MSCs are a crucial component of stem cell niche. MSCs regulate differentiation; maintenance and self-renewal of HSCs. MSCs deliver survival signals, stemness, and proliferation of HSCs and their progenitor cells. MSCs also protect HSCs from the chemotherapeutic agent and cytotoxic effect [3, 19].

3.2.1.2.1 Mesenchymal stem cells characterization

Mesenchymal and Tissue Stem Cell Committee (MTSCC) of the International Society of Cellular Therapy (ISCT) have been defining the minimal criteria for the characterization of MSCs which includes: plastic adherent property in culture; must be positive for MSCs

positive marker such as CD29, CD44, CD73, CD90, CD105 and Sca-1 and negative for MSCs negative markers such as CD11b, CD34, CD45, CD14, and HLA-DR (human leukocyte antigen D related); and differentiation into mesenchymal lineage such as chondrocytes, adipocytes, and osteocytes. Additionally, fibroblast cells like spindle-shaped morphology [3, 16, 20-21, 23, 72]. MSCs are the heterogeneous mixture of a subpopulation of cells may or may not fulfil the specified stem cell criteria. MSCs, those satisfy the criteria term as "mesenchymal SCs," and those do not call "multipotent mesenchymal stromal cells" [3] **(Table 2)**.

3.2.1.2.2 Origin of Mesenchymal stem cells

The origin of MSC is still mattered of conflict. Some researcher believes it is a mesodermal origin while other say neuroectodermal origin, even dual origin have been introduced. MSCs can differentiate into mesodermal lineages such as chondrocytes, osteocytes, and adipocytes in vitro, suggesting the MSC's mesodermal origin. Several reports proposed a neuroectodermal origin of MSC because of MSCs present in all vascular organ i.e. perivascular region. The previous report showed endosteal localized MSCs expressed only CD271, whereas MSCs in the perivascular region showed $CD146^{+}CD271^{+}$. Moreover, $CD146^{+}$MSC/pericytes were detected in hematopoietic microenvironment. Thus MSCs may be the mesodermal origin or neuroectodermal origin; it remains to explore [3, 73].

3.2.1.2.3 Dual effects of MSCs on Erythropoiesis

MSCs support HSCs and hematopoiesis but they also inhibit the erythroid differentiation ability of HSCs by soluble factors. Therefore, MSCs have the dual role toward erythropoiesis. IL-6, stroma cells secreted interleukin, inhibit erythroid development and favor the expansion of myeloid progenitor cells in the peripheral blood. Further, previous research published those MSCs initially with lower density or confluence of MSCs in culture discharge prostaglandin (PGE) which enhances erythropoiesis. As a result of growth, higher density or confluency of cells forms a monolayer of MSCs which produce no PGE, resulting in inhibition of blast forming unit-erythroid (BFU-E). Hence lower confluence MSCs favors erythropoiesis whereas higher confluency inhibits erythropoiesis [3].

3.2.1.2.4 Immunomodulation of MSCs

Immunomodulation property of MSCs includes immunosuppressive properties and systemic immunoregulatory. Since MSCs are not immune cells but they play a critical role in innate and adaptive immune response. Hence they are called "coordinator of the immune system." The fundamental mechanism of MSCs's immunomodulatory effect in modulating immune response is remaining to be disclosed. However, murine experiments expose that MSCs favor the generation of immunosuppressive immune cells subset including B regulatory cells, NK regulatory cells (NKregs) $CD4^+$ Tregs, $CD4^+$ Tregs, Regulatory DCs (DCregs). Immune suppressive regulatory cells make up a tolerogenic microenvironment which actively suppresses the immune response. Apart from favoring the production of immunosuppressive immune cells, MSCs simultaneously and forcefully overcome various pro-inflammatory immune cells [3].

The mechanism of an immunosuppressive capacity of MSCs is of two types, cell to cell contact dependent and independent mechanisms. In cell to cell contact-dependent mechanisms, MSCs control immunosuppressive or anti-inflammatory microenvironment by directly modulating of immune cells such as inhibition of activated neutrophils; strong inhibition of NKC function and proliferation, cytotoxicity and cytokine production such as PGE2 and IDO; inhibition of B-cell proliferation and activation and antibody generation, differentiation and function; inhibition of production of DCs cells from monocytes; direct inhibition of DC proliferation, maturation, differentiation, antigen-presenting capacity and pro-inflammatory function; strongly suppress $CD4^+$ T helper cells and cytotoxic $CD8^+$ T-cells' proliferation and activation, and completely repress Th1 and Th17 conversion. Whereas, Independent mechanisms of MSCs perform by mainly soluble anti-inflammatory factors secreted by MSCs (specifically MSCs type-2 cells) such as chemokines, cytokines and hormones which includes IL 1 receptor antagonist (IL1RA), IL2, IL6, macrophage colony stimulating factor (M-CSF), hepatocyte growth factor (HGF), monocyte chemotactic protein 1(MCP1), and intracellular adhesion molecule 1 indoleamine, 2,3-dioxygenase (IDO), human leukocyte antigen (HLA), CCL2, PGE2, and TGF-β. Interestingly, human MSCs use IDO whereas murine MSCs use NO to exert immunosuppressive response. IDO and NO act as a molecular switch which suppresses recognition and activation of immune response by inhibition of activation of proinflammatory monocytes & macrophage and direct activation of

regulatory cells such as Tregs. The anti-inflammatory environment is driving and converted MSCs to Type-2 cells that secret high level of chemokines, cytokines, and hormones [3, 74].

MSCs immunosuppressive capability requires activation or "licensing" and is not intrinsic. Inflammatory Microenvironment or inflammatory cytokines such as TNF-α, IL1, IL17, and IFN, activates MSCs and increase the expression of anti-inflammatory molecules and adhesion molecule present on the cell surface of MSCs. Surface adhesion molecules promote close inter-communication between MSCs and immune cells and participate and increase the impact of anti-inflammatory signals. Induced MSCs release anti-inflammatory molecules such as IDO, an enzyme that metabolizes L-tryptophan and produces L-kynurenine. Kynurenine is an inhibitor of erythropoietin and toxic for NKCs and T-cells whereas tryptophan shortage or starvation commands to cell cycle arrest in T-cells. Hence MSCs potently suppress proliferation of lymphocyte. MSCs directly (cell to cell contact) transfer inhibitory signal to immune cells, with the help of surface molecule such as Fas Ligand and programmed death ligand 1(PD-L1). Transferred inhibitory signal actively repress polarization of Th1 and TH17 [3].

Timing, kinetics of activation, ligand concentration, and type of activated TLR-signaling are some significant factors that polarized MSCs towards either Type-2 MSCs (anti-inflammatory MSCs) or Type-1 MSCs (pro-inflammatory MSCs). Bone marrow MSCs showed higher expression of TLR-3 and TLR-4. TLR-4 signaling in MSCs is also required and support proliferation and differentiation of HSCs. TLR-4 signaling polarize MSCs towards Type-1 MSCs (pro-inflammatory MSCs), whereas TLR-3 signaling polarize MSCs towards Type-2 MSCs (anti-inflammatory MSCs). In vitro study reveals that Type-1 MSCs (pro-inflammatory MSCs) are capable of releasing proinflammatory cytokines, presenting antigen, delivering chemokines for activation of inflammatory immune cells such as B-cells and T-cells. Type-2 MSCs (anti-inflammatory MSCs) discharge anti-inflammatory IL4, IDO, and PGE2 and inhibit lymphocyte proliferation and NKC function [3].

3.2.1.3 Multipotent adult progenitor cells (MAPCs) and functions

Multipotent adult progenitor cells (MAPCs), adult adherent stromal stem cells, are currently being practiced in clinical trials for acute graft versus host disease [75]. MAPCs are adult stem cells and capable for insert trophic effect and immunomodulatory properties. Also, MAPCs

are used for tissue regeneration. MAPCs are non-immunogenic, secrete angiogenic growth factors during the initial days after implantation, and could improve engraftment and survival. Chorioallantoic membrane assay study showed that human MAPCs generated significant amounts of angiogenic growth factors, including vascular endothelial growth factor, in vitro and in vivo. The existing data suggest that co-transplantation of mouse pancreatic islets with human MAPCs improve islet graft revascularization and subsequently improve islet graft function [76]. Moreover, MAPCs have immunomodulatory capabilities and the potential to improve serious autoimmune and inflammation-related diseases. MAPCs block PBMC proliferation via cell cycle arrest linked to metabolic stress in the form of tryptophan depletion. As a result, this activates GCN2 kinase, downstream signaling, and repression of cyclin D1 translation. These data explain the immune opportunity proclaimed with the administration of donor MAPCs [75]. Although new and originally isolated MAPCs exhibit robust differentiation towards neuro-dermal lineage and produce neuron-like cells [21]. However, MAPCs can differentiate into cells of all three germ layers such as mesodermal (e.g. endothelial cells, adipocytes, chondrocytes, and osteocytes), endodermal (e.g. hepatocytes), and ecto-dermal (e.g. astrocytes and neurons) [7]. MAPCs show robust endothelial expression as compared to MSCs. Human-MAPCs exhibits higher expression of CD44, CD13, CD73, and CD90 while MAPCs did not express mature hematopoietic markers such as CD34, CD45 CD56, CD105, and CD271 [21]. Rodent multipotent adult progenitor cells (MAPC) derived from bone marrow muscle, and brain shows c-Kit^{+}, CD9^{+}, CD13^{+}, CD31^{+}, and CD44^{-}, MHC-I^{-}, CD45^{-}, Thy1^{-} surface markers profile [25]. Moreover, Mouse cultured MAPC exhibit higher level of expression of stage-specific antigen (SSEA-1) and CD13, mMAPCs also express a low level of Sca-1, Thy-1and Flk-1 and also exhibit no expression of CD34, CD44, CD45, c-kit, major histocompatibility complex (MSC) class I and II [12, 77] **(Table 2)**. mMAPCs are significantly smaller than the MSCs and rodent MAPCs show resemblance with extra embryonic endoderm precursor cells and extra embryonic endoderm cells. MAPCs also show higher expression of pluripotency factors such as Oct3/4, Sox7, Sox17, Rex-1and endoderm-specific genes such as Gata4 and Gata6 [21, 77].

3.2.1.4 Bone marrow stroma cells and functions

Apart from stem cells, **endothelial cells (ECs)** are a significant part of the bone marrow (BM) microenvironment that controls the trafficking and homing of hematopoietic stem cells and

hematopoietic progenitor cells. Moreover, BM-ECs improves proliferation of hematopoietic progenitor cells by the discharge of lineage-specific cytokines [14, 78]. Endothelial cells secrete several factors like G-CSF (granulocyte colony-stimulating factor), M-CSF (macrophage colony-stimulating factor), GM-CSF (granulocyte–macrophage colony-stimulating factor), FLT3L (FMS-related tyrosine kinase 3 ligand), IL-6 (interleukin- 6) and SCF (stem cell factor or KIT ligand), which are required for in maintenance of HSCs hematopoiesis and microenvironment [79]. ECs also discharge the insulin-like growth factor binding protein, VEGF, and pleotrophin (PTN) and act as a regulator of stem cells fate [3]. Endothelial cells possess the expression of Notch l ligand and CXCL12 (CXC-chemokine ligand 12) chemokine that encourages HSCs homing and functions [14].

MSCs are the primary source of **osteoblasts** generation. Osteoblasts regulate HSCs activity and expansion by secretion of granulocyte colony-stimulating factor (G-CSF), angiopoietin and osteopontin. The bone surface lining osteoblasts termed as SNO (spindle-shaped N-cadherin$_+$ osteoblastic) cells. Osteoblast interacts with HSCs via Notch signaling, Bmp-1/Bmp-1 receptor signaling, parathyroid/ parathyroid receptor signaling and Wnt-catenin signaling and induces proliferation, migration, and quiescence of HSCs. Moreover, osteoblasts emit various factors like M- CSF, G- CSF, GM- CSF, IL- 1, IL- 6, IL- 7, and CXCL12 and express specific surface proteins, which involved in various HSCs functions, such as WNT ligands, Notch ligands, angiopoietin, thrombopoietin, N- cadherin, VCAM-1, ICAM-1, annexin II, CD44 and CD164. The scarcity of osteoblasts reduces the HSC mobilization, numbers, and functions [80-81].

Previous studies have shown condition deletion of Atr gene of osteoblasts cause hair greying, osteoporosis, alopecia (premature age-related phenotypes). Moreover, Atr mutant mice show depletion of HSCs and progenitor cells and their regenerative potential. Hence, osteoblasts also require in maintaining of bone marrow niche with aging process [16].

Adipocytes progressively replace vital hematopoietic tissues in BM with advancing age and serve as “space filler.” The abundance of adipose tissue is negatively correlated with the number of HSCs in the marrow. Previous studies showed that mice treated with peroxisome proliferator activated receptor-γ (PPAR-γ) inhibitor bisphenol A diglycidyl ether (BADGE), which inhibits adipogenesis showed accelerated bone marrow recovery after irradiation. Thus,

enhanced hematopoietic recovery after the inhibition of adipogenesis is suggesting the functions of adipocytes in hematopoietic cell regeneration [82].

Megakaryocytes (MKs) produce platelets and play as one of the crucial components of HSC niche. MKs secrete chemokine C-X-C motif ligand 4 (CXCL4) increased quiescence resulting in HSC reduction. Selective reduction of MKs starts the decline of quiescence of HSCs. CXCL4 knockout mice exhibited an enhanced propagation of HSCs. Moreover, studies identified that MKs produce thrombopoietin (TPO), crucial cytokine for HSC quiescence, mediated by the membrane protein C-type lectin-like receptor-2 (CLEC-2) signaling and regulate HSC quiescence [82]. Megakaryocytes required in the regulation of bone remodeling by secretion of RANKL, calcium-sensing receptors, NMDA-type glutamate receptors, TGF-β and TGF-β receptors, and estrogen receptors, osteonectin, osteocalcin [69].

Bone marrow macrophage is very essential niche-modulating cells in the BM. Macrophage-Fas-induced apoptosis transgenic mice, deletion of macrophages, revealed mobilization of HSCs and progenitor cells into the blood and reduction of niche factor-encoding genes. Moreover, $CD169^{+}$ macrophages support the excretion of CXCL12 from Nes-GFP^{+} stromal cells, which led to the holding of HSCs in the niche. Thus, these studies show that bone marrow macrophages associate in HSC regulation through bone marrow microenvironment [82]. Moreover, elimination of BM macrophages increases the HSCs mobilization with a reduction in expression of retention proteins. G-CSF induced the HSCs mobilization by inhibitory action the macrophage and modulates the localization of HSCs. Therefore, macrophages are participants in the modulation of HSC localization [83-85].

Dendritic cells (DCs) are colocalized with naïve B-cells and T-cells and restricted at the perisinusoidal space in BM. Elimination of DCs decreases the naive B-cells and IgM excretion, while progenitors of B-cells are not affected. DCs produce MIF (macrophage migration inhibitory factor) for residing naïve B-cells in the perisinusoidal region and factors needed for T-cells maintenance are less known [86]

Pericytes are stroma cells that communicate with other stromal cells through paracrine signaling or direct cell to cell contact. Pericytes regulate survival, stabilization, and maturation of other stromal cells such as ECs cells. Pericytes have contractile and phagocytic property.

They are associated with a neurovascular unit as an essential component and blood brain barrier. Differentiation capacity of pericytes makes them a "ubiquitous source of adult tissue stem cells." Nestin is a filamentous protein secreted by neuroepithelial neuronal precursor stem cells which are involved in HSC maintenance [3].

Non-myelinating Schwann cells support HSC quiescence by activating transforming growth factor-β (TGF-β). The sympathetic nerves coil these cells and moving along arteries and also contribute their role in cyclic release and migration of HSCs. Malfunction of nerve system leads impaired hematopoiesis. Hence autonomic nervous system acts as a "master regulator of hematopoiesis" [3]. Different types of nerves extremely electrify bone marrow and control hematopoiesis by the neural regulation. Sensitive catecholamine signals repress niche functions of Nes-GFP$^+$ stromal cells by β3 adrenaline receptor and control circadian liberation of HSCs from the BM. Sympathetic signals, provoked by granulocyte colony-stimulating factor (G-CSF), are also required in the process of HSC mobilization from the niche [82].

Nestin+ cells are mix cell population including ECs, MSCs, endothelial precursor cells, myofibroblasts. The endosteal niche includes nestin$^+$ MSC cells as an essential cell component which secretes CXCL12, a critical chemokine for HSC migration. **CXCL12$^+$ abundant reticular (CAR) cells** are identified as an essential component of the stem cell niche. Perivascular CAR cells have bi-lineage potential i.e. they can differentiate into both adipocytes and osteoblasts. CAR cells depleted (genetically engineered) mice showed a decline of HSCs. CAR cells involved in the maintenance of an undifferentiated state of HSCs, erythroid progenitor and lymphoid progenitors and retain HSCs in bone marrow [3].

Moreover, HSCs and other stem cells are also monitored by niche cells such as **adipocytes** which are a negative regulator of HSCs. **Osteoclasts** produce PGE2, **non-myelinating Schwann cells** which secret TGF, **sympathetic neurons** release CXCL12, and **BM macrophages** are a major source of PGE2 and involved in regulation of erythropoiesis [3] **(Table 1)**.

3.2.2 Soluble components of Bone marrow

Apart from a cellular component, soluble component is necessary for proper functioning of bone marrow. The soluble component includes cytokines, growth factors, hormones, calcium,

and chemokines. Stem cells and their progeny cells generate soluble factors. For instance, MSCs, ECs, osteoblasts and CAR cells secret stromal cell derived factor-1 (SDF-1, also known as CXC12), which is critical chemokines participating in HSCs maintenance and HSCs homing within HSC niche [3]. Sinusoidal endothelial cells synthesize Pleotrophin promotes HSC maintenance if added and deficiency is connected with impaired hematopoietic regeneration after myelosuppression and HSC depletion. Perivascular stromal cells express CXCL12 support HSC function. The Slit2 ligand is secreted by MSCs and other osteoblast lineage cells. Studies showed that Pleotrophin and Slit2 are essential elements of the perivascular niche [87]. Previous research showed that SDF-$1^{-/-}$ Mice's HSCs have colonization defect, and reinforced expression of SDF-1 in bone marrow vascular endothelial cells enhance colonization property of bone marrow by stem cells. Hence, bone marrow endothelial cells secreted SDF-1 is essential for hematopoietic colonization of bone marrow. SDF-1 also induce expression of VCAM-1 on ECs and very late antigen (VLA)-4 on megakaryocyte [14]. Niche cells also release SCF and TGF-β which is relevant to regulation and HSCs maintenance. TGF-β secretion is associated with osteoblastic differentiation of MSPC [3]. Previous separate studies revealed that an extract of soluble intracellular contents from whole bone marrow cells, named "Bone Marrow (BM) Soup," However, the active elements of BM Soup are unexplained. Protein arrays studies showed that BM Soup contain cytokines (IL-1ra, IL-16) and several angiogenesis-related factors (CD26, FGF, HGF, MMP-8, MMP-9, OPN, PF4, SDF-1) [88].

3.3 Interferon regulatory factors (IRFs)

Bone marrow confined in the central cavity of a bone. Bone microenvironment produced a variety of cytokines such as interferon gamma (IFN-γ), a pleotropic cytokine; perform a significant role in bone remodeling. pINF-γ injected mice revealed the disrupted cortical bone, trabecular bone, and bone marrow phenotype with an enhanced discharge of proinflammatory cytokine by bone marrow cells. Previous studies demonstrated that an increased IFN-γ synthesis in bone marrow might be enough to produce an inflammatory response [51].

Interferon (IFN) was detected as an agent that stops the replication of influenza virus. The IFN family of cytokines act as the first line of defense toward virus infection and critical components of the innate immune response [53, 89]. Moreover, interferons are connected with

many biological effects such as antiproliferative and immunomodulatory functions [90]. Three classes of IFN have been identified, named types I to III. Type I IFNs include IFN-α subtypes, IFN-β, IFN-κ, IFN-ε, IFN-ο, IFN-τ, and IFN-δ. The well-characterized function of type I IFNs is an active host response against viral infection. Type II IFN bears IFN-γ which mediates broad immune responses to pathogens other than viruses. Type III IFNs comprise IFN-λ which is known to regulate the antiviral response [89]. Type I IFNs and IFN-inducible genes are regulated by transcriptional regulators such as interferon (IFN) regulatory factors (IRFs). IRFs orchestrate and manage homeostatic mechanisms of host defense. Moreover, IRFs perform a pivotal role in the regulation of innate and adaptive immune responses. Moreover, they also involved in immune cell development, regulation of oncogenesis and metabolism [52, 58].

The mammalian IRF family of transcription factors includes nine members in humans and mice: IRF1, IRF2, IRF3, IRF4 (or PIP, or LSIRF, or ICSAT), IRF5, IRF6, IRF7, IRF8 (or ICSBP), and IRF9 (or ISGF3γ). In addition, IRF10 (absent in humans and mice) was recognized in chickens [52, 58, 90-91]. Previous studies showed that IRFs perform a very the significant involvement in many biological process such as in innate immune responses (IRF1, IRF3, IRF4, IRF5, IRF7, and IRF8) excited by pattern recognition receptors (PRRs), in the development of various immune cells (IRF1, IRF2, IRF4, and IRF8) and in the control of cell growth, cell survival, and oncogenesis (IRF1, IRF3, IRF5, and IRF8) [52, 58, 92].

3.3.1 Structure of Interferon regulatory factors (IRFs)

All IRF contains a well-conserved, ∼120 amino acids long, N-terminal DNA-binding domain (DBD). NMR spectroscopy revealed that DBD contains five conserved tryptophan residues at conserved positions, which are required for its tertiary structure, helix-turn-helix motif [52, 58, 93-94]. Helix-Turn-Helix domain identifies a DNA sequence similar to the IFN-stimulated response element (ISRE, A/GNGAAANNGAAACT) also known as IRF binding element (IRF-E) [52-53, 56, 95]. An investigation of the crystal structure of the DBD of IRF-1 bound to the PRDI of the IFN-β enhancer reported that 5`-GAAA-3` is the core recognition sequence of the helix-turn-helix motif [52, 96]. The following research of the crystal structure of the IRF-2 DBD in complex with a tandem repeat of GAAA explains that 5'-AANNGAAA- 3' is the consensus IRF recognizing sequence [52, 90].

The carboxy-terminal regions of all IRFs possess greater diversity and carry an IRF association domain (IAD). Two types of association modules, IRF associated domains 1 and 2 (IAD1 and IAD2) present in the carboxy-terminal regions of IRFs. IAD1 has Mad-homology 2 (MH2) domains of the Smad family of transcription factors like structure and conserved in all IRFs except IRF-1 and IRF-2, whereas IRF-1 and IRF-2 possess IAD2. IAD is responsible for participating in interactions with other members of the IRF family, co-factors, and other transcription factors. Thus, the carboxy-terminal region gives specificity to each IRF [52, 58, 97-98]. Moreover, the carboxyl-terminal region of IRF-1 is distinguished by the excess of acidic amino acids, while the corresponding area of IRF-2 is approximately rich in basic amino acids [53].

IRF-1 and IRF-2 were initially identified as transcription regulatory factors of the IFN-β gene. However, they have also required in the regulation of other virus or IFN inducible genes such as IFN-α and MHC Class I, respectively [90]. In addition to, a variety of cell types expresses IRF-1 at low levels or is undetectable. However, virus infection, treatment with both Type I and 11 IFN as well as other cytokines and activators such as tumor necrosis factor (TNF), interleukin-1 (IL-I), IL-6, leukemia inhibitory factor (L1F), double-stranded RNA (dsRNA; poly (rI):poly (rC)), concanavalin A (ConA), calcium ionophore and phorbol 12-myristate 13-acetate (PMA) induce its expression. In contrast, the IRF-2 is also inducible by Type I IFN and virus infection and its expression is constitutive in many cell types [90]. Previous studies showed that cDNA transfection experiments exhibited that IRF-1 activates IFN-α/β promoters and IRF-1 mRNA expression levels are dramatically up regulated upon viral infection or IFN stimulation. Unlike IRF-1, IRF-2 produced no such outcome; rather, it suppressed IRF-1-induced transcriptional activation. In addition, IRF-1 protein has a short half-life approximately 30 minis (highly unstable), whereas IRF-2 protein has a long half-life almost 8 hours (seemingly stable). These fundamental investigations were indicative that IRF-1 and IRF-2 function as a transcriptional activator and repressor, respectively, for the IFN-α/β genes. Further, previous studies revealed that IRF-1 associated with processes such as antiviral, antibacterial, autophagy, differentiation, tumor suppression, apoptosis, immune response, and cell growth and suppresses colorectal cancer cell growth and metastasis [99-102]. Apart from it repressor feature, IRF-2 functions as a transcriptional activator for vascular cell adhesion molecule-1 (VCAM-1) and cell-cycle-regulated histone H4 genes [53] **(Figure II)**.

3.3.1.1 Structure of IRF-1 protein

Co-crystallized IRF-1 (amino acids residues 1–113) with a 13-base pair (bp) DNA fragment includes the natural positive regulatory domain I (PRD I) sequence of IFN-β promoter. It exhibited that IRF-1 has three alpha helixes (α1-α3), made helix-turn-helix motif, four β-strands (β1-β4) and three loops (L1-L3) and created a sequence N-α1-β1-β2-L1-α2-L2-α3-β3-L3-β4-C. Recognition helix, α3-helix, identify DNA and situated in the DNA major groove. Amino acids, Arg 82, Cys 83, Asn 86 and Ser 87 of α3-helix make the connections (H-bond) with core major groove sequence 5`GAAA3` of the PRDI and His 40 from loop L1 negotiating the contact in the minor grove adjacent to the major groove where recognition helix is found. Three tryptophan residues out of five conserved Trp residues, Trp 11 of α1 helix, Trp 38 of an L1 loop and Trp 58 of α2 helix, build the hydrogen bonds and van der Waals bonds with sugar-phosphate back bone of DNA major groove. These three Trp residues form hydrophobic contacts with two conserved phenylalanines, Phe 55 of α2 helix and Phe 81 of α3 helix residues within the interior of the protein. These synergy bends the DNA toward the protein at an angle of ~22° and enables the intercommunication with other transcription factor and co-activator [103] **(Figure II A)**.

3.3.1.2 Structure of IRF-2 protein

IRF-1 and IRF-2 exhibit more than 76% homology between the amino acid sequences of their N-terminal 113 residues. This area identified as the DNA-binding domain (DBD). High sequence homology between their DNA-binding domains indicates that they possess almost the same three-dimensional structure. IRF-1 and IRF-2 bind particularly to AAGTGA hexamer repeat motifs, found in the transcription regulatory region of the IFN-β gene [104].

Heteronuclear multidimensional NMR spectroscopy showed that structure of IRF-2 exhibit similarities with IRF-1. Similar to IRF-1, structure elements of the DNA-binding domain of mouse interferon regulatory factor 2 (amino acids residues 1–113) showed that IRF-2 has three alpha helixes (α1-α3), made helix-turn-helix motif, four β-strands (β1-β4) and three loops (L1-L3) and created a sequence N-α1-β1-β2-L1-α2-L2-α3-β3-L3-β4-C [94, 104]. Despite the absence of possible amino acid sequence homology, it is quite similar to that of the winged helix–turn–helix (wHTH) family, which consists of proteins such as heat shock factor (HSF), catabolite gene activator protein (CAP), and ETS-1 [104].

IRF-1 identifies AAGTGA hexamer repeat motifs and displays supportive binding with other DNA-binding proteins, such as activation transcription factor-2 (ATF-2)/c-Jun, nuclear factor kB (NF-kB), and a high mobility group protein, HMG-I(Y). They make a protein complex called the enhanceosome, which activates the transcription of the IFN-β gene. While IRF-2 act as a competitor and binds to the same site as IRF-1 and suppresses the transcription of the IFN-β gene by its C-terminal repression domain. The IRF recognizing DNA sequence is also located in the regulatory regions of IFN-α and IFN-inducible genes [104].

IRF-1 is a modular transcription factor. It is assumed that IRF family of transcription factors develop by gene duplication and further diversification. According to the exon shuffling hypothesis, an evolutionary process by which new genes are created by recombinational events to form novel combinations of pre-existing exons, the IRF-1 and IRF-2 gene generation could be a candidate. Structural IRF-1 and IRF-2 are similar, but their functions are different [105-106].

Human IRF-1 gene shows high homology with mouse gene (IRF-1 and IRF-2). Gene is comprised of 9 exons. N-terminal DNA-binding domain (amino acids 1±120) covering exons 1, 2 and 3 (corresponding to amino acids 1±123), most of the NLS (amino acids 117±141) includes exon 4 (amino acids 124±138). The domain which is required for heterodimerization (between amino acids 164 and 219) comprise exons 5 and 6 (amino acids 139±224), and the acidic part of the transactivation domain (amino acids 220±256) held exon 7 (amino acids 225±242). Interestingly, the protein sequence encoded by exons 8 and 9 is not connected with any other known activity. Since deletions in this region do not affect any other activities, it shows that they do not significantly participate in the overall IRF-1 structure [105] **(Figure II B)**.

3.3.2 IRF-1 and IRF-2 pathway

Originally, it was discovered that expression of IRF mRNAs was provoked against the viral infection for the host defense [107]. Cells identify the pathogen-associated molecular patterns (PAMPs) such as viral nucleic acids, flagellin, peptidoglycan, microbial toxin, and lipopolysaccharide (LPS) through the membrane attached, or cytosolic PAMPs receptors called pattern recognition receptors (PRRs). Cells possess different types of PRRs such as Toll-like receptors (TLRs), Nod-like receptor (NLR), Retinoic acid inducible gene-I [RIG]-

like receptors (RLRs), C-type lectin receptors (CLRs) and other nucleic acid sensing receptors. They play an essential role in the expression of type I or II IFNs, chemokines and proinflammatory cytokines [52, 108].

PRRs of cells are of two types cytosolic and membrane bound [52]. The cytosolic PRRs involve the nucleotide-binding oligomerization domain (NOD) proteins, a retinoic acid inducible gene I (RIG-I) family and DNA-dependent activator of IRFs (DAI), IFN inducible double-stranded RNA (dsRNA)-dependent protein kinase (PKR) [52, 109-110]. PKR is a sensor of double stranded viral RNA and produces the type I IFNs in response to polyriboinosinic polyribocytidylic acid (poly rI:rC). NOD, RIG-1, and DAI identify the cytoplasmic bacterial PAMPs, cytoplasmic viral RNA, and pathogenic DNA, respectively [52, 110-111]. Membrane bound PRRs comprises TLRs family which include 10 and 12 types of TLRs in human and mouse, respectively and observed to identify a variety of PAMPs derived from viruses, bacteria, fungi, and protozoa to trigger immune responses such as induction of proinflammatory and type I IFN genes [52]. TLRs mediate signaling pathways are of two kinds: the MyD88-dependent pathway and MyD88-independent pathway [TRIF (Toll/IL-1 receptor domain containing adaptor inducing IFN-β)-dependent pathway] [52, 108]. Except for TLR3, all TLRs activate the MyD88-dependent pathway, while TLR3 and TLR4 start the MyD88-independent pathway. Although most TLRs directly unite with either MyD88 or TRIF upon PAMP stimuli, TLR4 needs the extra adaptors TIRAP and TRAM for the recruitment of MyD88 and TRIF, respectively [52, 58]. Both MyD88-dependent pathway and MyD88-independent pathway start activation of at least three major downstream molecules: IRFs, NF-κB, and mitogen-activated protein kinases (MAPKs). These factors provoke the expression of IFNs, chemokines or proinflammatory cytokines [112-115]. The myd88-dependent pathway starts with the recruitment of IL-1 receptor-associated kinases 1/4 (IRAK1/4) by the MyD88 and then TRAF6 and transforming growth factor (TGF)-β-activated kinase 1 (TAK1). TAK1 initiates the activation of NF-κB and MAPKs through the phosphorylation of IKKβ and MAPK kinase 6 (MKK6), respectively [52]. IFN-α/β and IFN-γ stimulate or inactivate the family of the transcription factors, IRFs (including IRF-1 and IRF-2) and STAT through IFNAR and IFNGR receptors. IFNR1 and IFNR2 activate the Tyk2 and Jak1 protein tyrosine kinases (PTKs) upon ligand binding. Activated PTKs phosphorylate the STAT1 and STAT2 which linked with IRF-9 to make a heterotrimeric transcription factor

complex, ISGF3 (IFN-stimulated gamma factor 3). ISGF3 translocate to the nucleus and activate the IFN-stimulated genes [56, 116-119]. Phosphorylated STAT1 undergoes homodimerization and produce IFN-γ activated factor/IFN-α activated factor (GAF/AAF), which attaches to the IFN-γ activated sequence (GAS) on the promoter of the target gene [53, 56, 116, 120]. Binding of the dimeric structure of IFN-γ to the IFNGR1 favor the participation of the IFNGR2 and stimulates PTKs Jak1 and Jak2. Activated Jak1 and Jak1 phosphorylate the STAT1 or STAT2. Phosphorylated STAT1 dimerize and make the complex STAT1-p48 with IRF-9 [116-118, 121]. Normal cells express IRF-1 at a low level, and viral infection, LPS, IFNs, TNF-α, IL-1, IL-6, and LIF provokes its expression through STATs and NF-κB [53, 122-124]. MyD88 signaling pathway for IRF-1 activation involves direct interaction of IRF-1 with MyD88. Full activation of IRF-1 by type II IFN (IFN-γ) required TLR9 engagement which causes MyD88-associated IRF-1 to undergo post-translational modifications and move into the nucleus more efficiently compared to non-MyD88-associated IRF-1. Activated IRF-1 associates with other transcription factors and promote the expression IFNs, iNOS, IL-12p35, p21 and surface adhesion molecules [52, 125].

3.3.3 Functions or Roles of IRF-1 and IRF-2 in bone marrow derived immune cells

The family of IRFs transcription factors was initially recognized in the connection of the type I interferon system in host defense. Their roles are extended further in immune cell development, immune responses and regulation of oncogenesis. Various studies confirmed the role of IRF-l and IRF-2 in bone marrow cells differentiation and development [52-53] **(Table 3 and 4)**.

3.3.3.1 IRF-1 and IRF-2 in development of dendritic cells (DCs)

DCs are equipped antigen-presenting cells (APCs) that are essential in initiating innate and adaptive immune responses. Importantly, mouse splenic DCs are a heterogeneous population of multiple subtypes $CD4^+$ DCs, $CD8\alpha^+$ DCs, $CD4^-CD8\alpha^-$ (double negative, DN) DCs, and pDCs with diverse functions. DCs smell the attacking pathogens through PRRs and upregulating the expression of major histocompatibility complex (MHC) II and costimulatory molecules on their cell surface and secrete cytokines. DCs processed the antigenic microbial products at the time of the DANGER and fixed on the surface and display antigenic peptides on MHC molecules to T cells, thereby exciting Th1 and Th2 responses [52, 58, 126-129].

IRF-1$^{-/-}$ mice exhibit a constant increment in pDC and drop in CD8α^{+} DC numbers. *IRF-1*$^{-/-}$ DCs show defective in IL-12p40 production and express higher levels of IL-10, TGF-β, and the tolerogenic enzyme IDO. As a result, *IRF-1*$^{-/-}$ DCs fail to mature fully. They are also incapable of inducing an IL-10-mediated suppressive activity in allogeneic CD4^{+}CD25^{+} regulatory T cells and stimulating the proliferation of allogeneic T cells. These studies suggest a novel role of IRF-1 in regulating the tolerogenic characteristics of DCs and critically involved in the regulation of DC development and function. In contrast, *IRF-2*$^{-/-}$ mice show abnormally augmented type I IFN signaling and a selective loss of splenic and epidermal CD4^{+}CD8α^{-} DCs. Interestingly, type I IFNs cytokines attenuate differentiation during the early stages of DC development if added and promote the late stage differentiation or maturation of DCs [52, 58, 130] **(Figure III A)**.

3.3.3.2 IRF-1 and IRF-2 in development of Natural Killer (NK) cells

NK cells are cytotoxic lymphocyte which mediates the first line of defense in innate immune response toward microbial pathogens or tumor growth. NK cell-mediated cytotoxicity is MHC unrestricted and does not expect prior sensitization to the pathogen [131-132]. Initially, it was discovered that *IRF-1*$^{-/-}$ mice failed to produce IL-12, a cytokine critical for NK cells and T helper (Th cells) and incapable of eliminating syngeneic, MHC class I negative tumor cells in vivo. IL-12 is beneficial for stimulation of NK cells, which produce IFN-γ and provoking T helper (Th) 1-type immune response. Several studies have shown that *IRF-1*$^{-/-}$ spleen and liver cells were failed to provide NK cell–mediated cytolytic activity, and consistently, the number of NK (NK1.1^{+}TCRα/β^{-}) cells was dramatically reduced in both spleen and liver. Also, *IRF-1*$^{-/-}$ mice also show degeneration the numbers of NK-T (NK1.1^{+}TCRα/β^{+}) cells and γδT cells. These conclusions indicate that NK cell development is damaged in *IRF-1*$^{-/-}$ mice. Transplanted *IRF-1*$^{-/-}$ bone marrow (BM) cells of irradiated mice can produce mature, functional NK cells in vitro, when cultured with IL-15, indicating that the IL-15 gene is transcriptionally controlled by IRF-1[52-53, 58].

Recently, *IRF-2*$^{-/-}$ mice were shown to carry defects in NK cell function and development and selectively lack mature CD11bhigh Dx5high NK cells. Furthermore, *IRF-2*$^{-/-}$ mice were shown dramatically decreased the number of NK cells (NK1.1^{+}TCRα/β^{-}). In contrast to *IRF-*

1$^{-/-}$ BM cells, the number of NK-T cells was normal in *IRF-2*$^{-/-}$ mice and *IRF-2*$^{-/-}$ BM cells were incapable of generating NK cells when cultured with IL-15 [52-53, 58] **(Figure III B)**.

3.3.3.3 IRF-1 and IRF-2 in macrophage function

Macrophages are phagocytic cells that participate in the elimination of cell debris after cell death and antigen presentation of immune cells to stimulate the adaptive immune response. IRF-1 is required for differentiation and activation of macrophage. Phorbol 12-myristate 13-acetate (PMA) provokes the monocyte/macrophage differentiation of human monoblastic U937 cells by the upregulation of IRF-1 [133].

IFN-β and lipopolysaccharide (LPS) treated WT macrophages induce the inducible nitric oxide synthetase (iNOS) gene, which encoded the enzyme nitric oxide synthetase, which is the producers of nitric oxide (NO), a short-lived volatile gas. NO performs a significant function in the effectors phase of Th1 immune response; i.e., macrophage cytotoxicity against bacteria, tumor cells, and other targets. Moreover, neutrophils and macrophages perform an important role in restricting Listeria monocytogenes infection in the early phase of primary infection in mice [53, 102].

Previous studies showed that *IRF-1*$^{-/-}$ macrophages were inadequate to induce the inducible nitric oxide synthetase (iNOS) gene. Mycobacterium bovis infected *IRF-1*$^{-/-}$ mice produce severe symptoms matching military cutaneous tuberculosis. In addition, IRF-1 has also required for the induction of the gene encoding the p40 subunit of IL-12, the cytokine crucial for Th1- type differentiation of the immune system [53, 134]. Various studies explained that IRF-1 expression is upregulated during myeloid differentiation. *IRF-1*$^{-/-}$ bone marrow cells exhibit decreased colony-forming ability (both G-CSF and M-CSF) and an increased number of immature granulocytic precursors, proposing a defective maturation process. Moreover, IRF-1, an IFN-inducible transcriptional activator for the ISRE-containing genes, targets many genes, including GBP, iNOS, Caspase-1, Cox-2, CIITA, and gp91phox in IFN-stimulated Macrophages. Moreover, in IFN- γ-stimulated cells, IRF-1 induces a subset of genes such as those encoding IL-12p40, IL-12p35, iNOS, IL-18, and IFN-β by the TLR-MyD88 pathway [52].

IRF-2$^{-/-}$ mice are extremely susceptible to Listeria infection. Consequently, IRF-2 is significant for IFN-γ mediated protection against Listeria, which induces the production of reactive oxygen intermediates (ROIs) and probably others in macrophages [53, 135]. *IRF-2*$^{-/-}$ mice exhibit a development of basophils, resulting in an increase in IL-4 production. *IRF-2*$^{-/-}$ mice show abnormalities of Th2 polarization. An in vitro ectopic expression study indicates that IRF-2 inhibits granulocyte differentiation and trigger differentiation of megakaryocytes. *IRF-2*$^{-/-}$ Macrophages treated with a fungal metabolite gliotoxin, or IFN-γ plus LPS found to be diminished induction of genes encoding IL-12p40 and Cox-2 and enhanced expression of the gene encoding Caspase-1, which is sufficient for the accelerated apoptosis [52]. IRF-1 and IRF-2 are confirmed to control IFN-γ dependent Cyclooxygenase (Cox)-2 expressions, which are upregulated by proinflammatory agents, starting many prostanoid mediated pathological conditions of inflammation [53] **(Figure IV A)**.

3.3.3.4 IRF-1 and IRF-2 in development of T-cells

Previous studies showed that *IRF-1*$^{-/-}$ mice exhibit a sharp decline (10 fold) of mature $CD4^{-}CD8^{+}$ T cells in spleen, lymph node peripheral lymphoid organs and the thymus, while immature T cells (i.e., double-positive $TCR\alpha\beta^{+}CD4^{+}CD8^{+}$) were capable of developing into mature $CD4^{+}$ [136]. These results indicate IRF-1 is essential in a lineage-specific thymocyte development (hematopoietic progenitor cells located in the thymus, differentiate into mature T lymphocytes) in between double-positive and single-positive stage [137]. Further studies revealed that *IRF-1*$^{-/-}$ H-Y and *IRF-1*$^{-/-}$ P14 transgenic mice show impaired positive and negative T cell selection, suggesting IRF-1 control the positive and negative selection of $CD8^{+}$ thymocytes. Also, *IRF-1*$^{-/-}$ thymocytes and thymic stromal cells display low expression of LMP2, TAP1, and MHC class I on the cell surface, indicating the deficiency of $CD8^{+}$T cell maturation does not remain in the thymic environment. Moreover, in vivo bone marrow chimeras and in vitro reaggregation cultures studies revealed *IRF-1*$^{-/-}$ stromal cells fully support the development of $CD8^{+}$ thymocytes [136].

Moreover, *IRF-1*$^{-/-}$ thymocytes displayed impaired induction of negative selection in TCR, and TCR-mediated signal transduction and *IRF-1*$^{-/-}$ mice thymocytes expected a 1000-fold higher level of the selecting peptide compared to control mice. Thus, IRF-1 manages the expression of the gene(s) in developing thymocytes, which is needed for selection and lineage

commitment of $CD8^+$ thymocytes. *IRF-1*$^{-/-}$ mice $CD8^+$ T cells possess cytotoxic effector functions, showed significant reduction of cytotoxic T lymphocyte (CTL) response against LCMV (lymphocytic choriomeningitis virus)-infected target cells, while $CD8^+$ T cells of *IRF-2*$^{-/-}$ mice showed normal CTL activity to LCMV-infected target cells. These outcomes collectively announce that IRF-1, IRF-2, contribute to the induction of CTL activity[137]. *IRF-1*$^{-/-}$ mice $CD8^+$ T cells, containing Bcl2 transgene driven by the Eμ or lck promoter, exhibit recovers the development of $CD8^+$ T cells but not NK, NKT, or $TCR\gamma\delta^+$ cells. This study was suggesting that IRF-1 is required for survival signals involving Bcl2 to support $CD8^+$ T cell development [52-53, 58, 138].

Recently, the $CD8^+$ T cell abnormality in naive *IRF-2*$^{-/-}$ mice exhibit an inflammatory skin disease resembling psoriasis which involves pathogenic association of $CD8^+$ and upregulation of the expression of genes induced by IFN-α/β. Furthermore, both infection development and $CD8^+$ T cell abnormality are control by the introduction of genes product that positively regulates the IFN-α/β signaling pathway. Thus, IRF-2 acts as a novel negative regulator. In addition, IRF-2 attenuates type I IFN induced gene transcription, which is essential for balancing harmful and the beneficial effects of IFN-α/β signaling within the immune system. These studies confirmed a new link between the IFN-α/β system and the $CD8^+$ T cell-mediated adaptive immune system [52-53, 58, 137, 139] **(Figure IV B)**.

3.3.3.5 IRF-1 and IRF-2 function in regulation of Th1/Th2 differentiation

IRF-1 absence leads to the induction of Th2-type immune response, while it is essential required for the development of Th1-type immune response. IRF-1 controls Th1 immune response by regulating the generation of IL-12 by macrophages and development of IFN-γ producing NK cells and DCs [140]. The undifferentiated $CD4^+$ T cells of *IRF-1*$^{-/-}$ mice fail to appropriately counter to wild type antigen-producing cells to differentiate into Th1 cells. Further studies revealed that Stat4 interfere in IL-12-induced upregulation of IRF-1 in Th1 cells but not in Th2 cells, which binds to the GAS sequence in the promoter area of the IRF-1 gene. IRF-1 deficiency also impairs the response of $CD4^+$ T cells to IL-12 [53, 141]. IFN-γ supports Th1 cells development by producing the expression of cytokine IL-12 and receptor IL-12. However, IFN-γ attenuates the development of Th2 cells by repressing the IL-4 expression by the coupling of IRF-1 and IRF-2 at IL-4 gene promoter [142].

IRF-2 was first reported as an opponent of the IRF-1-mediated transcriptional regulation of IFN-inducible genes. As *IRF-1*$^{-/-}$ mice exhibit impaired Th1 cell development and NK cell development, it was speculated that *IRF-2*$^{-/-}$ mice might prove different phenotypes. However, *IRF-2*$^{-/-}$ mice are defected in Th1 cell differentiation and confirm sensitivity to Leishmania major infection; and *IRF-2*$^{-/-}$ macrophages exhibit suppression of IL-12 production. Consequently, IRF-2 may offer to IL-12 gene expression in combination with other factors, instead of performing as a negative regulator [53, 58].

The new emerging subset of $CD4^+$ T-cells is TH-17. $CD4^+$ T-cells differentiate into TH-17 cells in response to TGF-β and IL-6. IL-23 is expected for population development and maintenance of TH-17 cells [143] **(Figure IV B)**.

3.3.4 Role of IRF-1 and IRF-2 in diseases

Clinical studies have also registered that the loss of IRF-1 is associated with the development of life-threatening disease such as human leukemia. Leukemia or preleukemic myelodysplastic syndrome (MDS) patients showed cytogenetic abnormalities including deletion of region 5q31.1 (IRF-1 gene region) of the chromosome. Thus, the failure of the IRF-1 function is very crucial in the development of human leukemias. In addition to, several reports have indicated that esophageal and gastric cancers showed frequent loss of an IRF-1 allele, which is also associated with hematopoietic malignancies. Two alternative mechanisms that point to the loss-of-function of IRF-1 were published. Splicing aberrations in the IRF-1 gene also consider for the loss of IRF-1 expression. Other studies proposed that Nucleophosmin (NPM), a putative ribosome assembly factor often over expressed in leukemic cells, adheres to IRF-1 and inhibits its functions [52-53]. In contrast to IRF-1, IRF-2 acts as a transcriptional attenuator. In NIH3T3 cells, the overexpression of IRF-2 generates oncogenic transformation, while concomitant constitutive expression of IRF-1 induces these cells to return to the non-transformed phenotype. Moreover, IRF-2 stimulates gene(s) involved in oncogenesis, such as Histone 4. These investigations indicate IRF-1 and IRF-2 play a very crucial role in various cancers [52-53, 98].

3.4 Connection between IRF-1 and IRF-2 and pluripotent associated transcription factors

Interferon (IFN) was initially detected as an agent that stops the replication of influenza virus. Three classes of IFN have been identified, named types I to III. Type I IFNs, include IFN-α, IFN-β, and others play a crucial role in an active host response against viral infection. Type II IFN bears IFN-γ, is associated with broad immune responses to pathogens other than viruses. Type III IFNs comprise IFN-λ which is known to regulate the antiviral response [89].

Previous studies showed that IRF-1 gene expression is induced by IFN-α/β and IFN-γ and by other cytokines [140]. Type III IFN uses a receptor complex different from that of type I IFN. However, both types of IFN provoke STAT1, STAT2, and STAT3 activation. In vitro as well as in vivo examinations exhibited that type I IFN functionally matches type III, IFN-λ, inducing antiviral protection. Activated IFN-λ receptor drives to the phosphorylation of STAT1, STAT2, and STAT3 and the construct the interferon-stimulated gene factor 3 (ISGF3) transcription factor, resulting in induction of typical IFN-induced genes. Previous research showed that IRF2 induction was also at the borderline of detection with this cell line, whereas both IFN-α and IFN-λ induce the IRF1 gene in Hep2G cells. It has been determined that IFN-α-dependent STAT3 and IRF1 derive a weak recruitment to the ISG56 promoter. IFN-α and IFN-λ stimulation resulted in a reduced ISG56 promoter occupation of IRF2 [144].

ESC pluripotency is associated with the activation of Janus kinase/signal transducer and activator of transcription 3 (Jak/Stat3) signal pathway. Previous research showed that activated Stat3 is crucial in MEFs during reprogramming for installation of the pluripotency. Leukemia inhibitory factor (LIF) activate Jak/Stat3 signal pathway. Artificially activated Stat3 maintains ESC self-renewal in the deficiency of LIF. It has been confirmed that LIF/Stat3 up regulates Klf4 and Myc expression in mouse ESCs. Moreover, inhibiting Jak/Stat3 activity prevents demethylation of Oct3/4 and Nanog regulatory elements in induced cells, which are characterized by suppressed endogenous pluripotent gene expression. Thus Jak/Stat3 activity represents a fundamental role in supporting pluripotency establishment at the epigenetic level, by promoting open-chromatin formation during late-stage reprogramming, DNA demethylation/de novo methylation [145].

Thus these studies confirm that both interferon regulatory factors (IRF-1 and IRF-2) and pluripotency associated factors (such as Oct3/4, Sox-2, Nanog, KLF, and cMyc) are linked with each other by Stat3. In addition, IRF-1 and Oct3/4 are also interlinked by Sumo-1 **(Figure V)**.

3.5 Alteration or Damage of Bone marrow

Bone marrow is extremely unsafe to cytotoxicity caused by environmental factors, certain chemotherapeutic agents, accidental or deliberate exposure to a moderate or high dose of total body irradiation (TBI) resulting bone marrow (BM) suppression, and aging [42].

3.6 Alteration or damage of bone marrow due to radiation

Previous studies results showed that radiation induces cytogenetic damage, transformation, chromosome aberrations and decline cell survival rate [146]. Ionizing radiation produces reactive species of oxygen (ROS), nitrogen (RNS), and free radicals in biological systems which damage the vital cellular DNA and membranes, depletion of stem cells, depletion of antioxidants, altered cell division, organ system dysfunction, resulting in cell death and finally death of the organism [147]. The microenvironment in the bone marrow includes stromal cells containing osteoclasts and osteoblasts for stem cell self-renewal and differentiation. These cells were diluted after irradiation [43]. It is well documented that ionizing radiation is one of the first causes of unrepaired genotoxic damage, stem cell pool depletion, impairing lineage functionality, cell death and accelerating aging, resulting in hematopoietic syndrome, one of the most dangerous radiation effects [44] Moreover, ionizing radiation induces a decline in the bone marrow cellularity and hematopoietic dysfunction, resulting in higher risk of bone marrow failure [45]. The previous literature revealed that total body irradiation provoked a quantitative and qualitative reduction of HSCs. In addition, long-term effects of radiation exposure initiate senescence and impairment of HSC self-renewal via activation pathways including p16/Rb and p53/p21. Radiation exposure also accelerates HSC aging, increasing spontaneous mutation, phenotypic changes, impaired reconstitution, increased apoptosis and accumulated DNA damage [44]. Previous studies revealed that exposure to total body irradiation (TBI) induces long-term or residual bone marrow (BM) injury which includes decreased long-term repopulating capacity, permanent damage to hematopoietic stem cells (HSCs), myeloid skewing, and impaired self-renewal. These HSC injuries were related to

significant increases in a generation of reactive oxygen species (ROS) due to radiation [46]. In addition to HSCs experience senescence after radiation which is linked to a defect in self-renewal of HSCs and decline of HSCs frequencies qualitatively and quantitatively [47]. Other investigations revealed that a most of the hematopoietic cells of bone marrow died by apoptosis after exposure to IR in vitro and those survived after IR damage failed their clonogenic function and showed an enhanced SA-β-gal activity, a biomarker for senescent cells [42, 47-48].

3.7 Alteration or Damage of Bone marrow due to aging (with time)

3.7.1 Aging

People are trying to defeat the aging since the millennium to achieve immortality and gave different theory or hypothesis for aging. Critical and bone marrow associated explanation for aging are **(Figure VII)**

3.7.1.1 Alteration of bone marrow/stem cells and axis or theory of aging

3.7.1.1.1 Stem cell theory of aging

Millions of cells from bone marrow, gut and skin tissues are removed after completing their biological job or lifespan. For example, 100-120 days erythrocytes (lifespan of erythrocyte) are eliminated from blood tissue after finishing lifespan. The lifespan of tissues depends on the replacement of these removed cells and supply of new ones. Tissue-specific stem cells sustain the supply and replacement of these cells throughout the life. For instance, a pool of hematopoietic stem cells (HSCs) in the bone marrow produces millions of new erythrocyte per second to maintain the homeostate between lost erythrocyte and new erythrocytes for a lifetime. That is why; the rate of the aging process of tissue depends upon tissue-specific stem cells [148]. Moreover, these tissue-specific stem cells maintain the homeostate in the tissue by differentiation of tissue-specific stem cells to produce required cell type and producing more stem cells in the tissue to sustain and repair the tissues; protect tissue or organ failure and struggle with the aging process. However, tissue homeostate is not constant during the age because of the functional inability of tissue-specific stem cells [149-150], increasing number of progenitor cells, side population (SP) HSCs and adipocytes instead of stem cells of age [149] **(Figure VIII)**.

3.7.1.1.2 Gene Expression Changes

During age, genes that are regulated by age include genes which mostly involve in differentiation. For instance, lymphoid lineage-specific genes were deactivating whereas myeloid lineage-specific genes, megakaryocyte-associated genes and many protoncogenes were found to be more activated with aging. As a result, the risk of age-associated lineages specific diseases increases such as myelodysplastic syndrome, myeloproliferative disorders, or leukemia, myeloid leukemia [16, 61, 150] **(Figure IX)**. Moreover, microarray study found that aging process activates inflammatory response genes & stress genes and deactivate some genes including DNA repairing, chromatin remodeling regulatory genes, and genomic integrity genes. Inflammatory response genes product lead to creating an inflammatory microenvironment within aging bone marrow and down-regulate some genes such as P-selecting gene. P-selecting genes encode adhesion protein that showed crucial involvement in the mobilization and engraftment. Thus, mobilization and engraftment potential of stem cells reduce within aging bone marrow. Thus, epigenetic irregularities of genes can dysregulate the transcriptional activity across the genome and leads to abnormal cellular function. As a result, functional defects of stem cells increases and decline the regenerative capability of stem cells. These findings explore, numerous and diverse changes at the molecular, cellular, tissue-level and organism levels, and it also explains why we feel inflammation in our tissues or body during aging and why we face a high risk of diseases at age [149-150]. Up-regulated inflammatory response genes, loss of DNA repairing gene, chromatin remodeling regulatory genes, and genomic integrity genes cause functional defects of stem cells, diminish the age-dependent stem cells, and reduce self-renewal ability and regenerative capability of stem cells. Hence gene expression changes explain decline bone marrow potential of aging bone marrow.

3.7.1.1.3 Epigenetic mechanisms

The previous report revealed that Epigenetic mechanisms linked with aging processes. Epigenetic modification such as DNA methylation is involved in many biological activities including gene imprinting, regulation of chromatin structure and genomic instability. Global DNA methylation declines slowly and increases at promoter region during aging. Previous studies exposed that 5-methylcytosine (5mC) and 5-hydroxymethylcytosine (5hmC); both epigenetic marks coexist in the genome. 5mC is a stable DNA modification but an epigenetic regulatory enzyme such as Ten-eleven Translocation (TET) family of protein enzymatically

oxidizes 5mC to 5hmC, and then thymine-DNA glycosylase (Tdg) produce unmethylated cytosine [151]. Previous researchers have shown that catalytic activity of TET-2 is required for maintenance of HSC progenitor development. In addition, mouse model study showed that somatic mutation in Ten-eleven Translocation-2 (TET-2) of HSCs generates atherosclerosis [152]. Hence, hydroxymethylation of 5mC is associated with silencing effect of 5mC and potential involvement in demethylation. Moreover, DNA methyltransferase-1 (DNMT1) has a lower affinity for 5hmC and unable to maintain the methyl transfer to DNA during cell division [151] **(Figure X)**.

Genome-wide research revealed that regulatory regions in embryonic stem cells and differentiated cells, gene bodies and promoter showed high enrichment of 5-hydroxymethylcytosine (5hmC). During age, depletion of 5mC and gaining of the 5hmC level exhibit an age-associated change in MSCs. Aged-Bone marrow derived mesenchymal stem cells acquire global loss of DNA methylation. Thus, 5hmC associated DNA demethylation has a crucial role in aging. Furthermore, 5hmCCpG sites occur in chromatin region marked by H3K4me1, are associated with poised enhancers in MSCs whereas 5hmC related to active enhancers marked by H3K4me1 and H3K27ac in differentiated and embryonic stem cells. Interestingly, “stemness” of stem cells is associated with a change of 5hmC at H3K4me1, H3K27me3 and H3k29me3 regions of chromatin. Hence, low-density CpG region, intron, enhancer, cell adhesion and morphogenesis-related genes showed the higher level of 5hmC whereas embryonic stem cells and differentiation related gene express a small degree of 5hmC. Moreover, proliferation and development associated related genes showed increased level of 5hmC in mice brain, in combination with decreased level of 5mC during aging. Deregulation of 5hmC involved in various diseases such as degenerative diseases and cancer [151].

3.7.1.1.4 ROS affect HSC aging

Aging of stem cells also depends on intracellular oxidative stress. This stress comes from reactive oxygen species (ROS) level within the cell which causes DNA damage and decline self-renewal capacity of stem cells. Impaired mitochondrial function and ATP generation in the cells elevate the level of intracellular ROS. Mitochondrial function, turnover, and biogenesis are associated with transcription factors such as FOXO transcription factors and

Bmi1 which regulate the level of intracellular ROS [153]. The higher level of ROS activate MAP kinase (MAPK) which in turn activates Cdk inhibitors which block HSC division required for self-renewal, and Atm expression participated in DNA damage and genomic stability. On the basis of intracellular ROS level, HSCs can be divided into two subtypes. ROShigh HSCs which loses self-renewal ability due to activation of Cdk (cyclin dependent kinase) inhibitors and differentiation capability because of damage DNA and ROSlow HSCs contain both, higher self-renewal potential and repopulating ability. Hence, intracellular ROS levels regulate HSCs activation, differentiation, proliferation, function, and homeostasis as well as aging of stem cells and hence raising the aging process [150] **(Figure XI)**.

3.7.1.1.5 Metabolic pathways in aging

The extreme consequences of aging are tissue failure, unable to regeneration processes, diseases and lastly death. In recent year, advance medical science, nutrition, and education have increased health span and lifespan, but we have many quotations since millennia such as what are principle rule of aging, can aging be prevented, how we can increase lifespan further.

The first breakthrough came in 1990; worm having mutated daf-2 gene which encodes insulin/insulin-like growth factor 1 (IGF1) like receptor, showed double the lifespan [153]. After that, various metabolic pathways are being searching which derives aging process. For instance, Ames mice having a low level of IGF1 pathways showed longevity. Decrease insulin, and IGF1 signaling (IIS) activates FOXO transcription factors, which activate the catalase and antioxidant such as manganese superoxide dismutase (MnSOD). Moreover, FOXO transcription factors also improved mitochondrial biogenesis and function by activation of PPARγ coactivator 1α (PGC1α). FOXO also inhibit the activity of p53, which involved in other longevity pathways, such as mTOR and AMPK [153]. Previous studied showed that FOXO deficient mice had shown lymphoid development abnormalities, myeloid lineage expansion, and higher ROS level in HSCs compared to normal mice HSCs of bone marrow. Moreover, FOXO deficient bone marrow showed defective long-term repopulating activity, cell cycle arrest by regulation of downstream targets such as p27, p21, and cyclin protein of cell cycle, increased apoptosis and depletion of HSCs. Hence, the association of evolutionary conserved metabolic pathways (insulin/insulin-like growth factor 1 (IGF1) like receptor→PI3K-AKT→FOXOs), stem cells depletion, and imbalance HSCs homeostate in

bone marrow indicate that it plays a significant function in the restriction of aging [154-155]. Moreover, the complex metabolic system in mammal reduces the role of insulin/insulin-like growth factor 1 (IGF1) in aging. However, genetic and metabolic studies show the conserved IIS pathway has a crucial role in human aging [156] **(Figure XI)**.

3.7.1.1.6 Telomeres and aging

Culture study of human fibroblasts emerges the role of telomeres linked to the aging process. Telomere, a repetitive TTAGGG sequence, acts as a cap and protect chromosome from the damage [153]. A telomere is a highly conserved sequence from primitive organism to humans [157]. Telomerase maintains elongation of telomeres and prevents senescence, a nondividing state, in fibroblast. However, lack an adequate level of telomerase resulting the loss or shorter the telomeres with each round of DNA replication which push the fibroblast cells to enter in senescence state [153]. It is thought that the rate of telomere shortening is approximately 20pb per year, which is more gradual and continuous rate [158]. The loss of telomeres activates p53 via DNA damage pathway. p53, further, induce apoptosis, growth arrest, and senescence in stem cells. Thus the loss of telomeres acts as the molecular clock of stem cells during the aging process. Previous studies have shown telomere shortening is strictly associated with age-related diseases. Moreover, a patient with dyskeratosis congenital having shorter telomeres, a premature aging syndrome, contains a mutation in TERC (the RNA component of telomerase) and TERT (the catalytic component of telomerase). Furthermore, functional loss of TERC and TERT is associated with several diseases such as bone marrow failure syndrome. Hence, telomeres dysfunction decline tissue's function and organ failure particularly highly proliferative organ such as bone marrow, promote short lifespan and aging. Thus, these studies speculate that telomere-based aging is primarily a bone marrow stem cells defect caused by increased p53 activity, induction of growth arrest, senescence and high level of apoptosis of stem and progenitor cells in the bone marrow [153].

Furthermore, inhibition of p53 by metabolic pathways, mild DNA damage and lower level of p53 activation allow repair and maintenance of cellular function resulting decline aging process, whereas excessive DNA damage and p53 activation lead p53 dependent cellular senescence and apoptosis which accelerate aging. However, how players of aging such as mitochondria, p53 increase, and decrease lifespan remain to be clear [153].

3.7.2 Bone marrow and aging

Aging is a universal process. All cells, tissues, organs, and organisms undergo changes with age. Age-related bone marrow alterations include deterioration bone marrow cellularity, fat cells deposition, and decrease hematopoietic tissue. Thus, age-related changes in bone marrow reflected by a higher risk of myeloproliferative disorder, anemia and decline immunity. With age, fat infiltration reduces space occupied by hematopoietic tissue from 90% (at birth) to 30% (at age 70). Diminished volume of hematopoietic tissue in bone marrow produces small native lymphocytes which decline the adaptive immunity with age [159]. Accumulated bone marrow fat (BMF), different from subcutaneous or visceral tissues fat, secrete adipokines such as leptin and adiponectin. Higher accumulation of BMF leads osteoporosis and weak bone mass during aging [160] **(Figure VI)**.

Furthermore, HSCs also showed several age-related changes including skewed X-chromosome inactivation, telomere shortening, accumulation of mitochondrial DNA mutations and micronuclei formation. These age-related variations cause HSCs dysfunction and inactive hematopoiesis. Impaired hematopoiesis decline production of Red Blood Cells (RBCs) with advancing age which causes Anemia, a significant health problem in the elderly. However, mechanism of age-related expansion of bone marrow fat and reduction of hematopoietic tissue (decline cellularity) remains to explore [159]. Moreover, previous reports disclose that old rat treated with growth hormone explains decline fat deposition within the bone marrow and increase hematopoietic tissue. Hence decrease growth hormone production with age, dysregulation of insulin growth factor signaling, and changes in the composition of the extracellular matrix also play a significant role in fat accumulation within the bone marrow [16, 159].

Almost all niches cells including accessory cells such as blood lineage and stem cells such as MSCs and HSCs undergo change with age. However, the exact mechanism is still unclear. Published research explained transplantation of young BMCs into old recipient mice, show reduces B cell generation, and transplantation of old BMCs into young recipient mice show a decline of peripheral B lymphocytes. Further decrease homing efficiencies of engagements (BMCsyoung to old mice, BMCs old to young mice) and generation potential toward myeloid lineage have been shown in both situations [150]. Previous studies indicate Aged-HSCs

showed higher CD150 expression which favors the expansion of myeloid-biased HSCs, resulting myeloid-biased HSCs fraction dominate the entire aged-HSCs pool in the bone marrow niche with the aging process. Age-associated myeloid bias could be due to cell-intrinsic modifications which turn lymphoid-biased HSC clones into myeloid-biased HSC clones within the aged-HSC pool in the bone marrow, i.e. clonal evolution, or clonal selection/expansion, in which myeloid-biased HSC clone expand more and dominate the entire aged HSCs pool i.e. clonal shift. Moreover, myeloid-biased HSCs showed higher self-renewal potential and long-term repopulating capacity than lymphoid-biased HSCs. Additionally, myeloid-biased HSC clone expansion reduces occupied space of lymphoid-biased HSC clone, resulting in a decrease the number of lymphoid progenitor cells and lymphopoiesis. Thus, aging process favors the expansion of homogeneous population (myeloid population) and reduces heterogeneity (lymphoid and myeloid cells population) of the bone marrow niche [16, 150]. The decrease in lymphopoiesis leads several blood diseases such as anemia.

3.7.3 Bone marrow cells and aging

3.7.3.1 Hematopoietic stem cells (HSCs) and aging

Hematopoiesis is a process in which hematopoietic stem cells and hematopoietic progenitor cells generate all mature cells that form the whole blood and immune system throughout the lifespan [161]. Hematopoiesis confined to proximal ends of long bones such as femora and humeri. Hematopoietic cellularity of marrow reduces with advancing age compared to young adults. However, peripheral blood count does not show alteration significantly with aging process [16, 158]. During age, HSCs receive phenotypic and functional abnormalities including altered homing efficiency, mobilization properties, repopulating ability. These changes in aging HSC are due to aberrant chromatin modification, down-regulated DNA repair mechanism, protein misfolding, higher inflammatory and stress response. Moreover, an increased level of reactive oxygen species (ROS) inserts more DNA damage in aged-HSCs of bone marrow. It was shown aged-HSCs dysregulates DNA methylation of differentiating genes controlling myeloid and lymphoid balance, impaired histone modification, disturbed cell polarity and activate mammalian target of rapamycin (mTOR) [16]. Also, HSCs exhibit abnormal differentiation and differential potential with advancing age. This abnormal

differentiation of HSCs drives to the immunosenescence or “immunoaging” in which lack of function of lymphoid cells such as B cells, T cells, and NK cells. Previous studies have shown that B cells generation and their diversity decrease significantly, while production of memory B cells and autoantibodies producing B cells which lead autoimmunity, expand more with advancing age. Additionally T cell production and their affinity towards antigen decrease with the aging process. Further, differentiated lymphocytes are inadequate to recognize the new pathogen. NK cells also exhibit decline cytokine secretion and cytotoxicity with age. Erythropoiesis also decreases with age causing anemia. Furthermore, aged bone marrow microenvironment pushes young HSCs to produce more myeloid cells compared to the young microenvironment. Although, myeloid cells number increase due to aged bone marrow microenvironment, and abnormal differentiation of HSCs, but their functionality decrease causing inflammatory surrounding known as “inflammaging.” Thus, both immunoaging and inflammaging motivates the deterioration of both adaptive and innate immune system, immunosenescence. The failure of the immune system (immunosenescence) with age induces high susceptibility to infection, disease including autoimmune disease, MDS, and cancer and also affects the entire body [16, 150]. Moreover, HSCs generated blood cells such as B cells, T cells, monocytes, macrophages and dendritic cells also have been revealed impaired functional elevation with advancing age. Aged Dendritic cells unable to activate B-cell and T cells and low expression of Toll-like receptors at macrophages and monocytes, reduced secretion of cytokines and chemokines, and altered B cell and T cell compartments are also correlated with the aging process [162].

HSCs highly express TWIST which is a master transcriptional regulator that regulates HSCs' myeloid lineage development and HSC self-renewal. Furthermore, TWIST is also involved in regulation of neural crest differentiation toward MSCs, cell lineage determination, induce expression of Stro1 (an MSC stemness marker), development of MSC progenitors and play a significant role in MSC differentiation, maintenance, and self-renewal [3].

3.7.3.2 Mesenchymal stem cells and aging

Similar to HSCs, MSCs also exhibit age-associated change with advancing age. Aged MSCs show decline proliferative capacity, clonogenic and differentiation potential. Moreover, MSCs have shown more differentiation towards adipocytes lineage, which leads accumulation of

adipocytes in the bone marrow with the aging process and turns red bone marrow (at birth) to yellow marrow (at elderly). The magnify deposition of adipocytes in aged bone marrow inhibits B-lymphogenesis and HSC function and positively regulates myelopoiesis. Age-dependent adipocyte differentiation (adipogenesis) of MSCs is not entirely understood. However, some speculation has been proclaimed including adipogenesis may dysregulate insulin/insulin growth factor 1(IGF1) receptor signaling (IIS), decrease bone formation and changes in the composition of extracellular matrix [16]. MSC dysfunction may cause a metabolic disorder such as accelerated aging associated metabolic syndrome. Production of adipocytes consumed MSCs in this syndrome. Also, type 2 diabetes and pre-diabetes are more commonly observed in metabolic syndrome, may also lead MSC dysfunction by the generation of advanced glycan end-products. These product stores in bone matrix and induce apoptosis, ROS production and suppress proliferation of MSCs during the age. Similar metabolic alteration is detected in severe disease of accelerated aging such as Hutchinson-Gilford progeria syndrome (HGPS) [20]. One report showed that age-related switch promotes MSCs toward adipocyte differentiation, instead of osteoblasts differentiation via NFATc (nuclear factor of activated T cell)/Maf and WNT signaling [162]. Previous literature publishes that aged MSCs associated with higher level of ROS and nitric oxide (NO), impaired DNA methylation, dysregulation of histone acetylation, telomere shortening and p53 mediated DNA damage [16].

3.7.3.3 Multipotent adult progenitor cells (MAPCs) /function and aging

Catherine Verfaillie group, in 2002, isolated multipotent adult progenitor cells (MAPCs) from rat and mouse bone marrow. Bone marrow derived MAPCs are adult stem cells and capable for insert trophic effect and immunomodulatory properties. Also, MAPCs are used for tissue regeneration. Although new and originally isolated MAPCs exhibit robust differentiation towards neuro-dermal lineage and produce neuron-like cells [21]. However, MAPCs can differentiate into cells of all three germ layers such as mesodermal (e.g. endothelial cells, adipocytes, chondrocytes, and osteocytes), endodermal (e.g. hepatocytes), and ecto-dermal (e.g. astrocytes and neurons) [7]. Human-MAPCs exhibit higher expression of CD44, CD13, CD73, and CD90 while MAPCs did not express mature hematopoietic markers such as CD34, CD45 CD56, CD105, and CD271 [21]. Rodent multipotent adult progenitor cells (MAPC) derived from bone marrow muscle, and brain shows c-Kit^{+}, CD9^{+}, CD13^{+}, CD31^{+}, and CD44^{-},

MHC-I$^-$, CD45$^-$, Thy1$^-$ surface markers profile [25]. Moreover, Mouse cultured MAPC exhibit higher level of expression of stage-specific antigen (SSEA-1) and CD13, mMAPCs also express a low level of Sca-1, Thy-1and Flk-1 and also exhibit no expression of CD34, CD44, CD45, c-kit, major histocompatibility complex (MHC) class I and II [12, 77] **(Table 2)**. Previous studies showed that cells infused in irradiated animals (treated with a low dose of radiation) which show a very low damage of the blood-brain barrier, and non-irradiated animals. An animal generates thymus lymphoma and spleen lymphoma which is commonly seen in aging NOD/SCID mice. mMAPCs exhibit higher level of differentiation and engraftment in low dose irradiated intestinal epithelium and hematopoietic system, and impart their function to neoangiogenesis in host tissue [77].

3.7.3.4 Bone marrow stroma cells and functions and aging

Apart from stem cells, **endothelial cells (ECs)** that line blood vessels in bone marrow also undergo the aging process and loss their numbers and function with advancing age. ECs secrete the insulin-like growth factor binding protein, VEGF, and pleotrophin (PTN) and act as a regulator of stem cells fate [3]. Previous studies have disclosed that Aged ECs showed the decline secretion of stem cell factor and ligand such as CXC motif ligand (CXCL) 12 that support bone marrow stem cells such as HSCs. Moreover, aged ECs show decreases Notch signaling and NO production that involved in vasodilation and mobilization of HSC. Thus, Aged ECs might be linked with defective mobilization and maintenance of stem cells in the bone marrow with aging process [16]. Previous studies have shown condition deletion of Atr gene of osteoblasts cause hair graying, osteoporosis, alopecia (premature age-related phenotypes). Moreover, Atr mutant mice show depletion of HSCs and progenitor cells and their regenerative potential. Hence, osteoblasts also require in maintaining of bone marrow niche with aging process [16].

MSCs are the primary source of osteoblasts generation. **Osteoblasts** regulate HSCs activity and expansion by secretion of granulocyte colony-stimulating factor (G-CSF), angiopoietin and osteopontin. The bone surface lining osteoblasts termed as SNO (spindle-shaped N-cadherin$^+$ osteoblastic) cells. Osteoblast interacts with HSCs via Notch signaling, Bmp-1/Bmp-1 receptor signaling, parathyroid/ parathyroid receptor signaling and Wnt-catenin signaling and induces proliferation, migration, and quiescence of HSCs. Further, HSCs and

other stem cells are also monitored by niche cells such as adipocytes which are a negative regulator of HSCs. Osteoclasts produce PGE2, non-myelinating Schwann cells which secret TGF, sympathetic neurons release CXCL12, and BM macrophages are a major source of PGE2 and involved in regulation of erythropoiesis [3]. Megakaryocytes required in the regulation of bone remodeling by secretion of RANKL, calcium-sensing receptors, NMDA-type glutamate receptors, TGF-β and TGF-β receptors, and estrogen receptors, osteonectin, osteocalcin [69].

Pericytes are stroma cells that communicate with other stromal cells through paracrine signaling or direct cell to cell contact. Pericytes regulate survival stabilization and maturation of other stromal cells such as ECs cells. Pericytes have contractile and phagocytic property. They are associated with a neurovascular unit as an essential component and blood brain barrier. Differentiation capacity of pericytes makes them a "ubiquitous source of adult tissue stem cells." Nestin is a filamentous protein secreted by neuroepithelial neuronal precursor stem cells which are involved in HSC maintenance. $Nestin^{+}$ cells are mix cell population including ECs, MSCs, endothelial precursor cells, myofibroblasts. The endosteal niche includes $nestin^{+}$ MSC cells as an essential cell component which secretes CXCL12, a critical chemokine for HSC migration. Sympathetic Nerves, surrounding arterioles, also contribute their role in cyclic release and migration of HSCs. Malfunction of nerve system leads impaired hematopoiesis. Hence autonomic nervous system acts as a "master regulator of hematopoiesis."$CXCL12^{+}$ abundant reticular (CAR) cells are identified as an essential component of the stem cell niche. Perivascular CAR cells have bi-lineage potential i.e. they can differentiate into both adipocytes and osteoblasts. CAR cells depleted (genetically engineered) mice showed a decline of HSCs. CAR cells involved in the maintenance of an undifferentiated state of HSCs, erythroid progenitor and lymphoid progenitors and retain HSCs in bone marrow [3].

3.8 Bone marrow related diseases

3.9 Bone marrow related diseases due to aging

3.9.1 Cancers

HSCs showed changes with age and produce no cell population or uncontrolled cell population of a particular cell lineage (known as cell autonomous mechanism for functional decline) and decrease the fitness of stem cells and progenitor cells (term as a non-cell-autonomous mechanism). The reduced fitness of stem cells and progenitor cells favor the oncogenic mutation which encourages the initiation of cancer. For instance, Fitness decline of aged B lymphopoiesis is connected with impaired receptor-associated kinase signaling. Moreover, impaired IL-7 signaling promotes selection of Bcr-Alb expression in aged-B progenitors which develop leukemias [163]. Altered bone marrow microenvironment particularly stems cell niche including MSCs, and their progeny leads the uncontrolled growth of a particular population produces several blood diseases. Most common malignant heterogeneous diseases of HSCs and progenitors cells are myelodysplastic syndromes (MDS), acute myeloid leukemia (AML) and acute lymphoblast leukemia (ALL) [3, 164-165]. Previous literature showed that altered bone marrow niche, the particular stem cells piece of niches such as mesenchymal cells and their progeny which have a strong immunomodulatory capacity, releasing trophic factors and communicate with all other immune cells, involved in development and propagation of MDS [3]. Later on, MDS turns into AML [164]. AML is a most common cancer affecting older adults and incidence increase with advancing age. Moreover, rapid progress and more resistant to standard chemotherapy of AML in the elderly increased mortality rate in elder patient if left untreated [158]. It is characterized by overproduction of abnormal white blood cells such as myeloblasts, monoblasts, and megakaryoblasts in the bone marrow and represses the generation of healthy blood cells. Unlike AML, Overproduction, and accumulation of lymphoblast, immature cancerous white blood cells in the bone marrow drive ALL, most common in the childhood. Although age-dependent factors including gene expression, epigenetic change cellular physiology of HSC that leads AML and ALL but the exact age-dependent molecular mechanism of AML and ALL are still to be investigated [165].

3.9.2 Altered B lymphopoiesis

Previous studies have shown altered bone marrow microenvironment with advancing age inhibit B lymphopoiesis, the developmental process of B cells. Moreover, Aged B cells are more proinflammatory in nature which further reduces B cell development. Thus, impaired B lymphopoiesis promotes decline number, functions and humoral immunity during aging process [166]. Microarray study reveals that antibody secreting cells (ASCs) undergo alteration with advancing age such as a defect in energy production and higher ROS level has been identified [167].

3.9.3 Osteoporosis

BM-MSCs can differentiate into osteoblasts, chondrocytes, and adipocyte under the controled mechanism/condition. Under the normal mechanism, RANKL (receptor activator factor kappa- B ligand) binds to osteoclast's RANK (receptor activator factor kappa- B) receptor. Receptor-ligand binding activates osteoclastogenesis, resulting in the generation of osteoclasts. Aging process pushes bone marrow MSCs towards adipogenesis instead of osteogenesis. As a result, some osteoblasts and their activity decline and interestingly a number of adipocytes increase. Moreover, osteoblasts and osteocytes mainly produce osteoprotegerin (OPG), a cytokine receptor, which mimic as RANK. RANKL-OPG binding inhibits the downstream signaling and blocks the osteoclastogenesis. Thus, the ratio of OPG/RANKL is an indicator of skeletal integrity and bone mass. Furthermore, OPG which is a member of tumor necrosis factor receptor (TNFR), interfere with activities of MSCs differentiated osteoblasts and promote MSCs differentiation towards adipogenesis during the aging process. As a result, MSCs differentiated adipocytes instead of osteoblasts accumulate in the bone marrow cavity, the primary characteristic of aged bone. Moreover, increased number of adipocytes leads osteoporosis in the bone with advancing age [168].

Moreover, previous researchers showed that cells expressing pre-adipocyte marker Pref-1 showed down-regulation of osteoprotegerin, RANKL-positive and exhibited a higher number of cells with advancing age. These cells generate osteoclasts from BM-macrophage. Hence, cells at pre-adipocyte stage favor osteoclastogenesis and bone destruction with advancing age [169] **(Figure XII)**.

Previous ex vivo study showed that IRF-1 plays a crucial role in regulation and maturation of bone metabolism, and also involved in the activity of osteoblasts and osteoclasts. IRF-1 deficiency is closely associated with increased mineralization activity and also linked with decline proliferation of BM-derived osteoblasts. *IRF-1*$^{-/-}$ mutant mice exhibit increased cellularity and cortical thickness, altered bone architecture and bone morphology [170].

3.9.4 Age-related macular degeneration (AMD)

Vision loss disease such Age-related macular degeneration (AMD) is irreversible blindness and more common of the age of 60 to 70 that continuously rise. AMD is characterized by the deposition of drusen between the Bruch's membrane and basement membrane of the retinal pigment epithelium (RPE) [171]. AMD is associated with degeneration or death of cells such as choroidal endothelial cells (CECs), retinal pigment epithelial cells and photoreceptor cells. Since Outer retina depends on the choriocapillaris for maintain metabolic support and loss of endothelial cells of the choriocapillaris which cause a severe problem. With advancing age, choroid and Bruch's membrane which is an essential component of healthy vision, exhibit changes in the molecular composition and the structure of these tissues. Alteration in tissues produce inflammatory environment and promote disease progression [172]. Since tissue-specific stem cells may be unable to generate RPE-like cells during age, resulting in AMD. Bone marrow-derived stem cells, embryonic stem cells (ESC), and tissue-specific stem cells may produce RPE-like cells. Hence RPE transplantation could be a future technique for treatment of AMD [171].

3.10 Bone marrow therapy in bone marrow related diseases

Extensive application of nuclear energy and radioisotopes in various activities, increase the risk of radiation exposures to human life-forms. Depending on the dose of the exposure, ionizing radiation damages the bone marrow and hematopoietic system. Thus, protecting people from the damaging effects of ionizing radiation is a major challenge [147]. The previous studies have demonstrated that bone marrow transplantation, approved therapy for bone marrow failure, is practiced for the treatment of many diseases such as non-malignant, malignant blood diseases [50]. Moreover, allogeneic bone marrow transplantation (BMT) is recommended treatment for both systemic and organ-specific autoimmune diseases associated with stem cell [49]. Bone marrow derived mesenchymal stromal cells (BM-MSC) are

practiced for therapeutic organ treatment because they can be comparatively easy to isolate, culture in a significant number, and in vitro, BM-MSC can differentiate into cells of all three germ layers. The collected preceding data revealed multiple mechanisms and pathways of BM-MSCs contribution to injury compensation. Current notions on radiation-induced insults are based on the assumption that an effective treatment should be given quickly, within a few hours after radiation exposure to defend and stop the death of the critically irradiated cells [63]. Thus, transplanted bone marrow or bone marrow derives stem cells such as MSC, HSCs may be an excellent help under such conditions.

3.10.1 Bone marrow transplantation

Accumulation of damage within the stem cells with age creates a deficiency of immune system, which leads to age-related diseases such as cancer, Alzheimer's disease (AD), Parkinson's disease, and osteoporosis. Previous research showed bone marrow transplantation (BMT) or stem cell transplantation (SMT) is a choice of age-related diseases **(Table 5 and 6)**.

3.10.1.1 Type 2 diabetes mellitus (T2DM)

Nutritional factors such as over nutrition, physical inactivity, genetic factors, and lifestyle cause obesity which leads age-related disease such as T2DM. T2DM is systemic, slowly progressing and chronic disease and life-threatening disease if left untreated. T2DM incidences are increasing among the people with age. The deterioration of insulin secretion by pancreatic β-cells and insulin-stimulated glucose uptake in highly active tissues such as adipose, muscle and liver tissues known as insulin resistance [173]. Stem cell transplantation therapy could be a useful approach for T2DM which mainly involved decrease hyperglycemia and improve insulin sensitivity and maintain normal blood glucose level all time in the body. Previous research showed transplantation of embryonic stem cell (ECS)-derived insulin-producing cells reduces hyperglycemia in streptozotocin-treated diabetic mice. Moreover, transplantation of human embryonic stem cell (ECS)-differentiated insulin-producing cell in NOD/SCID diabetic mice decreases hyperglycemia. Since MSCs have an immunomodulatory effect, having homing properties, differentiate insulin-producing cell like islets cell is a better choice of stem transplantation therapy for T2DM among the researchers **(Figure XIII)**. MSCs transplantation favors PDX1 expression and protects islets cells from pro-inflammatory effect and improves hyperglycemia in diabetic mice. Thus, stem cell transplantation decreased blood

glucose level in blood, increase insulin sensitivity, restore islet β-cell function and normalize hyperglycemia [162].

3.10.1.2 Osteoporosis

The most common age-related bone disease is osteoporosis which characterized by dysregulation of bone absorption and bone formation. The bone formation includes osteoblastogenesis process which generates osteoblasts, and osteoclastogenesis process which produces osteoclasts. Both process osteoblastogenesis and osteoclastogenesis are controlled by TNF-α, IL-6, and TGF-β. TNF-α provoke osteoblasts for producing IL-6 which in turn accelerate TRAICR/RANKL (TNF-related activation-induced cytokine receptor/receptor activator of nuclear factor- kb ligand) signaling and activate osteoclastogenesis resulting production of osteoclasts. Osteoclasts produce TGF-α which regulate the osteoblastogenesis. SAMP-6 (senescence accelerated mouse prone-6) is a mouse model of age-related osteoporosis disease. Previous researchers disclosed bone marrow microenvironment of SAMP-6 showed dysregulation of TNF-α, IL-6, and TGF-β. Bone marrow transplantation increases the level of RANKL, IL-6, and IL-11 which control the imbalance of bone formation and bone absorption and prevent the osteoporosis in a mouse model [162] **(Figure VIII)**.

3.10.1.3 Alzheimer's disease (AD)

The most familiar age-related neurodegenerative diseases are Alzheimer's disease (AD), Parkinson's disease. AD is characterized by learning and memory loss, behavioral depression, brain atrophy, loss of neurons, neuronal synapses, neuronal dendrites, dendritic spines, and β amyloid deposition in the brain. Previous research showed SAMP-8/10 (senescence accelerated mouse prone-8/10) is well-accepted mouse model for study of AD, which reflects cognitive deficit similar to AD patient such as decrease catecholamine synthesis in the cerebral cortex, neuronal DNA damage, and decrease hippocampal receptors, reduce neurotrophic factors and elevated oxidative stress in the brain with the aging process. Bone marrow transplantation normalizes HO-1 (oxidative stress marker) level, IL-6, IL-1β, iNOS and reduces β-amyloid deposition and thereby prevents the progression of AD [162].

3.10.1.4 Bone marrow stem cell therapy for AMD

A preclinical study showed that bone marrow transplantation (BMT) could be used to treat vision loss or retinal dysfunction which is age-related molecular degeneration. Stem cell transplantation approach are being discovered for regeneration of retina and treatment can cure ischemic and degenerating retina. Stem cells are known for secreting paracrine trophic factors which can reach multiple damaged cells and impart regenerative effect. Therefore, stem directly transplant into damaged tissue. Stem cell therapy has no limitations to AMD diseases. Stem cell such as mesenchymal stem cell is more commonly administered cell for treatment of diseases such as AMD, because of their homing and trophic properties [174].

4 STATEMENT OF PROBLEM

Bone marrow is a soft, gelatinous, and dynamic tissue which serves as an organ of the immune system. It is confined in the center and the epiphysis of long bones like femora, tibia, humeri, ribs, pelvis, vertebrae, and skull [2]. Bone marrow possesses cellular component and soluble component. The cellular component encompasses stem cells such as HSCs, MSCs, MAPCs and bone marrow stroma cells such as endothelial cells (ECs), osteoclasts, osteoblasts, fibroblasts, tissue macrophages, and adipocytes whereas soluble component constitutes of cytokines, chemokines, growth factors, and hormones [3]. Bone marrow includes two cellular components, Parenchyma or hematopoietic component which comprise HSCs and hematopoietic progenitor cells (HPCs) and Stoma or Vascular component receives non-hematopoietic progenitor cells such as MSCs and MAPCs [4]. Bone marrow is a large reservoir of pluripotent stem cells such as hematopoietic stem cells (HSCs) [5], mesenchymal stem cells (MSCs) [3, 6], and multipotent adult progenitor cells (MAPCs) [7]. Stem cells have unique ability to proliferate and differentiate into an unspecified lineage of cells of the body. Each cell of bone marrow performs its particular function and maintains bone marrow structure and functions [3].

Bone marrow is the primary site of hematopoiesis, which is a continuously dynamic process of production and consumption of all terminally differentiated blood cells to operate various functions throughout a lifetime [16]. HSCs, having self-renewal capacity and reconstitution ability of hematopoiesis following transplantation, differentiated into lineage-committed and multi-potential progenitor cells. HSCs and progenitor cells are not randomly scattered; rather they are protected and resided in a highly organized bone marrow microenvironment or bone marrow niche [3]. HSCs are primary stem cells of bone marrow, and capable of producing all hematopoietic lineages [17].

A primary source of MSCs is bone marrow. Other studies show that the other most important sources of mesenchymal stem cells are the umbilical cord, endometrial polyps, menses blood, adipose tissue, placenta, cruciate ligament and fallopian tubes, etc. [175]. MSCs are significantly involved in tissue homeostasis and formation of bone marrow niche structure and organization. MSCs maintain immunomodulation properties and capable of suppressing and regulate the immune system. Since MSCs are not immune cells but they control both innate

immunity and adaptive immunity. Therefore, to emphasizing their role in modulating the immune response, MSCs are termed as "coordinators of the immune system." MSCs are a crucial component of stem cell niche. MSCs regulate differentiation; maintenance and self-renewal of HSCs. MSCs deliver survival signals, stemness, and proliferation of HSCs and their progenitor cells. MSCs also protect HSCs from the chemotherapeutic agent and cytotoxic effect [3, 19]. Mesenchymal and Tissue Stem Cell Committee (MTSCC) of the International Society of Cellular Therapy (ISCT) have been defining the minimal criteria for the characterization of MSCs which includes: plastic adherent property in culture; must be positive for MSCs positive marker such as CD29, CD44, CD73, CD90, CD105 and Sca-1 and negative for MSCs negative markers such as CD11b, CD34, CD45, CD14, and HLA-DR (human leukocyte antigen D related); and differentiation into mesenchymal lineage such as chondrocytes, adipocytes, and osteocytes. Additionally, fibroblast cells like spindle-shaped morphology [3, 16, 20-21, 23, 72]. MSCs are the heterogeneous mixture of a subpopulation of cells may or may not fulfill the specified stem cell criteria. MSCs, those satisfy the criteria termed as "mesenchymal SCs," and those do not call "multipotent mesenchymal stromal cells" [3].

Bone marrow derived MAPCs are adult stem cells and capable for insert trophic effect and immunomodulatory properties. Also, MAPCs are used for tissue regeneration. Although new and originally isolated MAPCs exhibit robust differentiation towards neuro-dermal lineage and produce neuron-like cells [21]. However, MAPCs can differentiate into cells of all three germ layers such as mesodermal (e.g. endothelial cells, adipocytes, chondrocytes, and osteocytes), endo-dermal (e.g. hepatocytes), and ecto-dermal (e.g. astrocytes and neurons) [7]. MAPCs show robust endothelial expression as compared to MSCs [21].

The soluble component is necessary for proper functioning of bone marrow. The soluble component includes cytokines, growth factors, hormones, calcium, and chemokines. Stem cells and their progeny cells generate soluble factors. For instance, MSCs, ECs, osteoblasts and CAR cells secret stromal cell derived factor-1 (SDF-1, also known as CXC12), which is critical chemokines participating in HSCs maintenance and HSCs homing within HSC niche [3]. Previous research showed that SDF-1-/- Mice's HSCs have colonization defect, and reinforced expression of SDF-1 in bone marrow vascular endothelial cells enhance colonization property of bone marrow by stem cells. Hence, bone marrow endothelial cells

secreted SDF-1 is essential for hematopoietic colonization of bone marrow. SDF-1 also induce expression of VCAM-1 on ECs and very late antigen (VLA)-4 on megakaryocyte [14]. Niche cells also release SCF and TGF-β which is relevant to regulation and HSCs maintenance. TGF-β secretion is associated with osteoblastic differentiation of MSPC [3].

Since MSCs are accessible to isolate, culture, natural adherence to plastic culture dishes and expand in laboratory conditions, mesenchymal stem cells (MSCs) isolated from mouse [22, 176], rat [177], and human bone marrow [178-179] have been extensively studied. However, selection of passage (s) cells from in vitro condition is extremely significant because initial cell passage (s) may receive cellular contaminants of hematopoietic cells, and other lineages cells [22, 176] and late passage MSCs are susceptive to experience senescence and even chromosomal abnormalities [180]. Moreover, self-renewal and differentiation potential of MSC depends on passage of cells [181]. Bone marrow derived cultured MSCs described as most adherent cells of bone marrow stroma [182]. MSC also was identified by another alternative name such as bone marrow stem cells, stromal stem cells, marrow progenitor cells, and marrow derived adult stem cells [183]. Arnold I. Caplan has described that MSCs generate regenerative microenvironment at the site of injury because these cells provided many bioactive molecules. These molecules have immunoregulatory features. This capacity of MSCs, contributing paracrine molecules at the site of injury, called "trophic activity" [6]. Mesodermal- MSCs have several characteristics traits like- self-renewal, multilineage differentiation (like all stem cells) and potential to adhere to plastic support [175]. Morphologically, MSCs look like fibroblast which has a large nucleus in long thin cell bodies [184].

The hallmark of all types of stem cells is the capability of differentiation and self-renew. This property is called “stemness” which primarily depends on cellular signaling pathways preferentially expressed in the stem cells [26], chromatin regulatory epigenetic pathways [28], the engagement of regulatory RNAs, such as the micro-RNAs (miRNAs) [36-37] &long noncoding RNAs (lncRNAs) [40], and expression of transcription factors, such as Oct3/4,Sox-2, Nanog, Olig, Klf4, c-Myc, SALL4 etc. are responsible for specifying the gene expression programs in the stem cells [28, 31-32].

It is well documented that ionizing radiation is the primary cause of bone marrow failure, which regulates hematopoiesis, suppresses differentiation of immune cells, and inhibits

proliferation of hematopoietic progenitor cells in the hematopoietic microenvironment [185]. Moreover, ionizing radiation may lead to a decline in hematopoietic precursors, hematopoietic dysfunction, a reduction in the bone marrow cellularity, reduce bone mineralization and a higher risk of bone marrow failure [45]. The previous researchers showed that bone marrow transplantation, a recommended treatment under conditions of bone marrow failure, is practiced for the treatment of many diseases such as non-malignant, malignant blood diseases, autoimmune diseases [49-50]. Transplanted bone marrow may be a great help under such conditions.

Interferon regulatory factors (IRFs)-1 and 2, are two very essential transcription factors for genes encoding type 1 interferons (IFNs) including IFN-α and IFN-β. Previous studies established assumption that IRF-1 is expressed constitutively at a low level in almost every cell type including bone marrow cells. It provokes expression of IFN-stimulated genes, such as MHC class I and iNOS. IRF-1 and IRF-2 are the members of IRF family that monitors the variety of genes performing central roles in the regulation of both innate and adaptive immunity, cell development of bone marrow, differentiation, and apoptosis. [32, 53, 97]. IRF-1 is a transcriptional activator of interferon (IFN). The functional inactivation of IRF-1 is supposed to guard against autoimmune phenomena. These IRF-1-induced alterations are connected with MDS pathogenesis and the regulation of abnormal hematopoiesis [186]. Moreover, IRF-1 knockout mice exhibited declined levels of $CD8^+$ T cells and greater susceptivity to infections [52]. It was reported that IRF- 2 act as a transcriptional suppressor of type 1 IFN-signalling, preserve the self-renewal and multilineage differentiation property of hematopoietic stem cells, thereby promoting the complete homeostatic erythropoiesis during the life as well as IRF-2 knockout mice showed defects in B lymphopoiesis [187]. The expected purpose of this study is to the regeneration of the bone marrow of the irradiated mouse by the transplantation of freshly isolated mouse bone marrow cells and explores the role of interferon regulatory factors during bone marrow regeneration. This study will elaborate the function of IRFs (IRF-1 and IRF-2) which was less focus.

Based on the above background, following objectives were studied:

1. Isolation and culture of bone marrow (BM) cells and enrichment, isolation, culture, and propagation of mesenchymal stem cells (MSCs) from the C57Bl6J mouse as well as their morphological and immunophenotypic characterization.

2. Transplantation of BM cells and MSCs into irradiated mouse and study of bone marrow regeneration by (a) cell cycle analysis by FACS, (b) CFU-F assay, (c) gene expression analysis by RT-PCR and (d) functional assay by measuring secretory factors.

3. Role of IRF-1 and IRF-2 transcription factors in this mouse model of bone marrow regeneration by (a) immunofluorescence, protein expression/ localization, (b) gene expression (RT-PCR) and (c) expression of IRF-1 and IRF-2-regulated genes by RT-PCR

To address the above objectives, following experiments were carried out:

1. Isolation of bone marrow from C57/BL6 mouse bone marrow, (b) culture and expansion of MS-P0 Cells were conducted by intrinsic adherence property of MSCs. (c) culture and development of MS-P1 Cells were carried out by fundamental adherence property of MSCs. (d) cell cycle status of bone marrow. (e) Stem cell potential of bone marrow by CFU-F assay.

2. Characterization of MSCs by: (a) morphological features by Microscopy (fibroblast-like spindle-shaped morphology), (b) immunophenotypic characterization by surface markers (e.g., (MSC-positive) CD29, CD44, Sca-1, and (MSC-negative) CD34, CD45 and CD11b by FACS.

3. Generation of the irradiated mouse model and transplantation of BM cells into irradiated mouse. Mice of 8 weeks of age were exposed to the 4 Gy radiations, and then BMCs ($10x10^6$ cells) were transplanted four hours post-radiation through tail vein injection. Post 24 hours mice (control, irradiated and transplanted mice) were sacrificed and bone marrow cells were analyzed.

4. Investigation of bone marrow regeneration by (a) cell cycle analysis by FACS, (b) CFU-F assay, (c) histological study of bone from control, irradiated and irradiated + transplanted mice

5. Examination of IRF-1 and IRF-2 transcription factors in this mouse model of bone marrow regeneration by (a) gene expression (Real-Time RT-PCR), (b) immunofluorescence for protein expression/ localization.

6. Study of IRF-1 and IRF-2 transcription factors in bone marrow derived MS-P1 cells by immunofluorescence of protein expression/ localization.

7. Examination of pluripotency-associated transcription factors (Oct3/4 and Sox-2) in bone marrow cells and bone marrow derived MS-P1 cells by immunofluorescence for protein expression/ localization.

5 MATERIALS AND METHODS

5.1 MATERIALS

5.1.1 Reagents

5.1.1.1 Antibodies

5.1.1.1.1 **Table 1: Antibodies used for immunophenotyping and FACS**

Marker- Fluorochrome	**Dilution ($\mu g/10^6$ cells)**	**Company**	**Catalogue no.**
Armenian Hamster IgG Isotype-PE	1.0	eBioscience	12-4888
Rat IgG2a K Isotype Control- FITC	0.5	eBioscience	11-4321
Rat IgG2b, k Isotype Control- FITC	0.5	BD Bioscience	553988
CD29-PE	1.0	eBioscience	12-0291
CD34- FITC	1.0	eBioscience	11-0341
CD44- FITC	0.125	BD Bioscience	553133
CD45- FITC	0.25	BD Bioscience	553079
CD11b- FITC	0.5	eBioscience	11-0112
Sca-1- FITC	0.5	eBioscience	11-5981

FITC: fluorescein isothiocyanate, PE: phycoerythrin.

5.1.1.1.2 **Table 2: Antibodies used for immunofluorescence**

Antibodies	**Dilution**	**Catalogue no.**	**Company**
Primary antibodies			
IRF-1 (Rabbit polyclonal antibody)	1:250	(H-205): sc-13041	Santa Cruz Biotechnology
IRF-2 (Rabbit polyclonal antibody)	1:250	(H-229): sc-13042	Santa Cruz Biotechnology

OCT3/4 (rabbit, affinity isolated antibody)	1.250	O8389	Sigma-Aldrich
SOX2 (rabbit, affinity isolated antibody)	1.250	S9072	Sigma-Aldrich

Secondary antibodies

Goat anti-rabbit IgG- TRITC labeled	1:400	RTC2	Bangalore GeNei
Goat anti-rabbit IgG- TRITC labeled, affinity purified antibody	1:400	03-15-06	KLP
Goat anti-rabbit IgG- FITC labeled	1.400	F0382	Sigma-Aldrich

FITC: fluorescein isothiocyanate, TRITC: Tetramethylrhodamine

5.1.1.2 Cell Culture Reagents

Chemicals Name	**Company**	**Catalogue No.**
Antibiotic-antimycotic solution,(100X)	Sigma	A5955
Bovine serum albumin	Sigma	A9647
Crystal violet	Sigma	C0775
DAPI	Vector Lab Inc	H-1200
DMEM-HG	Sigma	D5796
Fetal bovine serum	Sigma	F4049
Fetal bovine serum	Gibco	10082147
Eosin	Sigma	E4009
Giemsa stain	Merck	61803900251730
Hematoxylin	Sigma	H9627
KCl	Qualigen Excela	R19255
KH_2PO_4	Merk	MI5M552654
Na_2HPO_4	Sigma	S7907
NaCl	Merk	61751905001730
Sheath fluid	BD Bioscience	342003
Trypan blue	Sigma	T8154

Trypsin-EDTA	HiMedia	TCL007

5.1.1.3 Primers

Primers	Ori	Sequence	cDNA (µl)	Temp (^{0}C)	Amplicon (bp)
GAPDH	F	5' ACC ACA GTC CAT GCC ATC AC 3'	1.5	60	452
	R	5' TCC ACC ACC CTG TTG CTG TA3'			
IRF-1	F	5' GGC TGG GAC ATC AAC AAG GAT G 3'	2.5	63	332
	R	5' GAG CTG CTG AGT CCA TCA GAG AA 3'			
IRF-2	F	5' GTT AAG CAC ATC AAG CAA GAA CCA 3'	2.5	63	492
	R	5' GCT CTC CTC TTT GAT GGT GAC C 3'			

Abbreviations: F: forward primer, R: reverse primer, bp: base pair, Ori: Orientation

5.1.1.4 Plastic and glassware

Plastic/Glassware and Usage	Company	Catalogue No.
50 ml Centrifuge tube (Polypropylene) used to aliquot media and FBS for storage	Corning	430291
15 ml Centrifuge tube (Polypropylene) to collect BMCs	Corning	430052
0.2 µm syringe filter used for media filtration	MDI	SYKG0601MNXX204
70 µm Cell strainer to filter cells and remove debris	BD Biosciences	352350
5 ml Dispo Van single use sterile syringe to flush bone marrow from bones	Dispo Van syringe	needle 0.55×25 mm
Eppendorf tubes and tips (DNase, RNase and Pyrogen free)	Tarson	500000-20,521000-20

FACS Tube used for FACS experiments	Genaxy	MTS-11-C
Microscopic coverslip/coverglass for growing and culturing on it	Blue Star	22 mm, No. 1
Micro slides	Blue Star	75 mm × 25 mm
5 ml Steripette for preparation of media	Corning	4501
Tissue culture plate-6 well (Polystyrene) for CFU assay and cell differentiation	Corning	3501
Tissue culture plate-96 well (Polystyrene)	Corning	CLS 3628
T-25 Canted culture flask (Polystyrene) used for culture and propagate bone marrow and mesenchymal stem cells	Corning	CLS 430639

5.1.1.5 Common Reagents

Chemicals	**Preparation**
Agarose	Routinely, 1% - 2% agarose (Sigma, A9539)
Acetic acid	Acetic acid glacial (Merck-GR). Stored at room temperature (RT)
Acid Alcohol	Add 1 ml concentrated HCl in 100 ml 70% ethanol (C_2H_5OH)
Bovine Serum Albumin (10mg/ml)	Dissolved 1gram BSA in 100ml double distilled water (Sigma, Fraction V, A9647) Stored at -20 ^{0}C.
Deionized water	10 g Mixed Bed Resin (Sigma, M 8157) added to 100 ml double-distilled water and kept at RT for overnight for a horizontal shaker. Aliquots the deionised water in 1.5 ml eppendorf tube and eventually autoclaved. Stored at -20 ^{0}C (used for PCR etc.)
DEPC water	1 ml Diethyl pyrocarbonate (DEPC) (Sigma, D5758) dissolved into 1 litre double distilled water at a final concentration of 0.1%, stored at 37 ^{0}C for overnight and then autoclaved. Finally stored at RT.
Enzymes and dNTP	Oligo $(dT)_{15}$ Primer (Promega, C1101) M-MLV Reverse Transcriptase, 10,000 U (Promega, M-1701) dNTPs (Promega, U120B, U122B, U121B, U123B)

	Recombinant RNasin$^{(R)}$ Ribonuclease inhibitor-2500U (Promega, N-2511)
	Taq DNA Polymerase (NEB, M0273L)
EtBr (10 mg/ml)	Dissolved 10 mg of ethidium bromide (EtBr) (Sigma, E 8751) in1 ml double distilled water. Stored at 4 ^{0}C.
NaOH	Sodium Hydroxide Merk (61757305001046). Store at RT
PBS-T	Dissolved 100µl (0.1%) Tween-20 in 100ml 1X-PBS, pH 7.4.
Phosphate buffered saline, PBS,(10X, pH 7.4)	80 g NaCl (1.3 M) (Merck), 2 g KCl (20 mM) (Qualigen Excela R, 19255), 14.4 g $Na_2HPO_4.2H_2O$ (78 mM) (Sigma, S7907), 2.4 g KH_2PO_4 (14mM) (Merk Germany, MI5M552654) mixed in 900 ml double distilled water, pH was adjusted to 7.4 with 1N NaOH, final volume made up to 1 litre and autoclaved. Stored at 4 ^{0}C.
PI (10 mg/ml)	10 mg propidium iodide (Sigma P4170) dissolved in 1.0 ml double distilled water. Stored at 4 ^{0}C in the dark.
PFA (4%)	4.0 g paraformaldehyde (PFA; Sigma, P6148) was dissolved in 100 ml 1X-PBS (pH 7.4). Add 2-3 drop NaOH to dissolve PFA and heated at 60 ^{0}C in the water bath for 30 min and then stored at 4 ^{0}C. Suitable for use for about two weeks.
Tris-Acetate-EDTA (TAE) Buffer-50 X	121 g Trizma (Sigma, T1503), 28.55 ml glacial acetic acid (Merck) and 9.50 g EDTA (Sigma, E5134) dissolved in 500 ml double distilled water, and autoclaved. Stored at RT.
Tris-Borate-EDTA (TBE) Buffer-5X	54 g Trizma (Sigma, T1503), 27.5 g Boric acid (Sigma, B6768) and 3.803 g EDTA (Sigma, E5134) dissolved in 1 litre double distilled water, and autoclaved. Stored at RT in the dark.
Tween 20 detergent	Molecular biology grade (Calbiochem, 655204) was used as a mild detergent to permeabilize cells. Stored at RT.
Triton X-100	Used as mild detergent
TRI Reagent	(Sigma, T9424), store at 4 ^{0}C
Paraffin wax	(Merck, 61782305001730)

5.1.2 Experimental animal

Eight week old Inbred C57BL/6 mice were used for all kind of experiments. All animals were maintained and bred in the animal house facility (25 ^{0}C, 50 % relative humidity) at Jawaharlal Nehru University, New Delhi, India. All mice related experiments were conducted as per Jawaharlal Nehru University guideline on animal care and ethics.

5.2 Methods

5.2.1 Isolation and culture of bone marrow cells (BMCs) and mesenchymal stem cells (MSCs)

5.2.1.1 Isolation of bone from mouse

BMCs were isolated from mice (C57BL/J6, 7-8 weeks old) (Dominici et al. 2006, Soleimani and Nadri 2009, Zhu et al. 2010). Mice were sacrificed by cervical displacement under anesthesia. Then, the external body surface of mice was sterilized by 70% (vol/vol) ethanol. Femurs, tibiae-fibulae, and humeri were separated out carefully from the mice body and removed associated muscle and tissue of the bones using a dissecting scissor. After cleaning, bones were stored in 5 ml complete media containing Dulbecco Modified Eagle's Medium (DMEM, Sigma-Aldrich, cat no. D5796), 15% heat-inactivated fetal bovine serum (FBS, Sigma-Aldrich, cat no. F4135), and 1x antibiotics/antimycotic solution (Sigma-Aldrich, cat no. A5955).

5.2.1.2 Isolation of bone marrow from bones

One end of the bone was cut using scissor under the proper sterile condition in the hood. Then BMCs were harvested by inserting and flushing of 5 ml complete media at the non-cut end of the bones with the help of a 24-gauge needle with 5 ml syringe and collected BMCs in 15 ml polypropylene tube. Two min vertex formed the bone marrow single cell suspension, and then cell suspension was refined through 70 μm cell strainer to extract precise single cell suspension without any significant cell clump, bone spicules, muscle, and debris.

After collecting filtered single cell suspension of the bone marrow in 15 ml polypropylene tube. We counted BMCs and seeded them in the T-25 culture flask. We did not centrifuge BMCs as mentioned in many pieces of literature because we believe; first, it can cause low yield, and secondly, as a result of centrifugation, some cells, specifically having low density

unable to settle down, resulting in loss of these particular cells. All types of cells in the bone marrow not only play their distinct function but also helping and maintaining the bone marrow niche structure. Cultured BMCs in the culture flask may be unhealthy in the absence of secretory factors release by lost cells during centrifugation; resulting culture takes more time to reach 70% confluence as compared to non-centrifuged culture as we have observed.

5.2.1.2.1 **Yield of bone marrow cells (BMCs) or cell viability assay**

Trypan blue assay determined the yield and viability of the cells. BMCs were enumerated on a hemocytometer. We found total BMCs per mouse were 66.9 million and total live 65.47 million (97.86 %), and dead cells 1.43 million (0.021 %) per mouse respectively.

5.2.1.3 Culture of bone marrow cells (BMCs) and mesenchymal stem (Passage-0) stem cells (MS-P0 cells or primary MSCs)

BMCs were cultured in the T-25 culture flask. BMCs ($25x10^6$ cells) were seeded at a density of $1x10^6$ cells/cm^2 area of the T-25 culture flask. Then culture flask was incubated at 37 ^{0}C in 5% CO_2 cell culture incubator. Then, let them grow until cell density reached 70%, It takes 12-15 days. Media (3ml out of 5 ml) was replenished with fresh media on every 3rd day.

5.2.1.3.1 **Passaging or Trypsinization or harvesting cultured mesenchymal stem (Passage-0) cells (MS-P0 cells or primary MSCs)**

Mature spindle-shaped and adhere a layer of MS-P0 cells were rinsed with 5 ml 1X-PBS twice. MS-P0 cells were detached from the culture flask by 2 ml 0.25% trypsin/EDTA for 2 min at 37 ^{0}C followed by vortex for 3 min at RT and then complete media, 3 ml, was added to discontinue the activity of trypsin. Pipetting was done for 2 min for mixing the entire media and trypsin, resulting in complete deactivation of the trypsin and detaching more cells. As a result, increase the yield of harvested cells. Then, the cell suspension was subjected to centrifuge at 2000 rpm (380 g) for 5 min at RT. The pellet was resuspended in 5 ml fresh complete media. MS-P0 cells were enumerated on a hemocytometer. Then harvested cells mesenchymal stem (Passage-1) cells (MS-P1 cells) were distributed and seeded into three culture flasks. Then culture flasks were incubated at 37 ^{0}C in 5% CO_2 cell culture incubator. Then, let them grow until cell density reached 70%, It takes 18-21 days. Media (3ml out of 5 ml) was replenished with fresh media on every 3rd day [22-23, 188-190].

5.2.2 Characterization of Bone marrow cells (BMCs) and mesenchymal stem (Passage-1) cells (MS-P1 cells)

BMCs were isolated, filtered and counted on hemocytometer from 7-8 week old C57BL/6J mouse [22-23, 188-189]. And cultured, mature, and spindle-shaped attached MS-P1 cells were rinsed with 5 ml 1X-PBS twice. MS-P1 cells were detached from the culture flask by 2 ml 0.25% trypsin/EDTA for 3 min at 37 ^{0}C followed by vortex for 3 min at RT and then complete media, 3 ml, was added to arrest the action of trypsin. Pipetting was performed for 2 min for mixing the entire media and trypsin, resulting in complete deactivation of the trypsin and detaching more cells. Then, the cell suspension was subjected to centrifuge at 2000 rpm (380g) for 5 min at RT. The resuspended pellet cells in 5 ml fresh complete media were enumerated on a hemocytometer. Then harvested BMCs and MS-P1 cells were aliquot ($1x10^6$ cells/ml in 1X-PBS) was made. Then, the cell suspension of BMCs and MS-P1 cells were subjected to centrifuge at 2000 rpm (380 g) for 5 min at RT. The pellets were rinsed with 1X-PBS and resuspended in 100 µl staining buffer (2%). The cell suspension was stained with PE-conjugated anti-mouse CD29, FITC-conjugated anti-mouse CD44, Sca-1 [MSC-positive markers], CD11b, CD34, and CD45 [MSC-negative markers], and isotype antibodies as a control respectively. After thirty min ice incubation, cells were subjected to centrifugation at 2000 rpm (380g) for 5 min at RT followed by washing with cold immunostaining buffer (2%). Cells were resuspended in 100ul of staining buffer (4%). PI was used to measure cell viability. Data were collected on BD FACS Calibur. 50,000 events per sample were acquired using FL1 and FL2 channels. FACS Calibur software analyzed data and FSC and SSC gating excluded dead cells.

5.2.3 Crystal violet staining

Crystal violet (0.05%, 50mg dissolved in 100ml double distilled water) was formed in water. The stain was suspended thoroughly by moving bottle for 5-10 min at RT. The solution was filtered through 0.45 µm filter before use. BMCs, MS-P0 cells, and MS-P1 cells were washed with 1X-PBS at RT and then fixed with 3.7% paraformaldehyde for 10 min. paraformaldehyde was carried out; cells were rinsed with PBS, and then stained with crystal violet for 10 min. After staining, cells were washed, and images were captured under the bright field microscope.

5.2.4 Development of mouse model for bone marrow regeneration

5.2.4.1 Irradiation

Recipient mice (C57BL/6J, male, 7-8 weeks) were placed in a specifically design irradiator having holes for continuous air flow. Irradiator with mice placed in gamma chamber (at CIF, JNU). A single dose of total body, sub-lethal, 4 Gy γ-radiations was given to recipient mice with gamma rays at the rate of 4 rads/second according to published ligatures [185, 191].

5.2.4.2 Bone marrow transplantation

Bone marrow transplantation was performed as per the information available in published literature with some modifications [49, 191]. Donor mice (C57BL/6J, male, 7-8 weeks) were sacrificed cervical displacement under anesthesia. Then, the external body surface of mice was sterilized by 70% (vol/vol) ethanol. Femurs, tibiae-fibulae, and humeri were separated out carefully from the mice body and then BMCs were harvested by inserting and flushing of 5 ml 1X-PBS at the end of the bone with the help of a 24-gauge needle with 5 ml syringe and collected BMCs in 15 ml polypropylene tube. Then cell suspension was refined through 70 μm cell strainer to extract precise single cell suspension without any significant cell clump, bone spicules, muscle, and debris. BMCs were enumerated on a hemocytometer. Four hours after irradiation, donor BMCs ($10x10^6$ BMCs) were intravenously transplanted into irradiated recipient mice via the tail vein using a 24 gauge needle [191].

5.2.5 Cell cycle analysis by FACS

Cell cycle was analyzed during the bone marrow regeneration. One million harvested BMCs from control, irradiated, and transplanted mice were fixed in 70% ethanol, and then cells were rinsed with 1X-PBS. Resuspended cells in 100 μl of 1X-PBS were administered with 100 μg/ml RNase A at 37 ^{0}C for 1 hour. Then after, Propidium iodide (10 μg/μl) was added cell suspension. Cells were incubated on ice for 15 min. Cell cycle data were acquired on BD FACS Calibur. 50,000 events per sample were acquired using FL1 and FL2 channels. Finally, Data was analyzed by FACS Calibur software, and FSC and SSC gating excluded dead cells [192-193].

5.2.6 Colony forming unit-fibroblasts (CFU-Fs) assay

Stem cell potential of bone marrow was analyzed by CFU-F assay of control, irradiated and transplanted mice bone marrow. Different cell densities (1, 2 and 4 million BMCs per 2 ml media) of bone marrow were seeded into the 6-well plate of control, irradiated and transplanted mice and placed them humidified incubator at 37 ^{0}C in a 5% CO_2 and let them grow. Fresh media was supplied at every 3rd day. At day 12th, cells were stained with 0.05% Crystal Violet stain followed by fixation and counted the number of colonies. MSCs developed colonies of different shape, size and cell densities in control irradiated and transplanted panel [194-195].

5.2.7 Histological Study

5.2.7.1 Tissue Fixation and Paraffin Wax Embedding

Isolated longs bones from control, irradiated and transplanted mice were washed twice with 1X-PBS then fixed in 4% paraformaldehyde solution for 24 hours at RT. The fixed bones were decalcified with 20% EDTA solution for 2-3 days at RT. The decalcified bones were containing bone marrow dehydrated in a series of grade ethanol, 30% for 30 min, 50% for 30 min, 70% for 30 min, 95% for 1 hr, 100% for 1 hr at 4 ^{0}C. The dehydrated bones were incubated in xylene solution for 15 min at RT. Finally, bones were immersed in pre-melted paraffin wax for 3 hours at 60 ^{0}C. Bones were embedded in a metal block in a proper orientation and with care to avoid the formation of air bubbles. The paraffin block containing bones were fixed on a metal peg and 5-10 µm thin sections were cut using radial microtome. The sections were expanded at pre-warmed 37 ^{0}C water. Then after, sections were mounted on gelatine-coated slide carefully. The slides were stored overnight at RT [196-197].

5.2.7.2 Hematoxylin and Eosin staining

Paraffinized tissue sections were deparaffinized with xylene for 2 min, and sections were hydrated with a series of grade ethanol (100%, 95%, 70%, 50%, and 30%) for 5 min at RT. Then after, sections were first stain with Hematoxylin for 1min. Slides excess stain was removed off by acid alcohol dip and differentiated in Scott's solution for blueing of nuclei. The slides were subsequently dehydrated through upgrade ethanol series up to 70% ethanol and were stained with Eosin for 1 min followed by quick dehydration with 95% ethanol and absolute ethanol. The slides were finally treated with xylene and mounted with DPX mountant

(A synthetic resin mixture of a polystyrene-distyrene, a plasticizer-tricresyl phosphate, and xylene). The slides were examined under the microscope and images were taken at 10x, 20x, and 60x magnification [2, 196, 198]. Images were analyzed by Image J software and the bone marrow cellularity was measured.

5.2.8 Real Time RT-PCR analysis of genes

Expression of IRF1 and IRF2 mRNAs in BMCs of control, irradiated and transplanted was analyzed by real-time reverse transcriptase-polymerase chain reaction (RT-PCR) [199-200]. RNA was isolated from BMCs by the TRI-reagent method. Isolated BMCs from the control, irradiated and transplanted mice were cleaned with 1X-PBS, and a pellet of 10 million cells was resuspended in one ml of Trizol reagent at RT and stored at -80 ^{0}C. Next day, BMCs were thawed at RT for 5 min, then chloroform (300 µl) was added to it and mixed for 15 min at RT and incubated for 15 min at 4 ^{0}C. The mixture was centrifuged at 13,000 rpm (15,856xg) for 15 min at 4 ^{0}C, the top colorless aqueous phase containing the RNA was transferred to a fresh centrifuge tube, and isopropanol (500 µl) was added to it and incubated for 10 min at 4 ^{0}C. The solution was centrifuged at 10,000 rpm (9,382xg), the supernatant was discarded, and the pellet was rinsed twice in 1 ml of 80% ethanol (prepared in DEPC-treated water), dried at RT and dissolved in 10 µl DEPC-treated water. The RNA concentration was measured by Nanodrop (ND1000) spectrophotometer, its integrity and purity were verified by electrophoresis of 1.0 µg of RNA in 1.5% agarose-TBE gel containing 0.5 µg/ml ethidium bromide, and RNA was stored at -80 ^{0}C. Quantitative reverse transcriptase polymerase chain reaction (qRT-PCR) was carried out. For 1st strand cDNA synthesis, the reaction mixture contained M-MLV RT buffer (1x), dNTPs (0.5 mM), RNAsin (20 U), oligo dT (12-18) primer (0.5 µg), RNA (1.0 µg), MMLV Reverse Transcriptase (200 U) in a 25 µl reaction mixture and incubated at 37 ^{0}C. The real-time PCR was carried out by using IRF-1 (5' GGC TGG GAC ATC AAC AAG GAT G 3' and 5' GAG CTG CTG AGT CCA TCA GAG AA 3') and IRF-2 (5' GTT AAG CAC ATC AAG CAA GAA CCA 3' and 5' GCT CTC CTC TTT GAT GGT GAC C 3') forward and reverse primers, respectively. RT-PCR for the GAPDH mRNA was carried out (forward and reverse primers: 5' ACC ACA GTC CAT GCC ATC AC 3' and 5' TCC ACC ACC CTG TTG CTG TA3' respectively) and used as an internal reference for normalization of IRF-1 and IRF-2 mRNA expressions. The KAPA SYBR FAST qPCR Kit (KK4601) was utilized according to the manufacturer's instructions by using an Applied

Biosystems 7500 Fast real-time PCR machine. The data were evaluated by the comparative CT method [200]. For quantitative normalization, IRF-1 and IRF-2 expressions were compared to the internal reference, GAPDH mRNA. The comparative CT (threshold cycle) method also known as the $2^{-\Delta\Delta CT}$ method was used for quantification of the relative gene expression of IRF-1 and IRF-2 [199-200].

5.2.9 Immunofluorescence of IRF-1, IRF-2, Oct3/4, and Sox-2 in the bone marrow cells (BMCs) and MSCs (P1 cells)

Immunofluorescence was performed to analyze the intracellular localization of IRF-1, IRF-2, Oct3/4, and Sox-2 in BMCs and MS-P1 cells. BMCs were isolated from 7-8 weeks C57BL6/J mice as previous. Cells were filtered, counted, and resuspended into DMEM-high glucose. Two million cells were seeded on pre-treated with poly-L-lysine coated coverslip and incubated in the CO_2 incubator for 30 min at 37 ^{0}C. BMCs and culture MS-P1 cells on coverslip were washed with 2ml 1X-PBS followed by cells was fixed with 2 ml, 4% paraformaldehyde for 30 min at RT. After that, paraformaldehyde was aspirated, and cells were washed with 2ml, 3X-PBS. Cells were permeabilized with 2ml, 0.1% Triton X-100 (in 1X-PBS) for 10 min at RT, followed by cells were cleaned twice with 1X-PBS. Blocking was done with 2ml, 1% BSA in 1X-PBS, for 10 min at RT, followed by cells were washed twice with 1X-PBS. After that, cells were incubated with primary rabbit anti-IRF-1 (Santa Cruz sc-13041), primary rabbit anti-IRF-2 (Santa Cruz sc-13042), rabbit anti-Oct3/4 (Sigma O8389), and rabbit anti-Sox-2 (Sigma S9072), antibodies at 1:250 dilutions, overnight at 4 ^{0}C. Lose Primary antibodies were eliminated by washing three times with 2 ml, 0.1% Tween 20 in 1X-PBS (PBST). Then after, cells were incubated with secondary goat anti-rabbit IgG-TRITC (Bangalore GeNei, RTC2), goat anti-rabbit-FITC (Sigma F0382), and rabbit anti-goat IgG-FITC (Bangalore GeNei, FTC2) antibodies at 1:500 dilution, for 30 min at RT. Untied secondary antibodies were eliminated by washing three times with 2 ml, 0.1% Tween 20 in 1X-PBS (PBST), followed by cells were mounted with Vectasheild with DAPI (Vector Labs H-1200). Nikon TiE fluorescence microscopy captured images [201]. Images were analyzed by Image J software and total intensity of control, irradiated and transplanted mice BMCs were measured.

6 RESULTS

6.1 Chapter 1: Isolation, culture, and propagation of bone marrow-derived mesenchymal stem (P0 and P1) cells (MS-P0 cells and MS-P1 cells)

6.1.1 Isolation of long bones, and isolation of bone marrow cells (BMCs)

BMCs were isolated from 7-8 weeks old C57BL/J6 mice **(Figure 1A)** as reported earlier [22-23, 190] with certain modifications. All animal experiments were approved by the Institutional Animal Ethics Committee (IAEC). The mice were sacrificed by cervical displacement following anesthesia. The external body surface of mice was sterilized by 70% (vol/vol) ethanol. The femora, tibiae-fibulae, and humeri were separated out carefully and eliminated from the associated muscles. The bones were kept in 5 ml complete culture medium, i.e., Dulbecco's Modified Eagle's Medium (DMEM) supplemented with 15% heat-inactivated fetal bovine serum (FBS) and 1X antibiotic/antimycotic solution. The freshly isolated femora, tibia, and humeri appeared reddish **(Figure 1B)** due to the presence of BMCs. One end of the bone was cut open using scissors in the laminar flow hood under tissue culture standard sterile conditions. BMCs were collected by inserting a 24-gauge needle, fitted with a syringe, at the uncut end and the marrow was flushed out with 5 ml complete culture medium, and then bone turned whitish **(Figure 1C)** after flushing bone marrow. BMCs were collected in a 15 ml polypropylene culture tube, dissociated by vortex to make a single cell suspension and passed through a 70 μm cell strainer to clear the single cell suspension from any cell clump, bone spicules, muscle, and debris. Single cell suspension centrifuged at 5000 rpm for 5-10 min at room temperature; the cell pellet was resuspended in DMEM-HG medium. BMCs were appropriately diluted and enumerated on a hemocytometer under the bright field microscope by Trypan blue assay to determine the yield and viability of the cells. We found total BMCs per mouse [average 22.93 g body weight **(Graph 1I)**] were 66.9 million **(Graph 1J)** and total live 65.47 million (97.86 %), and dead cells 1.43 million (2.12 %) per mouse respectively **(Graph 1K)**. Then BMCs seeded in a T-25 culture flask at a density of $1x10^6$ BMCs per cm^2 **(Figure 1D)** and images were captured. BMCs images at a different magnification such as 10X **(Figure 1E),** 20X **(Figure 1F)**, 60X **(Figure 1G)**, and 100X **(Figure 1H)** exhibit round shape with different size.

6.1.2 Culture and propagation of bone marrow stem cells or mesenchymal stem (Passage-0) cells (MS-P0 cells) and mesenchymal stem (Passage-1) cells or (MS-P1 cells)

6.1.2.1 Culture and propagation of bone marrow cells (BMCs) or mesenchymal stem (Passage-0) cells (MS-P0 cells)

BMCs were counted on hemocytometer and cultured in the T-25 culture flask. BMCs ($25x10^6$ cells) were seeded at a density of $1x10^6$ cells/cm^2 area of the T-25 culture flask. Then culture flask was incubated at 37 ^{0}C in 5% CO_2 humidified cell culture incubator. Then, let them grow for three days. Post 3 days incubation, the 2/3 old medium was replaced with fresh and pre-warm complete DMEM media in each culture flask. Non-adherent cells washed out during media change and left plastic-adhere cell in the culture flask. Images were captured under bright field microscope on the 3rd day at different magnification. Most of the cells appeared round-shaped with various sizes **(Figure 1A and 1B)**. The adherent cells in culture flask were further incubated at 37 ^{0}C in 5% CO_2 humidified cell culture incubator and cells were cultured until cell confluency reached 70-80% with the replacement of old media with fresh media at every 3rd day. On the other hand, another culture flask were stained with Crystal Violet at 3rd day **(Figure 2A and 2B)** and physical properties such as average length (8.69 µm) **(Figure 2C and Graph 2D)**, average area of BMCs (47.06 µm2) **(Figure 2E and Graph 2F)**, and circularity of BMCs **(Figure 2G, Graph 2H, and 2I)** were measured. At seven-day, 40-50% adhered cells on the surface in culture flask exhibit bidirectional elongated morphology **(Figure 3C and 3D)**. BMCs take 14-15 days to reach 70-80% confluency **(Figure 3E and 3F)**. By this time, around 8-10% cells were round-shaped, 10-15% cells were flatted-shaped, and 60-80% cells were elongated and spindle-shaped, and their number varies culture flask to culture flask. These cells are MS-P0 cells. Images were captured after crystal violet staining under bright field microscopy at different magnification **(Figure 3G and 3H)**. MS-P0 cells culture having plastic adhere property and three types of cells, i.e., round shaped, flatted and fibroblast-like spindle-shaped cells **(Figure 3I)**. The lengthwise size measurement of three distinct cells i.e. round shaped, flatted-shaped, and spindle-shaped cells showed a significant difference in the length of cells **(Figure 3J and Graph 3K)**. The cells at the end of passage 1 were enumerated and prepared the graph **(Graph 3L)**.

6.1.2.2 Culture and propagation of mesenchymal stem (Passage-1) cells or (MS-P1 cells)

Mature spindle-shaped and adhere a layer of BMCs (or MS-P0 cells) were rinsed PBS and detached from the culture flask by trypsin/EDTA. Then, harvested cells (MS-P1 cells) were distributed and seeded into three culture flasks. Then culture flasks were incubated at 37 ^{0}C in 5% CO_2 cell culture incubator. Then, let them grow until cell density reached 70% which takes around 18-21 days. Media (3ml out of 5 ml) was replenished with fresh media on every 3rd day as previous. Images were captured under bright field microscope on the 6th day of culture at different magnification. The density of cells was low at 6th day. Most of the cells of culture appeared spindle-shaped along with some round-shaped cells with various sizes **(Figure 4A and 4B)**. With time, cell number and cell growth increase and confluency were higher at 12th day compared to 6th day **(Figure 4C and 4D)**. The adherent cells in culture flask were further incubated at 37 ^{0}C in 5% CO_2 humidified cell culture incubator until cell confluency reached 70-80%. MS-P1 cells take 21-23 days to reach 70-80% confluency **(Figure 4E and 4F)**. By this time, 80-90% cells show fibroblast-like elongated and spindle-shaped morphology. Images were captured after crystal violet staining under bright field microscopy at different magnification **(Figure 4G and 4H)**. The MS-P1 cells at the end of passage-2 were enumerated and prepared the graph and compared with MS-P0 cells **(Graph 4I)**.

6.1.3 Colony forming unit-fibroblasts (CFU-Fs) assay

Stem cell potential of BMCs was analyzed by CFU-F assay. CFU-F assay is an important parameter that shows the presence of Mesenchymal stem cells in the bone marrow. MSCs have the capability to form colonies of various shapes and sizes during in vitro culture. It is assumed that each colony in a CFU-F assay is produced from a single stem cell. Colonies were fixed, stained with 0.05% Crystal Violet **(Figure 5A)** and most of the colonies were circular or round shaped **(Figure 5B),** but it is not a thumb rule. Size, shape, and number of cells within the colony may vary. The number of colonies was counted **(Table 5C)**. The increase in seeding density did not correlate proportionately with the CFU-Fs count in our experimental set-up ($P > 0.05$) and circumstances **(Graph 5D)**.

6.1.4 Cell cycle status of bone marrow cells (BMCs)

One million harvested BMCs from mice C57BL6/J were fixed in ethanol, and then cells were washed PBS and stained with Propidium iodide. Cell cycle data were acquired on FACS Calibur using FL1 and FL2 channels. We found that histogram **(Figure 6A)** of BMC population shows percentage of Sub G1 phase cells (dead cells) were 0.13± 0.05%, G1 phase cells (activated cells' potential) were 67.94 ± 0.94 %, S-phase 8.17 ± 0.27% and G2M phase cells 10.37 ± 0.24%. Percentage of cells expressing different phases of the cell cycle were tabulated **(Table 6B)** and translated into a graph **(Graph 6C)** which clearly exhibit that bone marrow has the highest percentage of active cells i.e. G1 phase cells.

6.1.5 Characterization of bone marrow cells (BMCs) and mesenchymal stem P1 cells (MS-P1 cells)

6.1.5.1 Immunophenotyping of bone marrow cells (BMCs)

We analyzed the expression of the surface marker of BMCs by FACS, to know, what is the surface marker profile of BMCs for BMCs transplantation? BMCs, the primary cell source of MSCs, were immunophenotype for MSC-positive markers, such as CD29, CD44 & Sca-1, and MSC-negative markers CD34, CD45 and CD11b. Before immunophenotyping, we quantified the live and dead cells by Propidium Iodide (PI) staining method and analyzed live and dead cells in the bone marrow sample. The dot plot, **(Figure 7A)**, indicate the relative size of BMCs. Histogram **(Figure 7B)** shows the cell numbers of unstained and PI stained BMCs. Dot plot, **(Figure 7C),** exhibit unstained or clean BMCs. Dot plot, **(Figure 7D)** of PI stained BMCs which show the percentage of live and dead cells in bone marrow sample. We the found 83.75% cells were live and 4.45% cells were dead. In our study, we found that BMCs show MSC-positive marker expression such as CD29 (68.54 ± 5.45 %) **(Figure 8A)**, CD44 (79.39 ± 4.47 %) **(Figure 8B)**, and Sca-1 (21.39 ± 5.54 %) **(Figure 8C)**. In addition, along with MSC-positive markers expression, we also found that BMCs express low level of MSC-negative markers such as hematopoietic markers CD11b (54.61 ± 2.35 %) **(Figure 8D)**, CD34 (21.12 ± 6.75 %) **(Figure 8E)**, and CD45 (71.34 ± 4.67 %) **(Figure 8F)**. We found BMCs show expression of MSC-positive markers **(Table 8G and Graph 8H)** as well as MSC-negative markers **(Table 8I and Graph 8J)**. Thus, results of FACS analysis show that bone marrow contains a heterogeneous population of cells **(Figure 9A and Graph 9B)**.

6.1.5.2 Immunophenotyping of mesenchymal stem (Passage-1) cells (MS-P1 cells)

MSCs in the bone marrow are capable of moving to damage site. Expression of surface markers of is one of the very fundamental criteria to define MSCs. MSCs characterization includes the very high expression of MSCs positive markers CD29, CD44, Sca-1, CD51, CD73, CD105, and LepR, and negative or very less expression of MSCs negative markers CD11b, CD31, CD34, CD45, and CD86 [22-23, 189-190]. In this study, cultured, mature and spindle-shaped, and plastic adheres MS-P1 cells were characterized by MSCs-positive markers CD29, CD44, Sca-1, and MSCs-negative markers CD11b, CD34, CD45. We found that MS-P1 cells show MSC-positive marker expression such as CD29 (96.90 ± 0.58 %) **(Figure 10A)**, CD44 (39.86 ± 6.47 %) **(Figure 10B)**, and Sca-1 (32.70 ± 14.67 %) **(Figure 10C)**. In addition, along with MSC- positive markers expression, we also found that MS-P1 cells also exhibit very low amount of MSC-negative markers expressions such as CD11b (28.28 ± 0.57 %) **(Figure 10D)**, CD34 (22.63 ± 0.29 %) **(Figure 10E)**, and CD45 (2.47 %) **(Figure 10F)**. We found MS-P1 cells show expression of MSC-positive markers **(Table 10G and Graph 10H)** as well as the low amount of MSC-negative markers **(Table 10I and Graph 10J)**. Thus FACS analysis showed that MS-P1 cells population shows both MSC-positive and very deficient MSC-negative markers expression **(Figure 11A and 11B)**. Comparative quantitative expression analysis of markers on BMCs and MS-P1 cells indicate that MS-P1 cells show decline expression of the MSC-negative marker with the passage **(Figure 12)**.

6.2 Chapter 2: Development of irradiated mouse model and transplantation of bone marrow cells (BMCs) and MSCs into irradiated mouse and study of bone marrow regeneration

6.2.1 Generation of irradiated mouse model

6.2.1.1 Irradiated mouse model

Our purpose of bone marrow transplantation is to regenerate/reconstitute irradiated and damaged bone marrow. Bone marrow transplantation is a choice for the cure of many diseases. The mice were exposed to the total 4Gy (2.14Gy/min), sub-lethal, whole body irradiation in a gamma ray chamber so that freshly isolated bone marrow cells can be transplanted into irradiated mice to study bone marrow regeneration **(Figure 13)**.

6.2.1.2 Isolation of bone marrow cells (BMCs) from donor mouse for transplantation

BMCs were isolated from 7-8 weeks old C57BL/J6 mice **(Figure 1A)** as described earlier [22-23, 189-190] with certain modifications. All animal experiments were approved by the Institutional Animal Ethics Committee (IAEC). The mice were sacrificed by cervical displacement under anesthesia. The external body surface of mice was sterilized by 70% (vol/vol) ethanol. The femora, tibiae-fibulae, and humeri were separated out carefully and removed from the associated muscles. The bones were kept in 5 ml Ix-PBS. The freshly isolated femora, tibia, and humeri appeared reddish **(Figure 1B)** due to the presence of BMCs. One end of the bone was cut open using scissors in the laminar flow hood under tissue culture standard sterile conditions. BMCs were harvested by inserting a 24-gauge needle, fitted with a syringe, at the uncut end and the marrow was flushed out with 5 ml 1x-PBS, and then bone turned whitish **(Figure 1C)** after flushing bone marrow. BMCs were collected in a 15 ml polypropylene culture tube, dissociated by vortex to make a single cell suspension and passed through a 70 μm cell strainer to clear the single cell suspension from any cell clump, bone spicules, muscle and debris **(Figure 1G and H)**. BMCs were appropriately diluted and enumerated on a hemocytometer under the bright field microscope by Trypan blue assay to determine the yield and viability of the cells. A single cell suspension containing $10x10^6$ BMCs centrifuged at 5000 rpm for 5 min at room temperature. The cell pellet was dissolved in 200μl 1x-PBS.

6.2.1.3 Transplantation of donor bone marrow cells (BMCs)

In this study, a dose of 10 million fresh BMCs from healthy donor mouse was transplanted through tail vein injection into irradiated mouse. Four hours post-irradiation, donor BMCs were intravenously transplanted into irradiated recipient mouse via tail vein injection. After 24 hours of transplantation, the control, irradiated and irradiated+transplanted mice were sacrificed by cervical dislocation and BMCs were isolated as mentioned above and study bone marrow regeneration **(Figure 13)** by cell cycle analysis, CFU-F assay and Histological analysis.

6.2.2 Cell cycle analysis of bone marrow cells (BMCs) of control, irradiated and bone marrow transplanted mice by FACS

One million harvested BMCs from control, irradiated, and transplanted mice C57BL6/J were fixed in ethanol, and then cells were washed PBS and stained with Propidium iodide, and cell cycle data were acquired on FACS Calibur using FL1 and FL2 channels. We found Dot plots (SSC versus FSC) **(Figure 14A, 14B, and 14C)** show relative size and granularity of cell of control, irradiated and transplanted mice bone marrow respectively. Dot plots (FL2-A versus FL2-W) **(Figure 14D, 14E, and 14F)** used for doublet discrimination of control, irradiated and transplanted mice the bone marrow respectively. We observed that cell death due to radiation generates more doublets because of sticky nature of dead cells. Histograms **(Figure 14G, 14H, and 14I)** of control, irradiated and transplanted mice bone marrow shows some bone marrow in particular phase of the cell cycle at FL2-A on X-axis versus counts on Y-axis. In irradiated mice (no transplantation), G1 phase cells (activated cells' potential) were significantly lower, i.e., from 62.50 ± 4.18 % in control **(Figure 15A)** to 38.74 ± 3.43 % in irradiated mice **(Figure 15B)**. There was up to 38.01% damage in the G1 phase cells. In the sub G1 phase cells (damaged cells' potential), it increased from 7.08 ± 3.36 % in control **(Figure 15A)** to 30.86 ± 6.08 % in irradiated mice **(Figure 15B)**, i.e. there were about 335.17 % rise in the sub G1 phase cells. In transplanted mice **(Figure 15C)**, G1 phase cells increased from 38.74 ± 3.43 % in irradiated mice **(Figure 15B)** to 48.04 ± 2.70 % in the transplanted mice **(Figure 15C)**, i.e. there was about 24 % recovery of the G1 phase cells and the sub G1 phase cells decreased from 30.86 ± 6.08 % in irradiated to 24.66 ± 5.27 % in transplanted mice, i.e. there were about 12.31 % reduction in the sub G1 phase cells. Other phases S phase and G2M phase cells were also affected but to lesser extents **(Figure 15D)**.

6.2.3 CFU-F assay (stem cell potential of bone marrow) of control, irradiated and transplanted mice during bone marrow regeneration after transplantation

Study of bone marrow recovery considers CFU-F assay as an important parameter that shows the presence of MSCs in the bone marrow. Stem cell potential of the bone marrow was analyzed by CFU-F assay from the control, irradiated and transplanted mice. Different cell densities (1, 2 and 4 million cells) per well were plated in 6 well plate. At day 14th, colonies were fixed, stained with 0.05% Crystal Violet **(Figure 16A)**. Each colony in a CFU-F assay is produced from a single stem cell **(Figure 16B)**, and the number of colonies was counted **(Table 16C)**. We found that one million cells seeded per well showed a significant decline in CFU counts, i.e., from 46.33 in controls to 6.33 in irradiated mice and the damage due to radiation were up to 86.34%. Further, CFU count significantly increased from 6.33 in irradiated to 22.33 in transplanted mice, i.e., the recovery (regeneration) due to transplantation was 34.53 %. Similarly, two million cells seeded per well showed significant decline in CFU count from 66.33 in control to 13.67 in irradiated mice, i.e. damage due to radiation was 79.39 %, further CFU count significantly increased from 13.67 in irradiated to 35.00 in transplanted mice, i.e. the recovery (regeneration) due to transplantation was 32.16 %. Four million cells seeded per well showed a similar trend, but due to too many cells results were at low level, i.e. CFU count declined **(Graph 16D)**. We found that damage to bone marrow potential due to radiation was 86.34 %, 79.39 %, and 54.77 % and recovery of bone marrow potential due to transplantation was 34.53 %, 32.16 % and 8.71 % in one, two and four million seeded cells respectively **(Table 16E)**.

6.2.4 Histological analysis of femur bone of control, irradiated and transplanted mice to study the bone marrow regeneration

Since histological study reveals the internal structure of the tissue, it could be an important parameter to study bone marrow regeneration. Long bones such as femur bone from the mice were isolated, washed twice with PBS, fixed in paraformaldehyde solution and decalcified with EDTA solution. Finally, 5-10 μm thick sections were cut by using a radial microtome. Hematoxylin and eosin stained section of femur bone of control, irradiated, and transplanted mice show cellular density in the bone of control, irradiated, and transplanted mice respectively. Irradiated mice bone is having lower cellularity and contains a large central cavity after radiation. Transplanted mice bone also includes cavity of small size, because

cellularity was increased after transplantation of BMCs **(Figure 17A)**. Higher magnification images of femur bone of control, irradiated, and transplanted mice clearly show that the cellular density of irradiated bone marrow was very little compared to control and it comes back in transplanted mice compared to irradiated mice bone marrow respectively **(Figure 17B)**. We analyzed cellularity; we found that 4 Gy irradiation caused 43.44 % decrease in cellularity of bone marrow of irradiated mice and formed a large cavity as compared to control **(Figure 17A)**. This cavity may be due to the radiation-induced DNA double strand breaks triggering genomic instability and cell death due to apoptosis and narcosis. However, as a result of transplantation, the freshly injected BMCs migrated towards the damaged sites in the bone marrow and repaired the damaged area. This regeneration process involves secretion of cell growth and differentiation factors and restoration of cellularity in bone marrow. We found that transplantation of 10 million BMCs to irradiated mice by the tail vein injection increased the cellularity up to 28.45% after 24 hours **(Graph 17C)** and decreased the cavity in the bone marrow formed due to the radiation-induced damage.

.

6.3 Chapter 3: Expression and localization of interferon regulatory factor 1 and 2 (IRF-1 and IRF-2)

6.3.1 Expression analysis of IRF-1, IRF-2 genes of control, irradiated and transplanted mice during bone marrow regeneration by real-time RT-PCR

IRF-1 and IRF-2 have various well-established functions in different kinds of BMCs such as B cells, T cells, and NK cell. However, their functional significance is yet to be investigated in bone marrow regeneration except very few findings associated with BMCs. Hence, we first decided to determine the function of IRF-1 and IRF-2 transcription factors during bone marrow regeneration. We measured their mRNA expressions in BMCs from the control, irradiated and transplanted mice by using quantitative real-time RT-PCR. We found that IRF-1 mRNA expression was significantly higher in irradiated (4.34x fold) and transplanted (3.85x fold) as compared to control mice **(Figure 18A)**. Similarly, IRF-2 mRNA expression was significantly higher in irradiated (3.87x fold) and transplanted (3.46x fold) as compared to control mice **(Figure 18B)**. Moreover, IRF-1 mRNA exhibited higher expression level compared to IRF-2 mRNA in BMCs of irradiated (1.12x fold) and irradiated+transplanted (1.11x fold) mice **(Figure 18)**. These results show that both IRF-1 and IRF-2 are radiation-responsive genes in BMCs and the extent of bone marrow regeneration by transplantation mentioned here is not sufficient to bring their mRNA expressions up to the normal state. It is presumed that genes regulated by IRF- 1 and IRF-2 may play a role in the cellular response to the radiation-induced damage in these cells.

6.3.2 Localization and expression of interferon regulatory factor 1 and 2 (IRF-1 and IRF-2) and pluripotency-associated transcription factors (Oct3/4 and Sox-2) in bone marrow cells (BMCs)

6.3.2.1 Localization of endogenous interferon regulatory factors (IRF-1 and IRF-2) in bone marrow cells (BMCs)

A variety of cells expressed both IRF-1 and IRF-2, e.g., BMCs, macrophages, monocytes and epithelial cells. IRF-1 and IRF- 2 are involved in cytokine regulation, immune response, cell growth regulation, apoptosis and cell differentiation under a variety of conditions. Real-time RT-PCR is confirming the expression of IRF1 and IRF2 at mRNA level. Further, we also wanted to check their expression at protein level in BMCs. Negative control shows no

bleeding of signals **(Figure 19)**. Confocal immunofluorescence microscopic image illustrates the expression of IRF-1 **(Figure 20)** and IRF2 **(Figure 21)**. Their expression further checked by double immunostaining of BMCs by anti-IRF-1 and anti-IRF-2 antibodies **(Figure 22)**.

6.3.2.2 Localization and expression pluripotency-associated transcription factors (Oct3/4 and Sox-2) in BMCs

Expression of pluripotency-associated transcription factors, such as Oct3/4, Sox-2, Nanog, Olig, Klf4, c-Myc, etc., is responsible for specifying the gene expression programs in the stem cells. In this study, we checked the expression of two pluripotency-associated transcription factors Oct3/4 and Sox-2 in BMCs. We found that Oct3/4 shows nuclear as well as cytoplasmic expression, but its localization were preferentially more peripheral in BMCs **(Figure 23)**. Whereas, Sox-2 shows stable expression i.e. uniformly express in nucleus and cytoplasm of BMCs **(Figure 24)**.

6.3.3 Localization of endogenous interferon regulatory factor 1 and 2 (IRF-1 and IRF-2) of control, irradiated and transplanted mice bone marrow cells (BMCs) during bone marrow regeneration

Intracellular localization of IRF-1, IRF-2 was studied in the BMCs by immunofluorescence. Expression of IRF-1 and IRF-2 in BMCs, of the control, irradiated and transplanted mice by confocal immunofluorescence microscopy showed low nuclear/cytoplasm ratio. Although the nucleus occupies most of the cellular space, BMCs mainly showed cytoplasmic expression of IRF-1 and IRF-2.

6.3.3.1 Localization of endogenous interferon regulatory factor-1 (IRF-1) of control, irradiated and transplanted mice bone marrow during bone marrow regeneration

In this study, we found that immunofluorescence for IRF-1 expression was cytoplasmic **(Figure 25A)**. Larger views of confocal immunofluorescence microscopic images show expression and cytoplasmic localization of IRF-1**(Figure 25B)**. We also found that IRF-1 showed significantly higher expression in irradiated (2.12x fold) and transplanted (1.73x fold) as compared to BMCs of control mice **(Graph 25C)**.

6.3.3.2 Localization of endogenous interferon regulatory factor-2 (IRF-2) of control, irradiated and transplanted mice bone marrow cells (BMCs) during bone marrow regeneration

Similar to the IRF-1, we found that immunofluorescence for IRF-2 expression was cytoplasmic **(Figure 26A)**. Larger views of confocal immunofluorescence microscopic images show expression and cytoplasmic localization of IRF-2 **(Figure 26B)**. We also found that immunofluorescence for IRF-2 was more in irradiated (1.71x fold) and transplanted (1.21x fold) as compared to control **(Graph 26C)**. These results showed that BMCs of irradiated mice expressed higher levels of IRF-1 and IRF-2 mRNAs and proteins and the elevated expressions did not decline to normal concentrations in transplanted mice up to 24 hours. Also, a higher number of cells expressed IRF-1 and IRF-2 in BMCs of irradiated mice compared to control and transplanted mice. Thus IRF-1 and IRF-2 are radiation-responsive genes in BMCs, and they may be involved in the bone marrow regeneration.

6.3.4 Localization and expression of interferon regulatory factor 1 and 2 (IRF-1 and IRF-2) and pluripotency-associated transcription factors (Oct3/4 and Sox-2) in mesenchymal stem (Passage-1) cells (MS-P1Cells)

6.3.4.1 Localization of endogenous interferon regulatory factor 1 and 2 (IRF-1 and IRF-2) in MS-P1 cells

After the confirmation of IRF-1 and IRF-2 expression and localization in bone marrow, this study was further extended to find out constitutive expression and Spatio-temporal localization of IRF-1 and IRF-2 proteins in MS-P1 cells. The control panel, wherein no primary antibody was added, did not show cross binding or non-specific binding by secondary anti-rabbit IgG **(Figure 27)**. Apart from BMCs which showed cytoplasmic expression of IRF-1 and IRF-2 in bone marrow, cultured MS-P1 cells displayed spatial specification, with IRF-1 consistently showing cytoplasmic preference **(Figure 28)**, while IRF2 was mainly localized in the nucleus **(Figure 29)**. Their expression further checked by double immunostaining of MS-P1 cells by anti-IRF-1 and anti-IRF-2 antibodies **(Figure 30A-G)**. Comparative analysis of intensities of IRF-1 and IRF-2 of MS-P1 cells showing that IRF-1 shows 3.11X time more cytoplasmic expression compared to nuclear expression and IRF-2 shows 4.19X time more nuclear expression compared to cytoplasmic expression in MS-P1 cells. Moreover, IRF-1

shows 1.57X time higher cytoplasmic expression compared to IRF-2 cytoplasmic expression, and IRF-2 shows 13.09X time higher nuclear expression compared to IRF-1 nuclear expression in MS-P1 cells **(Figure 30H)**.

6.3.4.2 Localization and expression pluripotency-associated transcription factors (Oct3/4 and Sox-2) in MS-P1 cells

Expression of pluripotency-associated transcription factors, such as Oct3/4, Sox-2, Nanog, Olig, Klf4, c-Myc, etc., are responsible for reprogramming of cells. In our study, we checked the expression of two pluripotency-associated transcription factors Oct3/4 and Sox-2 in MS-P1 cells similar to BMCs. We found that Oct3/4 shows nuclear as well as cytoplasmic expression, but its localization were preferentially more peripheral as compared to Sox-2 in MS-P1 cells **(Figure 31)**. Whereas, Sox-2 shows regular expression i.e. uniformly express in nucleus and cytoplasm in MS-P1 cells **(Figure 32)**.

6.3.5 Statistical analysis

The data presented are mean ± SEM from three independent experiments unless otherwise mentioned. ANOVA was used to find out the statistical significance between groups. P value < 0.05 was considered statistically significant *, $P \leq 0.05$, **, $P \leq 0.01$, ***, $P \leq 0.001$ and P value > 0.05 was considered statistically non-significant and represented as n.s. This notation has been used in the data mentioned in the figures. For analysis of microscopic images comparable fields were selected and a few fields were observed to record representative results.

7 DISCUSSION

The mammalian bone marrow, the largest semi-solid organ, resides in the center and the epiphysis of long bones like femora, tibia, humeri, ribs, pelvis, vertebrae, and skull [2]. Bone marrow is a major source of stem cells and immune cells, which creates and replaces the cells of the blood and immune system. Thus bone marrow functions as an immune regulatory organ and controls the immunity of the body [4]. Bone marrow contains three principal types of stem cells. Hematopoietic stem cells (HSCs), it develops all kinds of blood cells, localized in both endosteal niche and vascular niche [10]. Mesenchymal stem cells (MSCs) have trophic capabilities and immunomodulatory properties and found in all tissues, mostly vascularised tissues of the body [6, 11]. The multipotent adult progenitor cells (MAPCs) can differentiate into MSCs and hematopoietic lineage [7, 12].

Previous researchers have demonstrated that ionizing radiation is a primary cause of bone marrow failure, which restricts hematopoiesis, suppresses differentiation of immune cells, and inhibits proliferation of hematopoietic progenitor cells in the hematopoietic microenvironment [185]. Moreover, ionizing radiation may lead to a decline in hematopoietic precursors, cause hematopoietic dysfunction, a reduction in the bone marrow cellularity, reduce bone mineralization and pose a higher risk of bone marrow failure [45].

The previous studies showed that bone marrow transplantation, a recommended treatment under conditions of bone marrow failure, is practiced for the treatment of many diseases such as non-malignant, malignant blood diseases and autoimmune diseases [49-50]. Transplanted bone marrow may be a great help under such conditions. The collected preliminary data revealed that systemic administration of BM-MSCs could make a contribution to the treatment of radiation-induced injury or damage and radiation-induced insults. It has been observed that protection and prevention from the death of the critically irradiated cells depend on effective treatment modality, administered immediately within a few hours following radiation exposure [63].

The pluripotency of stem cells is regulated by pluripotency-associated transcription factors including Oct4, Sox-2, and Nanog. In addition to this, KLF, cMYC, and SALL4 have been detected to play a very crucial role in maintaining pluripotency. These pluripotency-associated

transcription factors are predominantly shown in pluripotent cell types such as ES, BMCs, HSCs, and MSCs and also required in several cellular processes such as differentiation, lineage specification, and self-renewal. It is expected that Oct4, Sox-2, Nanog, KLf, cMYC and SALL4 factors are significant for cell fate decisions [28, 31-32, 202]. We observed expression of Oct3/4 and Sox-2 proteins in BMCs and MS-P1 cells.

We expected that the interferon regulatory factor (IRF) transcription factors might also play a significant role in bone marrow cells (BMCs) and their regeneration. IRFs activate diversity of genes playing central roles in the regulation of both innate and adaptive immunity during bone marrow regeneration or recovery. IRF-1 plays an essential role in controlling the cell proliferation [56], while IRF-2 shows an antagonistic relationship with IRF-1 [52-53, 97, 203]. We have investigated expressions of IRF-1 and IRF-2 mRNAs and proteins in BMCs of the mice after radiation-induced bone marrow damage and recovery by transplantation of freshly isolated BMCs.

MSCs isolated from mouse [22, 176], rat [177], and human bone marrow [178-179] have been extensively studied, because they are easy to isolate, culture, easy for adherence to plastic culture dishes and to expand in laboratory conditions. However, selection of passage(s) cells from in vitro conditions is very critical because early cell passage(s) may contain cellular contaminants of hematopoietic cells, and other lineage of cells [22, 176] and late passage MSCs are susceptible to undergo senescence and even chromosomal abnormalities [180]. The previous study showed that late passage cells lost their fibroblast-like morphology and experienced decreased expression in the mRNA levels of CD73 and CD29 [204]. Moreover, self-renewal and differentiation potential of MSCs depend on the passage of cells [181].

Considering above facts, we need to work on improving isolation of BMCs and developing a new method for bone marrow transplantation to cure the radiation-induced bone marrow damage and bone marrow related diseases to make BMC-based cell therapy more effective, efficient and pragmatic. We have also made preliminary effort to evaluate the therapeutic potential of BMCs regarding cell cycle (G1 phase recovery), CFU-Fs recovery, and recovery of bone marrow cellularity by histology. Also, we need to improve the existing method of isolation, culture, propagation, characterization, and visualization of biological processes under in vitro conditions. In this study, we report that interferon regulatory factors (IRF-1 and

IRF-2) may play their role(s) during bone marrow regeneration in a radiation-induced bone marrow depletion experimental mouse model and their localization in BMCs and mesenchymal stem (Passage-1) cells (MS-P1 cells) appeared the cell type specific and the transcription factor specific. This aspect may be interesting and important for bone marrow stem cells' functions and bone marrow regeneration. Future study may be carried out in this direction.

7.1 Chapter 1: Isolation, culture, and propagation of bone marrow-derived mesenchymal stem (P0 and P1) cells (MS-P0 cells and MS-P1 cells)

7.1.1 Isolation of long bones, and isolation of bone marrow cells (BMCs)

Previous researchers have shown that BMCs are very useful in improving several diseases such as liver fibrosis [205], regenerate infarcted myocardium [206]. Thus study of BMCs required for clinical use of BMCs. BMCs were isolated from 7-8 weeks old C57BL/J6 mice **(Figure 1A)** as reported earlier [22, 176, 190] with certain modifications. The femora, tibiae-fibulae, and humeri were separated out carefully and eliminated from the associated muscles. The freshly isolated femora, tibia, and humeri appeared reddish **(Figure 1B)** due to the presence of BMCs and then bone turned whitish **(Figure 1C)** after flushing bone marrow. Trypan blue assay determined the yield and viability of the cells. We found total BMCs per mouse [average 22.93 g body weight **(Graph 1I)**] were 66.9 million **(Graph 1J)** and total live cells were 65.47 million (97.86 %), and dead cells 1.43 million (2.12 %) per mouse respectively **(Graph 1K)**. Then BMCs were seeded in a T-25 culture flask at a density of $1x10^6$ BMCs per cm2 **(Figure 1D)** and images were captured. BMCs images at different magnifications such as 10X **(Figure 1E),** 20X **(Figure 1F)**, 60X **(Figure 1G)**, and 100X **(Figure 1H)** exhibit round shape with different size. Round shape with different size, morphological appearance of freshly isolated BMCs at high magnification were very similar to previously reported observation [207].

7.1.2 Culture and propagation of bone marrow derived mesenchymal stem (Passage-0) cells (MS-P0 cells) and mesenchymal stem (Passage-1) cells or (MS-P1 cells)

Mammalian bone marrow is a rich source of stem cells, which create and replace the blood and immune system. There are four major types of stem cells in bone marrow, hematopoietic stem cells (HSCs) [10, 208], MSCs [6, 11, 18, 71, 209], multipotent adult progenitor cells

(MAPCs) [25, 210] and VSELs (very small embryonic-like stem cells) [8]. Bone marrow derived MSCs defined as most adherent cells of bone marrow stroma [182]. MSC was also known by another different name such as bone marrow stem cells, stromal stem cells, marrow progenitor cells, and marrow derived adult stem cells [183]. Previous studies have shown that primary tissue source of MSCs is bone marrow [22, 176, 189]. Other studies show that the most important sources of MSCs are the umbilical cord, endometrial polyps, menses blood, adipose tissue, placenta, cruciate ligament and fallopian tubes, etc. [175]. It is reported that one MSC is found in 10000 BMCs in the bone marrow [211]. Arnold I. Caplan has described that MSCs produce regenerative microenvironment at the site of injury because these cells produced many bioactive molecules. These molecules have immunoregulatory properties. This capacity of MSCs, providing paracrine molecules at the site of injury, called "trophic activity" [6]. MSCs have several characteristics properties like- self-renewal, multilineage differentiation (like all stem cells) and capacity to adhere to plastic support [175]. Morphologically, MSCs look like fibroblasts which have a large nucleus in long thin cell body [184]. Initially, BMCs, post 2 hours of isolation, appeared round-shaped with various sizes **(Figure 1)**. Bone marrow derived MS-P0 cells took 14-15 days to reach 70-80% confluency. The previous report showed that MS-P0 cells contained three different kinds of cells round-shaped, flattened-shaped, and elongated and spindle-shaped cells [212]. We found the similar results, after 14-15 days we got MS-P0 cells, around 8-10% cells were round-shaped, 10-15% cells were flattened-shaped, and 60-80% cells were elongated and spindle-shaped, and their number varied from culture flask to culture flask **(Figure 3)**. Cultured MS-P0 cells were rinsed with PBS and detached from the culture flask by trypsin/EDTA. Then, harvested cells (MS-P1 cells) were seeded again and cultured them until cell density reached 70% which took around 18-21 days. Previous research showed that MS-P1 cells exhibited fibroblast-like spindle-shaped morphology [189]. In our study we found similar results, MS-P1 cells took 21-23 days to reach 70-80% confluency. By this time, 80-90% cells showed fibroblast-like elongated and spindle-shaped morphology [213] **(Figure 4)**.

7.2 Characterization of bone marrow cells (BMCs) and mesenchymal stem (Passage-1) cells (MS-P1 cells)

7.2.1 Immunophenotyping of bone marrow cells (BMCs)

We analyzed the expression of the cell surface markers of BMCs by FACS, to know, what was the surface marker profile of BMCs for BMC transplantation? Bone marrow is the primary source of MS-P1cells. BMCs of bone marrow showed positive immunophenotype for MSC-positive markers: CD29, CD44 & Sca-1, and far less for MSC-negative markers: CD34, CD45 and CD11b. Before immunophenotyping, live and dead cells were quantified by the Propidium Iodide (PI) staining method. We found 83.75% cells were live and 4.45% cells were dead **(Figure 7)**. In a previous study, it was revealed that freshly isolated bone marrow Sca-1^+ and Sca-1^- cells initially expressed no or very less CD44 surface marker, CD29 expression was uniformly higher in bone marrow cells with Sca-1^+ and Sca-1^- background. Additional CD44 and Sca-1 surface marker expression increased with the passage of the cells in culture [194]. In our study, we found that BMCs showed relatively less expression of Sca-1 (21.39 ± 5.54 %) **(Figure 8C)**. In contrast to no or very less expression of CD44 expression in freshly isolated BMCs, we observed relatively higher expression of CD44 (79.39 ± 4.47 %) **(Figure 8B),** and CD29 (68.54 ± 5.45 %) **(Figure 8A)**. In addition, along with expression of the MSC-positive markers, we also found that BMCs expressed MSC-negative markers such as the hematopoietic markers CD11b (54.61 ± 2.35 %) **(Figure 8D)**, CD34 (21.12 ± 6.75 %) **(Figure 8E)** and CD45 (71.34 ± 4.67 %) **(Figure 8F)**. Thus FACS analysis showed that based on expression of cell surface markers, bone marrow contained a heterogeneous population of cells. Thus, we found BMCs showing expression of MSC-positive markers **(Table 8G and Graph 8H)** as well as MSC-negative markers **(Table 8I and Graph 8J)** as previously reported [214]. Thus FACS analysis demonstrates that bone marrow contains a heterogeneous population of cells **(Figure 9A and Graph 9B)**. We also found that our results, percentage of cells expressing CD29, CD44, Sca-1, and CD45, were somewhat similar to the other previously reported findings, except CD34, which showed a difference considerably [215].

7.2.2 Immunophenotyping of mesenchymal stem (Passage-1) cells (MS-P1 cells)

MSCs from bone marrow can move to damage sites in other tissues. Expression of cell surface markers is one of the crucial criteria to define MSCs [190]. Cultured MSCs differ from bone

marrow MSCs with respect to several markers, but researchers used different approaches to isolate and to characterize MSCs. That is why International Society for Cellular Therapy (ISCT) has set a minimal criterion to define MSCs which includes the following: MSCs must have plastic-adherence property, positive for surface markers such as CD105, CD73, and CD90, and negative for CD45, CD34, CD14 or CD11b, CD79α or CD19 and HLA-DR surface molecules and get differentiated into adipocytes, chondroblasts, and osteoblasts *in vitro* [190, 216]. MSCs show high expression of positive markers, e.g., CD29, CD44, Sca-1, CD51, CD73, CD105, and LepR, and negative expression for markers, e.g., CD11b, CD31, CD34, CD45 and CD86 [22, 176, 188, 217]. Previous reports showed that first passage MSCs express CD44 more that 98.1%, Sca-1 53.3%, while CD11b, CD34, and CD45 are expressed up to less that 1% [189]. In contrast to this expression of MSCs passage -1 surface markers, we found that MS-P1 cells showed MSC-positive marker expression such as CD29 (96.90 ± 0.58 %) **(Figure 10A)**, CD44 (39.86 ± 6.47 %) **(Figure 10B)**, and Sca-1 (32.70 ± 14.67 %) **(Figure 10C)**. In addition, along with MSC-positive markers expression, we also found that MS-P1 cells also exhibited very low amount of MSC-negative markers' expression such as hematopoietic markers CD11b (28.28 ± 0.57 %) **(Figure 10D)**, CD34 (22.63 ± 0.29 %) **(Figure 10E)**, and CD45 (2.47 %) **(Figure 10F)**. We found MS-P1 cells showed expression of MSC-positive markers **(Table 10G and Graph 10H)** as well as the low amount of MSC negative markers **(Table 10I and Graph 10J)**. Thus FACS analysis shows that MS-P1 cells population shows both MSC-positive and very little MSC-negative markers expression **(Figure 11A and 11B)**.

We also found that MSC-positive marker expression increased from BMCs to MS-P1 cells as CD29 increased from 68.54 ± 5.45 % to 96.90 ± 0.58 %, Sca-1 increased from 21.39 ± 5.54 % to 32.70 ± 14.67 %, whereas CD44 decreased from 79.39 ± 4.47 % to 39.86 ± 6.47 %. While MSC negative marker expression decreased from BMCs to MS-P1 cells as CD11b decreased from 54.61 ± 2.35 % to 28.28 ± 0.57 %, and CD45 decreased from 71.34 ± 4.67 % to 2.47 %, while CD34 remain unchanged around 21.12 ± 6.75 % to 22.63 ± 0.29 %. Thus, these results are suggesting an enrichment of MSCs during the culture. Comparative quantitative expression analysis of markers on BMCs and MS-P1 cells indicate that MS-P1 cells show a decline in the expression of the MSC-negative markers with the passage **(Figure 12)**.

7.3 Chapter 2: Development of irradiated mouse model and transplantation of bone marrow cells (BMCs) and MSCs into irradiated mouse and study of bone marrow regeneration

7.3.1 Generation of irradiated mouse model

7.3.1.1 Irradiated mouse model

Bone marrow is a major source of producing various types of blood cells, immune cells, like B and T lymphocytes that support the immune system. Bone marrow function could be affected by certain factors such as chemical, physical or biological. One of such factors is radiation which could cause damage to bone marrow. Ionizing radiation such as gamma- and X-rays are causes of DNA double-strand breaks and trigger generation of reactive oxygen species (ROS), which further causes damage of cells of various types, including hematopoietic stem and progenitor cells [48, 218]. Previously reported studies have demonstrated that ionizing radiation is the primary cause of bone marrow failure because of the change in the hematopoietic microenvironment. This situation results in a rise in the number of adipocytes in bone marrow that regulates hematopoiesis, suppresses differentiation of immune cells, and inhibits proliferation of hematopoietic progenitor cells [185]. Moreover, ionizing radiation may lead to a decline in hematopoietic precursors, a reduction in the bone marrow cellularity, hematopoietic dysfunction; reduce bone mineralization and a higher risk of bone marrow failure [219]. Bone marrow transplantation is recommended under conditions of bone marrow failure. The previous studies have shown that bone marrow transplantation is practiced for the treatment of many diseases such as non-malignant, malignant blood diseases, autoimmune diseases and metabolic diseases [49-50]. The regenerative potential of transplanted bone marrow is a great help under such conditions. Earlier clinical transplantation studies have shown that high dose of total body irradiation caused first, increased vascular permeability resulting in more bone marrow stem cells entering the site of damage, creating extra space in bone marrow, reducing the struggle between the host stem cells and transplanted donor stem cells and finally limiting the rejection of the donor graft [191]. Moreover, radiation causes the production of free radicals, affecting self-renewal, survival, and differentiation of the stem cells [220]. Furthermore, other studies have shown that high dose or lethal dose of total body irradiation reduced the retention of transplanted donor stem cells [191]. Therefore, in our

study, the mice were subjected to total 4Gy (2.14Gy/min), sub-lethal dose of whole body irradiation in a gamma ray chamber [185], so that freshly isolated BMCs can be transplanted into irradiated mice to study bone marrow regeneration **(Figure 13)**.

7.3.1.2 Transplantation of donor bone marrow cells (BMCs)

Our purpose of bone marrow transplantation is to regenerate/reconstitute irradiated and damaged bone marrow. Bone marrow transplantation is a choice for the cure of many non-malignant and malignant blood-related diseases. Hence, *in vivo,* preclinical mouse model study is very crucial because *in vitro* study cannot reveal the complications of the *in vivo* system [50, 191]. In our study of bone marrow regeneration, we irradiated mice that caused depletion of bone marrow, weakened the immune system and then carried out transplantation of BMCs by tail vein injection. The previous study has shown that transplanted BMCs shift the damaged bone marrow conditions towards healthy conditions by replacing the damaged cells, secreting important factors for proliferation, differentiation of cells and regenerate bone marrow [191]. The hematopoietic system of mouse contains 300 million HSCs that produce 260 million new blood cells in a day to maintain homeostasis in the peripheral blood system [221]. In this study, a dose of 10 million fresh BMCs from healthy donor mouse was transplanted through tail vein injection into irradiated mouse 4 hours after irradiation [49-50, 191]. After 24 hours of transplantation, control, irradiated and irradiated+transplanted mice were sacrificed by cervical dislocation and BMCs were isolated as mentioned above and to study the bone marrow regeneration **(Figure 13)**.

7.3.2 Cell cycle analysis of bone marrow cells (BMCs) of control, irradiated and bone marrow transplanted mice by FACS

Previous reports have shown that gamma radiation caused double strand DNA breaks in the genome mostly in actively dividing cells and seized their cell cycle. Consequently, cells having multiple DNA damage/breaks in the genome suffer from genomic instability and undergo cell death through apoptosis or necrosis because the cells could not repair the DNA damage to restore the normal state. Since mitotically active cells of bone marrow and hematopoietic system show high sensitivity towards irradiation, it causes inhibition of cell proliferation and severe damage to bone marrow [50, 191]. Our observation also showed a similar result. Therefore, transplantation of bone marrow may be a good way to restore

irradiated/damaged bone marrow to a healthy state. BMCs isolated from control, irradiated and transplanted mice were analyzed for cell cycle status by FACS. We found Dot plots (SSC versus FSC) **(Figure 14A, 14B, and 14C)** and Dot plots (FL2-A versus FL2-W) **(Figure 14D, 14E, and 14F)** used for relative size and granularity of cell and doublet discrimination of control, irradiated and transplanted mice bone marrow respectively. We observed that cell death due to radiation generated more doublets because of sticky nature of dead cells. Histograms **(Figure 14G, 14H, and 14I)** of control, irradiated and transplanted mice bone marrow showed some bone marrow in particular phase of the cell cycle at FL2-A on X-axis versus counts on Y-axis. In irradiated mice (no transplantation), G1 phase cells (activated cells' potential) were significantly lower, i.e., from 62.50 ± 4.18 % in control **(Figure 15A)** to 38.74 ± 3.43 % in irradiated mice **(Figure 15B)**. There was up to 38.01% damage in the G1 phase cells. In the sub G1 phase cells (damaged cells' potential), it increased from 7.08 ± 3.36 % in control **(Figure 15A)** to 30.86 ± 6.08 % in irradiated mice **(Figure 15B)**, i.e., there were about 335.17 % rise in the sub G1 phase cells. In transplanted mice **(Figure 15C)**, G1 phase cells increased from 38.74 ± 3.43 % in irradiated mice **(Figure 15B)** to 48.04 ± 2.70 % in transplanted mice **(Figure 15C)**, i.e., there was about 24 % recovery of the G1 phase cells and the sub G1 phase cells decreased from 30.86 ± 6.08 % in irradiated to 24.66 ± 5.27 % in transplanted mice, i.e. there were about 12.31 % reduction in the sub G1 phase cells. Other phases, S phase and G2M phase cells were also affected but to lesser extents **(Figure 15D)**.

7.3.3 CFU-F assay of normal, irradiated and transplanted mice or stem cell potential of bone marrow during bone marrow regeneration after transplantation

Study of bone marrow recovery considers CFU-F assay as an important parameter that shows the presence of MSCs in bone marrow of irradiated (not transplanted) and bone marrow transplanted mice indicating the stem cell potential of the marrow. It is assumed that each colony in a CFU-F assay is produced from a single stem cell [220]. The previous study has shown that the number of CFU-F increases and their absolute number decreases after three days of irradiation with a total 4Gy irradiation dose [185]. In contrast, it has also been shown that no CFU-F colonies were found at seven days after irradiation of total 20 Gy radiation dose [222]. Additionally, further research has shown that the CFU-F count decreases with age of mice [223], oxygen tension [194] and a number of passages in the culture [220]. Therefore, CFU-F assay was carried out to analyze bone marrow potential during bone marrow

regeneration after transplantation and under *in vitro* conditions of the culture of the repopulated cells. Different cell densities (1, 2 and 4 million cells) per well were plated in 6 well plate. At day 14th, colonies were fixed, stained with 0.05% Crystal Violet **(Figure 16A)**. Each colony in a CFU-F assay is produced from a single stem cell **(Figure 16B)**, and the number of colonies were counted **(Table 16C)**. We found that one million cells seeded per well showed a significant decline in CFU counts, i.e., from 46.33 in control to 6.33 in irradiated mice and the damage due to radiation were up to 86.34%. Further, CFU count significantly increased from 6.33 in irradiated to 22.33 in transplanted mice, i.e., the recovery (regeneration) due to transplantation was 34.53 %. Similarly, two million cells seeded per well showed significant decline in CFU count from 66.33 in control to 13.67 in irradiated mice, i.e. damage due to radiation was 79.39 %, further CFU count significantly increased from 13.67 in irradiated to 35.00 in transplanted mice, i.e. the recovery (regeneration) due to transplantation was 32.16 %. Four million cells seeded per well showed a similar trend, but due to too many cells the results were at low level, i.e. CFU count declined **(Graph 16D)**. We found that damage to bone marrow potential due to radiation was 86.34 %, 79.39 %, and 54.77 % and recovery of bone marrow potential due to transplantation was 34.53 %, 32.16 % and 8.71 % in one, two and four million seeded cells respectively **(Table 16E)**.

7.3.4 Histological analysis of femur bone of control, irradiated and transplanted mice to study the bone marrow regeneration

Bone marrow is a structurally extensive and functionally dynamic tissue residing in the central cavity of the long bones [2]. Since histological study reveals the internal structure of the tissue, it could be an important parameter to study bone marrow regeneration. Hematoxylin and eosin stained section of femur bone of control, irradiated, and transplanted mice showed cellular density in the bone of control, irradiated, and transplanted mice respectively. We got more or less similar results of histological analysis of control mice bone marrow as previously reported histological examinations of bone marrow [2] **(Figure 17A)**. Previous studies demonstrated that ionizing radiation reduces the bone marrow cellularity, and reduce bone mineralization [45]. We found the similar result as previous studies explained. We got that irradiated mice bone showed lower cellularity and contained a large central cavity after the radiation. Transplanted mice bone also included cavity of small size, because cellularity was increased after transplantation of BMCs **(Figure 17A)**. Higher magnification images of femur

bone of control, irradiated, and transplanted mice clearly showed that the cellular density of irradiated bone marrow was very little compared to control and it came back in transplanted mice compared to irradiated mice bone marrow respectively **(Figure 17B)**. We analyzed the cellularity, and we found that 4 Gy irradiation caused 43.44 % decrease in the cellularity of bone marrow of irradiated mice and formed a large cavity as compared to control **(Figure 17A)**. This decrease in the cellularity may be due to the radiation-induced DNA double strand breaks triggering genomic instability and cell death due to apoptosis and narcosis. However, as a result of transplantation, the freshly injected BMCs migrated towards the damaged sites in bone marrow and repaired the damaged area. This regeneration process involves secretion of cell growth and differentiation factors and restoration of cellularity in bone marrow. We found that transplantation of 10 million BMCs to irradiated mice by the tail vein injection method increased the cellularity up to 28.45% after 24 hours **(Graph 17C)** and decreased the cavity in bone marrow formed due to the radiation-induced damage. Later time points of the observation are expected to yield better results.

.

7.4 Chapter 3: Expression and localization of interferon regulatory factor-1 and -2 (IRF-1 and IRF-2)

7.4.1 Expression analysis of IRF-1 and IRF-2 genes of control, irradiated and transplanted mice bone marrow cells (BMCs) during bone marrow regeneration by real-time RT-PCR

We expected that IRF transcription factors might also play a significant role in BMCs and their regeneration. IRFs activate diversity of genes playing central roles in the regulation of both innate and adaptive immunity during bone marrow recovery. IRF-1 plays essential role in controlling cell proliferation [56], while IRF-2 shows an antagonistic relationship with IRF-1 [52-53, 97-98, 203, 224]. IRF-1 knockout mice showed decreased levels of $CD8^+$ T cells and higher susceptibility to infections [52] as well as IRF-2 knockout mice showed defects in B lymphopoiesis [187]. We have investigated expression of IRF-1 and IRF-2 mRNAs and proteins in BMCs of the mice after radiation-induced bone marrow damage and recovery from this due to bone marrow regeneration by transplantation of freshly isolated BMCs. To determine the function of IRF-1 and IRF-2 transcription factors during bone marrow regeneration, we measured their mRNA expressions in BMCs from control, irradiated and transplanted mice by using quantitative real-time RT-PCR. A previous report showed that gamma radiation inhibited phosphorylation of the transcription factor, signal transduction and activation of transcription-1 (STAT-1), which in turn decreased expression of IFN-γ-inducible genes such as IRF-1[225]. In contrast, we found that IRF-1 mRNA expression was significantly higher in irradiated (4.34x fold) and transplanted (3.85x fold) as compared to control mice **(Figure 18A)**. Similarly, IRF-2 mRNA expression was significantly higher in irradiated (3.87x fold) and transplanted (3.46x fold) as compared to control mice **(Figure 18B)**. Moreover, IRF-1 mRNA exhibited higher expression level compared to IRF-2 mRNA in BMCs of irradiated (1.12x fold) and irradiated+transplanted (1.11x fold) mice **(Figure 18)**. This result shows that both IRF-1 and IRF-2 are radiation-responsive genes in BMCs and the extent of bone marrow regeneration by the transplantation mentioned here is not sufficient to bring their mRNA expressions back to the normal state. It is expected that genes regulated by IRF-1 and IRF-2 may play a role in the cellular response to the radiation-induced damage in these cells as well as possibly in the bone marrow regeneration.

7.4.2 Localization of endogenous interferon regulatory factor-1and -2 (IRF-1 and IRF-2) of control, irradiated and transplanted mice bone marrow cells (BMCs) during bone marrow regeneration

Interferon regulatory factors function through gene expression-dependent and gene expression independent mechanisms. The previous one is an expression of IRF-1 and IRF-2 regulated mRNAs, and the latter involves protein-protein interactions with other transcription factors and signaling proteins. Previous studies have reported that a variety of cells expressed both IRF-1 and IRF-2, e.g., BMCs, macrophages, monocytes and epithelial cells [53]. IRF-1 and IRF-2 are involved in cytokine regulation, immune response, cell growth regulation, apoptosis and cell differentiation under a variety of conditions [53]. Expression of IRF-1 and IRF-2 in BMCs of control, irradiated and transplanted mice by confocal immunofluorescence microscopy showed low nuclear/cytoplasm ratio. Although the nucleus occupies most of the cellular space, BMCs mainly showed cytoplasmic expression of IRF-1 and IRF-2. In this study, we found that immunofluorescence for IRF-1 expression was cytoplasmic **(Figure 25A)**. Larger views of confocal immunofluorescence microscopic images show the cytoplasmic localization and expression of IRF-1**(Figure 25B)**. We also found that IRF-1 showed significantly higher expression in irradiated (2.12x fold) and transplanted (1.73x fold) as compared to BMCs of control mice **(Graph 25C)**. Similar to the IRF-1, we found that immunofluorescence for IRF-2 expression was cytoplasmic **(Figure 26A)**. Larger views of confocal immunofluorescence microscopic images show the cytoplasmic localization and expression of IRF-2 **(Figure 26B)**. We also found that immunofluorescence for IRF-2 was more in irradiated (1.71x fold) and transplanted (1.21x fold) as compared to BMCs of control **(Graph 26C)**. This data showed that BMCs of irradiated mice expressed higher levels of IRF-1 and IRF-2 mRNAs and proteins and the elevated expressions did not decline to normal levels in transplanted mice up to 24 hours. Also, a higher number of cells expressed IRF-1 and IRF-2 in BMCs of irradiated mice compared to control and transplanted mice. Thus IRF-1 and IRF-2 are radiation-responsive genes in BMCs, and they may be involved in bone marrow regeneration.

7.4.3 Localization and expression of interferon regulatory factor-1 and -2 (IRF-1 and IRF-2) and pluripotency-associated transcription factors (Oct3/4 and Sox-2) in bone marrow cells (BMCs) and mesenchymal stem (Passage 1) cells (MS-P1 cells)

7.4.3.1 Localization of endogenous interferon regulatory factor-1 and -2 (IRF-1 and IRF-2) in bone marrow cells (BMCs) and mesenchymal stem (Passage 1) cells (MS-P1 cells)

IRFs regulate expression of cytokine, chemokine, growth factor and immunomodulatory genes, mRNAs, and proteins. IRFs are involved in various cellular processes including development/differentiation of cells, the immune response against pathogens, cell growth/proliferation, tumorigenesis [52-53]. IRF-1, act as a tumor suppressor, its expression is associated with growth inhibition and anti-proliferation [56]. Whereas, IRF-2, having oncogenic property, activates VCAM-1, TLR-9, and histone genes, regulate cell cycle and is associated with various cancers [52]. IRF-1 and IRF-2 play crucial roles in the immune system, e.g., apoptosis, autophagy of cells, regulation of NK cell development, differentiation of Th1 and Th2 cells, macrophage function, regulation of T cells, B cells and dendritic cells and their functions [52-53, 58]. Moreover, abnormalities in the expression of IRF-1 and IRF-2 cause several diseases including cancer, bone marrow-related disease, e.g., myelodysplastic syndromes (MDS) [59]. However, the status of IRF-1 and IRF-2, regarding RNA and protein expression and localization, is not yet known in mouse bone marrow and bone marrow-derived MS-P1 cells.

A variety of cells expressed both IRF-1 and IRF-2, e.g., BMCs, macrophages, monocytes and epithelial cells at a basal level. During our investigation, real-time RT-PCR confirmed the expression of IRF-1 and IRF-2 at mRNA and the protein levels in BMCs. Negative control shows no bleeding of signals **(Figure 19)**. Confocal immunofluorescence microscopic images illustrate the expression of IRF-1 **(Figure 20)** and IRF-2 **(Figure 21)**. Double immunostaining of bone marrow cells by anti-IRF-1 and anti-IRF-2 antibodies further confirm their expression **(Figure 22)**.

After the confirmation of IRF-1 and IRF-2 expression and localization in BMCs, this study was further extended to find out constitutive expression and spatio-temporal localization of IRF-1 and IRF-2 proteins in MS-P1 cells. Control panel, wherein no primary antibody was

added, did not show cross-binding or non-specific binding by secondary anti-rabbit IgG **(Figure 27)**. Apart from BMCs which showed cytoplasmic expression of IRF-1 and IRF-2 in bone marrow, cultured MS-P1 cells displayed spatial specification, with IRF-1 consistently showing cytoplasmic preference **(Figure 28)**, while IRF2 was mainly localized in the nucleus **(Figure 29)**. Their expression was further checked by double immunostaining of (MS-P1 cells) by anti-IRF-1 and anti-IRF-2 antibodies **(Figure 30A-G)**. Comparative analysis of intensities of IRF-1 and IRF-2 of MS-P1 cells showed that IRF-1 showed 3.11x fold more cytoplasmic expression compared to nuclear expression and IRF-2 showed 4.19x fold more nuclear expression compared to cytoplasmic expression in MS-P1 cells. Moreover, IRF-1 showed 1.57x fold higher cytoplasmic expression compared to cytoplasmic expression of IRF-2. Moreover, IRF-2 showed 13.09x fold higher nuclear expression compared to IRF-1 in MS-P1 cells **(Figure 30H).** This cell-type, nuclear-cytoplasmic and transcription factor-type expression may be linked to the stem cell and immunomodulatory function(s) of MSCs.

7.4.3.2 Localization and expression of pluripotency-associated transcription factors (Oct3/4 and Sox-2) in bone marrow cells (BMCs) and mesenchymal stem (Passage-1) cells (MS-P1 cells)

The regenerative capacity of bone marrow-derived stem cells is associated with expression of pluripotency-associated transcription factors, such as Oct3/4, Sox-2, Nanog, Olig, Klf4, and c-Myc [28, 32-33]. Previous studies have shown that Oct3/4 expression is very critical to pluripotent cells such as cells of developing embryo. Downregulation of Oct3/4 is associated with trophectoderm differentiation, and overexpression induces extraembryonic mesodermal and endodermal differentiation. Thus, Oct3/4 concentration is dose-dependent and crucial for pluripotency in ESCs [226]. Previously published reports on human bone marrow derived mesenchymal stem cells (passage-1) have shown cytoplasmic Oct3/4 and Sox-2 expression [227], similar to this report we observed cytoplasmic Oct3/4 and Sox-2 expressions in the mouse bone marrow derived MS-P1 cells. Moreover, early passage MSCs show low-level expression of Oct3/4 and late passage MSCs exhibit no or very less expression of Oct3/4 [226]. We found that mouse bone marrow derived MS-P1 cells showed higher Oct3/4 expression as compared to control.

In this study, we investigated expression of two pluripotency-associated transcription factors, e.g., Oct3/4 and Sox-2 in BMCs. We found that Oct3/4 showed nuclear as well as cytoplasmic expression similar to the previous finding, but its localization was preferentially more peripheral in BMCs **(Figure 23)**. Sox-2 showed stable expression, i.e., uniformly expressed in nucleus and cytoplasm of BMCs **(Figure 24)**. In addition, MS-P1 cells showed similar results as BMCs; we found that Oct3/4 showed nuclear as well as cytoplasmic expression, more peripheral **(Figure 31)**. Sox-2 showed regular expression, i.e., uniformly expressed in nucleus and cytoplasm of MS-P1 cells **(Figure 32)**. The sub-cellular expression patterns of the two pluripotency-associated transcription factors in the BMCs and MSCs of mouse may be interesting but needs further investigation.

8 CONCLUSIONS

Experimental methods for isolation, culture, characterization and propagation of mouse bone marrow cells and bone marrow derived mesenchymal stem cells (passage 1) were optimized. A method for radiation-induced bone marrow damage in mouse was optimized and bone marrow regeneration (24%) was achieved up to 24 hours after the damage by transplantation of bone marrow stem cells through tail-vein injection in the mouse. Bone marrow cells and bone marrow derived mesenchymal stem cells showed expression of the transcription factors: interferon regulatory factor-1 (IRF-1) and IRF-2, which was sensitive and responsive to radiation-induced damage and bone marrow regeneration. This experimental mouse model system for stem cell therapy can be used for studying many human diseases related to the bone marrow.

9 TABLES

Table 1: Bone marrow cells and their functions

Cells	Properties and Functions	Reference
HSCs	Self-renewal, differentiation, and production of all blood cells	[16]
MSCs	Differentiate into adipocytes, chondrocytes, and osteocytes, homing efficiency, release trophic factors, and immunomodulation capabilities	[3]
MAPCs	Differentiate into mesodermal (e.g. endothelial cells, adipocytes, chondrocytes, and osteocytes); endodermal (e.g. hepatocytes) and ectodermal (e.g. astrocytes and neurons)	[7, 12]
Endothelial cells	Line blood vessels, secrete insulin-like growth factor binding protein, VEGF, and pleotrophin (PTN) and act as a regulator of stem cells fate	[3]
Osteoblasts	Regulate activity and expansion of HSCs; secrete granulocyte colony-stimulating factor (G-CSF), angiopoietin and osteopontin. The bone surface lining osteoblasts are termed as SNO (spindle-shaped N-cadherin^{+} osteoblastic) cells	[3]
Adipocytes	A negative regulator of HSCs	[3, 160]
Osteoclasts	Produce PGE-2, and involved in regulation of erythropoiesis	[3]
Non-myelinating Schwann cells	Secrete TGF, and regulate erythropoiesis	[3]
Sympathetic neurons	Involved in regulation of erythropoiesis and release CXCL12, act as a master regulator of hematopoiesis	[3]
BM macrophages	A major source of PGE-2 and involved in regulation of erythropoiesis	[3]
Megakaryocytes	Secrete RANKL, calcium-sensing receptors, NMDA-type glutamate receptors, TGF-β and TGF-β receptors, and estrogen receptors, osteonectin, osteocalcin and regulate bone	[69]

	remodeling	
Pericytes	regulate survival, stabilization and maturation of other stroma cells and having contractile and phagocytic property	[3]
CAR cells	an essential component of the stem cell niche and maintain an undifferentiated state of HSCs, erythroid progenitor, and lymphoid progenitors and retain HSCs in bone marrow	[3]

Table 2: Cell surface markers and transcription factors of BM derived stem cells

Stem cells	**Cell surface markers (A)**	**Expression of transcription factors (B)**	**Differentiation into**	**Reference**
HSCs	Positive- SCA-1, C-KIT, CD105, CD150, THY-1 and CD34 Negative- Lin, FLT3, CD38, and CD48	Zfx, Bmi-1, Tel/Etv6, and FoxO	All immune cells	(A) [17, 228] (B) [229] (C) [3]
MSCs	Positive- CD29, CD44, CD73, CD90, CD105, and Sca-1 Negative- CD11b, CD14, CD34, CD45, and CD86 [22]	Oct-4, Rex-1, and Sox-2	Mesenchymal lineages such as chondrocytes, adipocytes, and osteocytes	(A) [16, 23, 72] (B) [230] (C) [3, 16]
MAPCs	Positive- SSEA-1, CD13 FLK-1, SCA-1,and THY-1 Negative- CD34, CD44, CD45, c-KIT, MHC-I, and MHC-II	Oct-4, Rex-1	All three germ layers such as mesodermal (e.g. endothelial cells, adipocytes, chondrocytes, and osteocytes), endodermal (e.g. hepatocytes), and ectodermal (e.g. astrocytes and neurons)	(A) [12] (B) [12] (C) [7]

Table 3: A list of IRF-1 functions in bone marrow cells derived immune cells

Cell type	Function of IRF-1	Reference
T regulatory (Tregs) cells	Required in modulation of T regulatory (Tregs) cells via suppression of Foxp3	[59]
Macrophages ((Mφs)	Associated with M1 polarization (classically activated) of macrophages	[231]
Dendritic cells (DCs)	Improve function and maturation of DCs [232]	[232]
Th17 cells	Linked to inhibition of Th17 differentiation found in genetic deletion of IRF-1 in Sirt1-null DCs	[233]
Dendritic cells (DCs)	Associated with development of dendritic cells. *Irf1−/− mice* showed decline $CD8\alpha^+$ DC number and increase in number of plasmacytoid dendritic cells (pDCs)	[52]
Myeloid cells	Needed in differentiation and full maturation of myeloid cells such as macrophages and neutrophils. Irf1−/− bone marrow cells exhibit a higher number of immature granulocytic precursors	[52]
$CD8^+$ T cells	Support in function, development of $CD8^+$ T cells, cytotoxic T lymphocyte (CTL), for instance, $CD8^+$ T cells in *Irf1−/− mice* showed declined response against LCMV-infected target cells	[52].
$CD8^+$ T cells	Involved in maturation of $CD4^-CD8^+$ T cells in the thymus and peripheral lymphoid organs in *Irf1−/− mice*	[52].
Th1 cells	Required in activation of Th1 differentiation through MΦs/DCs (IL-12). *Irf1−/− mice* showed compromised Th1 differentiation of $CD4^+$ T cells and NK cells (IL-15)	[52, 234-235].
Natural Killer cells (NK cells)	Involved in development of NK cells. *Irf1−/− mice* exhibit dramatically reduced NK ($NK1.1^+$ $TCR\alpha/\beta^-$) cell number and showed declined NK cell activities such IL-12-dependent IFN-γ production and cytotoxic property	[52].

Monocyte/macrophage	Participated in differentiation of monocyte/macrophage	[236]
Natural Killer cells (NK cells)	Associated with severe deficiency of NK cells. Whereas IRF-1(-/-) bone marrow cells with IL-15 can produce functional NK cells	[237].

Table 4: A list of IRF-2 functions in bone marrow derived immune cells

Cell type	Function of IRF-2	References
T cells	Involved in a deficiency of $Ly49^+$ T cells. *Irf2−/− mice* exhibit lacking IFN-α/β R alpha-chain (IFNAR1) which is associated with IFN- α/β signaling in T cells	[238].
HSCs	Required for multilineage differentiation and preserved self-renewal capacity of HSCs. *Irf2−/− mice* exhibited selective loss and failed to produce HSCs	[239].
DCs subsets	Associated with development of DCs subsets. IRF2 also participated in Langerhans cells (LCs). *Irf2−/− mice* exhibit a selective loss of epidermal and splenic $CD4^+CD8\alpha^-$ cells	[52].
Granulocyte (Basophils)	Participated in inhibition of differentiation of granulocytes. *Irf2−/− mice* showed basophils expansion, resulting in higher expression of IL-4	[52, 240].
NK cells	Included in the development of NK cells. *Irf2−/− mice* exhibit lesser number of $CD11b^{high}$ $Dx5^{high}$ NK cells and impaired development and function of NK cells	[52].
$CD8^+$ T cells	Connected to development of $CD8^+$ T cells. *Irf2−/− mice* produced abnormal $CD8^+$ T-cells that caused hyperresponsiveness to antigen stimulation and psoriasis, a spontaneous inflammatory skin disease	[52].
Megakaryocyte	Associated with stimulation of megakaryocyte differentiation	[52]
Th1 cells	Required for differentiation of $CD4^+$ DCs (IL-12 in MΦs)	[52].
Th2 cells	Suppress Th2 differentiation (by basophils secreted IL-4), and *Irf2−/− mice* exhibit higher Th2 polarization	[52].

Table 5: Bone marrow transplantation (BMT) Therapy in Bone marrow age-related diseases

Age-related bone marrow disease	Therapy	References
Cancers	BMT	[3, 163-165]
Altered B lymphopoiesis	BMT	[166-170]
Osteoporosis	BMT	[162]
Age-related macular degeneration (AMD)	BMT	[174]
Type 2 diabetes mellitus (T2DM)	BMT	[162, 173]
Alzheimer's disease (AD)	BMT	[162]

Table 6: Stem cell potentials and regenerative capabilities of the bone marrow-derived stem cells

Stem Cells transplantation (SCT) Therapy

Stem cells	Tissue regeneration models by cell therapy (A)	Stem cell potential, Regenerative capabilities (B)	References
HSCs	Ischaemic myocardium GFP-transgenic C57BL/ Ka-Thy-1.1 mice C57BL/Ka-Thy-1.1 mice [241]	c-kit-1, Thy1.1^{lo}, Lin^{-}, Sca-1^{+} long-term reconstituting haematopoietic stem cells [241]	(A) [241] (B) [241]
MSCs	Myocardial infarction Immunocompetent Lewis rats C57BL/6 mouse MSCs [242]	Mouse MSCs derived Angiogenesis and cardiomyocytes regeration [242]	(A) [242] (B) [242]
MAPCs	lymphoma in thymus and spleen NOD/SCID mice Mouse MAPCs [12]	Play an important role in neoangiogenesis in mouse [12]	(A) [12] (B) [12]

10 REFERENCES

1. Murphy, D.T., et al., *Bone marrow.* Magn Reson Imaging Clin N Am, 2010. **18**(4): p. 727-35.
2. Travlos, G., *Normal structure, function, and histology of the bone marrow.* Toxicologic pathology, 2006. **34**(5): p. 548.
3. Pleyer, L., P. Valent, and R. Greil, *Mesenchymal Stem and Progenitor Cells in Normal and Dysplastic Hematopoiesis-Masters of Survival and Clonality?* Int J Mol Sci, 2016. **17**(7).
4. Zhao, E., et al., *Bone marrow and the control of immunity.* Cell Mol Immunol, 2012. **9**(1): p. 11-9.
5. Trumpp, A., M. Essers, and A. Wilson, *Awakening dormant haematopoietic stem cells.* Nature Reviews Immunology, 2010. **10**(3): p. 201-209.
6. Caplan, A.I., *Adult mesenchymal stem cells for tissue engineering versus regenerative medicine.* J Cell Physiol, 2007. **213**(2): p. 341-7.
7. Reyes, M., et al., *Donor origin of multipotent adult progenitor cells in radiation chimeras.* Blood, 2005. **106**(10): p. 3646-3649.
8. Shaikh, A., et al., *Mouse Bone Marrow VSELs Exhibit Differentiation into Three Embryonic Germ Lineages and Germ & Hematopoietic Cells in Culture.* Stem Cell Rev, 2017.
9. Pourrajab, F., S.K. Forouzannia, and S.A. Tabatabaee, *Molecular characteristics of bone marrow mesenchymal stem cells, source of regenerative medicine.* Int J Cardiol, 2013. **163**(2): p. 125-31.
10. Tamma, R. and D. Ribatti, *Bone Niches, Hematopoietic Stem Cells, and Vessel Formation.* Int J Mol Sci, 2017. **18**(1).
11. Regulski, M.J., *Mesenchymal Stem Cells: "Guardians of Inflammation".* Wounds, 2017. **29**(1): p. 20-27.

12. Jiang, Y., et al., *Pluripotency of mesenchymal stem cells derived from adult marrow.* Nature, 2002. **418**(6893): p. 41-9.

13. Urao, N. and M. Ushio-Fukai, *Redox regulation of stem/progenitor cells and bone marrow niche.* Free Radic Biol Med, 2013. **54**: p. 26-39.

14. Kopp, H.-G., et al., *The bone marrow vascular niche: home of HSC differentiation and mobilization.* Physiology, 2005. **20**(5): p. 349-356.

15. Calvi, L.M. and D.C. Link, *The hematopoietic stem cell niche in homeostasis and disease.* Blood, 2015. **126**(22): p. 2443-2451.

16. Kovtonyuk, L.V., et al., *Inflamm-Aging of Hematopoiesis, Hematopoietic Stem Cells, and the Bone Marrow Microenvironment.* Front Immunol, 2016. **7**: p. 502.

17. Wognum, A.W., A.C. Eaves, and T.E. Thomas, *Identification and isolation of hematopoietic stem cells.* Archives of medical research, 2003. **34**(6): p. 461-475.

18. Robey, P., *"Mesenchymal stem cells": fact or fiction, and implications in their therapeutic use.* F1000Research, 2017. **6**.

19. Ding, D.-C., W.-C. Shyu, and S.-Z. Lin, *Mesenchymal stem cells.* Cell Transplantation, 2011. **20**(1): p. 5-14.

20. Baker, N., L.B. Boyette, and R.S. Tuan, *Characterization of bone marrow-derived mesenchymal stem cells in aging.* Bone, 2015. **70**: p. 37-47.

21. Jacobs, S.A., et al., *Immunological characteristics of human mesenchymal stem cells and multipotent adult progenitor cells.* Immunology and cell biology, 2013. **91**(1): p. 32-39.

22. Zhu, H., et al., *A protocol for isolation and culture of mesenchymal stem cells from mouse compact bone.* Nat Protoc, 2010. **5**(3): p. 550-60.

23. Soleimani, M. and S. Nadri, *A protocol for isolation and culture of mesenchymal stem cells from mouse bone marrow.* Nature protocols, 2009. **4**(1): p. 102-106.

24. Cunha, J., et al., *Human multipotent adult progenitor cells enhance islet function and revascularisation when co-transplanted as a composite pellet in a mouse model of diabetes.* Diabetologia, 2017. **60**(1): p. 134-142.

25. Sohni, A. and C.M. Verfaillie, *Multipotent adult progenitor cells.* Best practice & research Clinical haematology, 2011. **24**(1): p. 3-11.

26. Guillerman, R.P., *Marrow: red, yellow and bad.* Pediatr Radiol, 2013. **43 Suppl 1**: p. 181-92.

27. Ahmadzadeh, A., et al., *Wnt/beta-catenin signaling in bone marrow niche.* Cell Tissue Res, 2016. **363**(2): p. 321-35.

28. Orkin, S.H. and K. Hochedlinger, *Chromatin connections to pluripotency and cellular reprogramming.* Cell, 2011. **145**(6): p. 835-50.

29. Bogdanović, O. and R. Lister, *DNA methylation and the preservation of cell identity.* Current Opinion in Genetics & Development, 2017. **46**: p. 9-14.

30. Lessard, J.A. and G.R. Crabtree, *Chromatin regulatory mechanisms in pluripotency.* Annual review of cell and developmental biology, 2010. **26**: p. 503-532.

31. Liao, W., et al., *Enhancing bone marrow regeneration by SALL4 protein.* J Hematol Oncol, 2013. **6**: p. 84.

32. Takahashi, K. and S. Yamanaka, *Induction of pluripotent stem cells from mouse embryonic and adult fibroblast cultures by defined factors.* Cell, 2006. **126**(4): p. 663-76.

33. Li, M. and J.C.I. Belmonte, *Ground rules of the pluripotency gene regulatory network.* Nature Reviews Genetics, 2017.

34. Fagnocchi, L. and A. Zippo, *Multiple Roles of MYC in Integrating Regulatory Networks of Pluripotent Stem Cells.* Frontiers in cell and developmental biology, 2017. **5**.

35. Kaikkonen, M.U., M.T. Lam, and C.K. Glass, *Non-coding RNAs as regulators of gene expression and epigenetics.* Cardiovascular research, 2011. **90**(3): p. 430-440.

36. Ong, S.G., et al., *MicroRNA-mediated regulation of differentiation and trans-differentiation in stem cells.* Adv Drug Deliv Rev, 2015. **88**: p. 3-15.

37. Lakshmipathy, U., J. Davila, and R.P. Hart, *miRNA in pluripotent stem cells.* Regen Med, 2010. **5**(4): p. 545-55.

38. Chen, Z.-H., et al., *The lncRNA HOTAIRM1 regulates the degradation of PML-RARA oncoprotein and myeloid cell differentiation by enhancing the autophagy pathway.* Cell Death & Differentiation, 2017. **24**(2): p. 212-224.

39. Huang, Y., et al., *Long non-coding RNA H19 inhibits adipocyte differentiation of bone marrow mesenchymal stem cells through epigenetic modulation of histone deacetylases.* Scientific reports, 2016. **6**.

40. Luo, M., et al., *Long non-coding RNAs control hematopoietic stem cell function.* Cell Stem Cell, 2015. **16**(4): p. 426-38.

41. Mohamed, J.S., et al., *Conserved long noncoding RNAs transcriptionally regulated by Oct4 and Nanog modulate pluripotency in mouse embryonic stem cells.* Rna, 2010. **16**(2): p. 324-337.

42. Wang, Y., et al., *Total body irradiation selectively induces murine hematopoietic stem cell senescence.* Blood, 2006. **107**(1): p. 358-366.

43. Cao, X., et al., *Irradiation induces bone injury by damaging bone marrow microenvironment for stem cells.* Proceedings of the National Academy of Sciences, 2011. **108**(4): p. 1609-1614.

44. Harfouche, G. and M.T. Martin, *Response of normal stem cells to ionizing radiation: a balance between homeostasis and genomic stability.* Mutation Research/Reviews in Mutation Research, 2010. **704**(1): p. 167-174.

45. Wilke, C., et al., *Marrow damage and hematopoietic recovery following allogeneic bone marrow transplantation for acute leukemias: Effect of radiation dose and conditioning regimen.* Radiotherapy and Oncology, 2016. **118**(1): p. 65-71.

46. Shao, L., Y. Luo, and D. Zhou, *Hematopoietic stem cell injury induced by ionizing radiation.* Antioxid Redox Signal, 2014. **20**(9): p. 1447-62.

47. Chang, J., et al., *28 Si total body irradiation injures bone marrow hematopoietic stem cells via induction of cellular apoptosis.* Life Sciences in Space Research, 2017. **13**: p. 39-44.

48. Wang, Y., et al., *Total body irradiation causes residual bone marrow injury by induction of persistent oxidative stress in murine hematopoietic stem cells.* Free Radical Biology and Medicine, 2010. **48**(2): p. 348-356.

49. Cui, Y.Z., et al., *Optimal protocol for total body irradiation for allogeneic bone marrow transplantation in mice.* Bone Marrow Transplant, 2002. **30**(12): p. 843-9.

50. Duran-Struuck, R. and R.C. Dysko, *Principles of bone marrow transplantation (BMT): providing optimal veterinary and husbandry care to irradiated mice in BMT studies.* J Am Assoc Lab Anim Sci, 2009. **48**(1): p. 11-22.

51. Agas, D., et al., *INF-γ encoding plasmid administration triggers bone loss and disrupts bone marrow microenvironment.* Journal of Endocrinology, 2017. **232**(2): p. 309-321.

52. Tamura, T., et al., *The IRF family transcription factors in immunity and oncogenesis.* Annu Rev Immunol, 2008. **26**: p. 535-84.

53. Taniguchi, T., et al., *IRF family of transcription factors as regulators of host defense.* Annu Rev Immunol, 2001. **19**: p. 623-55.

54. Mboko, W.P., et al., *Interferon Regulatory Factor 1 and Type I Interferon Cooperate To Control Acute Gammaherpesvirus Infection.* J Virol, 2017. **91**(1).

55. Upreti, M. and P.C. Rath, *Expression and DNA binding activity of the recombinant interferon regulatory factor-1 (IRF-1) of mouse.* Mol Biol Rep, 2005. **32**(2): p. 103-16.

56. Romeo, G., et al., *IRF-1 as a negative regulator of cell proliferation.* J Interferon Cytokine Res, 2002. **22**(1): p. 39-47.

57. Prakash, K. and P.C. Rath, *Mouse interferon regulatory factor-2: expression, purification and DNA binding activity.* Mol Biol Rep, 2012. **39**(1): p. 599-606.

58. Zhao, G.N., D.S. Jiang, and H. Li, *Interferon regulatory factors: at the crossroads of immunity, metabolism, and disease.* Biochim Biophys Acta, 2015. **1852**(2): p. 365-78.

59. Perazzio, A.S., et al., *Increase of IRF-1 gene expression and impairment of T regulatory cells suppression activity on patients with myelodysplastic syndrome: A longitudinal one-year study.* Leuk Res, 2017. **55**: p. 6-17.

60. Yu, V.W. and D.T. Scadden, *Hematopoietic Stem Cell and Its Bone Marrow Niche.* Curr Top Dev Biol, 2016. **118**: p. 21-44.

61. Pang, W.W., S.L. Schrier, and I.L. Weissman, *Age-associated changes in human hematopoietic stem cells.* Semin Hematol, 2017. **54**(1): p. 39-42.

62. Ganuza, M. and S. McKinney-Freeman, *Hematopoietic stem cells under pressure.* Current Opinion in Hematology, 2017. **24**(4): p. 314-321.

63. Vyalkina, M., et al. *Long-Term Effects of Stem Cells on Total-Body Irradiated Mice*. in *Journal of Physics: Conference Series*. 2017: IOP Publishing.

64. Blank, U., G. Karlsson, and S. Karlsson, *Signaling pathways governing stem-cell fate.* Blood, 2008. **111**(2): p. 492-503.

65. Hande, M.P., et al., *Past exposure to densely ionizing radiation leaves a unique permanent signature in the genome.* The American Journal of Human Genetics, 2003. **72**(5): p. 1162-1170.

66. Li, Q., et al., *Disease-specific hematopoietic stem cell transplantation in children with inherited bone marrow failure syndromes.* Annals of Hematology, 2017: p. 1-9.

67. Horowitz, M.M., et al., *Graft-versus-leukemia reactions after bone marrow transplantation.* Blood, 1990. **75**(3): p. 555-562.

68. Fliedner, T., et al., *Structure and function of bone marrow hemopoiesis: mechanisms of response to ionizing radiation exposure.* Cancer Biotherapy and Radiopharmaceuticals, 2002. **17**(4): p. 405-426.

69. Compston, J.E., *Bone marrow and bone: a functional unit.* J Endocrinol, 2002. **173**(3): p. 387-94.

70. Benayahu, D., I. Shur, and S. Ben-Eliyahu, *Hormonal changes affect the bone and bone marrow cells in a rat model.* J Cell Biochem, 2000. **79**(3): p. 407-15.

71. Zheng, C., et al., *Bone Marrow Stem Cells: Source, Characterization, Isolation, Culture, and Identification*, in *Bone marrow stem cell therapy for stroke*. 2017, Springer. p. 37-53.

72. Zhu, H., et al., *A protocol for isolation and culture of mesenchymal stem cells from mouse compact bone.* Nature protocols, 2010. **5**(3): p. 550-560.

73. Gökçinar-Yagci, B., D. Uçkan-Çetinkaya, and B. Çelebi-Saltik, *Pericytes: properties, functions and applications in tissue engineering.* Stem Cell Reviews and Reports, 2015. **11**(4): p. 549-559.

74. Atoui, R. and R.C. Chiu, *Concise review: immunomodulatory properties of mesenchymal stem cells in cellular transplantation: update, controversies, and unknowns.* Stem cells translational medicine, 2012. **1**(3): p. 200-205.

75. Burrows, G.G., et al., *Solution‐Phase Crosstalk and Regulatory Interactions Between Multipotent Adult Progenitor Cells and Peripheral Blood Mononuclear Cells.* Stem cells translational medicine, 2015. **4**(12): p. 1436-1449.

76. Cunha, J.P.M., et al., *Human multipotent adult progenitor cells enhance islet function and revascularisation when co-transplanted as a composite pellet in a mouse model of diabetes.* Diabetologia, 2017. **60**(1): p. 134-142.

77. Jiang, Y., et al., *Pluripotency of mesenchymal stem cells derived from adult marrow.* Nature, 2002. **418**(6893): p. 41-49.

78. Rafii, S., et al., *Human bone marrow microvascular endothelial cells support long-term proliferation and differentiation of myeloid and megakaryocytic progenitors.* Blood, 1995. **86**(9): p. 3353-3363.

79. Möhle, R., M.A. Moore, and S. Rafii, *The role of endothelium in the regulation of hematopoietic stem cell migration.* Stem Cells, 1998. **16**(S2): p. 159-165.

80. Taichman, R.S., *Blood and bone: two tissues whose fates are intertwined to create the hematopoietic stem-cell niche.* Blood, 2005. **105**(7): p. 2631-2639.

81. Arai, F., et al., *Tie2/angiopoietin-1 signaling regulates hematopoietic stem cell quiescence in the bone marrow niche.* Cell, 2004. **118**(2): p. 149-161.

82. Asada, N., S. Takeishi, and P.S. Frenette, *Complexity of bone marrow hematopoietic stem cell niche.* International Journal of Hematology, 2017: p. 1-10.

83. Winkler, I.G., et al., *Bone marrow macrophages maintain hematopoietic stem cell (HSC) niches and their depletion mobilizes HSCs.* Blood, 2010. **116**(23): p. 4815-4828.

84. Christopher, M.J., et al., *Expression of the G-CSF receptor in monocytic cells is sufficient to mediate hematopoietic progenitor mobilization by G-CSF in mice.* Journal of Experimental Medicine, 2011. **208**(2): p. 251-260.

85. Chow, A., et al., *Bone marrow CD169+ macrophages promote the retention of hematopoietic stem and progenitor cells in the mesenchymal stem cell niche.* Journal of Experimental Medicine, 2011: p. jem. 20101688.

86. Sapoznikov, A., et al., *Perivascular clusters of dendritic cells provide critical survival signals to B cells in bone marrow niches.* Nature immunology, 2008. **9**(4): p. 388-395.

87. Morrison, S.J. and D.T. Scadden, *The bone marrow niche for haematopoietic stem cells.* Nature, 2014. **505**(7483): p. 327.

88. Fang, D., et al., *Identification of the active components in Bone Marrow Soup: a mitigator against irradiation-injury to salivary glands.* Scientific reports, 2015. **5**.

89. Sadler, A.J. and B.R. Williams, *Interferon-inducible antiviral effectors.* Nature reviews. Immunology, 2008. **8**(7): p. 559.

90. Nguyen, H., J. Hiscott, and P.M. Pitha, *The growing family of interferon regulatory factors.* Cytokine & growth factor reviews, 1997. **8**(4): p. 293-312.

91. Nehyba, J., et al., *A novel interferon regulatory factor (IRF), IRF-10, has a unique role in immune defense and is induced by the v-Rel oncoprotein.* Molecular and cellular biology, 2002. **22**(11): p. 3942-3957.

92. Ikushima, H., H. Negishi, and T. Taniguchi. *The IRF family transcription factors at the interface of innate and adaptive immune responses*. in *Cold Spring Harbor symposia on quantitative biology*. 2013: Cold Spring Harbor Laboratory Press.

93. Fujita, T., et al., *Induction of endogenous IFN-α and IFN-β genes by a regulatory transcription factor, IRF-1.* Nature, 1989. **337**(6204): p. 270-272.

94. Uegaki, K., et al., *Secondary structure and folding topology of the DNA binding domain of interferon regulatory factor 2, as revealed by NMR spectroscopy.* FEBS letters, 1995. **359**(2-3): p. 184-188.

95. Honda, K. and T. Taniguchi, *IRFs: master regulators of signalling by Toll-like receptors and cytosolic pattern-recognition receptors.* Nature reviews. Immunology, 2006. **6**(9): p. 644.

96. Escalante, C.R., et al., *Structure of IRF-1 with bound DNA reveals determinants of interferon regulation.* Nature, 1998. **391**(6662): p. 103.

97. Paun, A. and P.M. Pitha, *The IRF family, revisited.* Biochimie, 2007. **89**(6-7): p. 744-53.

98. Yanai, H., H. Negishi, and T. Taniguchi, *The IRF family of transcription factors: Inception, impact and implications in oncogenesis.* Oncoimmunology, 2012. **1**(8): p. 1376-1386.

99. Yuan, L., et al., *IFN-γ-mediated IRF1/miR-29b feedback loop suppresses colorectal cancer cell growth and metastasis by repressing IGF1.* Cancer letters, 2015. **359**(1): p. 136-147.

100. Tanaka, N., et al., *Cellular commitment to oncogene-induced transformation or apoptosis is dependent on the transcription factor IRF-1.* Cell, 1994. **77**(6): p. 829-839.

101. Zhang, L., et al., *Interferon regulatory factor-1 regulates the autophagic response in LPS-stimulated macrophages through nitric oxide.* Molecular Medicine, 2012. **18**(1): p. 201.

102. Kamijo, R., et al., *Requirement for transcription factor IRF-1 in NO synthase induction in macrophages.* Science, 1994. **263**(5153): p. 1612-1616.

103. Escalante, C.R., et al., *Structure of IRF-1 with bound DNA reveals determinants of interferon regulation.* Nature, 1998. **391**(6662): p. 103-6.

104. Furui, J., et al., *Solution structure of the IRF-2 DNA-binding domain: a novel subgroup of the winged helix–turn–helix family.* Structure, 1998. **6**(4): p. 491-500.

105. SCHAPER, F., et al., *Functional domains of interferon regulatory factor I (IRF-1).* Biochemical Journal, 1998. **335**(1): p. 147-157.

106. Harada, H., et al., *Structurally similar but functionally distinct factors, IRF-1 and IRF-2, bind to the same regulatory elements of IFN and IFN-inducible genes.* Cell, 1989. **58**(4): p. 729-739.

107. MacDonald, N.J., et al., *Different pathways mediate virus inducibility of the human IFN-α1 and IFN-β genes.* Cell, 1990. **60**(5): p. 767-779.

108. Janeway Jr, C.A. and R. Medzhitov, *Innate immune recognition.* Annual review of immunology, 2002. **20**(1): p. 197-216.

109. Fritz, J.H., et al., *Nod-like proteins in immunity, inflammation and disease.* Nature immunology, 2006. **7**(12): p. 1250.

110. Akira, S., S. Uematsu, and O. Takeuchi, *Pathogen recognition and innate immunity.* Cell, 2006. **124**(4): p. 783-801.

111. Diebold, S.S., et al., *Viral infection switches non-plasmacytoid dendritic cells into high interferon producers.* Nature, 2003. **424**(6946): p. 324.

112. Moynagh, P.N., *TLR signalling and activation of IRFs: revisiting old friends from the NF-κB pathway.* Trends in immunology, 2005. **26**(9): p. 469-476.

113. Kawai, T. and S. Akira, *TLR signaling.* Cell death and differentiation, 2006. **13**(5): p. 816.

114. Takeda, K. and S. Akira. *TLR signaling pathways*. in *Seminars in immunology*. 2004: Elsevier.

115. Kawai, T. and S. Akira. *TLR signaling*. in *Seminars in immunology*. 2007: Elsevier.

116. Darnell Jr, J.E., I.M. Kerr, and G.R. Stark, *Jak-STAT pathways and transcriptional activation in response to IFNs and other extracellular signaling proteins.* Science-AAAS-weekly paper edition-including guide to scientific information, 1994. **264**(5164): p. 1415-1420.

117. Ihle, J.N. and I.M. Kerr, *Jaks and Stats in signaling by the cytokine receptor superfamily*. Trends in Genetics, 1995. **11**(2): p. 69-74.

118. Ihle, J.N., *Cytokine receptor signalling.* Nature, 1995. **377**(6550): p. 591-594.

119. Taniguchi, T., *Cytokine signaling through nonreceptor protein tyrosine kinases.* Science, 1995: p. 251-255.

120. Bluyssen, H.A., J.E. Durbin, and D.E. Levy, *ISGF3γ p48, a specificity switch for interferon activated transcription factors.* Cytokine & growth factor reviews, 1996. **7**(1): p. 11-17.

121. Bluyssen, H., et al., *Combinatorial association and abundance of components of interferon-stimulated gene factor 3 dictate the selectivity of interferon responses.* Proceedings of the National Academy of Sciences, 1995. **92**(12): p. 5645-5649.

122. FuJITA, T., et al., *Induction of the transcription factor IRF-1 and interferon-beta mRNAs by cytokines and activators of second-messenger pathways.* Proceedings of the National Academy of Sciences, 1989. **86**(24): p. 9936-9940.

123. Pine, R., A. Canova, and C. Schindler, *Tyrosine phosphorylated p91 binds to a single element in the ISGF2/IRF-1 promoter to mediate induction by IFN alpha and IFN gamma, and is likely to autoregulate the p91 gene.* The EMBO Journal, 1994. **13**(1): p. 158.

124. Harada, H., et al., *Structure and regulation of the human interferon regulatory factor 1 (IRF-1) and IRF-2 genes: implications for a gene network in the interferon system.* Molecular and cellular biology, 1994. **14**(2): p. 1500-1509.

125. Negishi, H., et al., *Evidence for licensing of IFN-γ-induced IFN regulatory factor 1 transcription factor by MyD88 in Toll-like receptor-dependent gene induction program.* Proceedings of the National Academy of Sciences, 2006. **103**(41): p. 15136-15141.

126. Ardavín, C., *Origin, precursors and differentiation of mouse dendritic cells.* Nature reviews. Immunology, 2003. **3**(7): p. 582.

127. Banchereau, J., et al., *Immunobiology of dendritic cells.* Annual review of immunology, 2000. **18**(1): p. 767-811.

128. Edwards, A.D., et al., *Relationships among murine CD11chigh dendritic cell subsets as revealed by baseline gene expression patterns.* The Journal of Immunology, 2003. **171**(1): p. 47-60.

129. Shortman, K. and L. Yong-Jun, *Mouse and human dendritic cell subtypes.* Nature reviews. Immunology, 2002. **2**(3): p. 151.

130. Gabriele, L., et al., *IRF-1 deficiency skews the differentiation of dendritic cells toward plasmacytoid and tolerogenic features.* Journal of leukocyte biology, 2006. **80**(6): p. 1500-1511.

131. Vivier, E., et al., *Functions of natural killer cells.* Nature immunology, 2008. **9**(5): p. 503.

132. Trinchieri, G., *Biology of natural killer cells.* Advances in immunology, 1989. **47**: p. 187-376.

133. Manzella, L., et al., *Role of interferon regulatory factor 1 in monocyte/macrophage differentiation.* European journal of immunology, 1999. **29**(9): p. 3009-3016.

134. Liu, J., et al., *Differential regulation of interleukin (IL)-12 p35 and p40 gene expression and interferon (IFN)-γ–primed IL-12 production by IFN regulatory factor 1.* Journal of Experimental Medicine, 2003. **198**(8): p. 1265-1276.

135. Fehr, T., et al., *Crucial role of interferon consensus sequence binding protein, but neither of interferon regulatory factor 1 nor of nitric oxide synthesis for protection against murine listeriosis.* Journal of Experimental Medicine, 1997. **185**(5): p. 921-932.

136. Penninger, J.M., et al., *The interferon regulatory transcription factor IRF-1 controls positive and negative selection of CD8+ thymocytes.* Immunity, 1997. **7**(2): p. 243-254.

137. Matsuyama, T., et al., *Targeted disruption of IRF-1 or IRF-2 results in abnormal type I IFN gene induction and aberrant lymphocyte development.* Cell, 1993. **75**(1): p. 83-97.

138. Ohteki, T., C. Maki, and S. Koyasu, *Overexpression of Bcl-2 differentially restores development of thymus-derived CD4− 8+ T cells and intestinal intraepithelial T cells in IFN-regulatory factor-1-deficient mice.* The Journal of Immunology, 2001. **166**(11): p. 6509-6513.

139. Hida, S., et al., *CD8+ T cell–mediated skin disease in mice lacking IRF-2, the transcriptional attenuator of interferon-α/β signaling.* Immunity, 2000. **13**(5): p. 643-655.

140. Taki, S., et al., *Multistage regulation of Th1-type immune responses by the transcription factor IRF-1.* Immunity, 1997. **6**(6): p. 673-679.

141. Coccia, E.M., et al., *Interleukin-12 induces expression of interferon regulatory factor-1 via signal transducer and activator of transcription-4 in human T helper type 1 cells.* Journal of Biological Chemistry, 1999. **274**(10): p. 6698-6703.

142. Elser, B., et al., *IFN-γ represses IL-4 expression via IRF-1 and IRF-2.* Immunity, 2002. **17**(6): p. 703-712.

143. Veldhoen, M., et al., *TGFβ in the context of an inflammatory cytokine milieu supports de novo differentiation of IL-17-producing T cells.* Immunity, 2006. **24**(2): p. 179-189.

144. Zhou, Z., et al., *Type III interferon (IFN) induces a type I IFN-like response in a restricted subset of cells through signaling pathways involving both the Jak-STAT pathway and the mitogen-activated protein kinases.* Journal of virology, 2007. **81**(14): p. 7749-7758.

145. Tang, Y., et al., *Jak/Stat3 signaling promotes somatic cell reprogramming by epigenetic regulation.* Stem Cells, 2012. **30**(12): p. 2645-2656.

146. Zaichkina, S., et al., *Low doses of gamma-radiation induce nonlinear dose responses in mammalian and plant cells.* Nonlinearity in biology, toxicology, medicine, 2004. **2**(3): p. 15401420490519861.

147. Chacko, T., et al., *Mitigation of whole-body gamma radiation–induced damages by Clerodendron infortunatum in mammalian organisms.* Journal of radiation research, 2017. **58**(3): p. 281-291.

148. Kramer, A. and G.A. Challen, *The epigenetic basis of hematopoietic stem cell aging.* Semin Hematol, 2017. **54**(1): p. 19-24.

149. Gross, L., *Mechanisms of aging in bone marrow stem cells.* PLoS Biol, 2007. **5**(8): p. e215.

150. Ergen, A.V. and M.A. Goodell, *Mechanisms of hematopoietic stem cell aging.* Exp Gerontol, 2010. **45**(4): p. 286-90.

151. Torano, E.G., et al., *Age-associated hydroxymethylation in human bone-marrow mesenchymal stem cells.* J Transl Med, 2016. **14**(1): p. 207.

152. Zhu, Y.P., C.C. Hedrick, and D.E. Gaddis, *Hematopoietic stem cells gone rogue.* Science, 2017. **355**(6327): p. 798-799.

153. Sahin, E. and R.A. DePinho, *Axis of ageing: telomeres, p53 and mitochondria.* Nat Rev Mol Cell Biol, 2012. **13**(6): p. 397-404.

154. Tothova, Z., et al., *FoxOs are critical mediators of hematopoietic stem cell resistance to physiologic oxidative stress.* Cell, 2007. **128**(2): p. 325-39.

155. Tothova, Z. and D.G. Gilliland, *FoxO transcription factors and stem cell homeostasis: insights from the hematopoietic system.* Cell Stem Cell, 2007. **1**(2): p. 140-52.

156. van Heemst, D., *Insulin, IGF-1 and longevity.* Aging Dis, 2010. **1**(2): p. 147-57.

157. Calado, R.T., *Telomeres and marrow failure.* Hematology Am Soc Hematol Educ Program, 2009: p. 338-43.

158. Pinto, A., et al., *Aging and the hemopoietic system.* Crit Rev Oncol Hematol, 2003. **48**(Suppl): p. S3-S12.

159. Prabhakar, M., W.B. Ershler, and D.L. Longo, *Bone marrow, thymus and blood: changes across the lifespan.* Aging health, 2009. **5**(3): p. 385-393.

160. Hardouin, P., V. Pansini, and B. Cortet, *Bone marrow fat.* Joint Bone Spine, 2014. **81**(4): p. 313-9.

161. Latchney, S.E. and L.M. Calvi, *The aging hematopoietic stem cell niche: Phenotypic and functional changes and mechanisms that contribute to hematopoietic aging.* Semin Hematol, 2017. **54**(1): p. 25-32.

162. Ikehara, S. and M. Li, *Stem cell transplantation improves aging-related diseases.* Front Cell Dev Biol, 2014. **2**: p. 16.

163. Henry, C.J., et al., *Declining lymphoid progenitor fitness promotes aging-associated leukemogenesis.* Proc Natl Acad Sci U S A, 2010. **107**(50): p. 21713-8.

164. Lim, M., et al., *Altered mesenchymal niche cells impede generation of normal hematopoietic progenitor cells in leukemic bone marrow.* Leukemia, 2016. **30**(1): p. 154-62.

165. Petrov, I., et al., *Molecular pathway activation features of pediatric acute myeloid leukemia (AML) and acute lymphoblast leukemia (ALL) cells.* Aging (Albany NY), 2016. **8**(11): p. 2936-2947.

166. Riley, R.L., *Impaired B lymphopoiesis in old age: a role for inflammatory B cells?* Immunologic research, 2013. **57**(1-3): p. 361-369.

167. Kannan, S., et al., *Age-related changes in the transcriptome of antibody-secreting cells.* Oncotarget, 2016. **7**(12): p. 13340.

168. Zhang, L., et al., *Role of Osteoprotegerin (OPG) in Bone Marrow Adipogenesis.* Cellular Physiology and Biochemistry, 2016. **40**(3-4): p. 681-692.

169. Takeshita, S., et al., *Age-related marrow adipogenesis is linked to increased expression of RANKL.* J Biol Chem, 2014. **289**(24): p. 16699-710.

170. Salem, S., et al., *A novel role for interferon regulatory factor 1 (IRF1) in regulation of bone metabolism.* Journal of cellular and molecular medicine, 2014. **18**(8): p. 1588-1598.

171. Ambati, J., et al., *Age-related macular degeneration: etiology, pathogenesis, and therapeutic strategies.* Survey of ophthalmology, 2003. **48**(3): p. 257-293.

172. Chirco, K., et al., *Structural and molecular changes in the aging choroid: implications for age-related macular degeneration.* Eye, 2017. **31**(1): p. 10-25.

173. Donath, M.Y., *Targeting inflammation in the treatment of type 2 diabetes: time to start.* Nature reviews Drug discovery, 2014. **13**(6): p. 465-476.

174. Park, S.S., et al., *Advances in bone marrow stem cell therapy for retinal dysfunction.* Progress in retinal and eye research, 2017. **56**: p. 148-165.

175. Ding, D.C., W.C. Shyu, and S.Z. Lin, *Mesenchymal stem cells.* Cell Transplant, 2011. **20**(1): p. 5-14.

176. Soleimani, M. and S. Nadri, *A protocol for isolation and culture of mesenchymal stem cells from mouse bone marrow.* Nat Protoc, 2009. **4**(1): p. 102-6.

177. Polisetti, N., et al., *Isolation, characterization and differentiation potential of rat bone marrow stromal cells.* Neurology India, 2010. **58**(2): p. 201.

178. Mareschi, K., et al., *Isolation of human mesenchymal stem cells: bone marrow versus umbilical cord blood.* Haematologica, 2001. **86**(10): p. 1099-1100.

179. Miao, Z., et al., *Isolation of mesenchymal stem cells from human placenta: comparison with human bone marrow mesenchymal stem cells.* Cell biology international, 2006. **30**(9): p. 681-687.

180. Jeon, B.-G., D.-O. Kwack, and G.-J. Rho, *Variation of telomerase activity and morphology in porcine mesenchymal stem cells and fibroblasts during prolonged in vitro culture.* Animal biotechnology, 2011. **22**(4): p. 197-210.

181. Bonab, M.M., et al., *Aging of mesenchymal stem cell in vitro.* BMC cell biology, 2006. **7**(1): p. 14.

182. Cmielova, J., et al., *Gamma radiation induces senescence in human adult mesenchymal stem cells from bone marrow and periodontal ligaments.* Int J Radiat Biol, 2012. **88**(5): p. 393-404.

183. Atoui, R. and R.C. Chiu, *Concise review: immunomodulatory properties of mesenchymal stem cells in cellular transplantation: update, controversies, and unknowns.* Stem Cells Transl Med, 2012. **1**(3): p. 200-5.

184. Kitada, M. and M. Dezawa, *Parkinson's disease and mesenchymal stem cells: potential for cell-based therapy.* Parkinsons Dis, 2012. **2012**: p. 873706.

185. Poncin, G., et al., *Characterization of spontaneous bone marrow recovery after sublethal total body irradiation: importance of the osteoblastic/adipocytic balance.* PLoS One, 2012. **7**(2): p. e30818.

186. Perazzio, A.S., et al., *Increase of IRF-1 gene expression and impairment of T regulatory cells suppression activity on patients with myelodysplastic syndrome: A longitudinal one-year study.* Leukemia research, 2017. **55**: p. 6-17.

187. Sato, T., et al., *Interferon regulatory factor-2 protects quiescent hematopoietic stem cells from type I interferon–dependent exhaustion.* Nature medicine, 2009. **15**(6): p. 696-700.

188. Li, H., et al., *Isolation and characterization of primary bone marrow mesenchymal stromal cells.* Ann N Y Acad Sci, 2016. **1370**(1): p. 109-18.

189. Nadri, S., et al., *An efficient method for isolation of murine bone marrow mesenchymal stem cells.* Int J Dev Biol, 2007. **51**(8): p. 723-9.

190. Dominici, M., et al., *Minimal criteria for defining multipotent mesenchymal stromal cells. The International Society for Cellular Therapy position statement.* Cytotherapy, 2006. **8**(4): p. 315-7.

191. Roy, S., et al., *Donor hematopoietic stem cells confer long-term marrow reconstitution by self-renewal divisions exceeding to that of host cells.* PLoS One, 2012. **7**(12): p. e50693.

192. Riccardi, C. and I. Nicoletti, *Analysis of apoptosis by propidium iodide staining and flow cytometry.* Nature protocols, 2006. **1**(3): p. 1458-1461.

193. Belloc, F., et al., *A flow cytometric method using Hoechst 33342 and propidium iodide for simultaneous cell cycle analysis and apoptosis determination in unfixed cells.* Cytometry Part A, 1994. **17**(1): p. 59-65.

194. Baustian, C., S. Hanley, and R. Ceredig, *Isolation, selection and culture methods to enhance clonogenicity of mouse bone marrow derived mesenchymal stromal cell precursors.* Stem Cell Res Ther, 2015. **6**: p. 151.

195. Quan, H., et al., *Optimization of growth inducing factors for colony forming and attachment of bone marrow-derived mesenchymal stem cells regarding bioengineering application.* The journal of advanced prosthodontics, 2014. **6**(5): p. 379-386.

196. Avwioro, G., *Histochemical uses of haematoxylin—a review.* Jpcs, 2011. **1**: p. 24-34.

197. Cho, A., et al., *A method for rapid demineralization of teeth and bones.* The open dentistry journal, 2010. **4**: p. 223.

198. Cho, A., et al., *A method for rapid demineralization of teeth and bones.* Open Dent J, 2010. **4**: p. 223-9.

199. Bustin, S.A., et al., *The MIQE guidelines: minimum information for publication of quantitative real-time PCR experiments.* Clin Chem, 2009. **55**(4): p. 611-22.

200. Schmittgen, T.D. and K.J. Livak, *Analyzing real-time PCR data by the comparative C(T) method.* Nat Protoc, 2008. **3**(6): p. 1101-8.

201. Cai, Y.-J., et al., *Up-regulation of intestinal epithelial cell derived IL-7 expression by keratinocyte growth factor through STAT1/IRF-1, IRF-2 pathway.* PLoS One, 2013. **8**(3): p. e58647.

202. Boyer, L.A., D. Mathur, and R. Jaenisch, *Molecular control of pluripotency.* Current Opinion in Genetics & Development, 2006. **16**(5): p. 455-462.

203. Nascimento, F.R., et al., *Interferon regulatory factor (IRF)-1 is a master regulator of the cross talk between macrophages and L929 fibrosarcoma cells for nitric oxide dependent tumoricidal activity.* PLoS One, 2015. **10**(2): p. e0117782.

204. Ahmed, M., M. Ghabriel, and A. Amleh, *Enrichment, Propagation, and Characterization of Mouse Testis-Derived Mesenchymal Stromal Cells.* Cellular Reprogramming (Formerly" Cloning and Stem Cells"), 2017. **19**(1): p. 35-43.

205. Cho, K.A., et al., *Transplantation of bone marrow cells reduces CCl4- induced liver fibrosis in mice.* Liver International, 2011. **31**(7): p. 932-939.

206. Orlic, D., et al., *Bone marrow cells regenerate infarcted myocardium.* Nature, 2001. **410**(6829): p. 701-705.

207. Huang, S., et al., *An improved protocol for isolation and culture of mesenchymal stem cells from mouse bone marrow*. Journal of Orthopaedic Translation, 2015. **3**(1): p. 26-33.

208. Trumpp, A., M. Essers, and A. Wilson, *Awakening dormant haematopoietic stem cells.* Nat Rev Immunol, 2010. **10**(3): p. 201-9.

209. Ren, G., et al., *Concise review: mesenchymal stem cells and translational medicine: emerging issues.* Stem cells translational medicine, 2012. **1**(1): p. 51-58.

210. Reyes, M., et al., *Donor origin of multipotent adult progenitor cells in radiation chimeras.* Blood, 2005. **106**(10): p. 3646-9.

211. Chamberlain, G., et al., *Concise review: mesenchymal stem cells: their phenotype, differentiation capacity, immunological features, and potential for homing.* Stem Cells, 2007. **25**(11): p. 2739-49.

212. Li, Y., et al., *Comparative study of mesenchymal stem cells from C57BL/10 and mdx mice.* BMC cell biology, 2008. **9**(1): p. 24.

213. Sung, J., et al. *Isolation and characterization of mouse mesenchymal stem cells*. in *Transplantation proceedings*. 2008: Elsevier.

214. Chaudhary J.K. and Rath P.C., *A Simple Method for Isolation, Propagation, characterization, andDifferentiation of Adult Mouse Bone Marrow-Derived Multipotent Mesenchymal Stem Cells.* J Cell Sci Ther 2017, 8:1

215. Marim, F.M., et al., *A method for generation of bone marrow-derived macrophages from cryopreserved mouse bone marrow cells.* PLoS One, 2010. **5**(12): p. e15263.

216. Karp, J.M. and G.S.L. Teo, *Mesenchymal stem cell homing: the devil is in the details.* Cell Stem Cell, 2009. **4**(3): p. 206-216.

217. Anjos-Afonso, F. and D. Bonnet, *Isolation, culture, and differentiation potential of mouse marrow stromal cells.* Curr Protoc Stem Cell Biol, 2008. **Chapter 2**: p. Unit 2B 3.

218. Huang, L., A.R. Snyder, and W.F. Morgan, *Radiation-induced genomic instability and its implications for radiation carcinogenesis.* Oncogene, 2003. **22**(37): p. 5848-5854.

219. Wilke, C., et al., *Marrow damage and hematopoietic recovery following allogeneic bone marrow transplantation for acute leukemias: Effect of radiation dose and conditioning regimen.* Radiother Oncol, 2016. **118**(1): p. 65-71.

220. Digirolamo, C.M., et al., *Propagation and senescence of human marrow stromal cells in culture: a simple colony-forming assay identifies samples with the greatest potential to propagate and differentiate.* Br J Haematol, 1999. **107**(2): p. 275-81.

221. Pallavicini, M.G., et al., *Rescue from lethal irradiation correlates with transplantation of 10-20 CFU-S-day 12.* Blood Cells Mol Dis, 1997. **23**(2): p. 157-68.

222. Cao, X., et al., *Irradiation induces bone injury by damaging bone marrow microenvironment for stem cells.* Proc Natl Acad Sci U S A, 2011. **108**(4): p. 1609-14.

223. Bruna, F., et al., *Regenerative Potential of Mesenchymal Stromal Cells: Age-Related Changes.* Stem Cells Int, 2016. **2016**: p. 1461648.

224. Liebermann, D.A. and B. Hoffman, *Good and bad IRF-1: role in tumor suppression versus autoimmune disease.* Leuk Res, 2009. **33**(10): p. 1301-2.

225. Han, S.K., et al., *Gamma irradiation-reduced IFN-gamma expression, STAT1 signals, and cell-mediated immunity.* J Biochem Mol Biol, 2002. **35**(6): p. 583-9.

226. Liu, T.M., et al., *Effects of ectopic Nanog and Oct4 overexpression on mesenchymal stem cells.* Stem cells and development, 2009. **18**(7): p. 1013-1022.

227. Izadpanah, R., et al., *Biologic properties of mesenchymal stem cells derived from bone marrow and adipose tissue.* Journal of cellular biochemistry, 2006. **99**(5): p. 1285-1297.

228. Wilson, A. and A. Trumpp, *Bone-marrow haematopoietic-stem-cell niches.* Nature Reviews Immunology, 2006. **6**(2): p. 93-106.

229. Galan-Caridad, J.M., et al., *Zfx controls the self-renewal of embryonic and hematopoietic stem cells.* Cell, 2007. **129**(2): p. 345-57.

230. Izadpanah, R., et al., *Biologic properties of mesenchymal stem cells derived from bone marrow and adipose tissue.* J Cell Biochem, 2006. **99**(5): p. 1285-97.

231. Xie, C., et al., *Effects of IRF1 and IFN-beta interaction on the M1 polarization of macrophages and its antitumor function.* Int J Mol Med, 2016. **38**(1): p. 148-60.

232. Guo, M., et al., *IFN Regulatory Factor-1 Modulates the Function of Dendritic Cells in Patients with Acute Coronary Syndrome.* Cell Physiol Biochem, 2015. **36**(2): p. 599-610.

233. Yang, H., et al., *Histone deacetylase sirtuin 1 deacetylates IRF1 protein and programs dendritic cells to control Th17 protein differentiation during autoimmune inflammation.* J Biol Chem, 2013. **288**(52): p. 37256-66.

234. Kano, S., et al., *The contribution of transcription factor IRF1 to the interferon-gamma-interleukin 12 signaling axis and TH1 versus TH-17 differentiation of CD4+ T cells.* Nat Immunol, 2008. **9**(1): p. 34-41.

235. Unutmaz, D. and J. Vilcek, *IRF1: a deus ex machina in TH1 differentiation.* Nature immunology, 2008. **9**(1): p. 9-10.

236. Manzella, L., et al., *Role of interferon regulatory factor 1 in monocyte/macrophage differentiation.* Eur J Immunol, 1999. **29**(9): p. 3009-16.

237. Ogasawara, K., et al., *Requirement for IRF-1 in the microenvironment supporting development of natural killer cells.* Nature, 1998. **391**(6668): p. 700-3.

238. Notake, T., et al., *Differential requirements for IRF-2 in generation of CD1d-independent T cells bearing NK cell receptors.* J Immunol, 2012. **188**(10): p. 4838-45.

239. Sato, T., et al., *Interferon regulatory factor-2 protects quiescent hematopoietic stem cells from type I interferon-dependent exhaustion.* Nat Med, 2009. **15**(6): p. 696-700.

240. Hida, S., et al., *Negative control of basophil expansion by IRF-2 critical for the regulation of Th1/Th2 balance.* Blood, 2005. **106**(6): p. 2011-7.

241. Balsam, L.B., et al., *Haematopoietic stem cells adopt mature haematopoietic fates in ischaemic myocardium.* Nature, 2004. **428**(6983): p. 668-73.

242. Barry, F.P. and J.M. Murphy, *Mesenchymal stem cells: clinical applications and biological characterization.* Int J Biochem Cell Biol, 2004. **36**(4): p. 568-84.

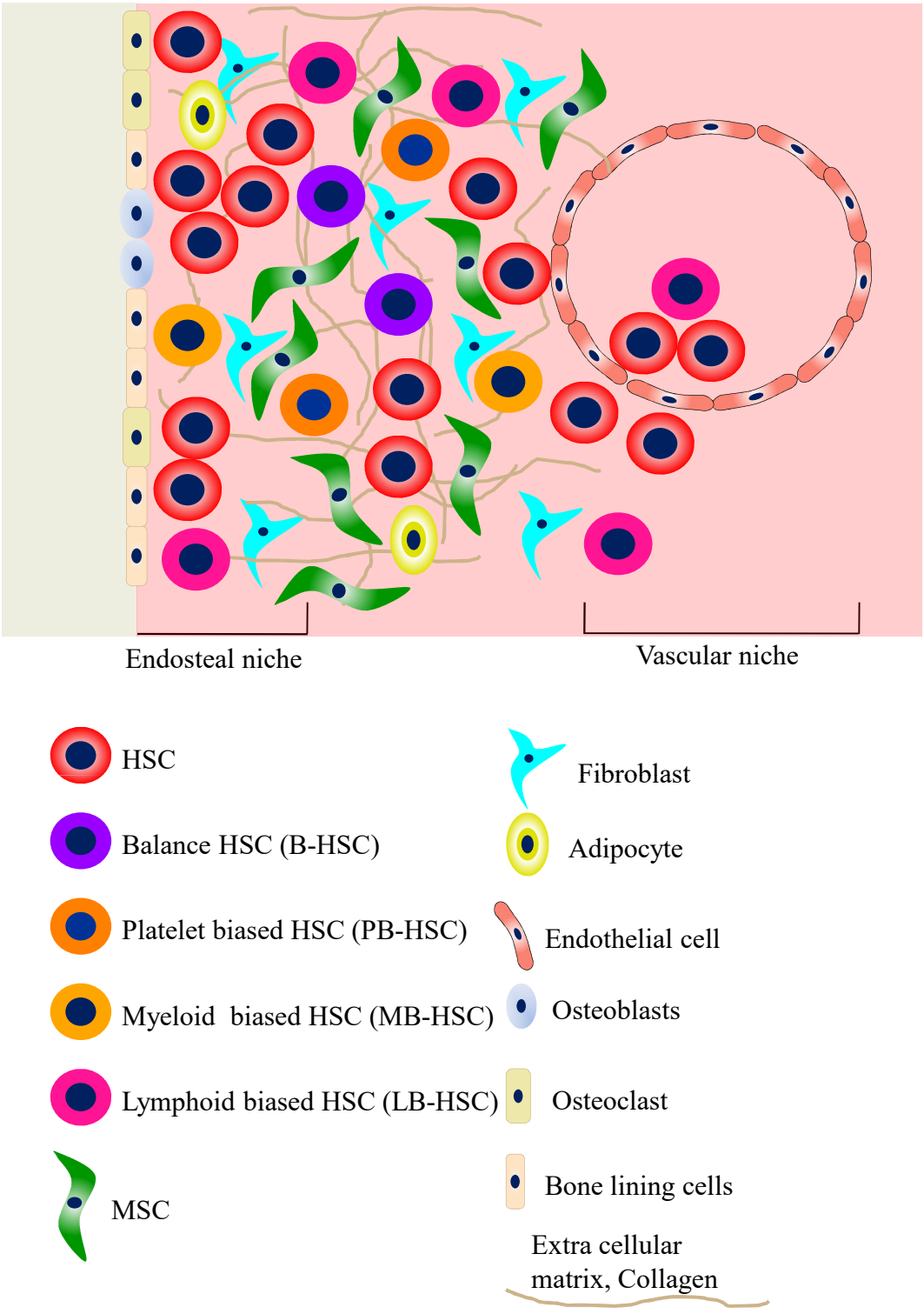

Figure I: Structure and cellular organization of adult bone marrow. Bone marrow shows the structural organization of bone marrow cells and niches such as endosteal niche and vascular niche. Bone marrow comprises various kinds of cells including HSCs, MSCs, MAPCs, adipocytes, endothelial cells, osteoblasts, and osteoclasts. Each cell performs its particular function. The overall functions of bone marrow have complex but highly coordinated regulations.

(A) Modular structure of interferon regulatory factor-1

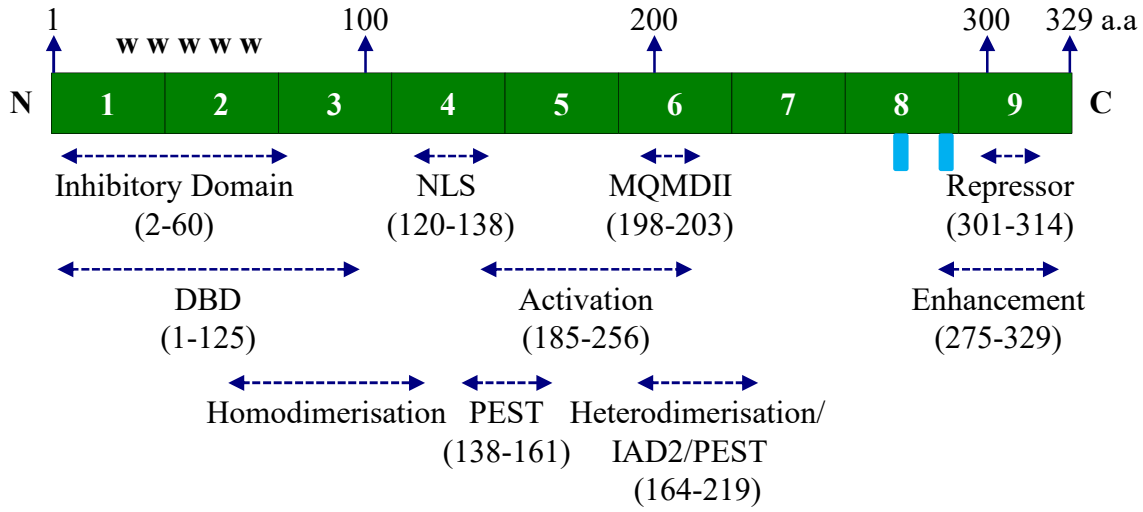

(B) Modular structure of interferon regulatory factor-2

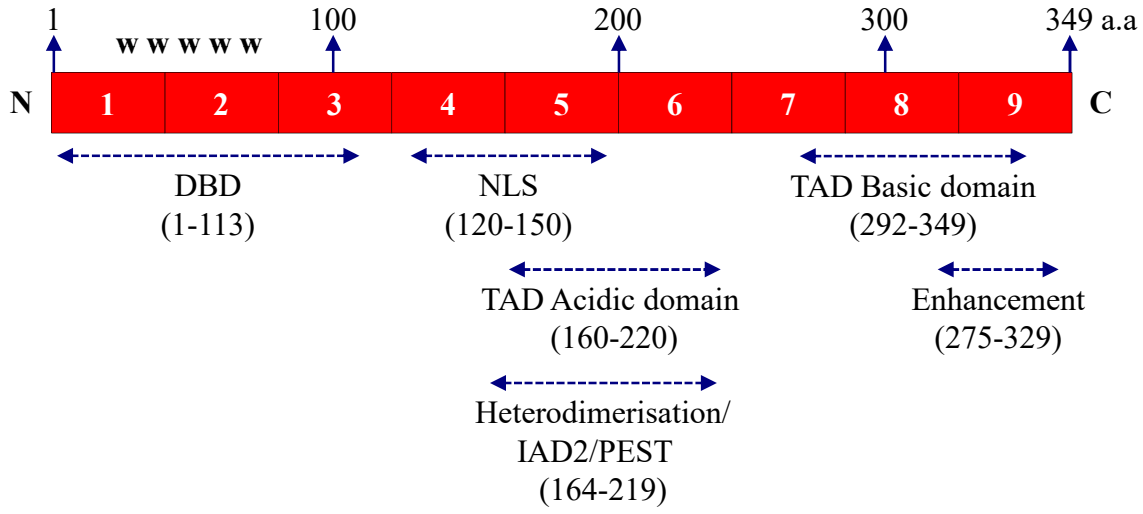

Figure II: The modular domain structure of IRF1 and IRF2. The modular structure of IRF-1 and IRF-2 transcription factors displaying multiple domains with N-terminal DNA binding domain (DBD), C-terminal regulatory domain, and different sites for several post-translational modifications. The DBD of IRF-1 and IRF-2 is precisely identified by the presence of five relatively well conserved tryptophan-rich repeats. IRF-1 and IRF-2 include an IRF association domain (IAD2) from 164th amino acid to the 219th amino acid (a.a.) residues in entire protein molecule. The other relevant domains are a nuclear localizing signal (NLS), trans-activating domain (TAD). Ref: DOI: DOI: 10.1146/annurev.immunol.26.021607.090400.

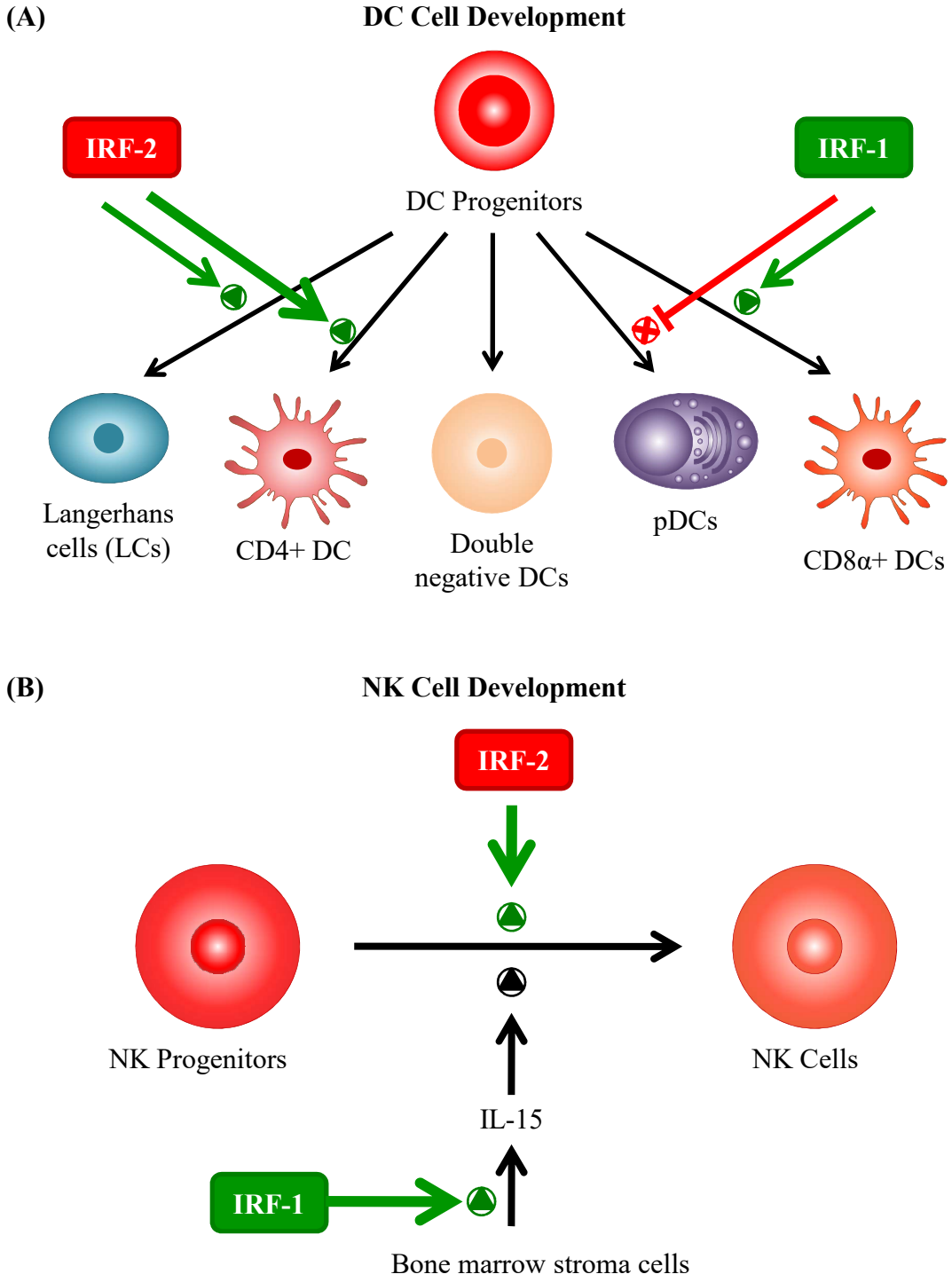

Figure III: Regulation of dendritic cell (DC) and natural killer (NK) cell development by IRF-1 and IRF-2. (A): IRF-1 positively controls CD8α + DC differentiation, whereas it negatively regulates pDC differentiation. IRF-2 is involved in the development of splenic CD4+ DCs as well as CD4+ LCs through negatively regulating type I IFN signaling. **(B):** IRF-1 is fundamental for NK cell development by regulating the expression of IL-15, a cytokine that promotes NK cell development in bone marrow stromal cells, while IRF-2 helps NK cell development in an NK cell–intrinsic manner. Ref: DOI: DOI: 10.1146/annurev.immunol.26.021607.090400.

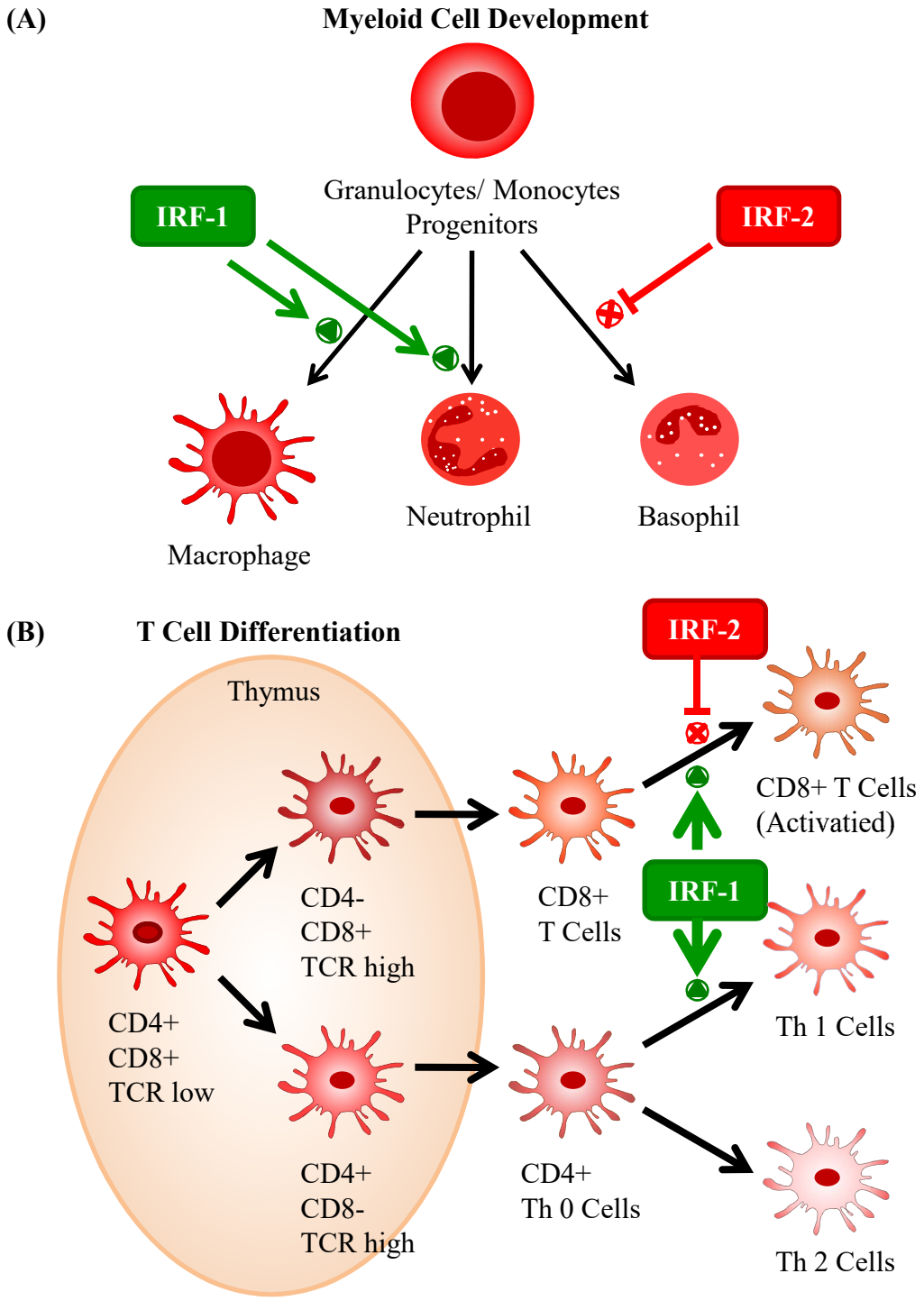

Figure IV: The role of IRF-1 and IRF-2 in myeloid cell development and T cell differentiation. (A): IRF-1 is needed for the sufficient maturation of neutrophils and macrophages. IRF-2 negatively controls the expansion of basophils. **(B):** In the thymus, IRF-1 performs a crucial role in CD8+ T cell development. IRF-1 positively regulates cytotoxic T lymphocyte (CTL) activation. IRF-1 is essential for CD4+ T cells to react to the Th1 cytokine IL-12. IRF-2 is suspected for preventing hyperresponsiveness of CD8+ T cells to antigen stimulation, which is mediated by IRF-2's negative regulation of type I IFN signaling. In addition, IRF-2 negatively controls Th2 polarization in mice by restricting the number of basophils that discharge the Th2 cytokine, IL-4. Th1 differentiation requires IRF-1 and IRF-2.
Ref: DOI: DOI: 10.1146/annurev.immunol.26.021607.090400.

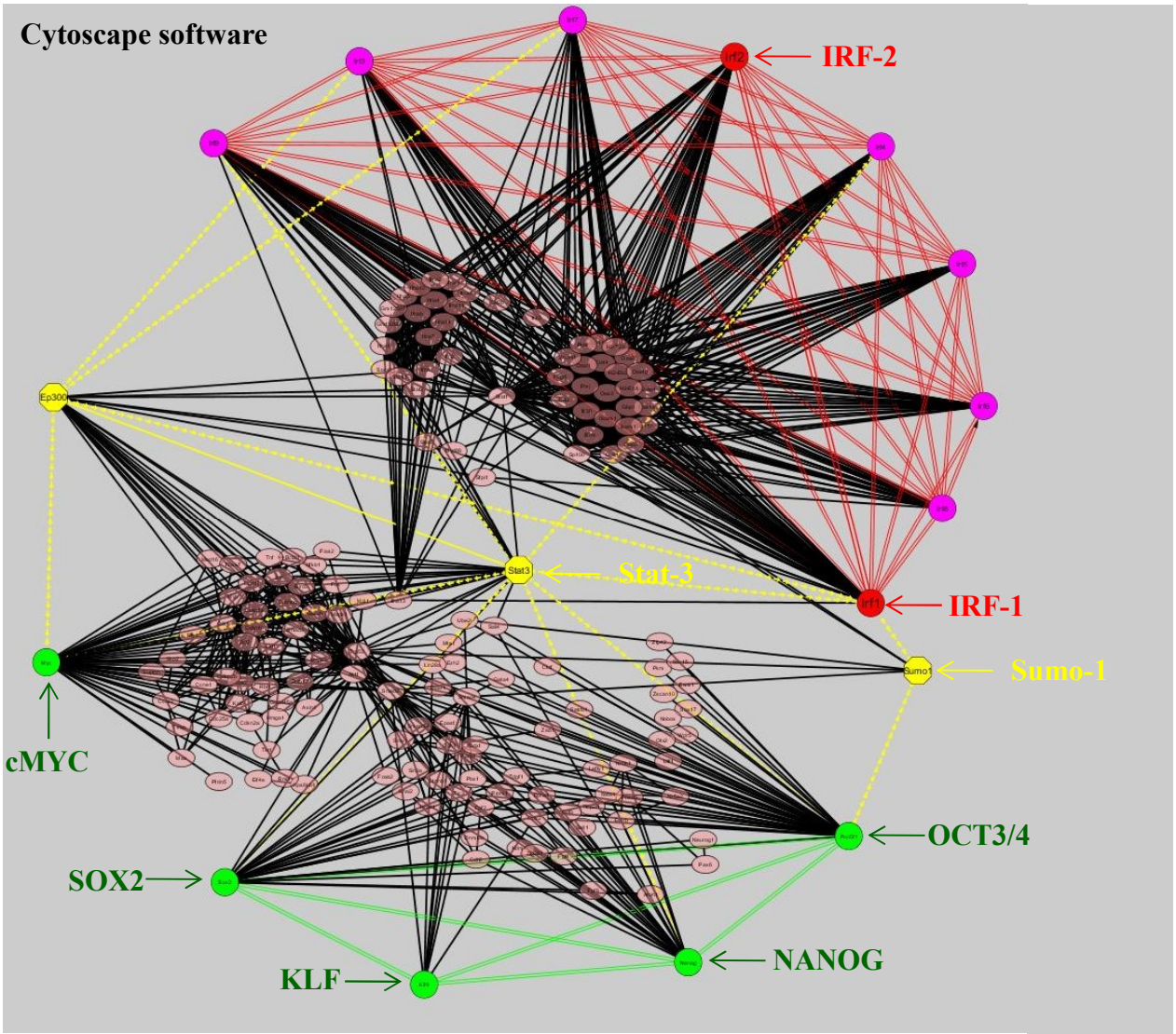

Figure V: Bioinformatic network between interferon regulatory factor(s) and pluripotency associated transcription factors explain the possible connection among them. This may propose for role of IRF-1 and IRF-2 in bone marrow stem cells.

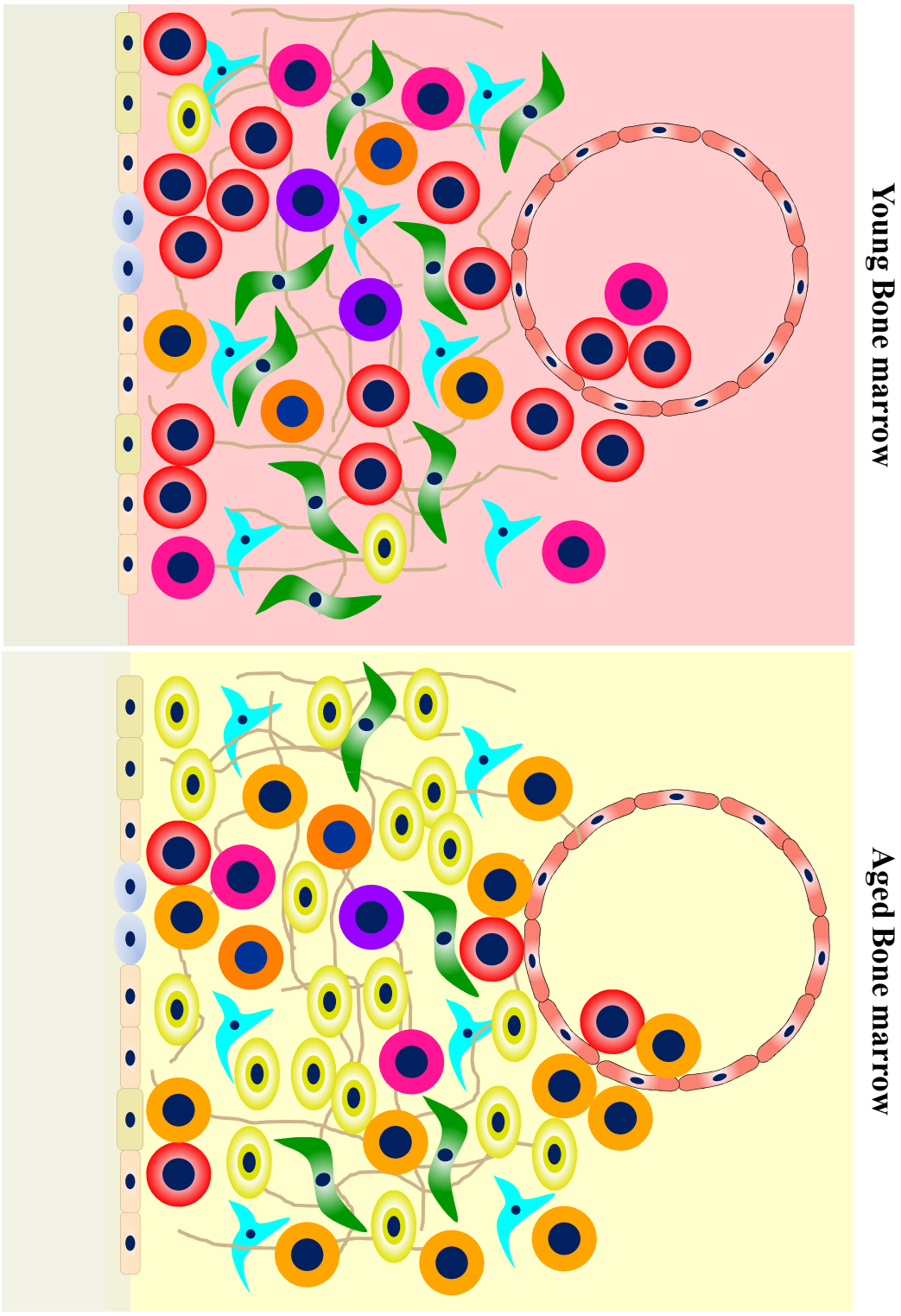

Figure VI: Differences between young bone marrow and aged bone marrow over the time. Young bone marrow is reddish due to high hematopoiesis activity, which turns into yellow or fatty marrow, which has great adipocyte deposition and shows insignificant hematopoiesis activity, over the time (age).

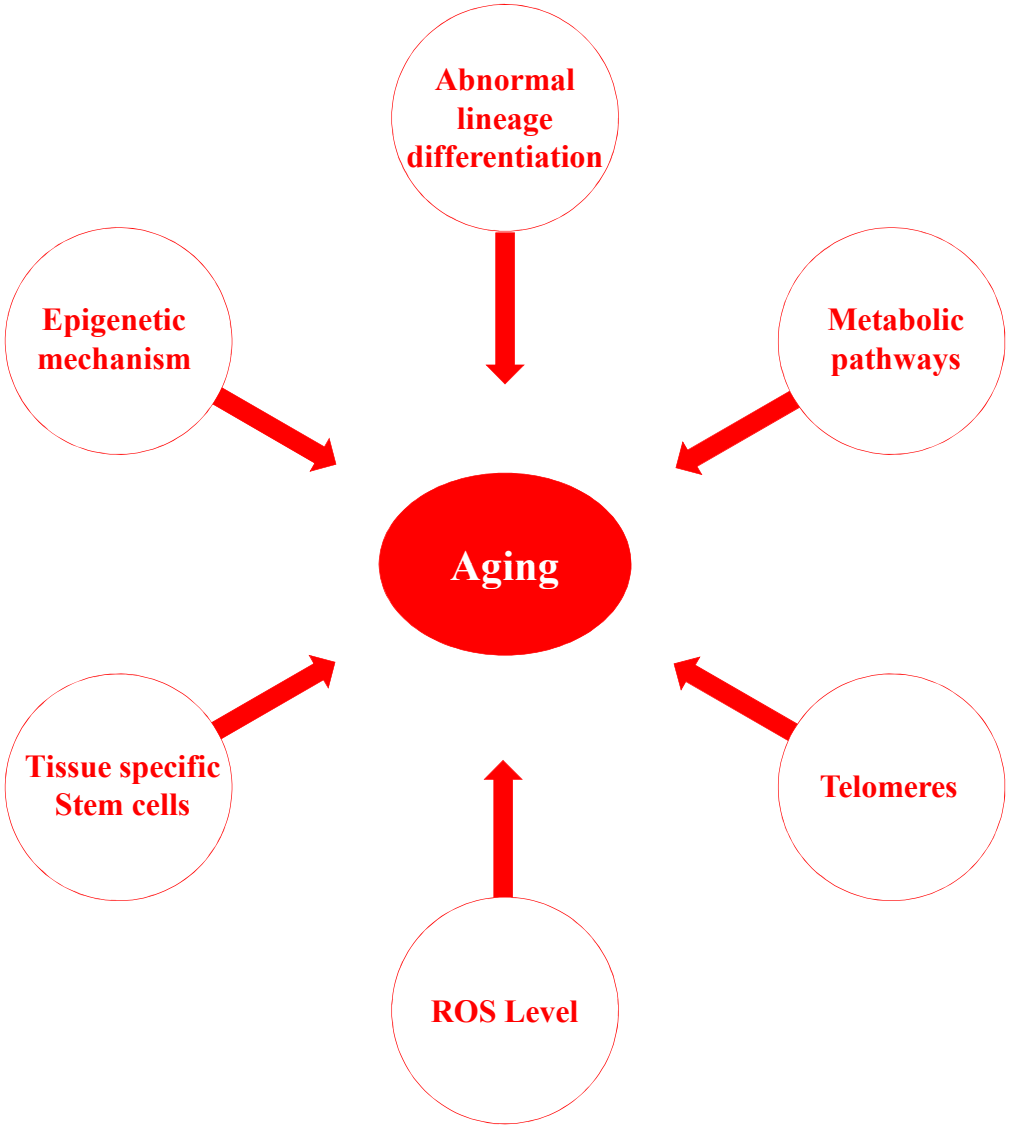

Figure VII: Axis or Theory of Aging. An aging process, which includes various theories such as stem cell theory, gene expression changes theory, ROS theory of aging, epigenetic mechanisms, metabolic pathways in aging and function of telomeres during aging.

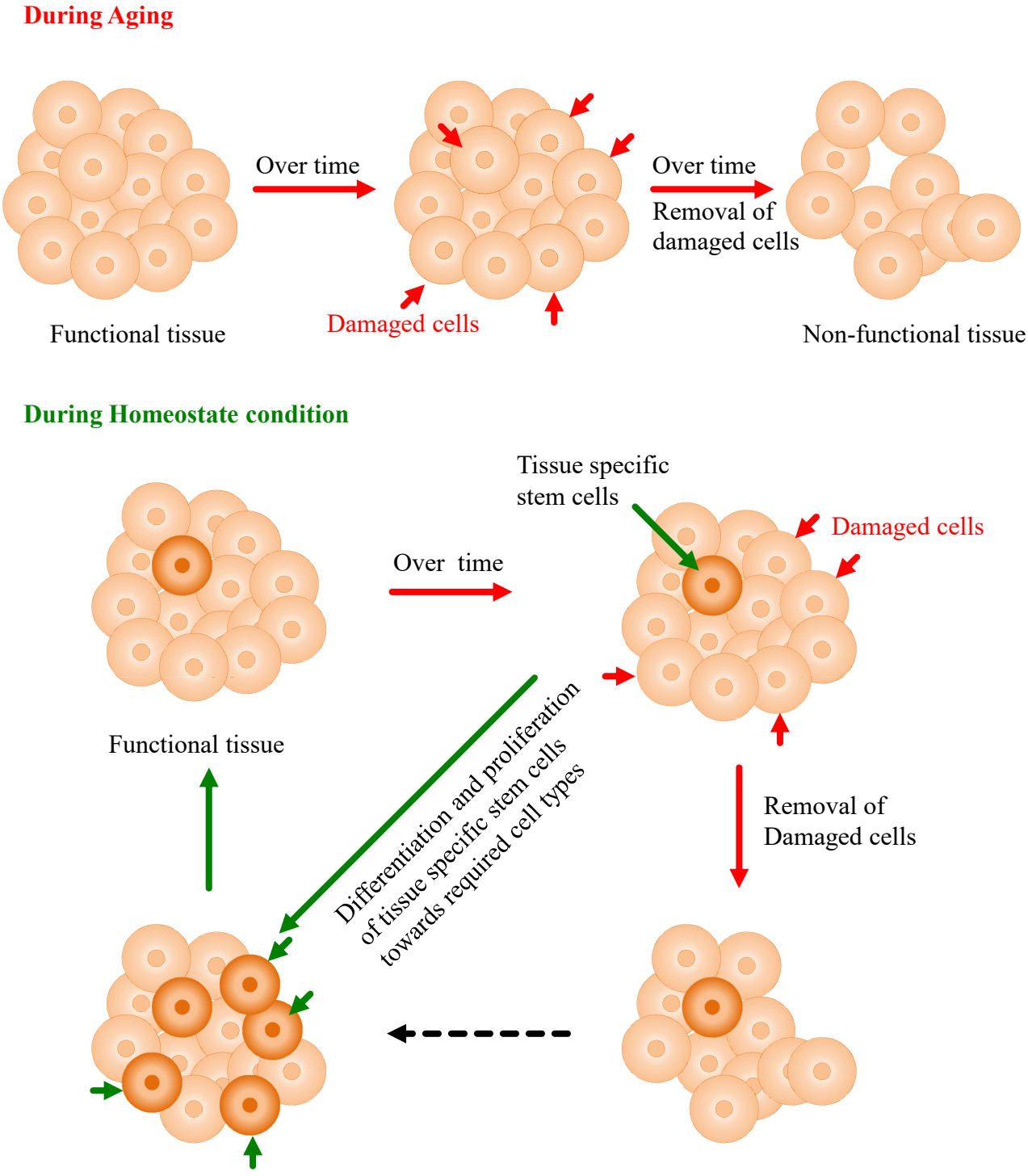

Figure VIII: Stem cell theory of aging. Tissue-specific stem cells support the homeostate in the tissue by differentiation of tissue-specific stem cells to generate the required cell types and provide more stem cells and differentiated cells in the tissue to sustain and rejuvenate the tissues and protect tissue or organ malfunction and struggle with the aging process.

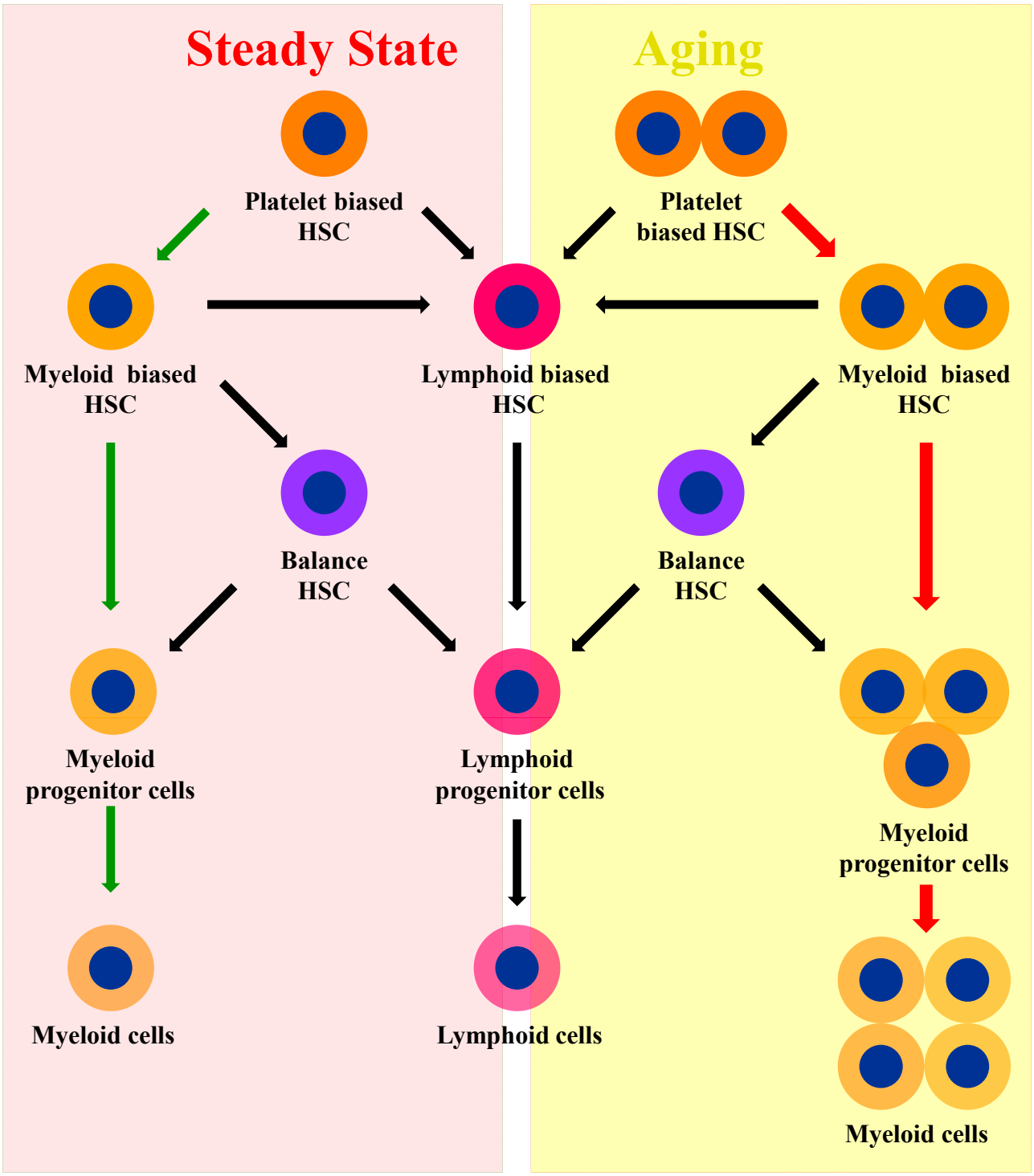

Figure IX: Modified image of abnormal lineage differentiation during aging. Lymphoid lineage-specific genes are deactivated, whereas myeloid lineage-specific genes, megakaryocyte-associated genes, and many protoncogenes were observed to be more activated with aging. As a result, myeloid cells increase in number as compared to lymphoid cells during aging process. Dysregulation of lineage differentiation leads to abnormal cellular and bone marrow function. Ref: DOI: 10.3389/fimmu.2016.00502.

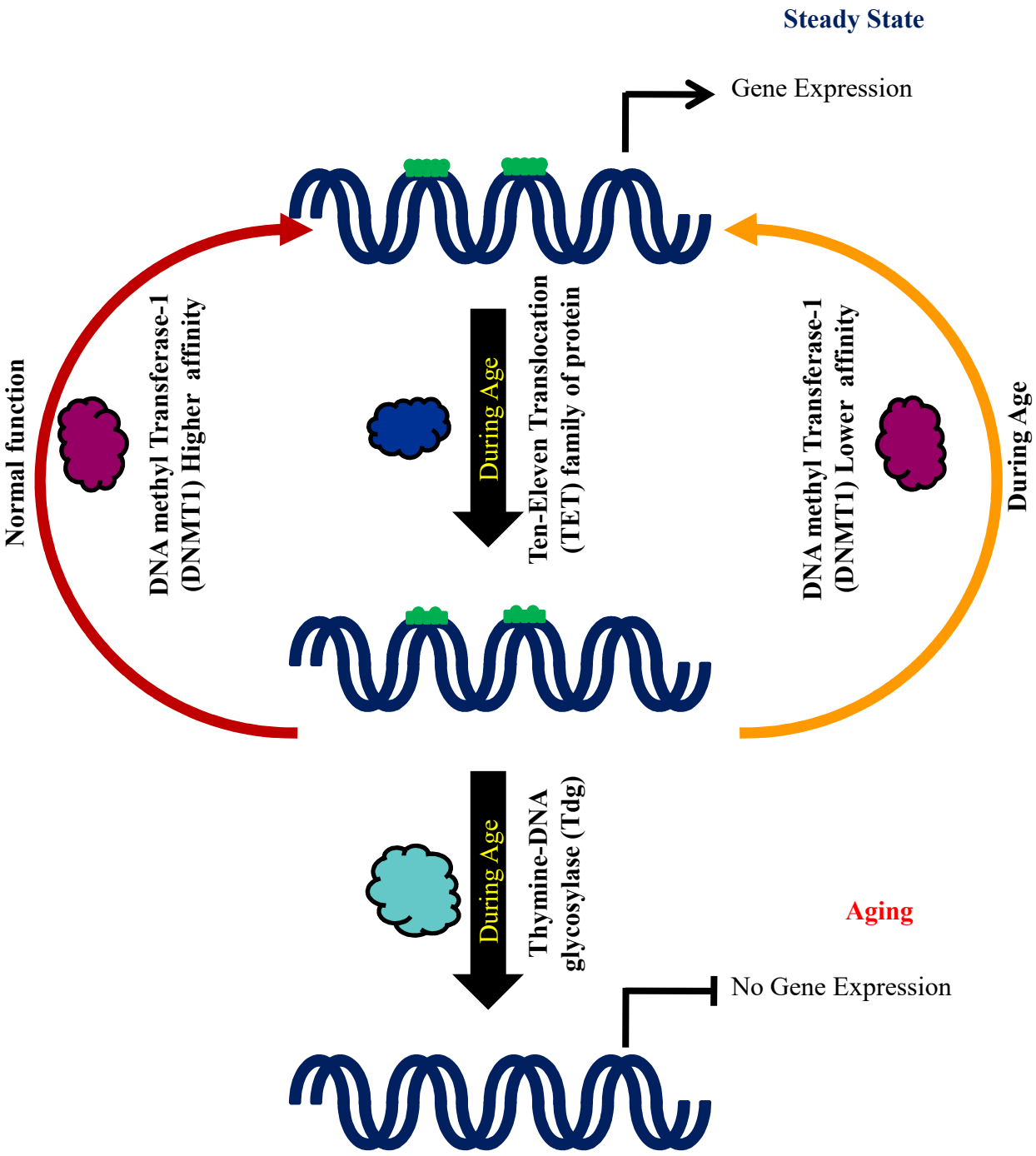

Figure X: Epigenetic Mechanism of Aging. Epigenetic modification such as DNA methylation causing global DNA methylation decreasing gradually and increasing at promoter regions during aging. Methylated cytosine (5mC) is a stable DNA modification, but an epigenetic regulatory enzyme such as Ten-eleven Translocation (TET) family of protein enzymatically oxidizes 5mC to 5hmC, and then thymine-DNA glycosylase (Tdg) generate unmethylated cytosine. Unmethylated cytosine is linked to the repression of many genes and poise the enhancer in differentiated and embryonic stem cells.

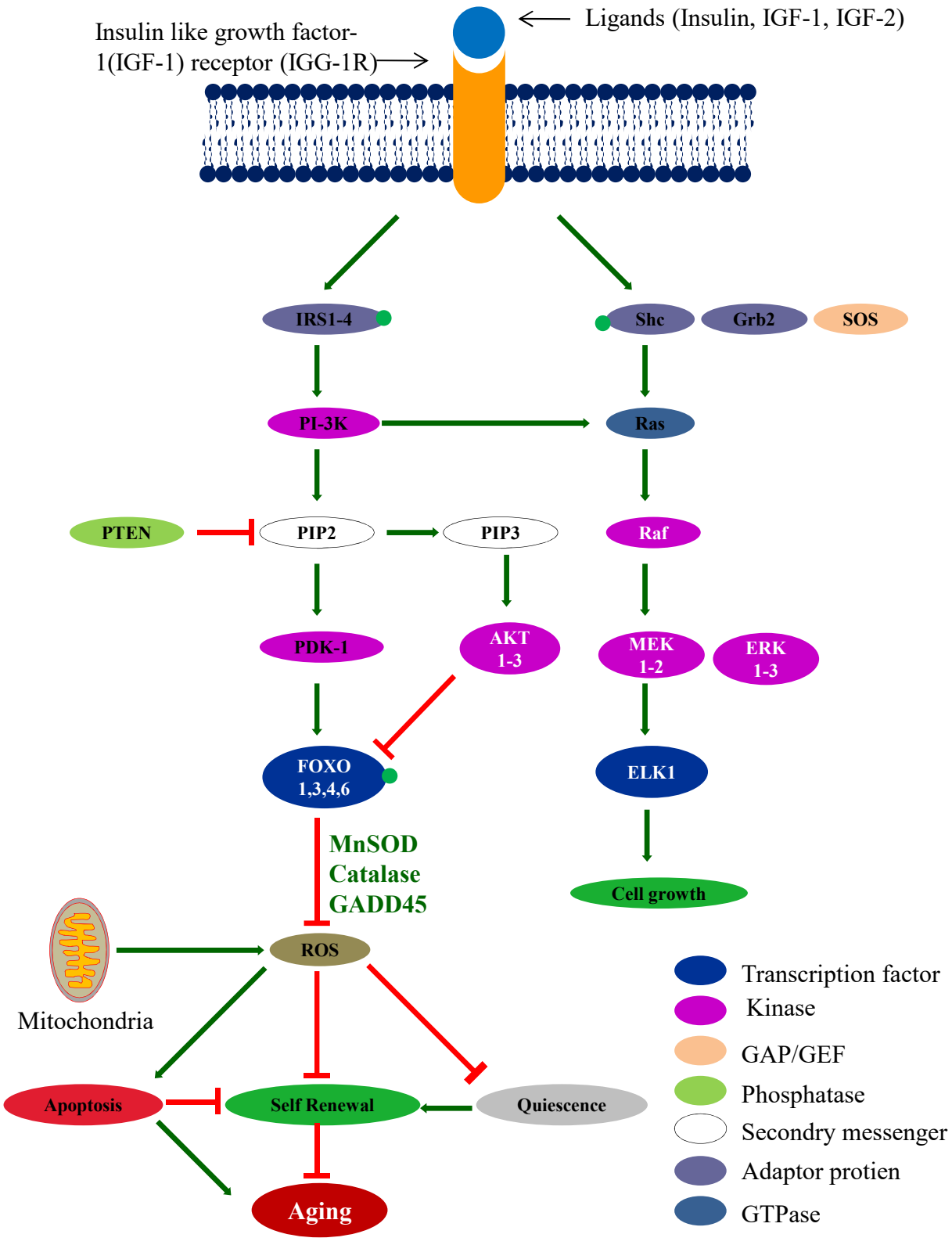

Figure XI: Modified simple representation of the metabolic mechanism of aging of stem cells in bone marrow. Relationship between metabolic pathways and aging process is depicted. Insulin and IGF-1 signaling (IIS) activate FOXO transcription factors, which inhibit ROS production, activity of p53 and enhanced mitochondrial biogenesis and self-renewal. Hence such metabolic pathway limits the aging process. Ref: DOI :10.1016/j.stem.2007.07.017

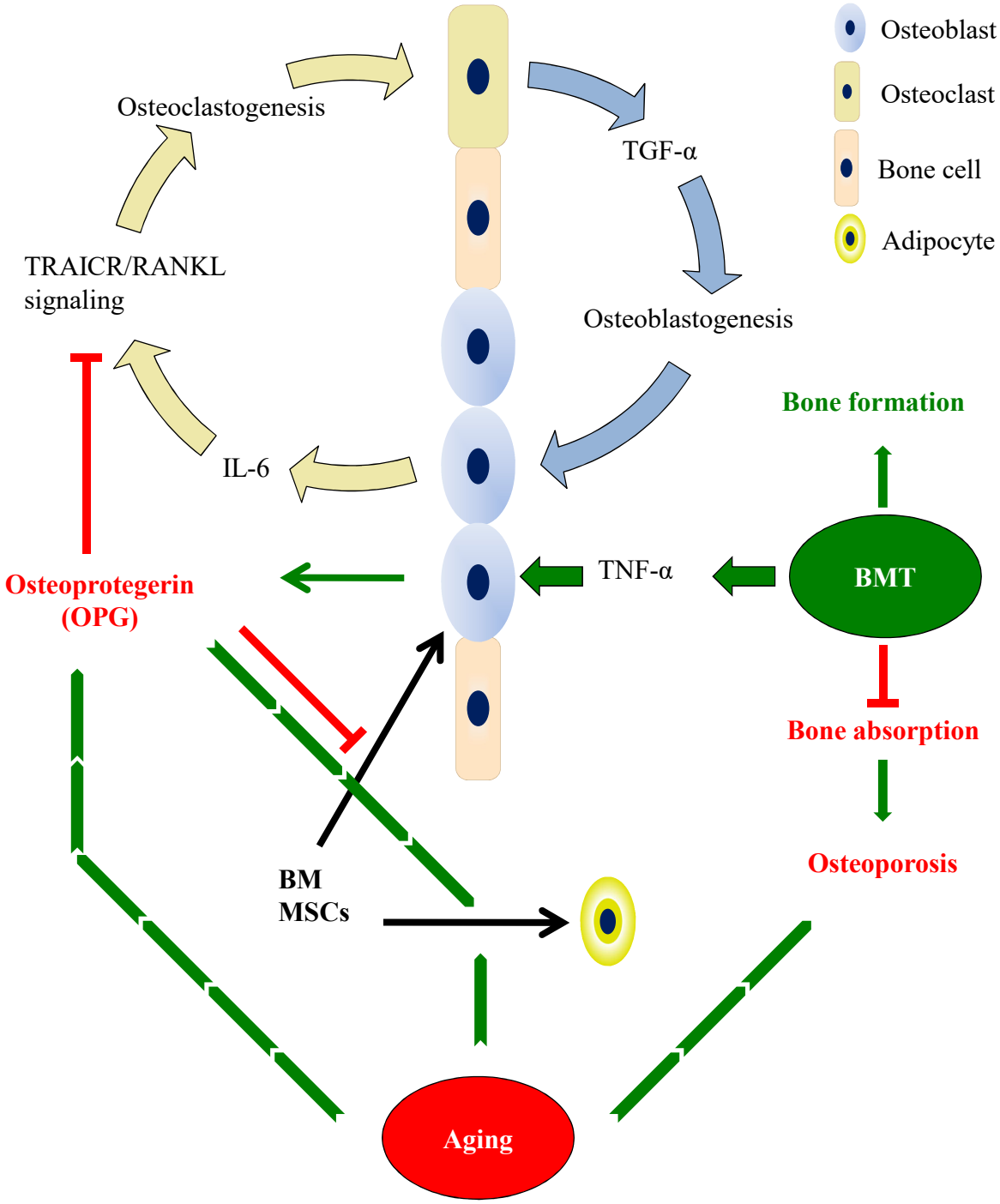

Figure XII: Bone formation, Osteoporosis, Adipogenesis. MSCs can differentiate into osteoblasts, chondrocytes, and adipocytes under the control mechanism/condition. Under normal conditions, osteoclasts secret TGF-α, which in turn activates osteoblastogenesis resulting osteoblast generation. Osteoblasts release IL-6, which is more crucial for TRAICR/RANKL signaling in osteoclasts, which are responsible for osteoclastogenesis. During aging process, osteoblasts and osteocytes mainly produce osteoprotegerin (OPG), a cytokine receptor, which mimic as RANK. RANKL-OPG binding inhibits the downstream signaling and blocks osteoclastogenesis. Moreover, MSCs differentiate into adipocytes, instead of osteoblasts, and accumulate in the bone marrow cavity, which leads to osteoporosis in the bone with advancing age. Bone marrow transplantation reduces bone absorption and inhibits osteoporosis.
Ref: DOI: 10.3389/fcell.2014.00016.

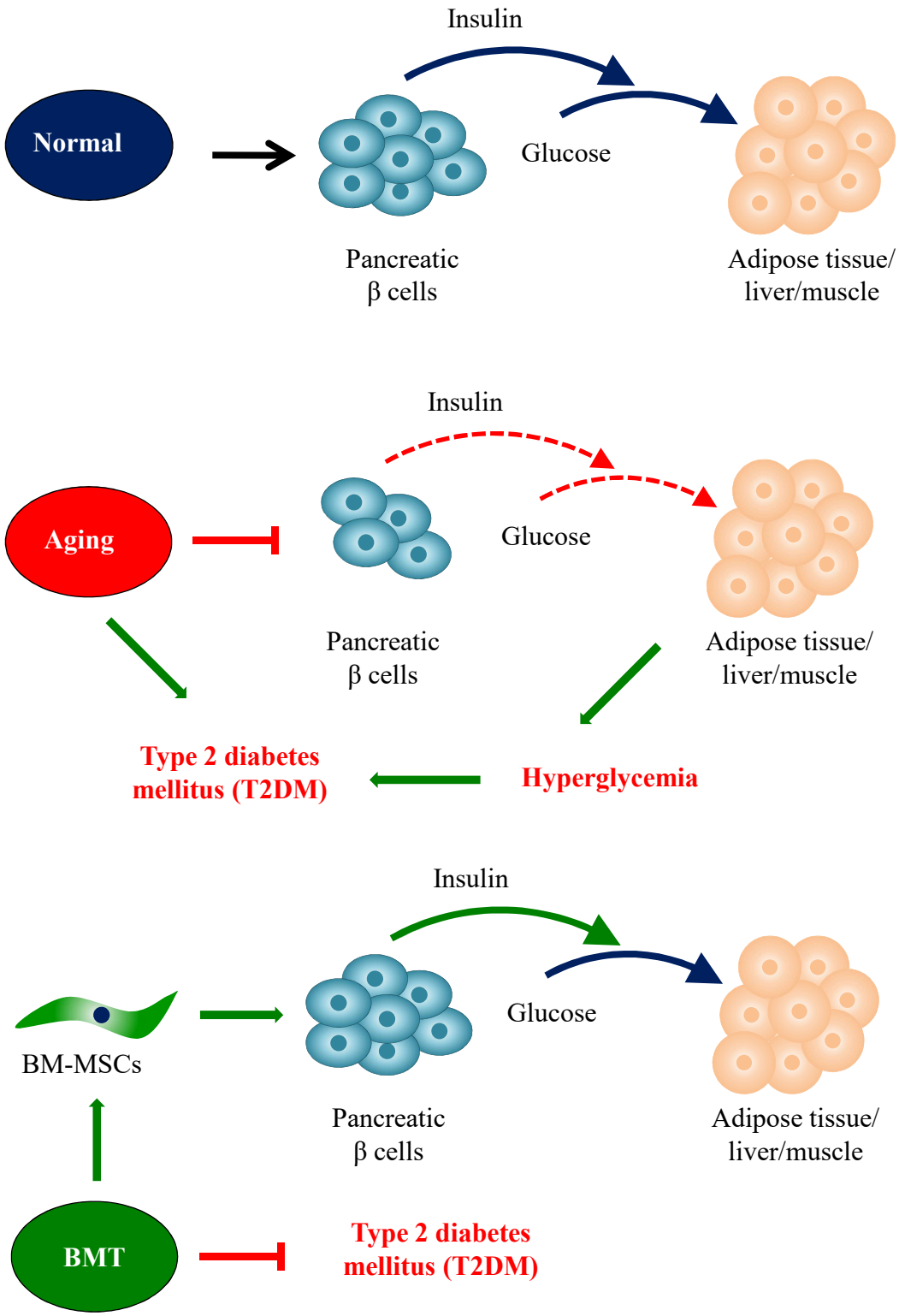

Figure XIII: Treatment of Type 2 diabetes mellitus (T2DM). T2DM patients number is increasing among the people with increasing age. During normal conditions, pancreatic β-cells discharge adequate amount of insulin in highly active tissues such as adipose, muscle, and liver. The deterioration of insulin secretion by pancreatic β-cells is increased with the aging process. As a result, hyperglycemia arises, which leads to T2DM. Stem cell transplantation therapy could be a useful approach for T2DM, which mainly involves decreasing blood glucose level in blood, increasing insulin sensitivity, restoring islet β-cell function and normalize hyperglycemia or T2DM. Ref : DOI:10.1038/nrd4275.

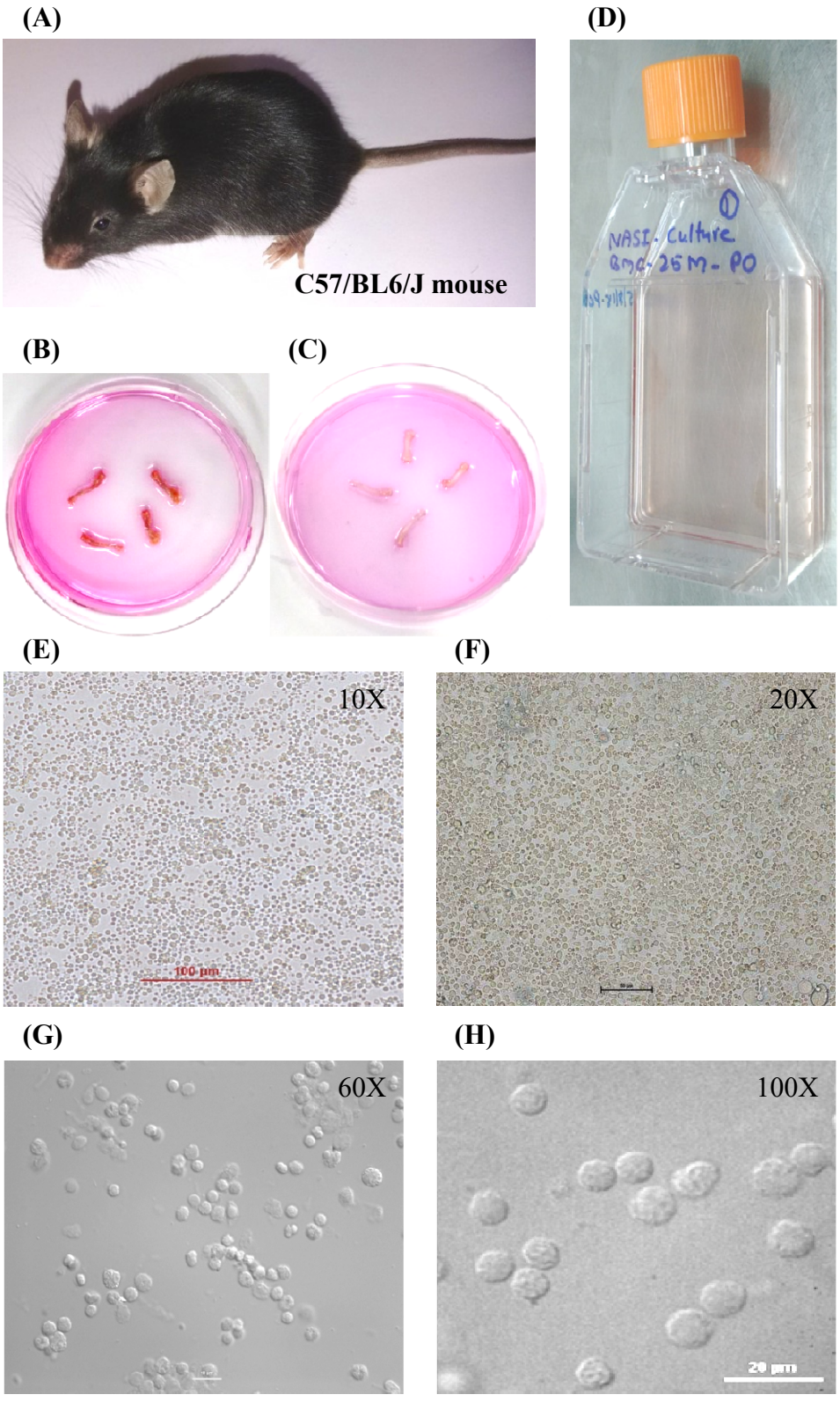

Figure 1(continued)

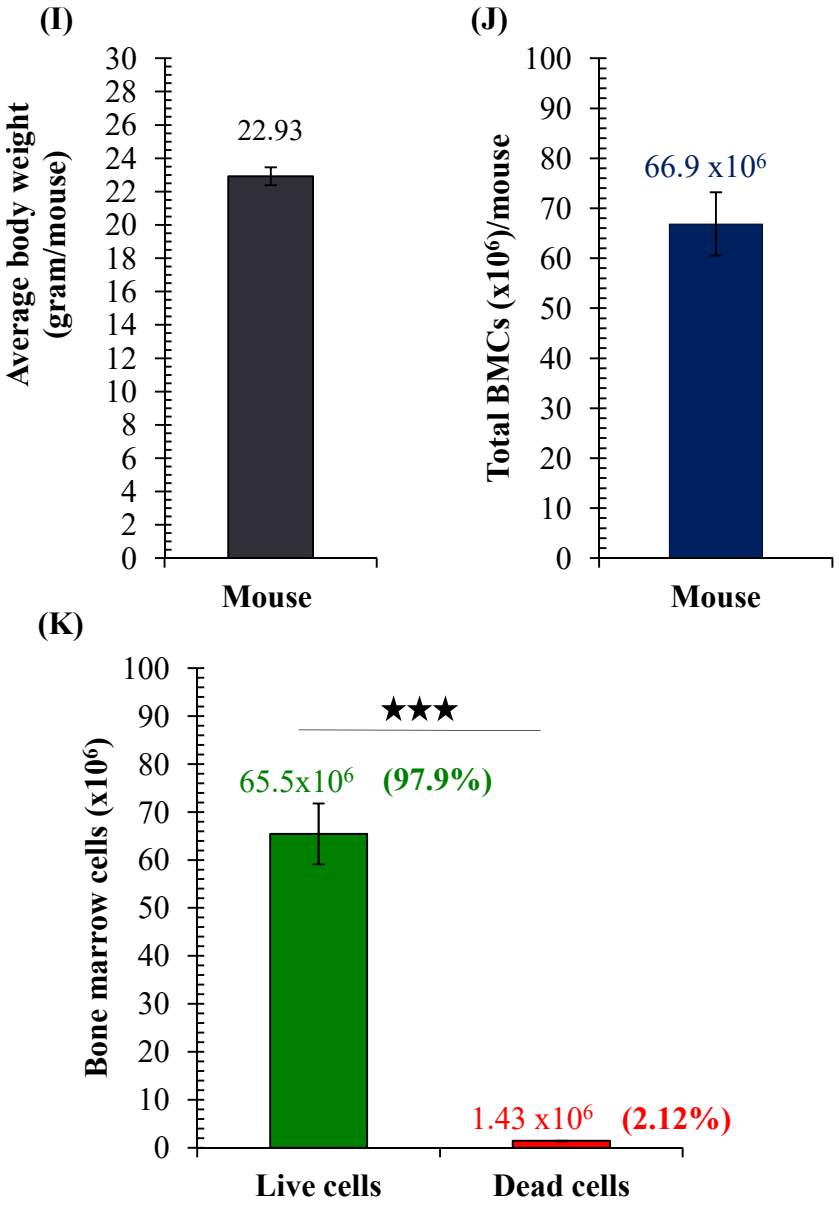

Figure 1: Dissection and removal of bones from long bones (hind & forelimbs) of mouse and isolation of bone marrow cells (BMCs). **(A):** Mouse C57BL6/J. Femurs, Tibiae and Humeri bones were isolated from the 7-8 week old male mouse sacrificed by cervical dislocation after wiping the animal with 70% ethanol. BMCs were harvested by flushing with DMEM-HG by 24 gauge needle. **(B)**: Humeri, femurs, tibia, and fibula appear reddish because of having bone marrow. **(C)**: Whitish bone after flushing of BMCs from the bone marrow cavity. **(D)**: Bone marrow was dissociated and filtered through 70 µm BD-cell strainer, centrifuged, counted and seeded at a density of 1×10^6 cells/cm^2 in T-25 tissue culture flask. **(E, F, G, and H)**: DIC image of BMCs at different magnifications (at 5 minutes post seeding). **(I):** Average body weight of mice C57BL6/J. **(J):** The average yield of total BMCs per mouse. **(K):** Total live and dead cells per mouse. Results shown are mean ± SEM of three independent experiments.

P value < 0.05 was considered statistically significant ★, P ≤ 0.05; ★★, P≤0.01; ★★★, P ≤ 0.001 and P value > 0.05 was considered statistically non significant and represented as n.s.

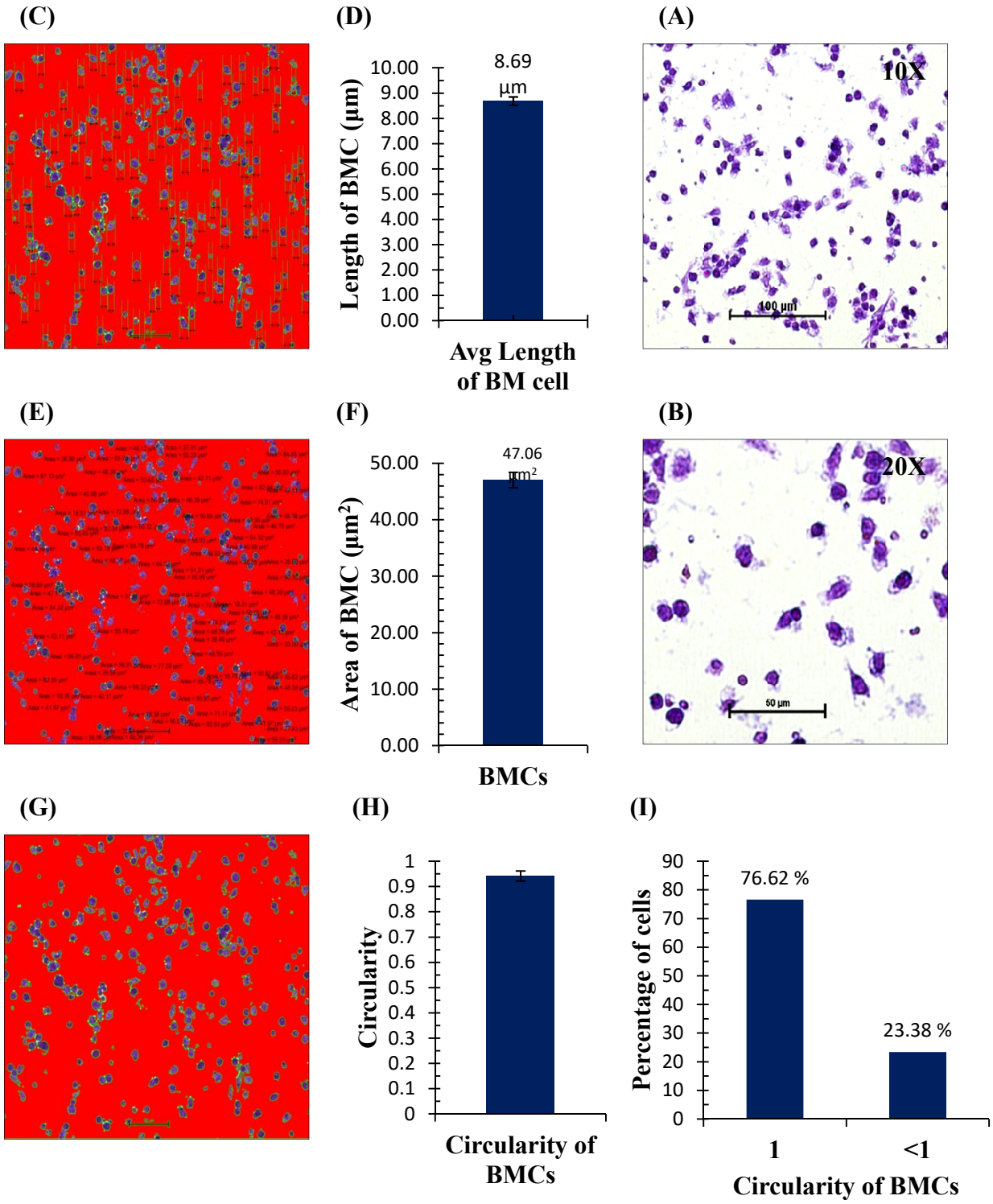

Figure 2: Physical properties of bone marrow cells (BMCs). Physical properties include staining, average length, average area and circularity of BMCs at 3rd day. **(A and B):** Images of different magnifications show the crystal violet staining of BMCs on the 3rd day. **(C** and **D):** Image and graph indicate the average length respectively. **(E** and **F):** Image and graph show the average area of BMCs respectively. **(G, H** and **I):** Image and graph indicate circularity of BMCs and percentage of cells showing circularity on 3rd Day respectively.

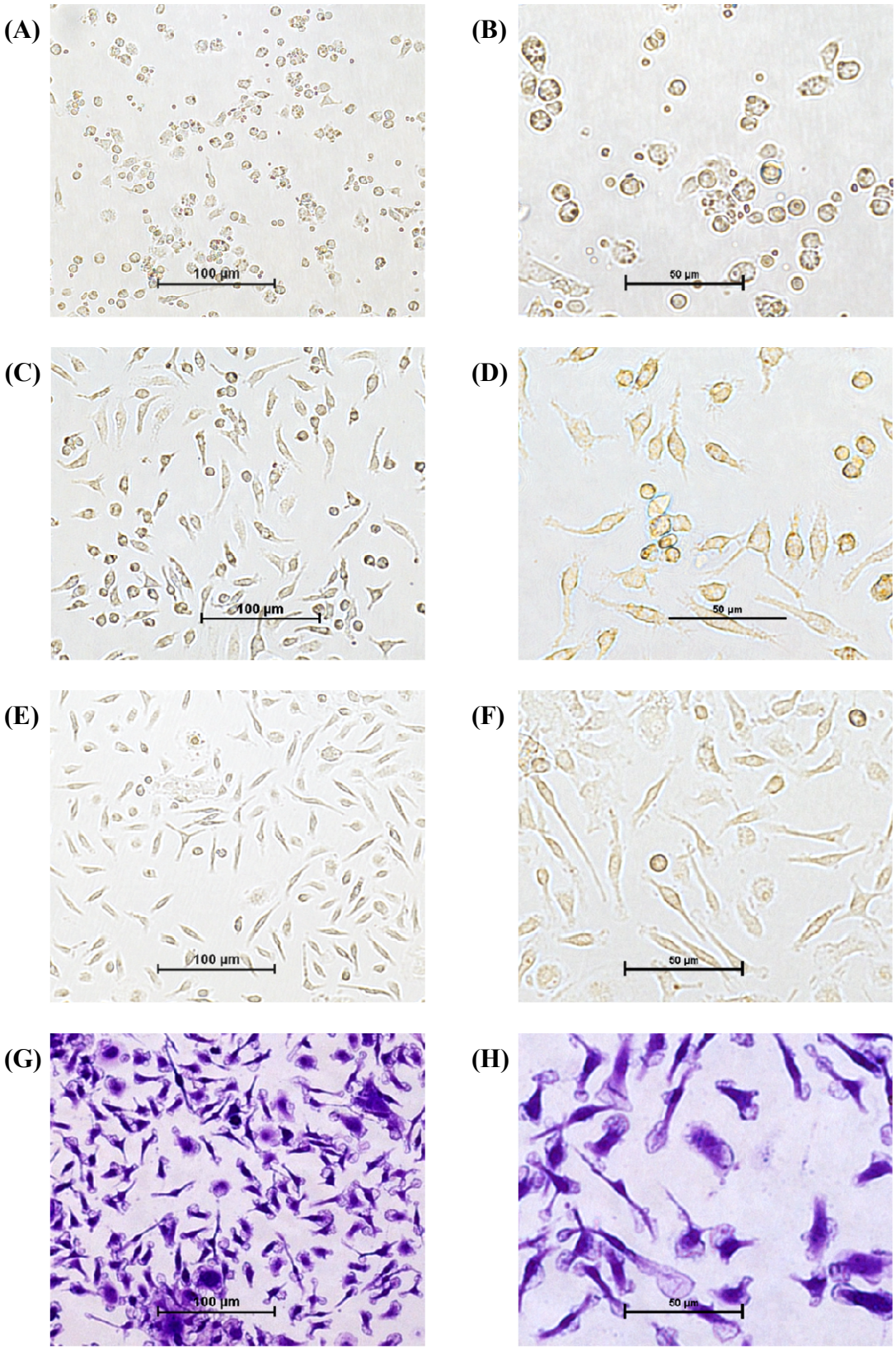

Figure 3 (continued)

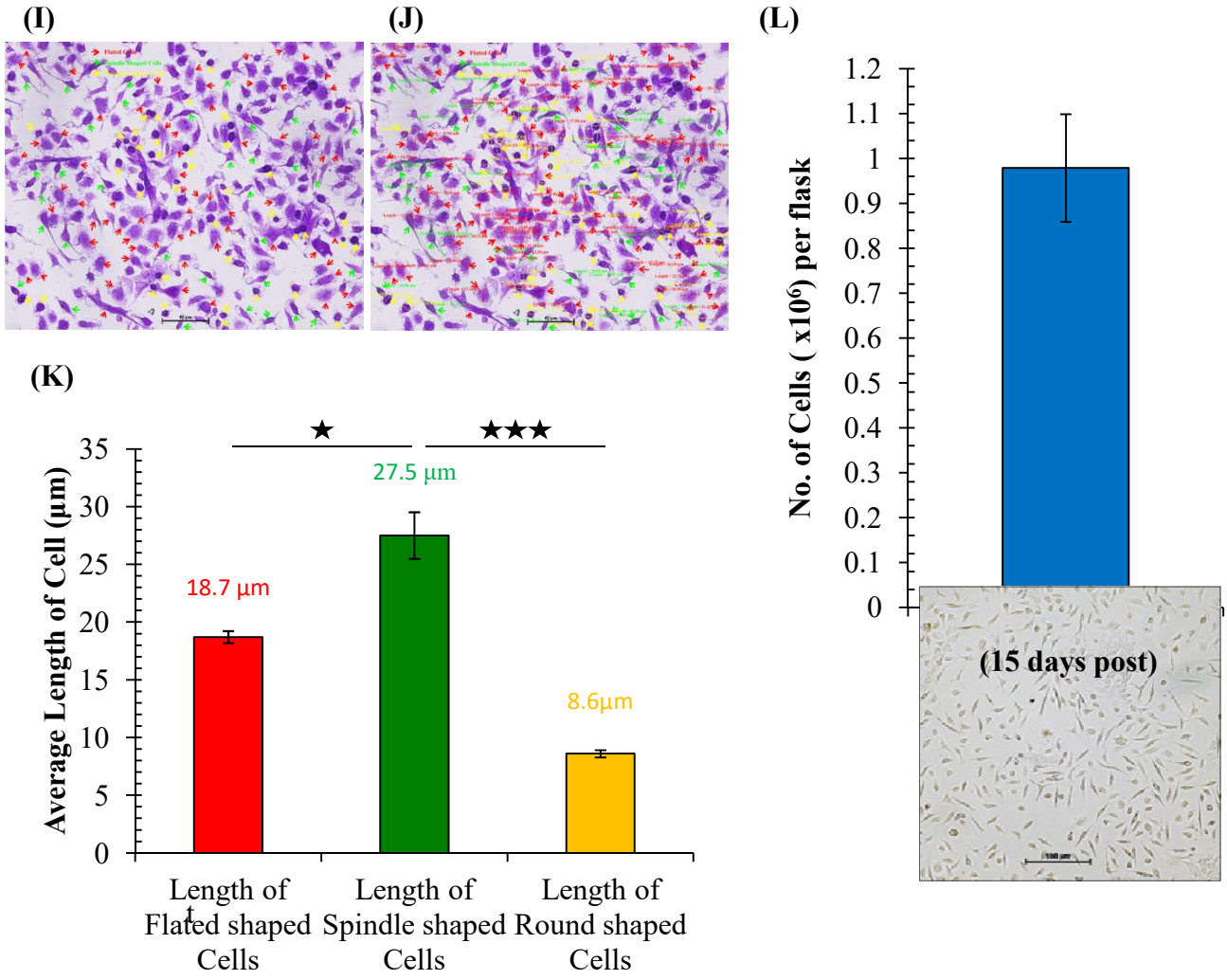

Figure 3: Culture and propagation of mouse bone marrow cells (BMCs) and propagation of mesenchymal stem (Passage-0) cells (MS-P0 cells). **(A** and **B):** Morphology of BMCs under bright field on day 3 at different 10X and 20X magnifications respectively. **(C and D):** Cultured cells at 7 days. **(E and F):** Morphology of cultured MS-P0 cells at 15 days at different 10X and 20X magnifications respectively. **(G and H):** MS-P0 cells stained with crystal violet (CV) at 15 days. **(I):** Culture of MS-P0 cells contain three types of cells such as round shaped, flattened-shaped and spindle-shaped cells. **(J):** Measurement of MS-P0 cells (round shaped, flattened-shaped and spindle-shaped cells) **(L):** Graph indicates harvested cultured bone marrow-derived MS-P0 cells yield after first passage. Results shown are mean ± SEM of three independent experiments. Scale bar: 50 µm (A, C, E, and G), 100 µm (B, D, F, and H).

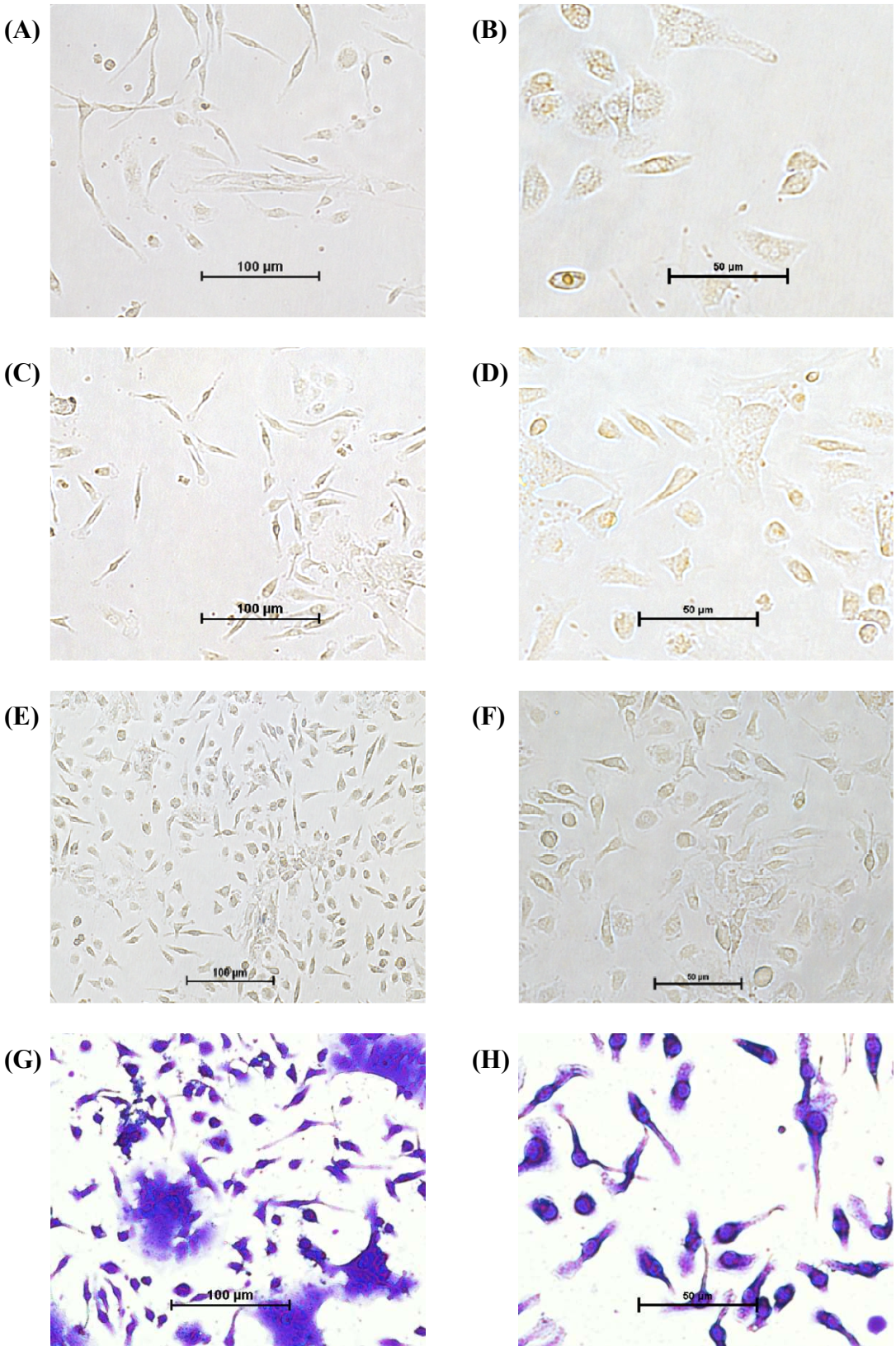

Figure 4 (continued)

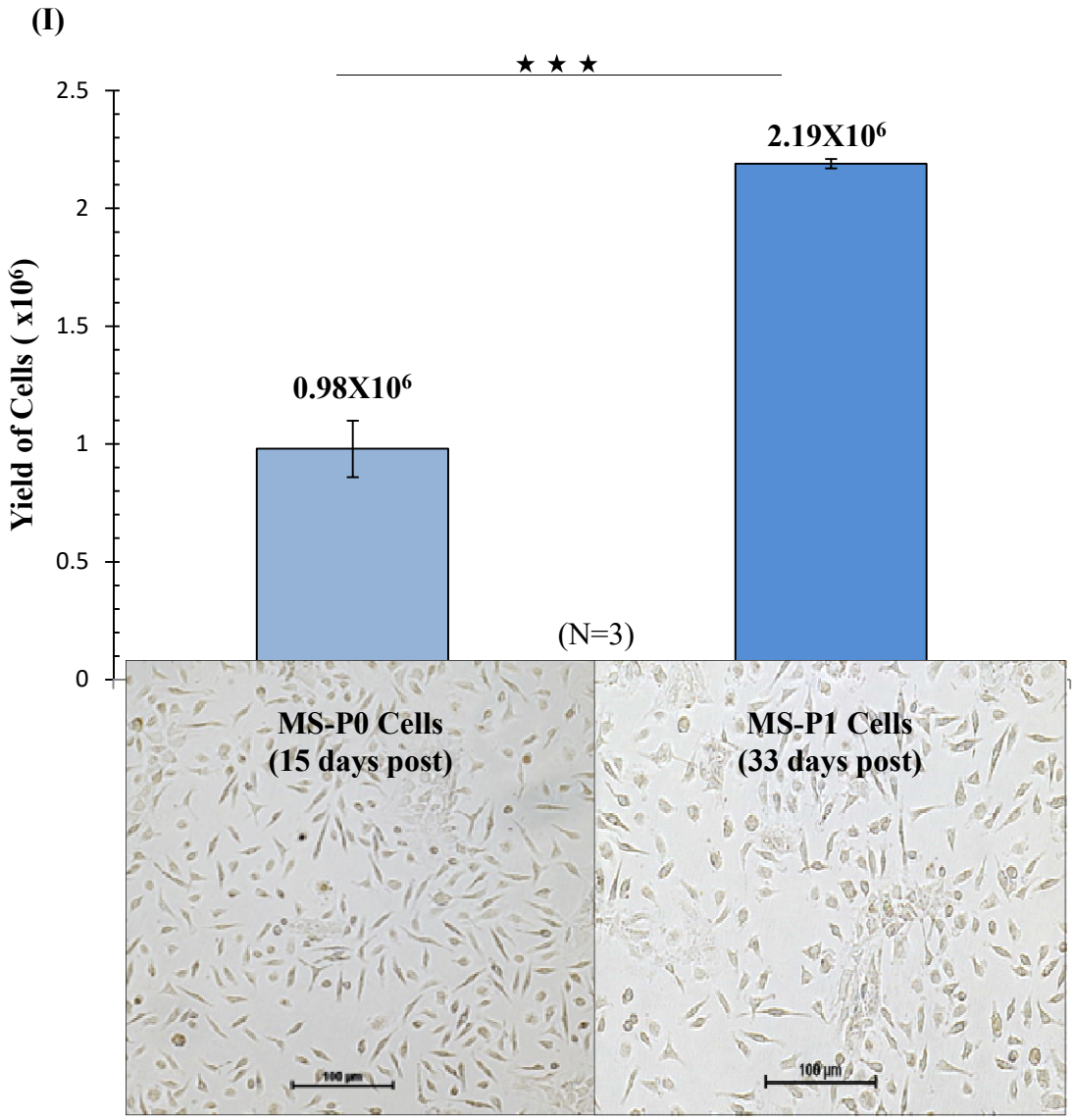

Figure 4: Culture and propagation of mouse bone marrow derived mesenchymal stem (Passage-1) cells (MS-P1 cells). **(A** and **B):** Morphology of bone marrow derived MS-P1 cells under bright field on day 6 at different 10X and 20X magnifications respectively. **(C and D):** Cultured MS-P1 cells at 12 days. **(E and F):** Morphology of cultured MS-P1 cells at 15 days at different 10X and 20X magnifications respectively. **(G and H):** MS-P1 cells stained with crystal violet (CV) at 15 days. **(I):** Graph indicates harvested cultured bone marrow-derived MS-P0 cells (after 15 days) and MS-P1 cells (after 33 days) yield after the passages respectively. Results shown are mean ± SEM of three independent experiments. Scale bar: 50 µm (A, C, E, and G), 100 µm (B, D, F, and H).

(A)

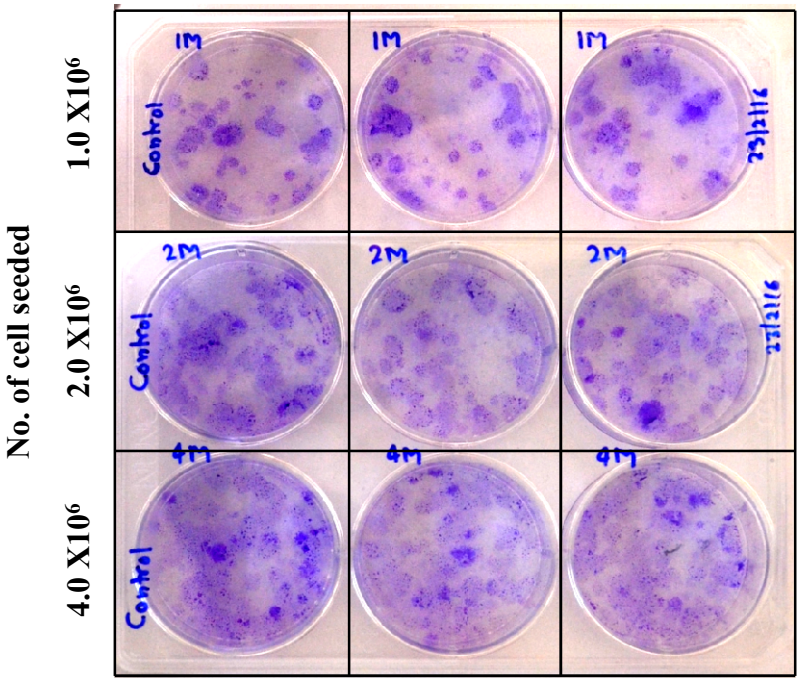

(B)

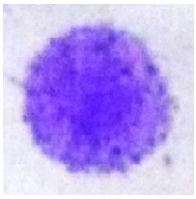

Single colony

(C)

MOUSE	Number of cells seeded		
	1 Million	2 Million	4 Million
MOUSE 1	43.33	63.33	86.33
MOUSE 2	26.67	33.00	46.33
MOUSE 3	31.00	54.00	67.00
Mean	33.67	50.11	66.56
± SEM	4.99	8.97	11.55

(D)

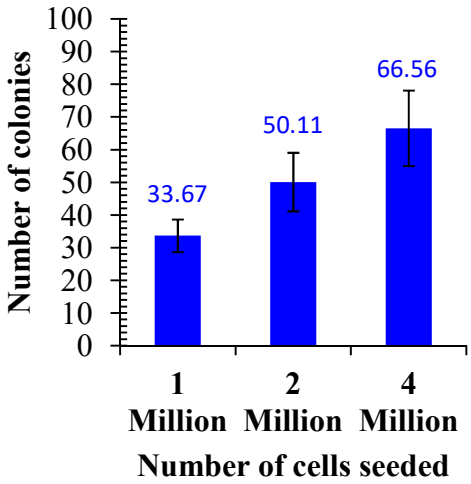

Figure 5: Bone marrow stem cell potential. (A): Bone marrow cells (BMCs) seeded in 6 well plates at different cell numbers and cultured for 14 days and stained with 0.5% crystal violet. Colony forming unit (CFU-F)-fibroblastic shows viable cells in the colony. **(B):** The image of a single colony. **(C):** Table shows the average CFU number at different cell density. **(D):** Graph showing the quantification of average CFU-Fs colonies means ± SEM of three independent experiments.

(A)

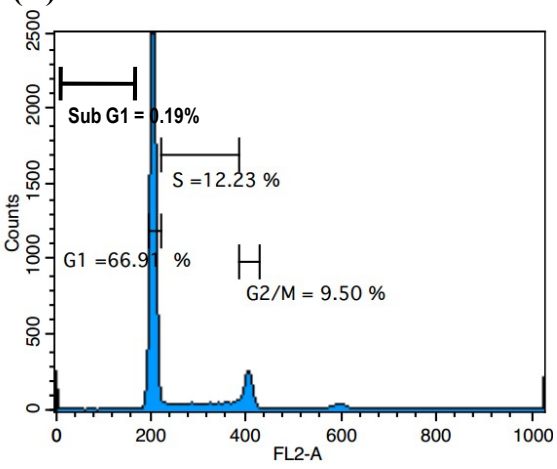

(B)

SAMPLE	Sub G1	G1	S	G2-M
Mouse 1	0.16	69.72	8.69	9.89
Mouse 2	0.19	66.54	8.02	10.51
Mouse 3	0.04	67.56	7.80	10.70
Mean	**0.13**	**67.94**	**8.17**	**10.37**
±SEM	0.05	0.94	0.27	0.24

(C)

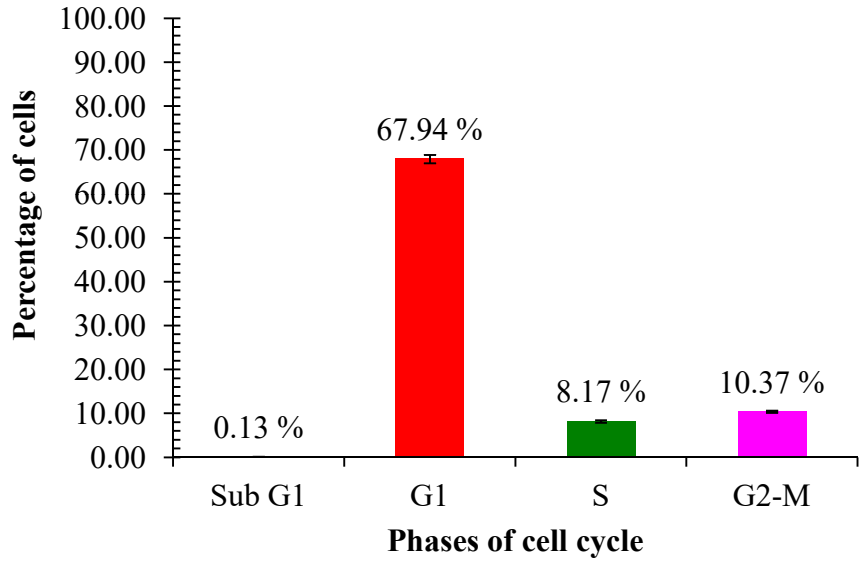

Figure 6: Cell cycle profile of bone marrow cells (BMCs). BMCs were stained with PI and analyzed by FACS (BD-Calibur). **(A):** Histogram shows a number of BMCs in particular phase of the cell cycle at FL2-A on X-axis versus counts on Y-axis. **(B** and **C):** Table and graph show the percentage of cells in different phases of cell cycle. Cell Quest-Pro software was used to calculate the fraction of cells. Results shown are mean ± SEM of three independent experiments.

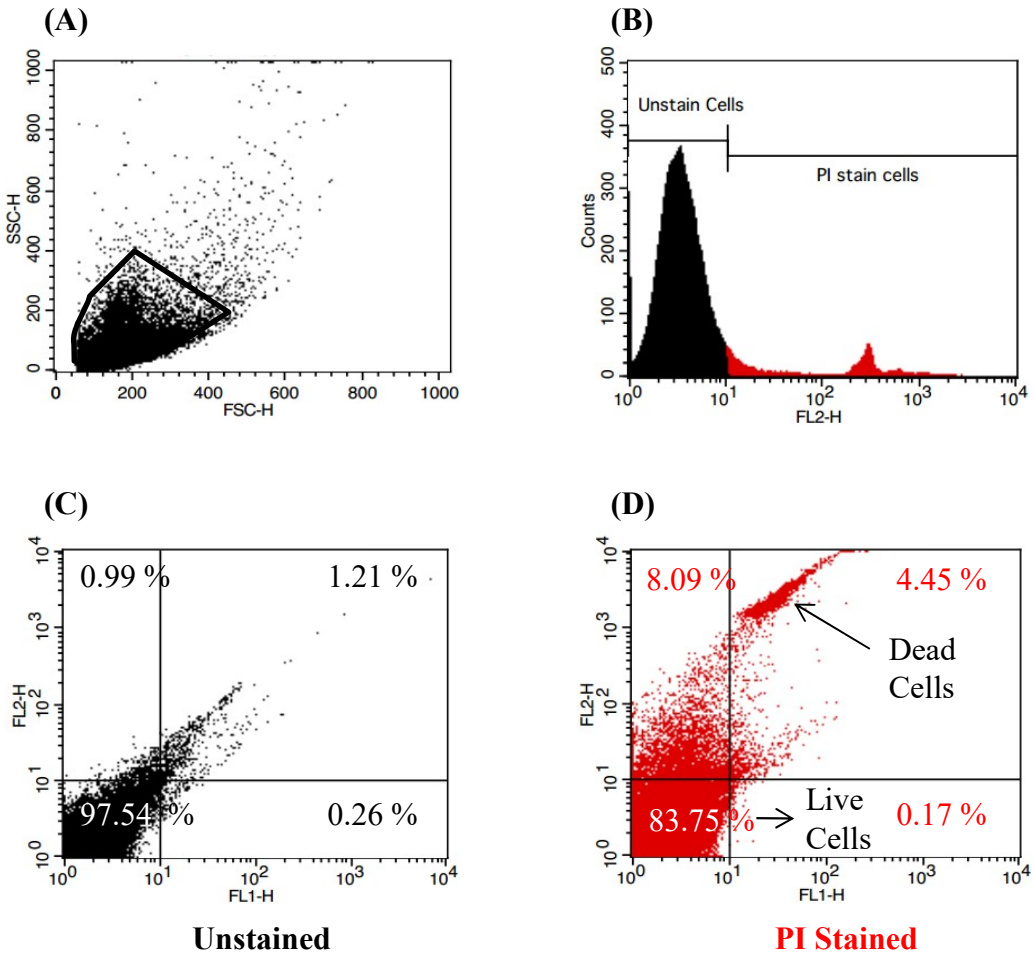

Figure 7: Live and dead cell quantification by propidium iodide (PI) method for immunophenotypic characterization of bone marrow cells (BMCs). BMCs were stained with PI and analyzed for live and dead cells in the bone marrow sample. **(A):** The dot plot indicates the relative size of BMCs. **(B):** Histogram shows the cell numbers of unstained and PI-stained BMCs. **(C):** Dot plot of unstained BMCs. **(D):** Dot plot of PI-stained BMCs, which shows the percentage of live and dead cells in bone marrow sample.

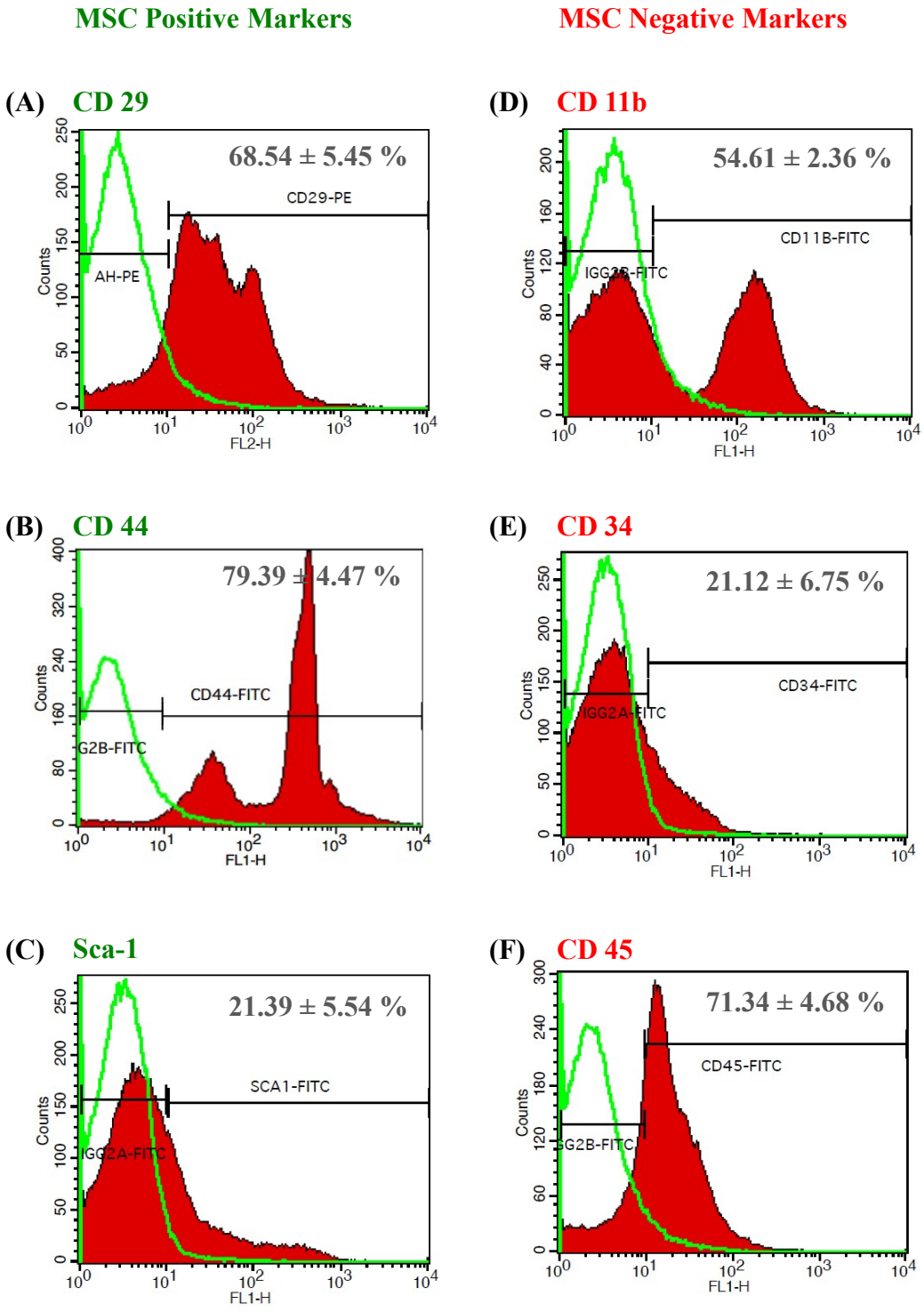

Figure 8 (continued)

(G)

MSC Positive Markers	Percentage of Cells (Mean)	±SEM
CD 29	68.55	5.46
CD 44	79.40	4.47
Sca-1	21.39	5.54

(I)

MSC Negative Markers	Percentage of Cells (Mean)	±SEM
CD 11b	54.62	2.36
CD 34	21.12	6.75
CD 45	71.35	4.68

(H)

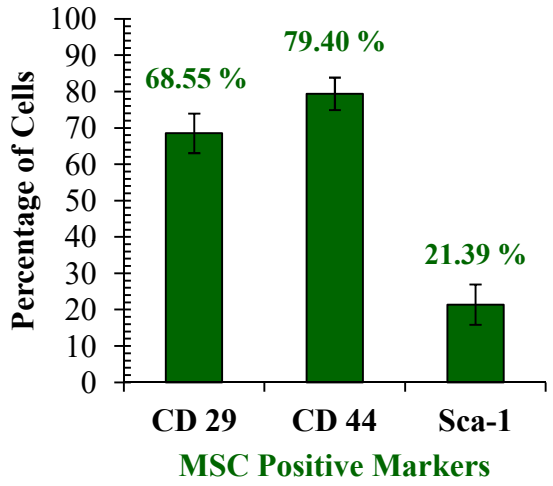

(J)

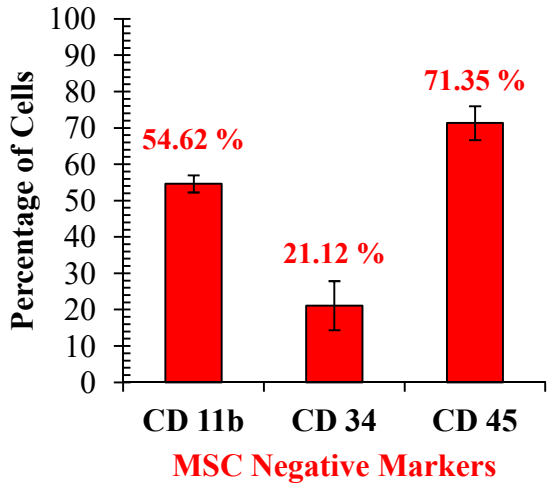

Figure 8: Immunophenotypic characterization of bone marrow cells (BMCs). BMCs were freshly isolated and then characterized by immunophenotypic markers with respect to the MSC-positive and MSC-negative cell surface markers. **(A):** BMCs were stained with phycoerythrin (PE)-conjugated anti-mouse CD29 and **(B):** fluorescein isothiocyanate (FITC)-conjugated anti-mouse CD44, **(C):** Sca-1, **(D):** CD34, **(E):** CD45 and **(F):** CD11b along with isotype control antibodies. (**G** & **I):** Table and Graph (**H** & **J**) show percentage of BMCs showing expression of MSC-positive and MSC-negative cell surface markers respectively. Results shown are mean ± SEM of three independent experiments.

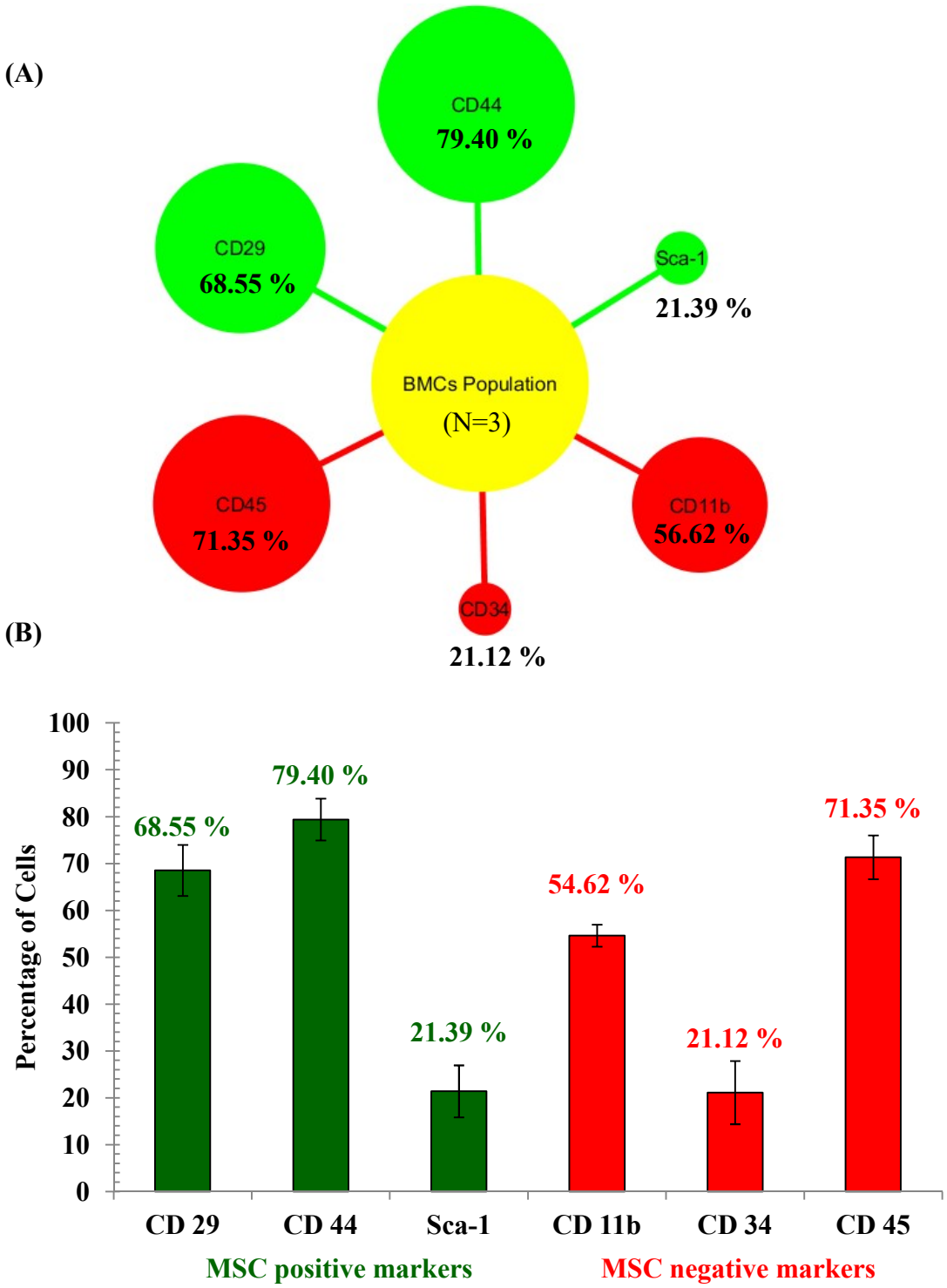

Figure 9: Overall expression of MSC-markers (positive and negative) in bone marrow cells (BMCs). (A and B): Image and graph show percentage of BMCs showing expression of MSC-positive and MSC-negative cell surface markers respectively. Results shown are mean ± SEM of three independent experiments.

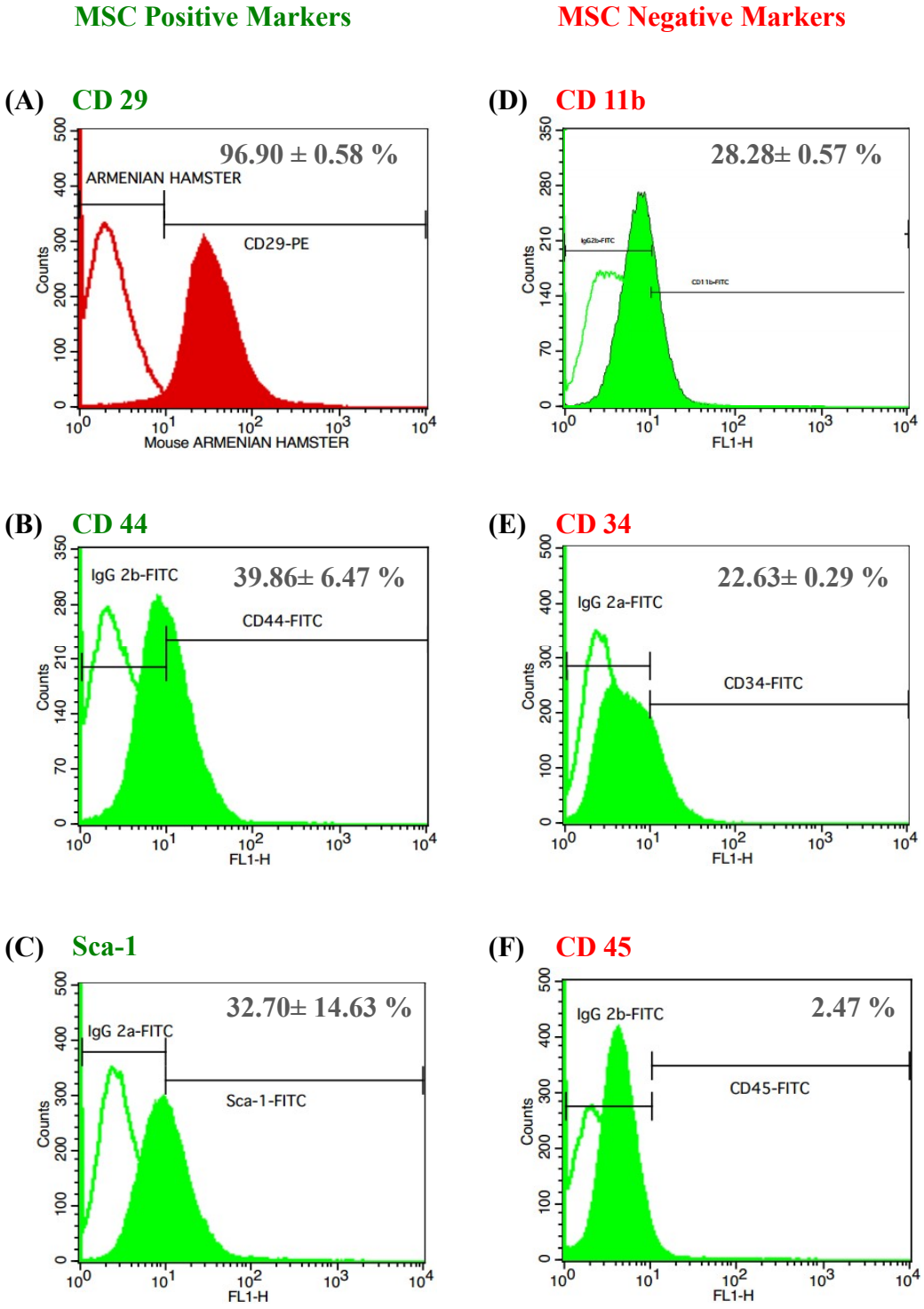

Figure 10 (continued)

(G)

MSC Positive Markers	Percentage of Cells (Mean)	±SEM
CD 29	96.90	0.58
CD 44	39.86	6.47
Sca-1	32.70	14.63

(I)

MSC Negative Markers	Percentage of Cells (Mean)	±SEM
CD 11b	28.28	0.57
CD 34	22.63	0.29
CD 45	2.47	

(H)

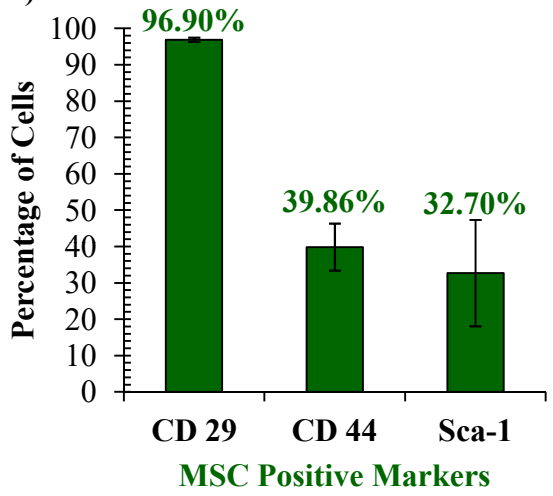

(J)

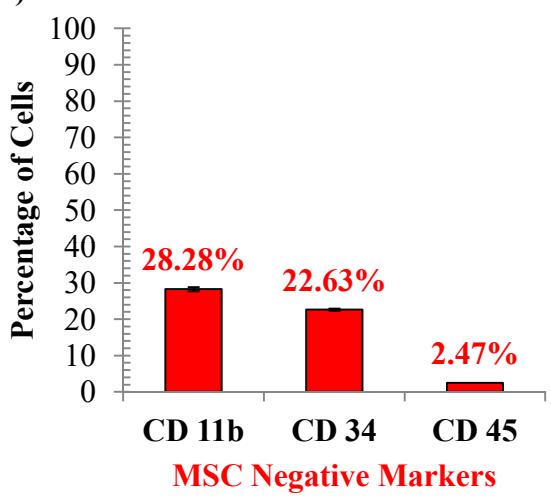

Figure 10: Immunophenotypic characterization of mesenchymal stem (Passage-1) cells (MS-P1 cells). MS-P1 cells were freshly harvested after 33 days of culture and then characterized by immunophenotypic markers with respect to the MSC-positive and MSC-negative cell surface markers. **(A):** MS-P1 cells were stained with phycoerythrin (PE)-conjugated anti-mouse CD29 and **(B):** fluorescein isothiocyanate (FITC)-conjugated anti-mouse CD44, **(C):** Sca-1, **(D):** CD34, **(E):** CD45 and **(F):** CD11b along with isotype control antibodies. (**G** & **I**)**:** Table and graph (**H** & **J**) show percentage of MS-P1 cells showing expression of MSC-positive and MSC-negative markers respectively. Results shown are mean ± SEM of three independent experiments.

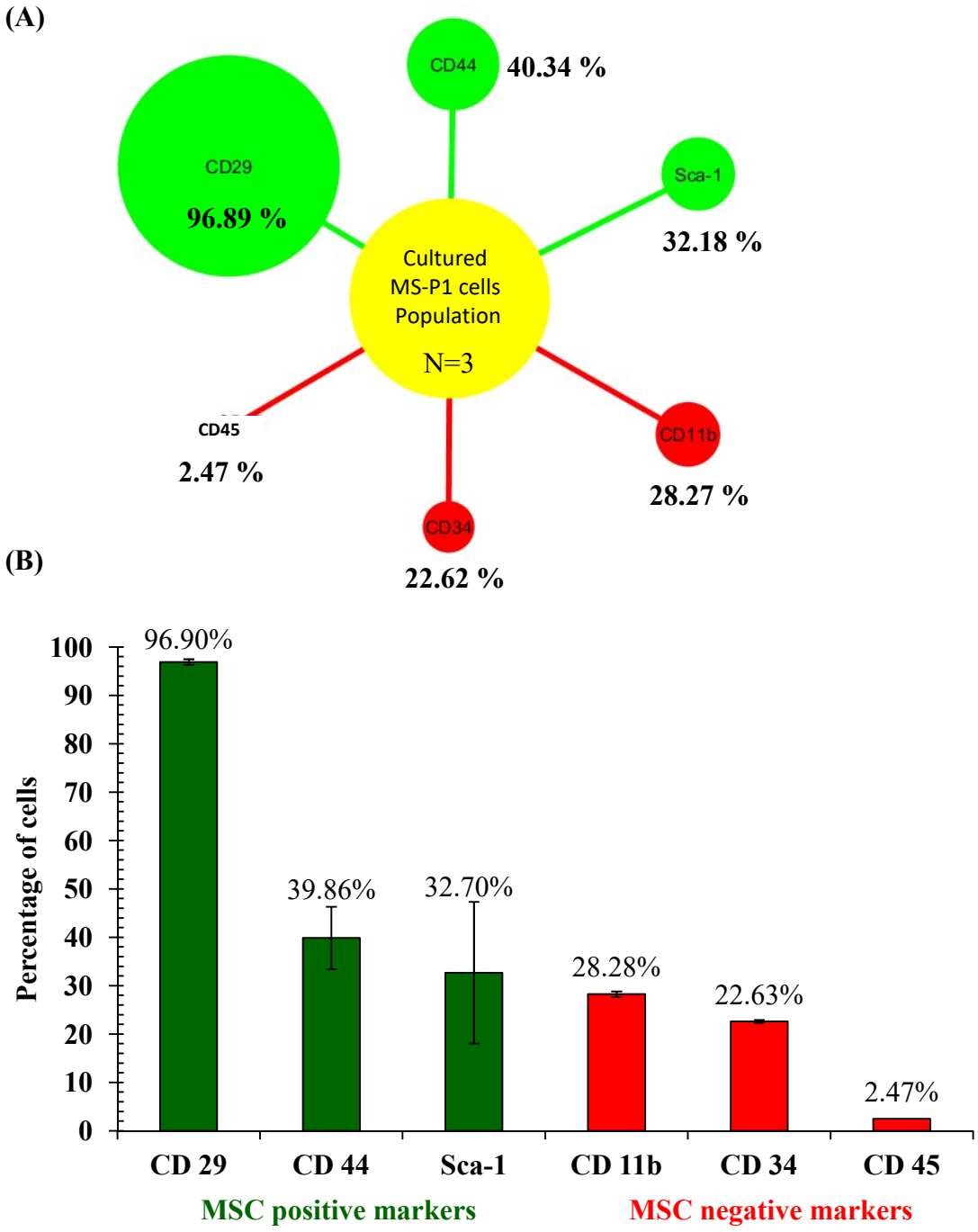

Figure 11: Overall quantitative expression of MSC-markers (positive and negative) on mesenchymal P1 stem cells (MS-P1 cells). (A and B): Image and graph show percentage of MS-P1 cells showing expression of MSC-positive and MSC-negative markers respectively. Results shown are mean ± SEM of three independent experiments.

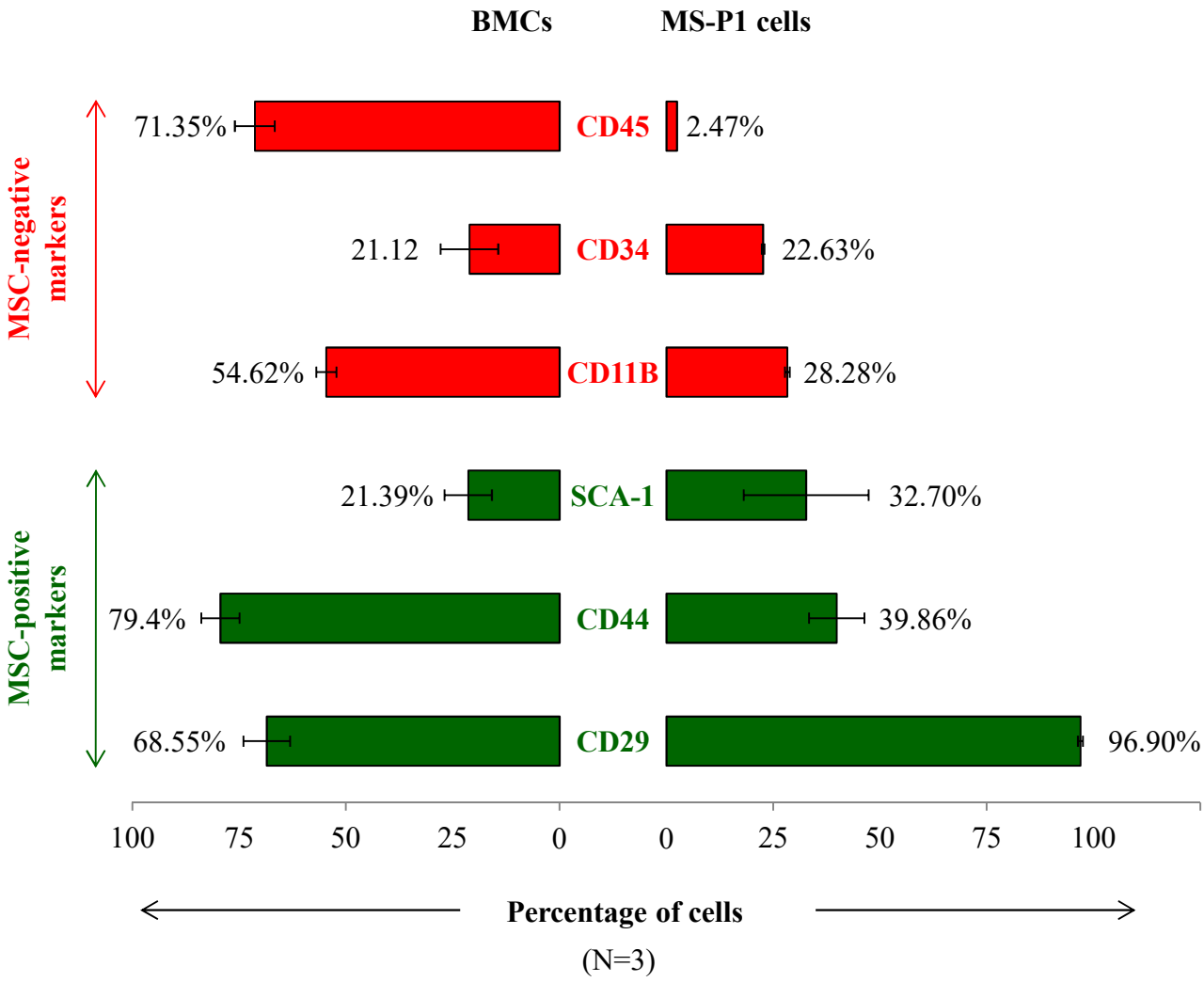

Figure 12: Comparative quantitative expression of cell surface markers on bone marrow cells (BMCs) and mesenchymal stem (Passage-1) cells (MS-P1 cells). The graph describes the percentage of cells in BMCs and MSC-P1 cells population showing expression of MSC-positive and MSC-negative markers on BMCs and MSC-P1 cells on left side and right side of the graph respectively. Results shown are mean ± SEM of three independent experiments.

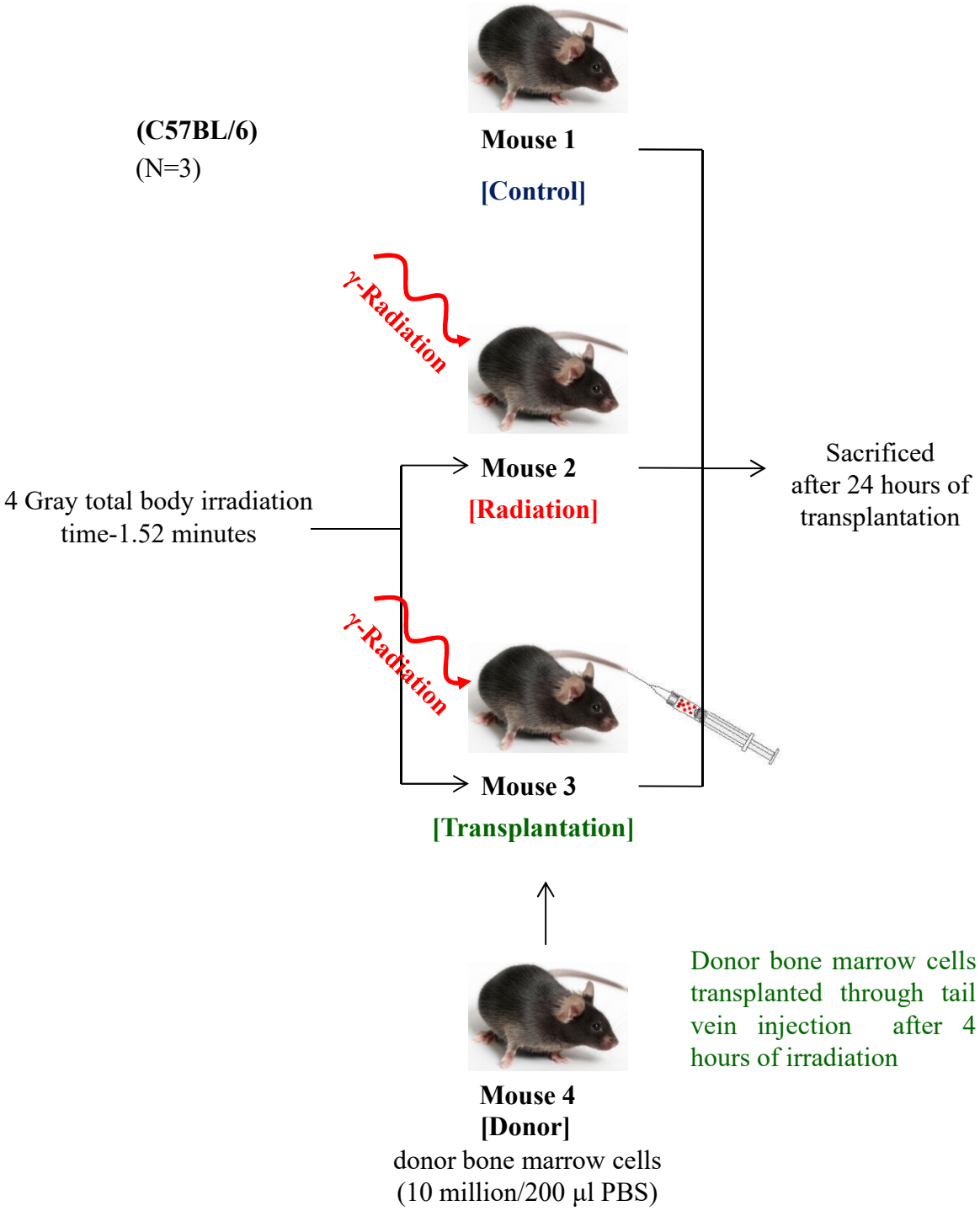

Figure 13: An irradiated mouse model for bone marrow regeneration after transplantation. Mouse 1 (no radiation and no transplantation) used as control. A single dose of total body, sub-lethal, 4 Gy γ-radiation was given to recipient mouse 2 and mouse 3 with gamma rays at the rate of 4 rads/second. Four hours post-irradiation, donor bone marrow cells (BMCs) isolated from the donor mouse i.e. mouse 4 ($10x10^6$ BMCs) were intravenously transplanted into the irradiated recipient mouse 3 via tail vein injection by using a 24 gauge needle. Results were analyzed 24 hours later.

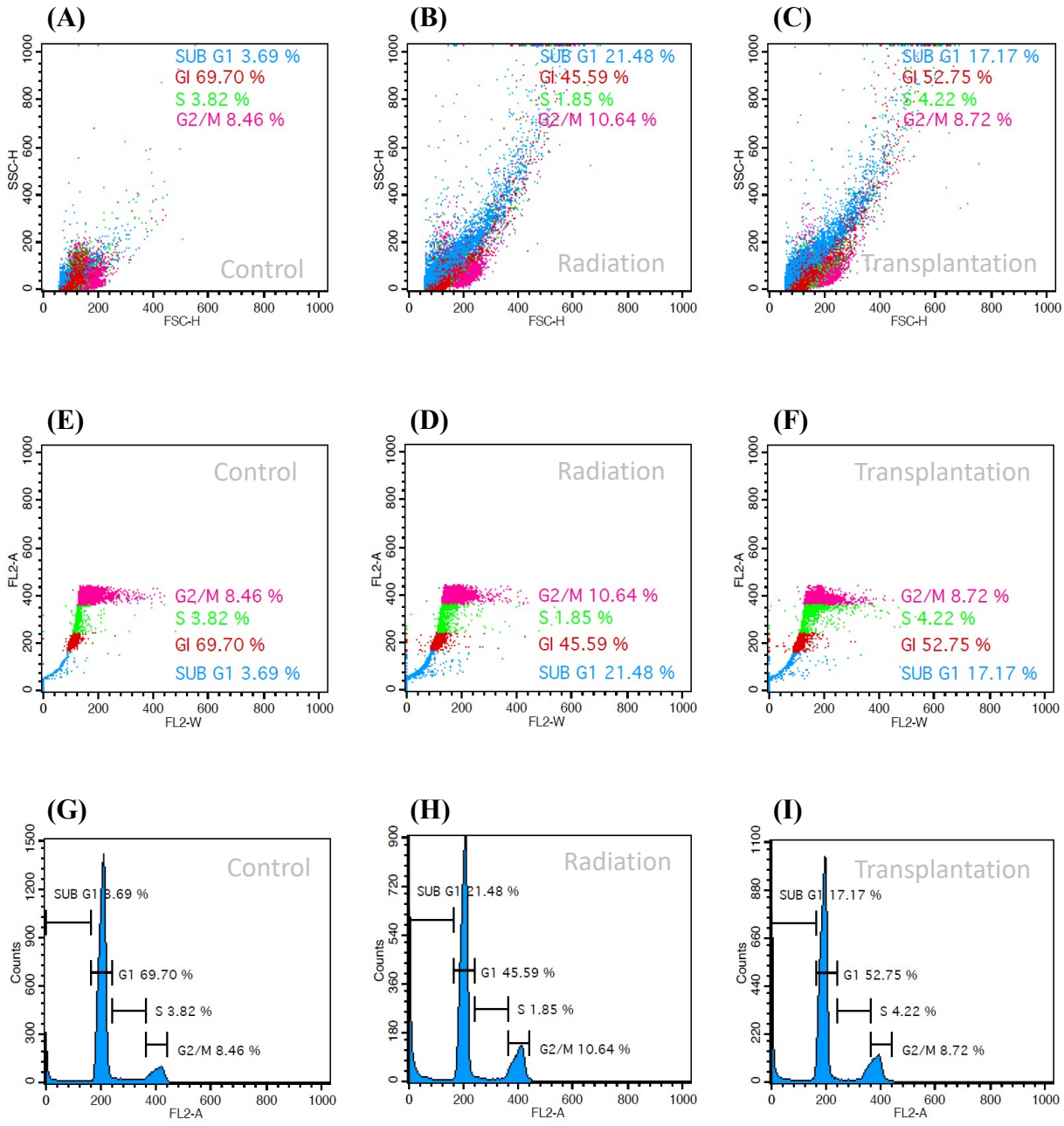

Figure 14: Cell cycle analysis of bone marrow cells (BMCs) of control, irradiated and bone marrow transplanted mice from 3 independent experiments by FACS. BMCs were stained with PI and analyzed by BD-FACS Calibur. Panel **(A, B** and **C):** Dot plots (SSC versus FSC) show relative size and granularity of cells of control, irradiated and transplanted mice using bone marrow cells respectively**.** Panel **(D, E,** and **F):** Dot plots (FL2-A verses FL2-W) used for doublet discrimination of control, irradiated and transplanted mice bone marrow cells respectively**.** Panel **(G, H** and **I):** Histograms of control, irradiated and transplanted mice bone marrow cells show a number of BMCs in particular phase of the cell cycle at FL2-A on X-axis versus counts on Y-axis. The results are obtained 24 hours after transplantation.

(A)

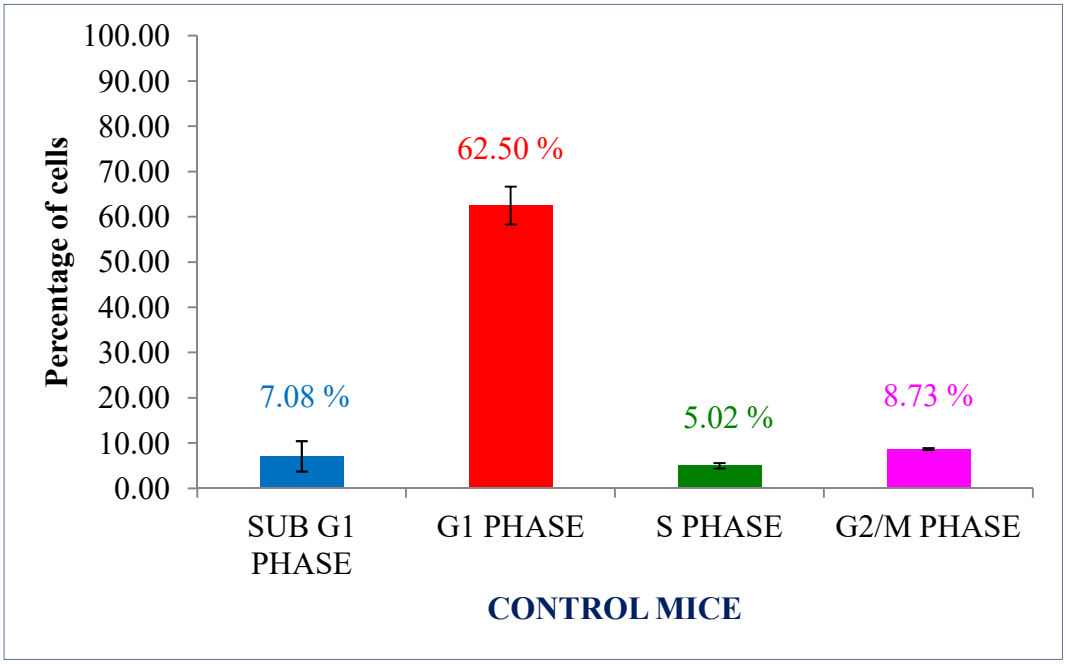

CONTROL MICE				
	SUB G1 PHASE	G1 PHASE	S PHASE	G2/M PHASE
MOUSE 1	13.80	55.23	5.65	8.57
MOUSE 2	3.75	62.58	5.58	9.13
MOUSE 3	3.69	69.70	3.82	8.48

CONTROL MICE				
	SUB G1 PHASE	G1 PHASE	S PHASE	G2/M PHASE
Mean	**7.08**	**62.50**	**5.02**	**8.73**
±SEM	3.36	4.18	0.60	0.20

Figure 15 (continued)

(B)

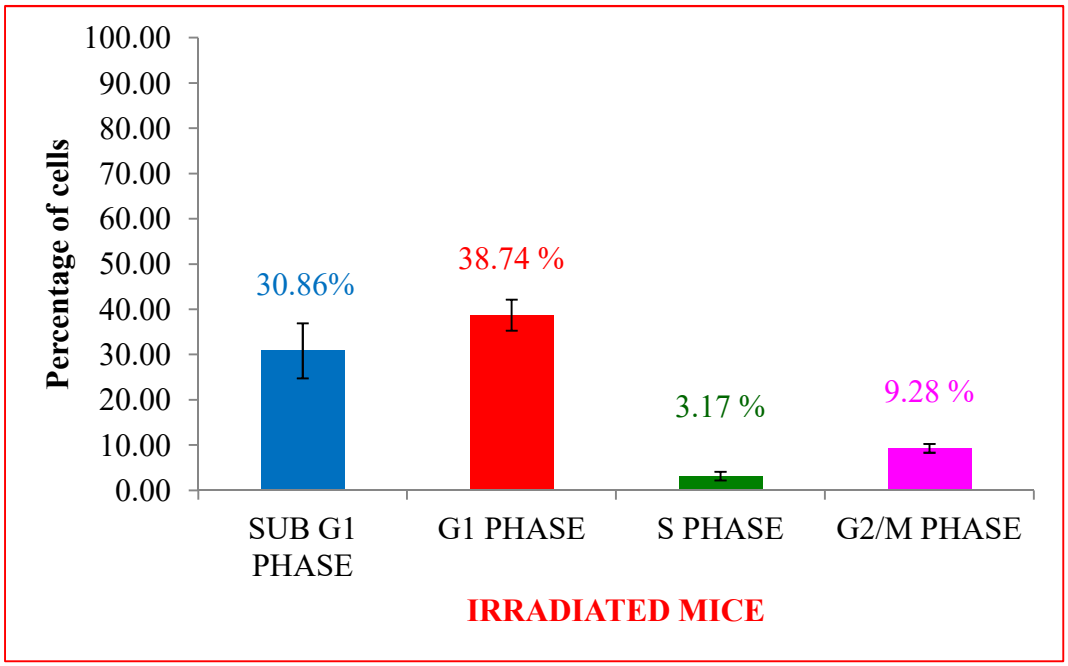

IRRADIATED MICE				
	SUB G1 PHASE	G1 PHASE	S PHASE	G2/M PHASE
MOUSE 1	42.26	35.54	2.66	7.43
MOUSE 2	28.85	35.09	5.00	9.77
MOUSE 3	21.48	45.59	1.85	10.65

IRRADIATED MICE				
	SUB G1 PHASE	G1 PHASE	S PHASE	G2/M PHASE
Mean	**30.86**	**38.74**	**3.17**	**9.28**
±SEM	6.08	3.43	0.94	0.96

Figure 15 (continued)

(C)

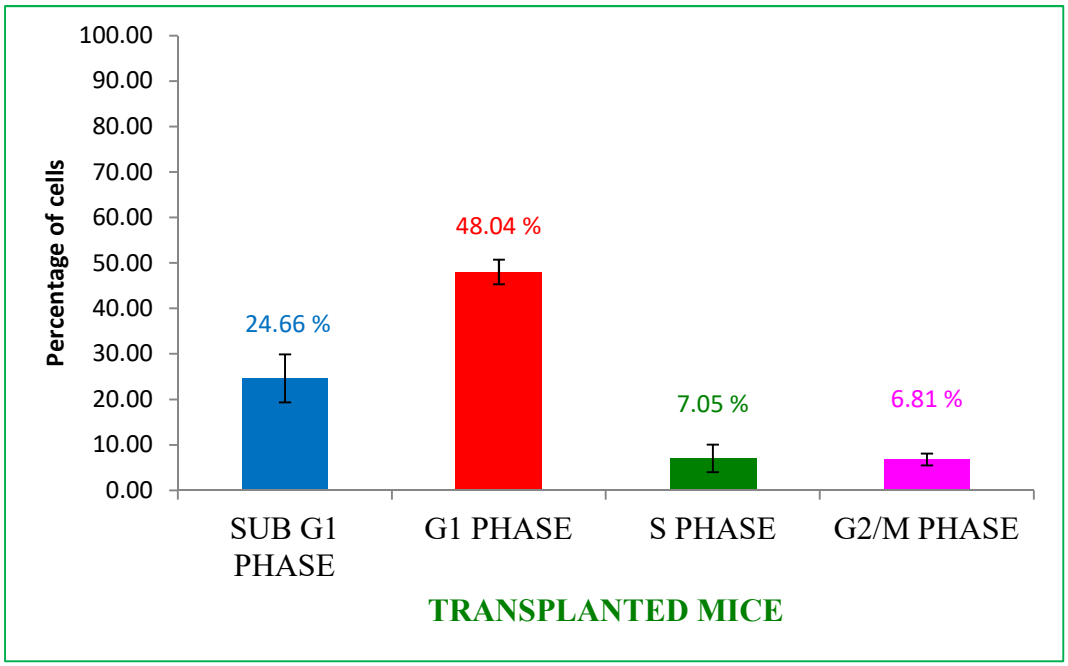

TRANSPLANTED MICE				
	SUB G1 PHASE	G1 PHASE	S PHASE	G2/M PHASE
MOUSE 1	34.84	43.41	3.81	7.42
MOUSE 2	21.98	47.97	13.12	4.30
MOUSE 3	17.17	52.75	4.22	8.72

TRANSPLANTED MICE				
	SUB G1 PHASE	G1 PHASE	S PHASE	G2/M PHASE
Mean	**24.66**	**48.04**	**7.05**	**6.81**
±SEM	5.27	2.70	3.04	1.31

Figure 15 (continued)

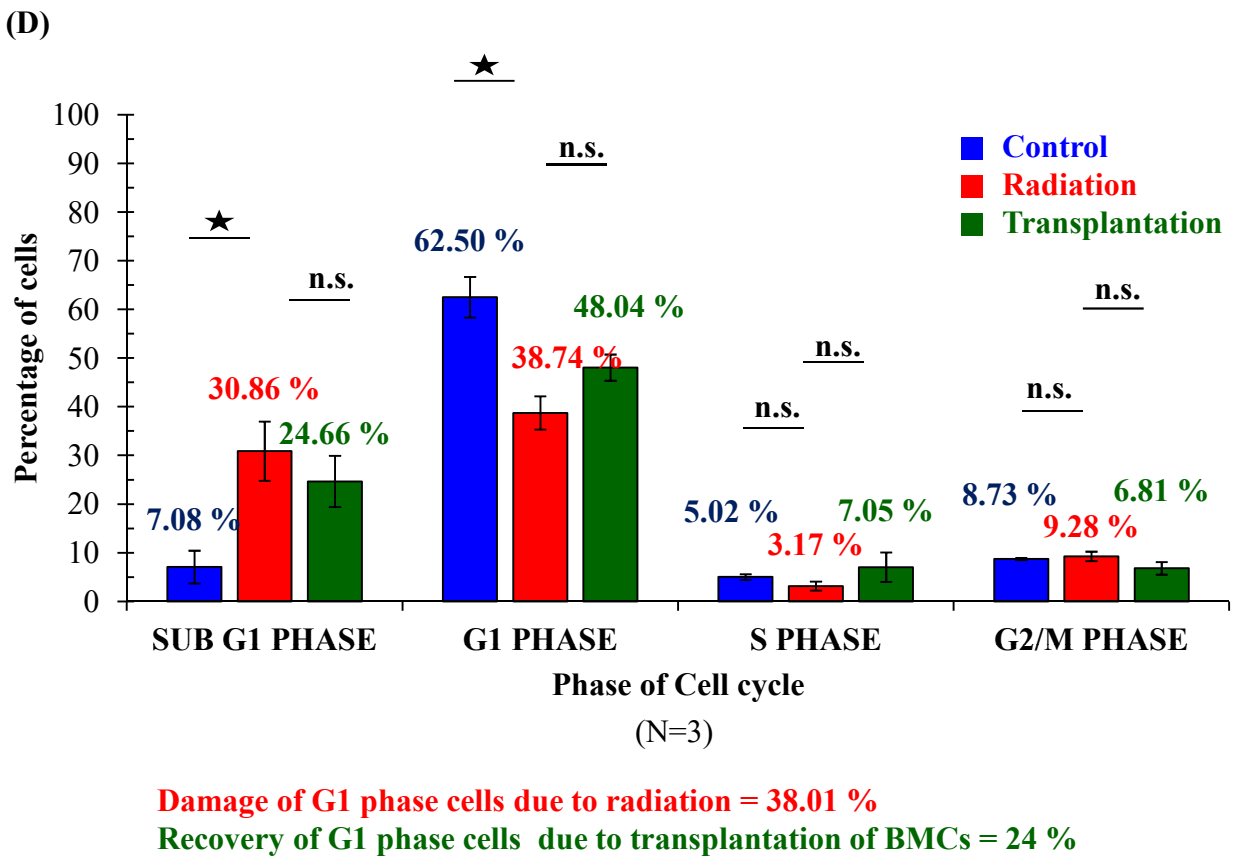

Figure 15: Comparative quantification of cell cycle analysis of bone marrow cells (BMCs) of control, irradiated and bone marrow transplanted mice from 3 independent experiments by FACS. BMCs were stained with PI and analyzed by BD-FACS Calibur. Panel **(A, B** and **C):** Graphs and tables show the cell cycle profile of control, irradiated and transplanted mice bone marrow cells respectively**. (D):** Graph shows the significant comparative analysis of cell cycle of control, irradiated and transplanted mice bone marrow cells respectively**.** Results show damage of G1 phase cells due to radiation was 38.01% and recovery of G1 phase cells due to transplantation of BMCs was 24%. Results shown are mean ± SEM of three independent experiments for 24 hours after transplantation.

(A)

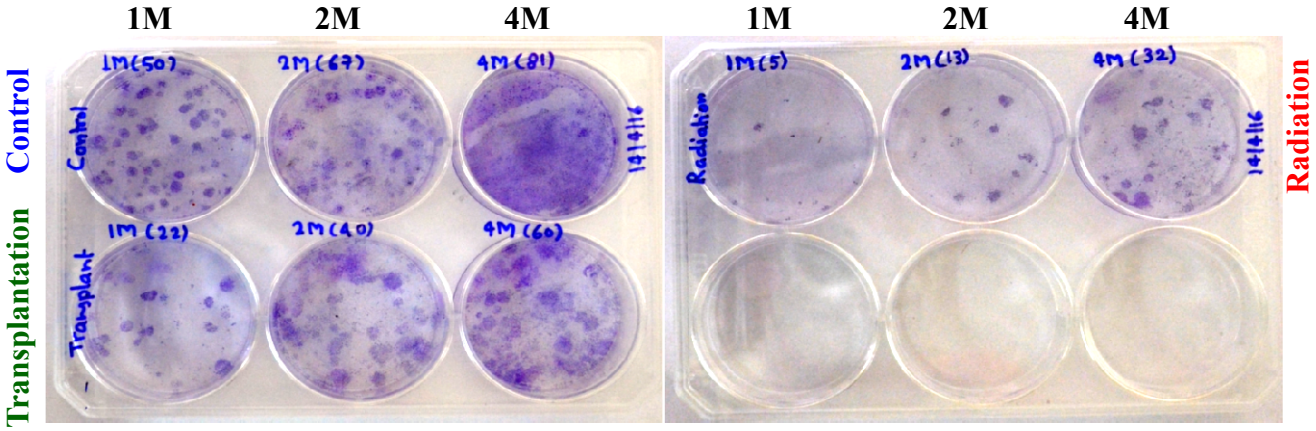

M = Millions cells seeded

(B)

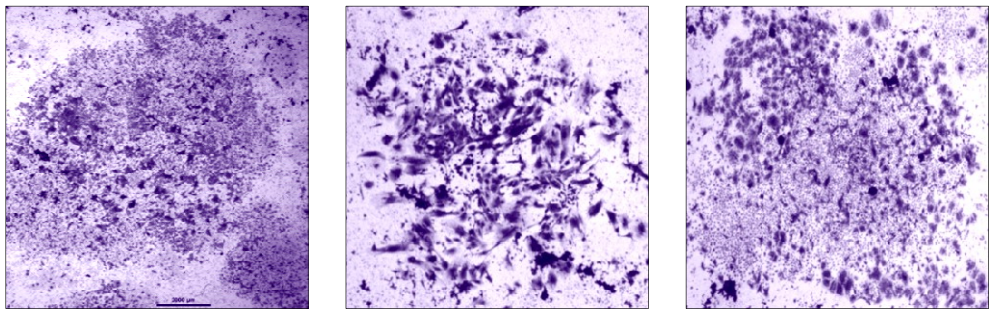

(C)

MOUSE	No. of cells seeded		
	1 Million	2 Million	4 Million
Control	33	60	75
Control	56	72	85
Control	50	67	81
Mean Control	46.33	66.33	80.33
SEM	6.89	3.48	2.91

MOUSE	No. of cells seeded		
	1 Million	2 Million	4 Million
Radiation	7	15	56
Radiation	7	13	21
Radiation	5	13	32
Mean Radiation	6.33	13.67	36.33
SEM	0.67	0.67	10.33

MOUSE	No. of cells seeded		
	1 Million	2 Million	4 Million
Transplantation	15	25	50
Transplantation	30	40	20
Transplantation	22	40	60
Mean Transplantation	22.33	35.00	43.33
SEM	4.33	5.00	12.02

Figure 16 (continued)

(D)

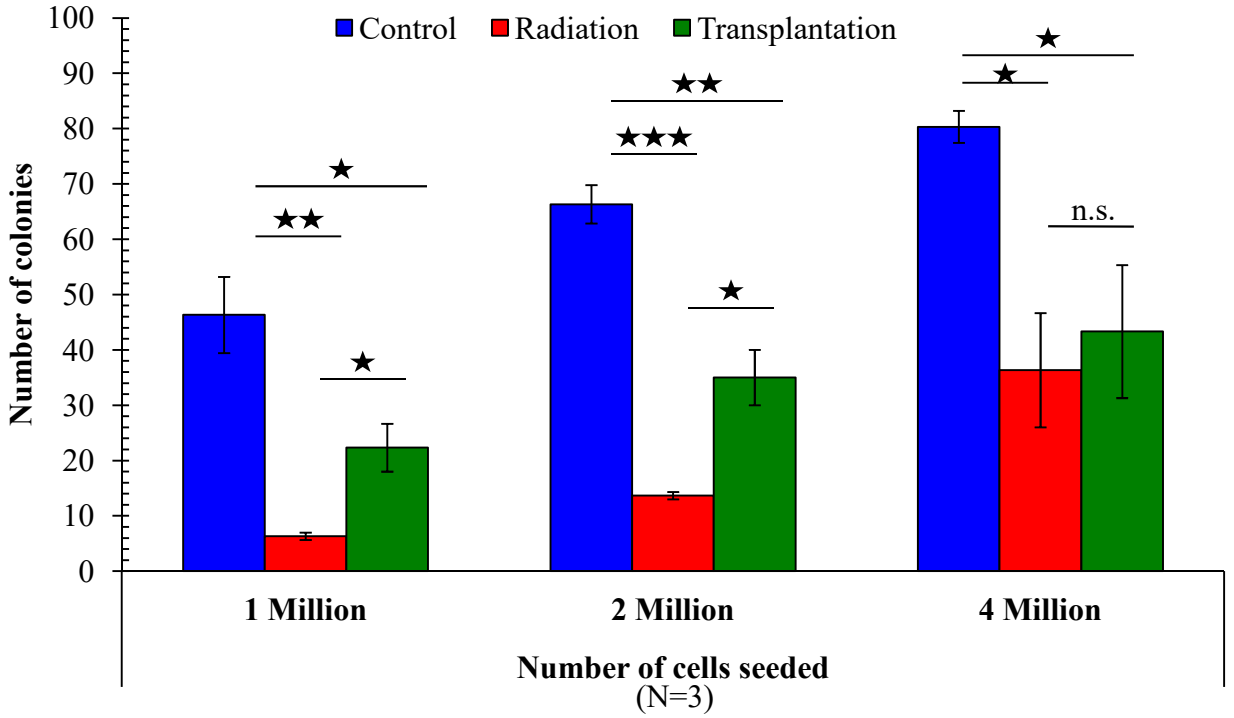

(E)

Damage of bone marrow potential due to radiation	
$1x10^6$ (seeded cells)	**86.34%**
$2x10^6$ (seeded cells)	**79.39 %**
$4x10^6$ (seeded cells)	**54.77%**

Recovery of bone marrow potential due to transplantation (24 hours)	
$1x10^6$ (seeded cells)	**34.53%**
$2x10^6$ (seeded cells)	**32.16%**
$4x10^6$ (seeded cells)	**8.71%**

Figure 16: CFU-assay (14 days) control, irradiated and transplanted mice. (A): Bone marrow cells (BMCs) from control, irradiated and transplanted mice were seeded in 6 well plates at different cell densities and cultured for 14 days and stained with crystal violet. Colony forming unit (CFU-F)-fibroblastic shows viable cells in the colony. **(B):** The images of the colony from each well were captured by Stereomicroscope. **(C):** Table shows the average numbers of CFU-F at different cell density. **(D):** Graph showing CFU-F mean ± SEM. **(E):** Table shows the extent of damage due to irradiation and recovery after transplantation for 24 hours at different cell densities of seeding. Scale bar: 2000 µm.

(A)

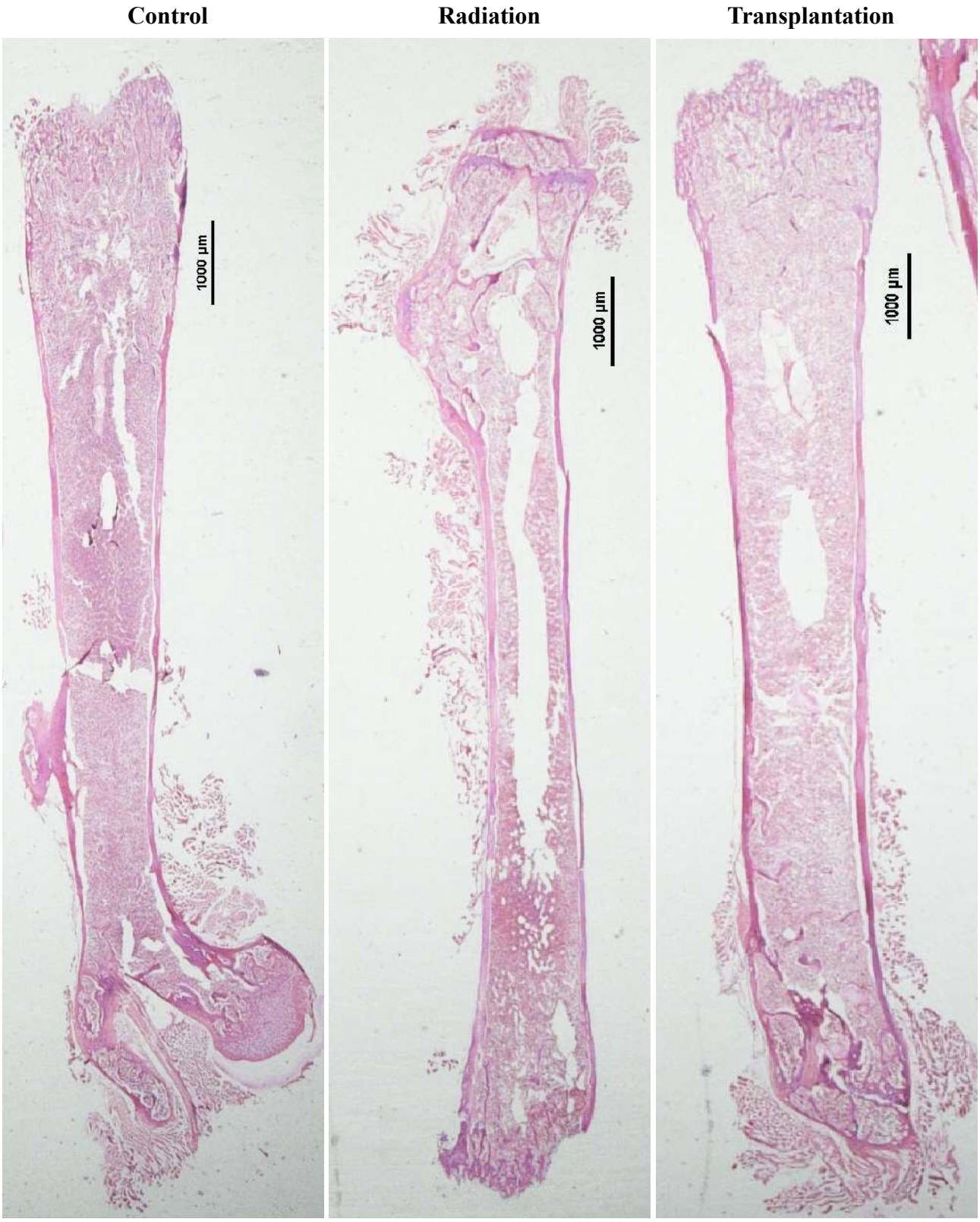

Figure 17 (continued)

(B)

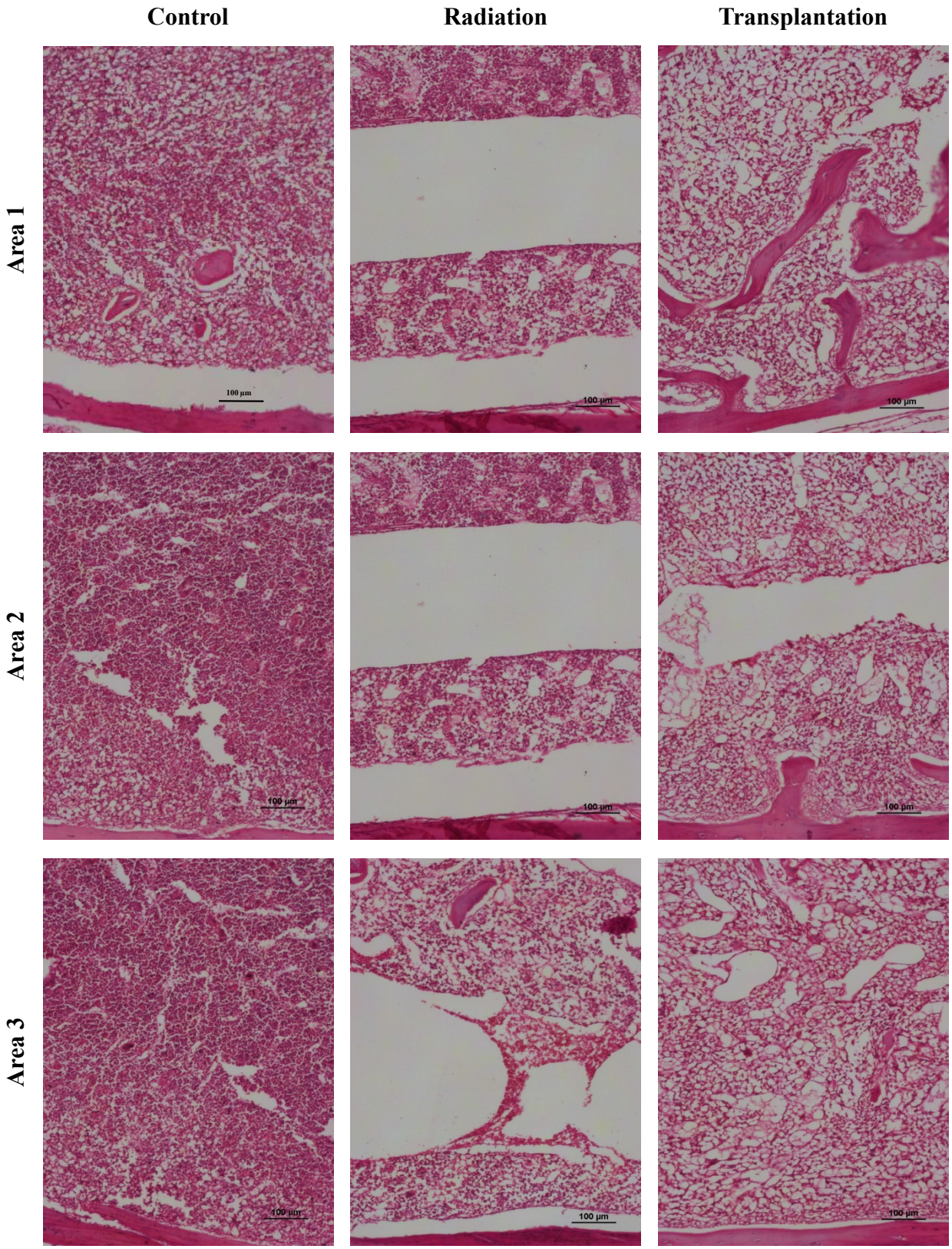

Figure 17 (continued)

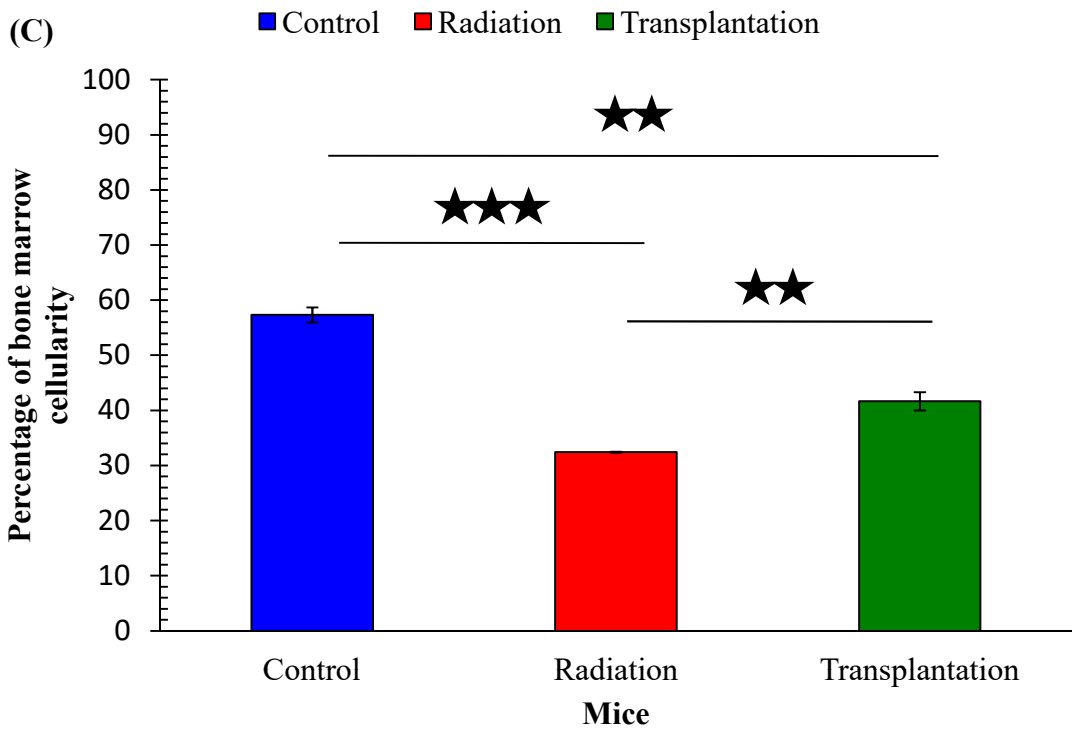

Figure 17: Histological analysis of femur bone of control, irradiated and transplanted mice to study the bone marrow regeneration in terms of cellularity. (A): Hematoxylin and eosin stained paraffin embedded sections of femur bone of control, irradiated, and transplanted mice show the cellular density (cellularity) of the bone of control, irradiated, and transplanted mice respectively. Irradiated mice bone is having lower cellularity and contains a large central cavity after loss of cells due to the radiation. Transplanted mice bone also includes cavity but of small size, because cellularity was increased after the transplantation of bone marrow cells (BMCs). **(B):** Higher magnification images of the different areas of femur bone of control, irradiated, and transplanted mice clearly show the density of BMCs in the bone marrow respectively. **(C):** Graph showing the significant difference between the average mean ± SEM in cellularity of BMCs of femur bone of control, irradiated, and transplanted (24 hours) mice respectively. Scale bar: 1000 µm and 100 µm.

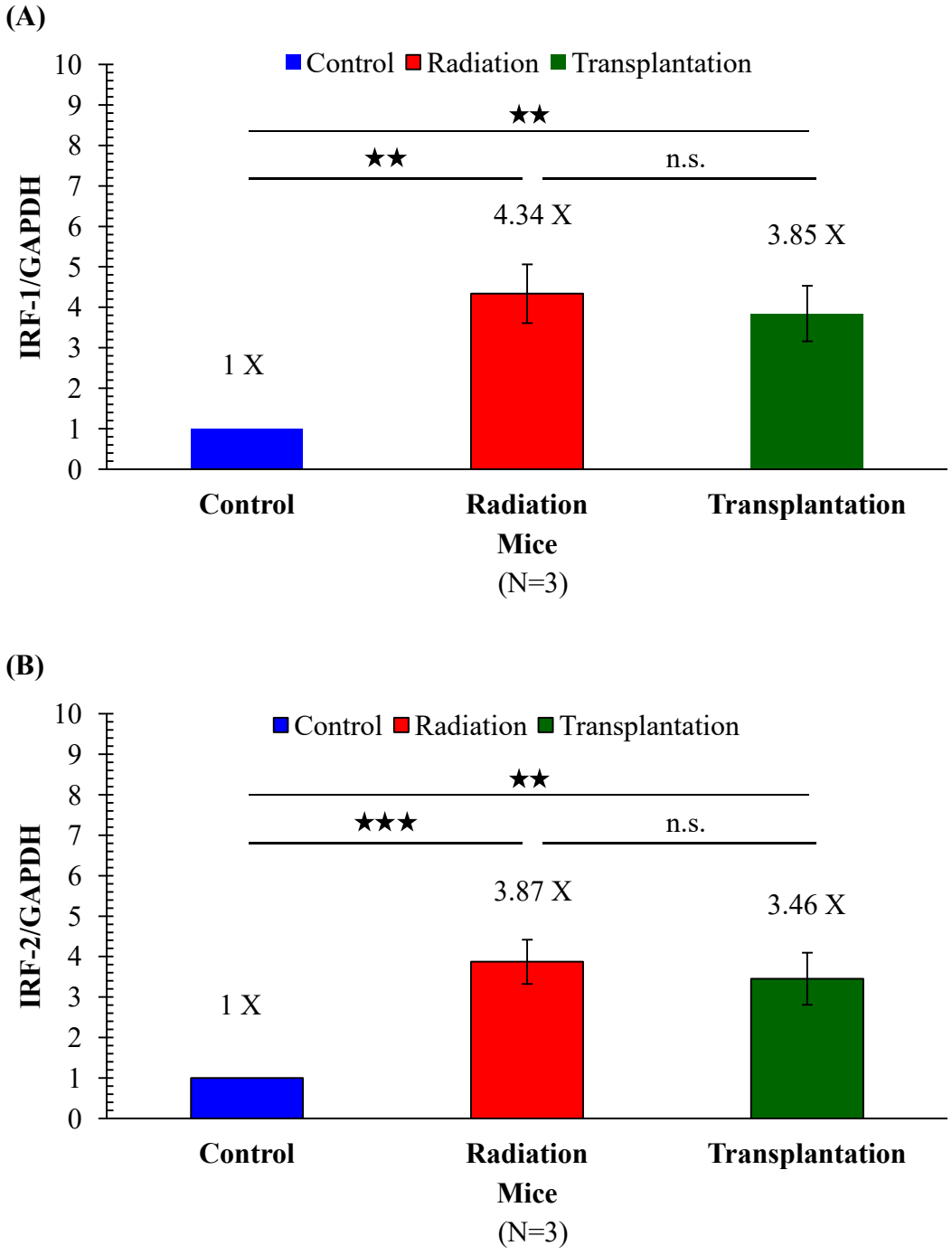

Figure 18: Expression of interferon regulatory factor-1 and -2 (IRF-1 and IRF-2) mRNAs in bone marrow cells (BMCs) of control, irradiated and transplanted (24 hours) mice by real-time RT-PCR. Expression of IRF-1 and IRF-2 mRNAs in BMCs during bone marrow regeneration. **(A** and **B):** expressions of IRF-1 and IRF-2 mRNAs were normalized to expression of GAPDH mRNA, in BMCs of control, irradiated and transplanted (24 hours) mice. Graph showing the average expression as mean ± SEM. Both IRF-1 and IRF-2 mRNAs' levels were up regulated up to 3-4X fold higher in BMCs due to radiation and radiation+ transplantation.

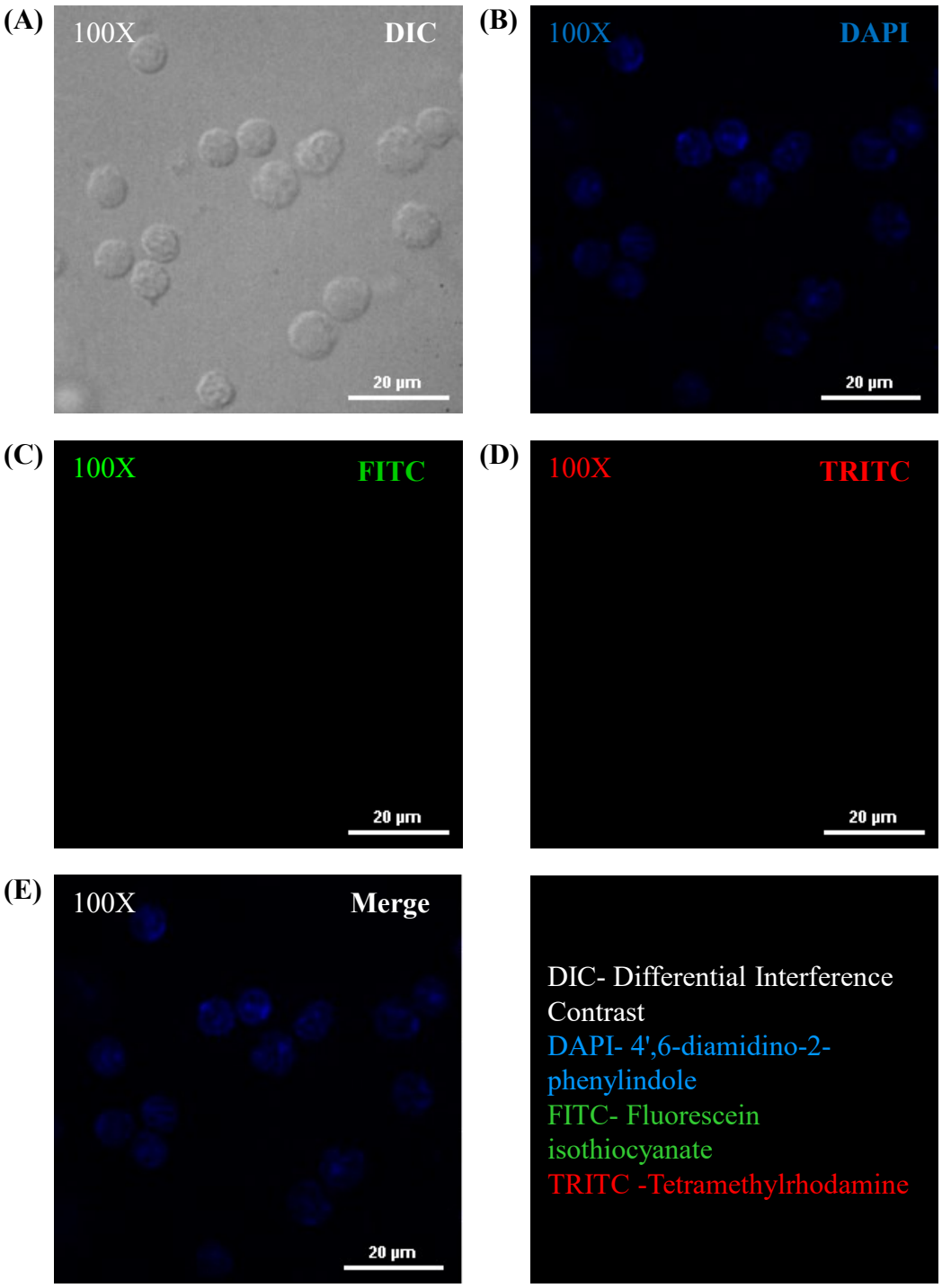

Figure 19: Negative control for expression and localization of interferon regulatory factor-1 and -2 (IRF-1 and IRF-2) in bone marrow cells (BMCs). (A): DIC image of BMCs. **(B):** DAPI staining of nuclei of BMCs showing the heterogeneous distribution of nuclear DNA. **(C** and **D):** Negative control without anti-IRF-1 and anti-IRF-2 primary antibodies to check bleeding of the signals, if any in FITC [Fluorescein isothiocyanate] fluorescence and TRITC [Tetramethylrhodamine] fluorescence channels. **(E):** Merge image showing DAPI [4, 6-diamidino-2-phenylindole] signal only. Scale bar: 20 µm.

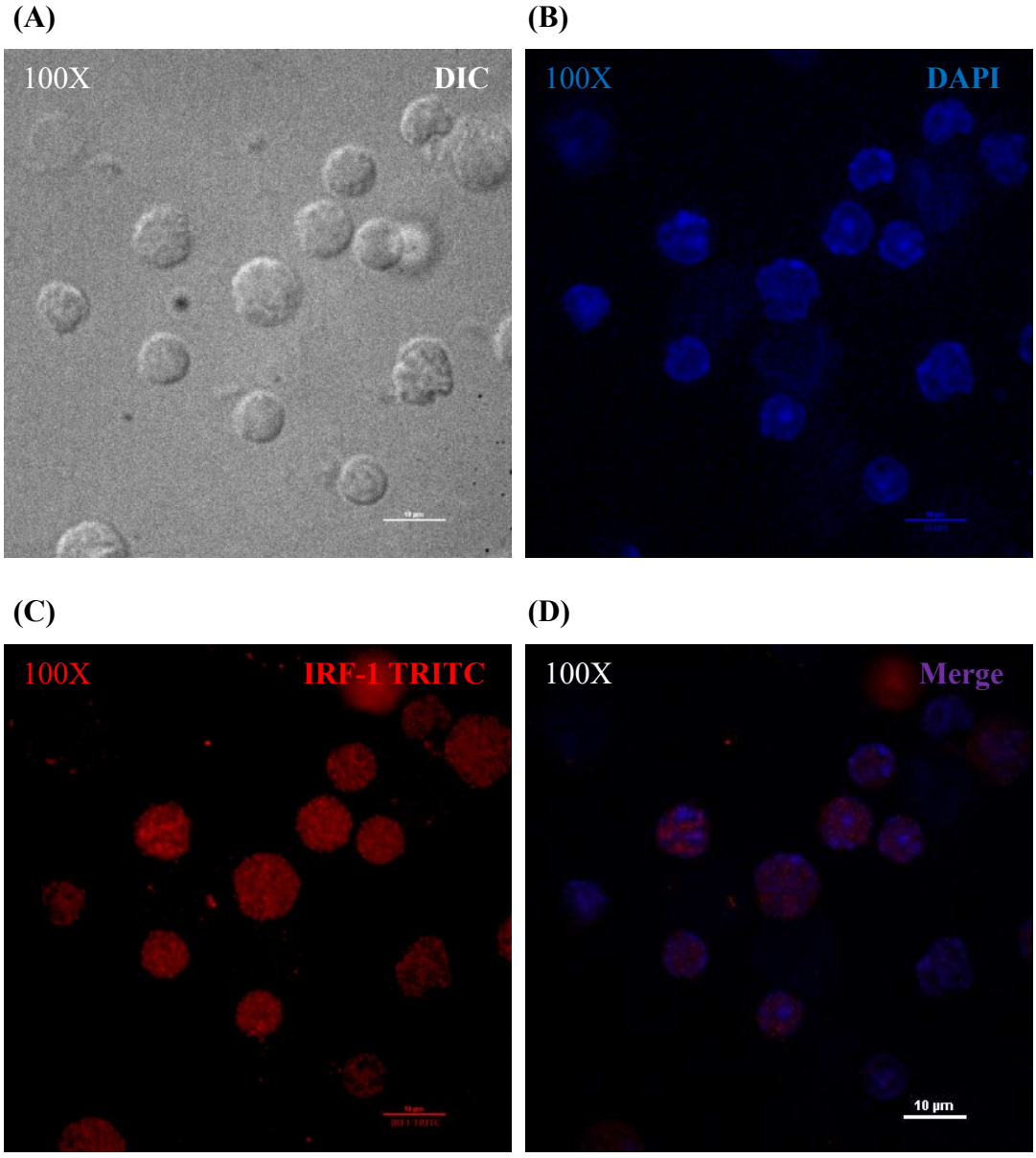

Figure 20: Expression and localization of interferon regulatory factor-1 (IRF-1) in the bone marrow cells (BMCs) by immunofluorescence. (A): DIC image of BMCs. **(B):** DAPI stained nuclei of BMCs showing heterogeneous distribution of nuclear DNA. **(C):** Confocal immunofluorescence microscopic image illustrates the expression of IRF-1 (red). **(D):** Merged image showing both DAPI and IRF-1 signals in the BMCs. Nuclear staining is in blue by DAPI [4, 6-diamidino-2-phenylindole]. IRF-1 staining is in red due to TRITC [Tetramethylrhodamine] fluorescence. Scale bar: 10µm.

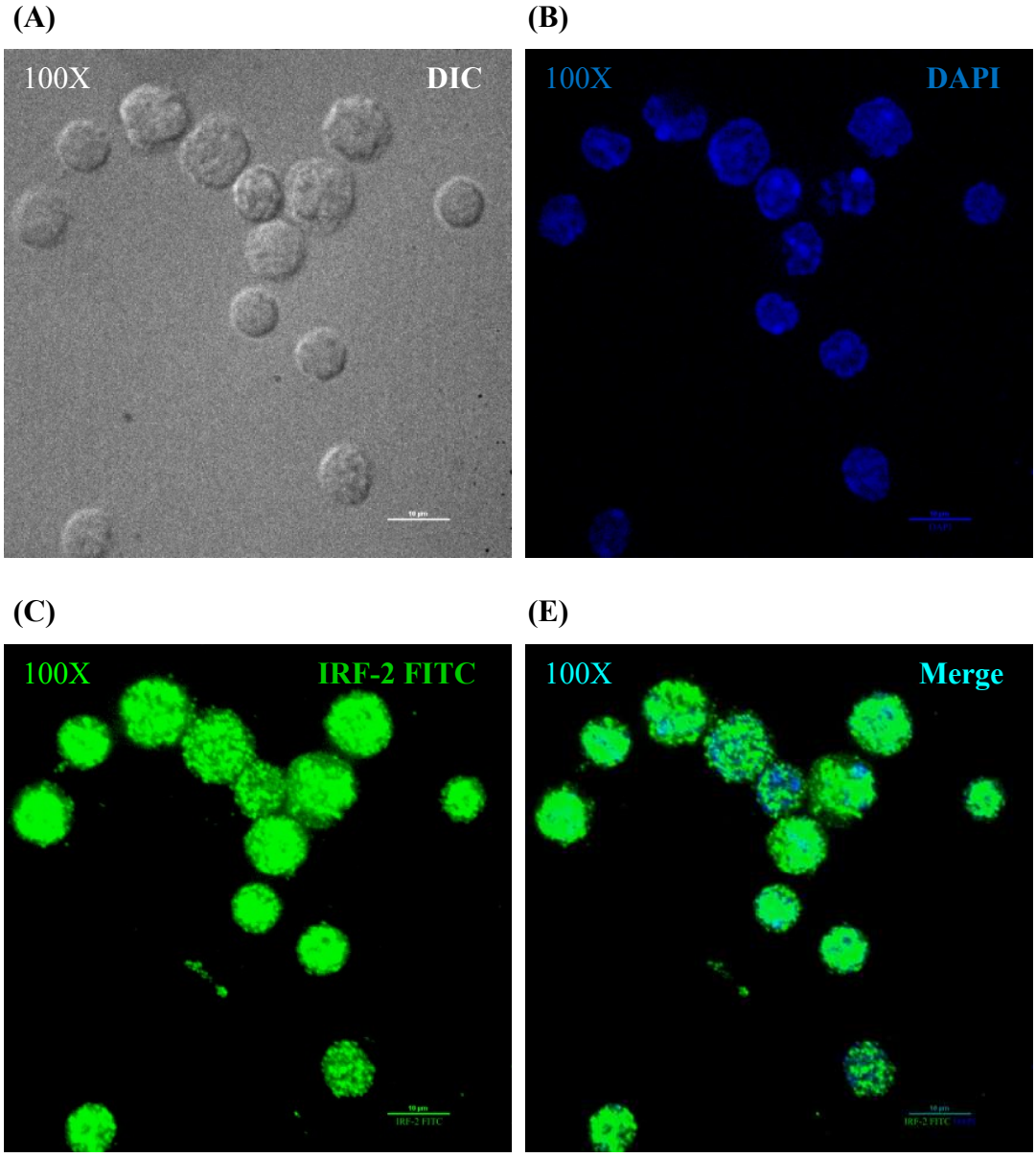

Figure 21: Expression and localization of interferon regulatory factor-2 (IRF-2) in the bone marrow cells (BMCs) by immunofluorescence. (A): DIC image of BMCs. **(B):** DAPI stained nuclei of BMCs showing heterogeneous distribution of nuclear DNA. **(C):** Confocal immunofluorescence microscopic image illustrates the expression of IRF-2 (green). **(D):** Merged image showing both DAPI and IRF-2 signals in BMCs. Nuclear staining is in blue by DAPI [4, 6-diamidino-2-phenylindole]. IRF-2 staining is in green due to FITC [Fluorescein isothiocyanate] fluorescence. Scale bar: 10µm.

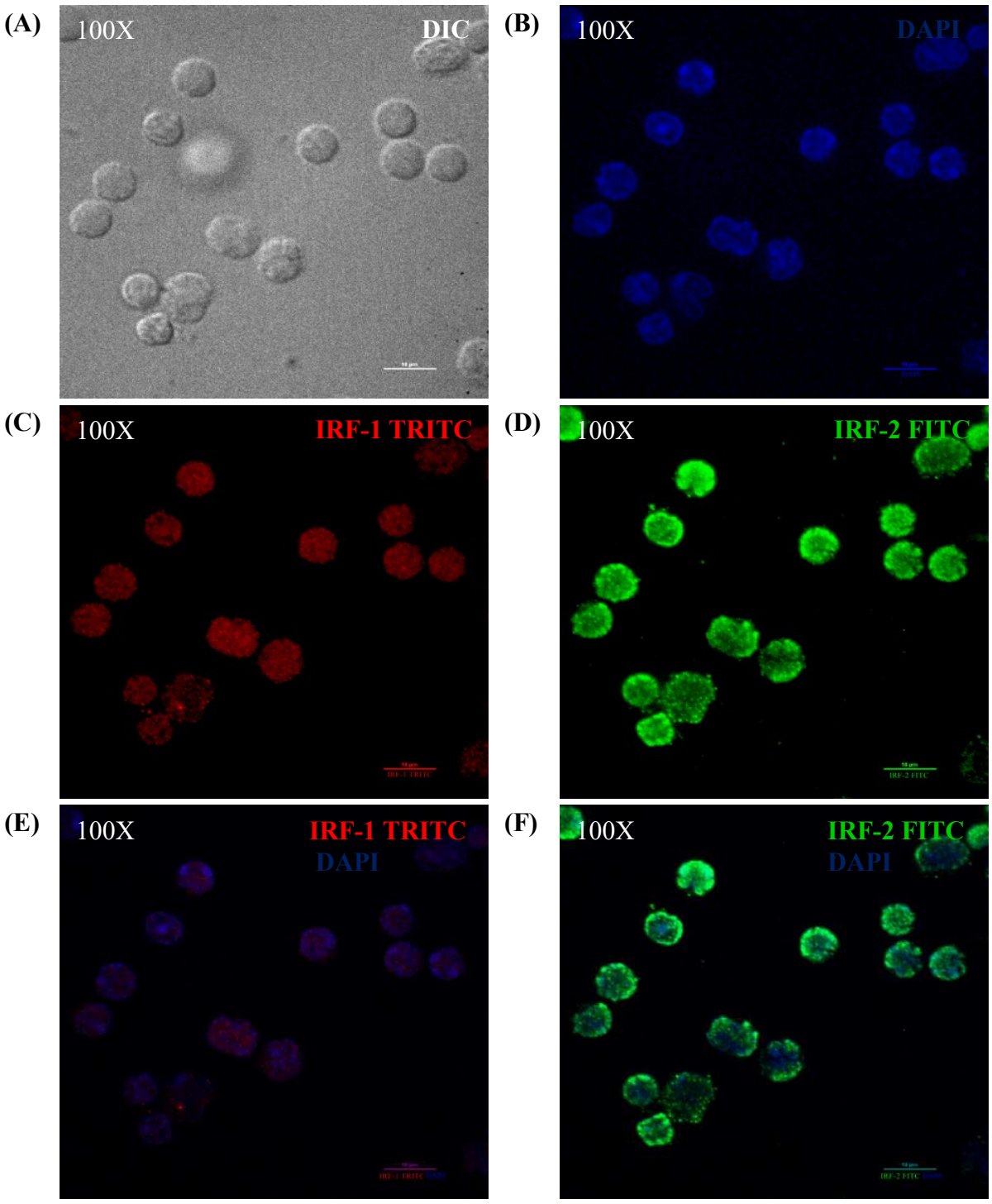

Figure 22 (continued)

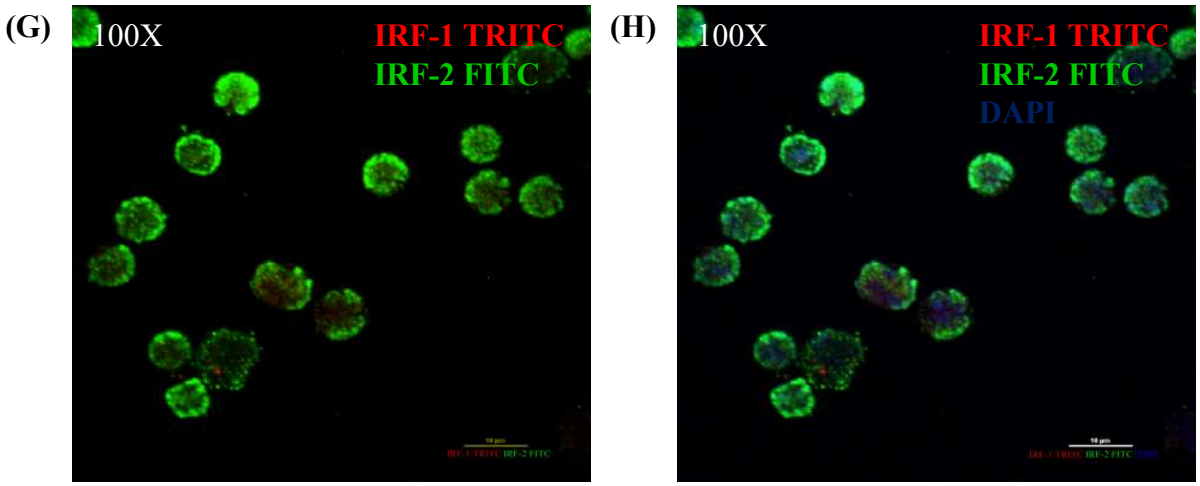

Figure 22: Expression and localization of interferon regulatory factor-1 and -2 (IRF-1 and IRF-2) in the bone marrow cells (BMCs) after double staining by immunofluorescence. (A): DIC image of BMCs showing the various sizes of BMCs. **(B):** DAPI stained nuclei of BMCs showing heterogeneous distribution of nuclear DNA. **(C** and **D):** Confocal immunofluorescence microscopic images showing the expression of IRF-1 (red) and IRF-2 (green) in the BMCs respectively. **(E** and **F):** Merged images showing DAPI & IRF-1 and DAPI & IRF-2 signals in the BMCs respectively. **(G):** Merged image showing IRF-1 and IRF-2 signals in the BMCs. **(H):** Merged image showing DAPI, IRF-1, and IRF-2 signals in the BMCs. Nuclear staining is in blue by DAPI [4, 6-diamidino-2 phenylindole]. IRF-1 staining is in red due to TRITC [Tetramethylrhodamine] fluorescence. IRF-2 staining is in green due to FITC [Fluorescein isothiocyanate] fluorescence. Scale bar: 10µm.

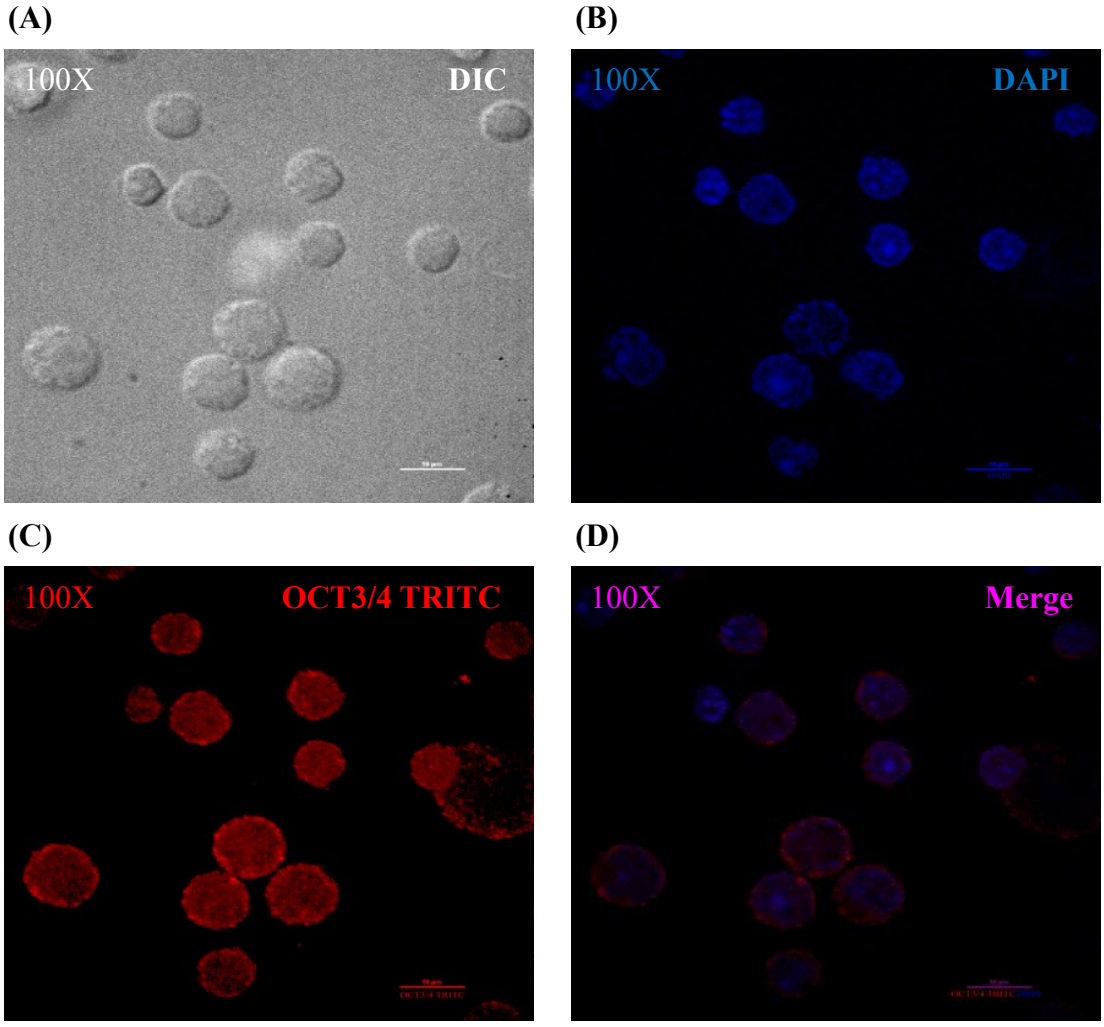

Figure 23: Bone marrow cells (BMCs) show expression and localization of pluripotency-associated transcription factor Oct3/4 (A): DIC image of BMCs. **(B):** DAPI stained nuclei of BMCs showing heterogeneous distribution of nuclear DNA. **(C):** Confocal immunofluorescence microscopic image illustrates the expression of Oct3/4 (red). **(D):** Merged image showing both DAPI and Oct3/4 signals in the BMCs. Nuclear staining is in blue by DAPI [4, 6-diamidino-2-phenylindole]. Oct3/4 staining is in red due to TRITC [Tetramethylrhodamine] fluorescence. Scale bar: 10µm.

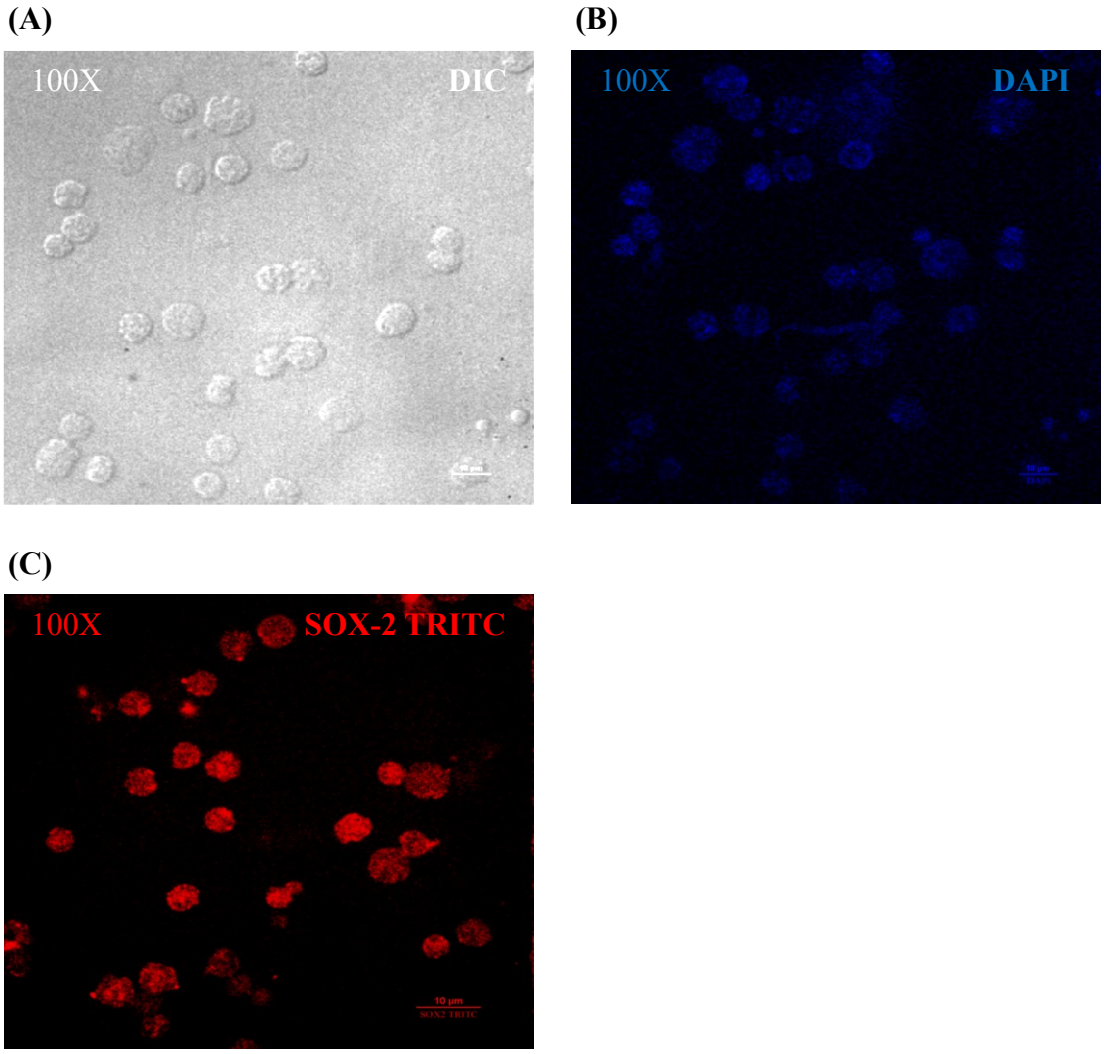

Figure 24: Bone marrow cells (BMCs) show expression and localization of pluripotency-associated transcription factor Sox-2 (A): DIC image of BMCs. **(B):** DAPI stained nuclei of BMCs showing heterogeneous distribution of nuclear DNA. **(C):** Confocal immunofluorescence microscopic image illustrates the expression of Sox-2 (red). Nuclear staining is in blue by DAPI [4, 6-diamidino-2-phenylindole]. Oct3/4 is in the red due to TRITC [Tetramethylrhodamine] fluorescence. Scale bar: 10µm.

(A)

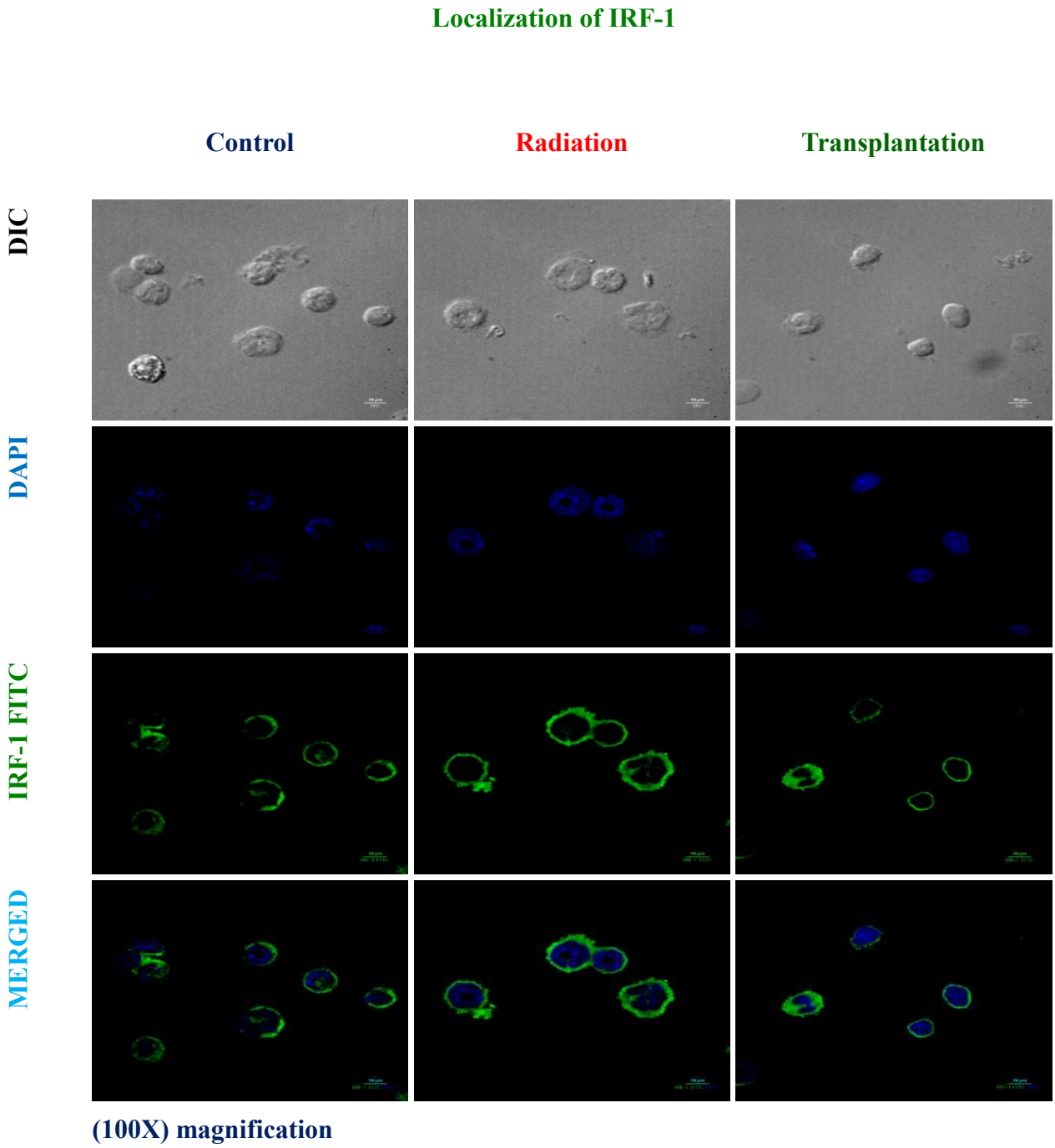

Figure 25 (continued)

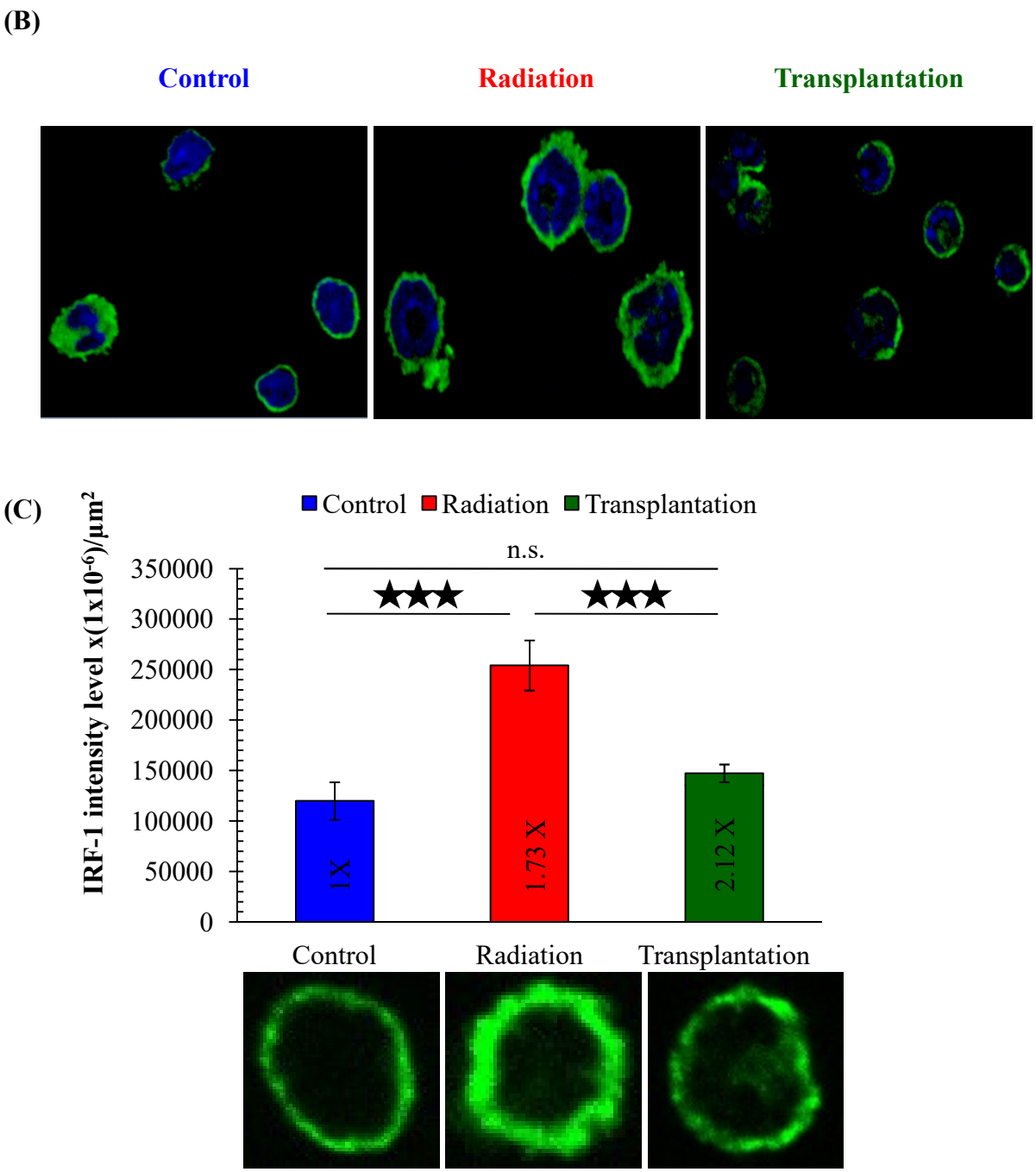

Figure 25: Expression and localization of interferon regulatory factor-1 (IRF-1) in the bone marrow cells (BMCs) during bone marrow regeneration. (A): Confocal immunofluorescence microscopic images show the expression of IRF-1 (green) in BMCs of control, irradiated and transplanted (24 hours) mice. **(B):** Larger view of confocal immunofluorescence microscopic images show the cytoplasmic localization and expression of IRF-1 (green) in BMCs during bone marrow regeneration. **(C):** Graph showing the average intensity of IRF-1 expression in BMCs of of control, irradiated and transplanted (24 hours) mice during bone marrow regeneration as mean ± SEM level. Nuclear staining is in blue by DAPI [4, 6-diamidino-2-phenylindole]. IRF-1 staining is in green due to FITC [Fluorescein isothiocyanate]. Scale bar: 10µm.

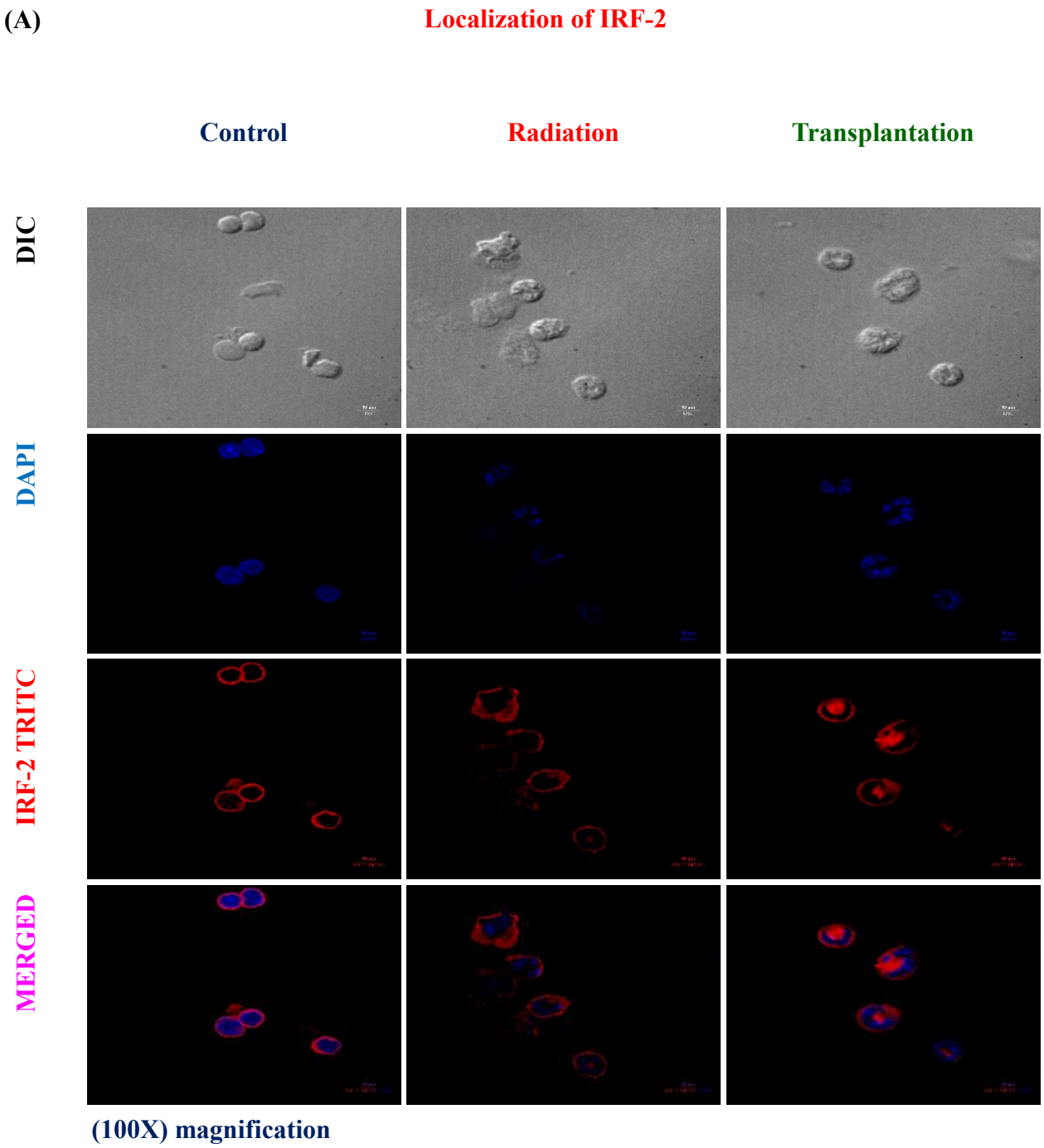

Figure 26 (continued)

(B)

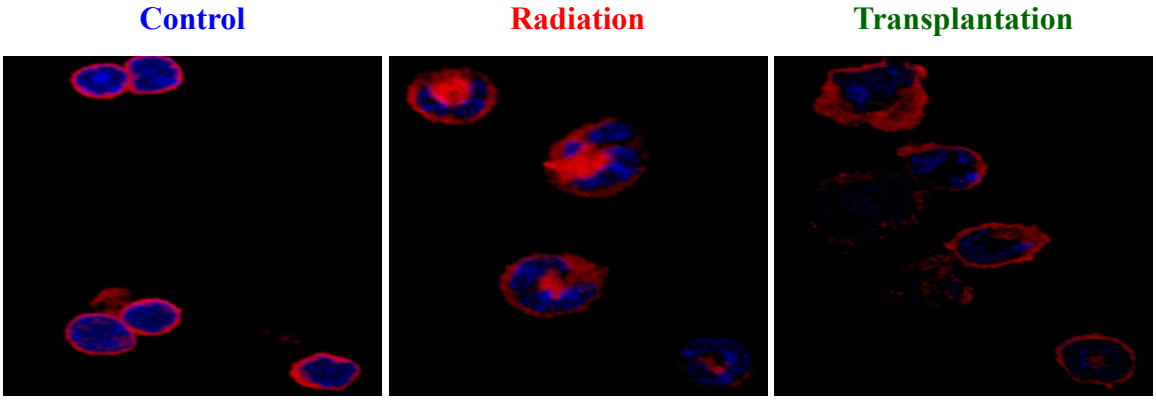

(C)

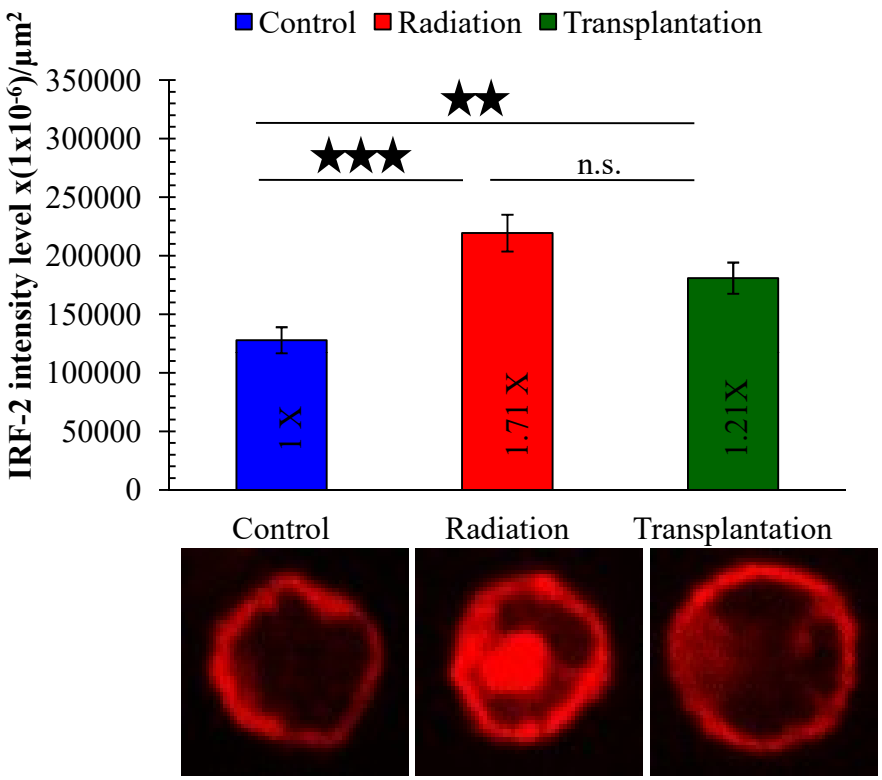

Figure 26: Expression and localization of interferon regulatory factor-2 (IRF-2) in the bone marrow cells (BMCs) during bone marrow regeneration. (A): Confocal immunofluorescence microscopic images show the expression of IRF-2 (red) in BMCs of control, irradiated and transplanted (24 hours) mice. **(B):** Larger view of confocal immunofluorescence microscopic images show the cytoplasmic localization and expression of IRF-2 (red) in the BMCs during bone marrow regeneration. **(C):** Graph showing the average intensity of IRF-2 expression in BMCs of control, irradiated and transplanted (24 hours) mice during bone marrow regeneration as mean ± SEM level. Nuclear staining is in blue by DAPI [4, 6-diamidino-2-phenylindole]. IRF-2 staining is in the red due to TRITC [Tetramethylrhodamine] fluorescence. Scale bar: 10µm.

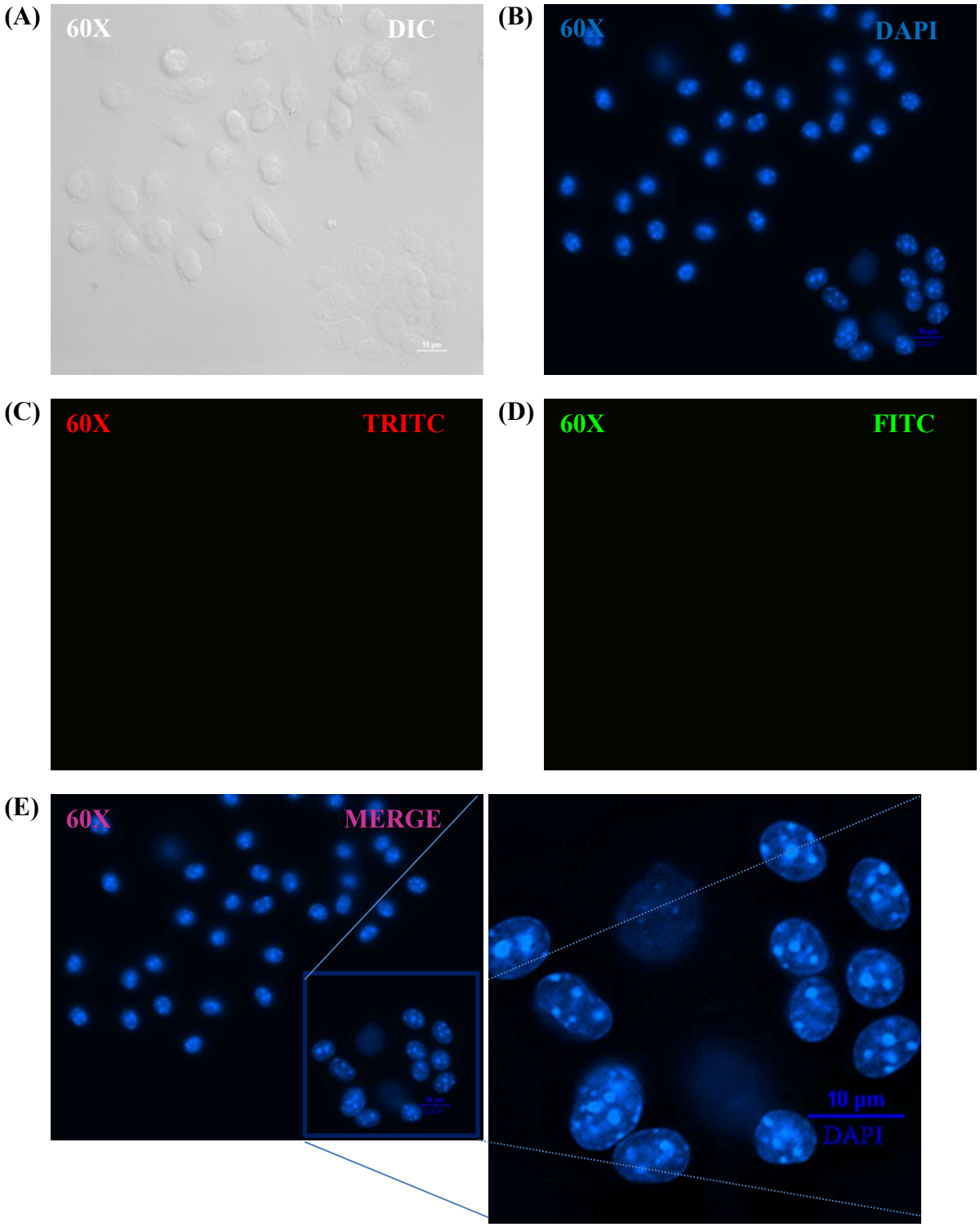

Figure 27: Negative control for expression and localization of interferon regulatory factor-1 and -2 (IRF-1 and IRF-2) in the mesenchymal stem (Passage 1) cells (MS-P1cells) derived from the bone marrow. (A): DIC image of MS-P1cells. **(B):** DAPI stained nuclei of MS-P1 cells showing heterogeneous distribution of nuclear DNA. **(C** and **D):** Negative control without anti-IRF-1 and anti-IRF-2 primary antibodies to check bleeding of the signals in FITC and TRITC channels. **(E):** Merged image showing DAPI signal only. Scale bar: 10 µm.

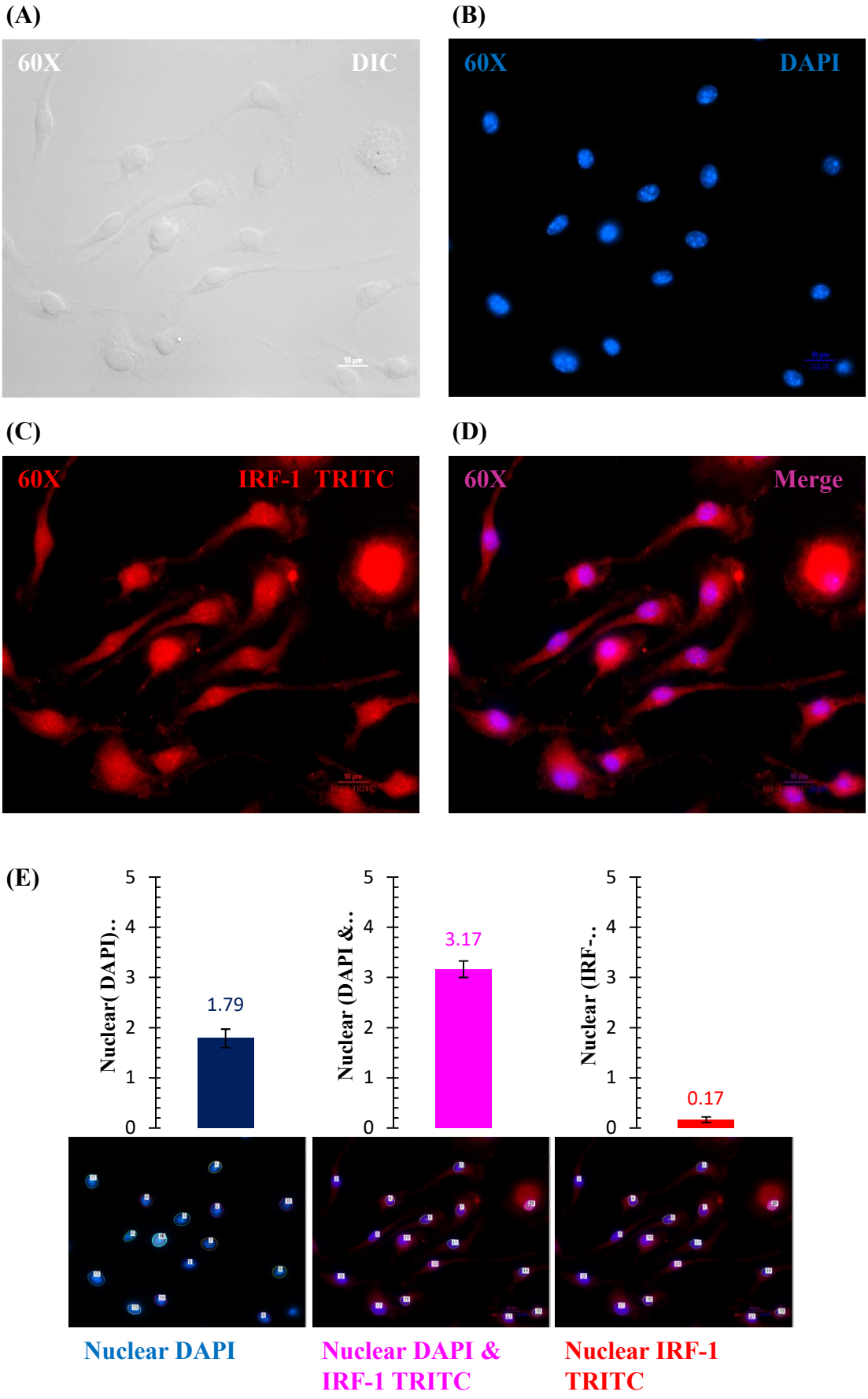

Figure 28 (continued)

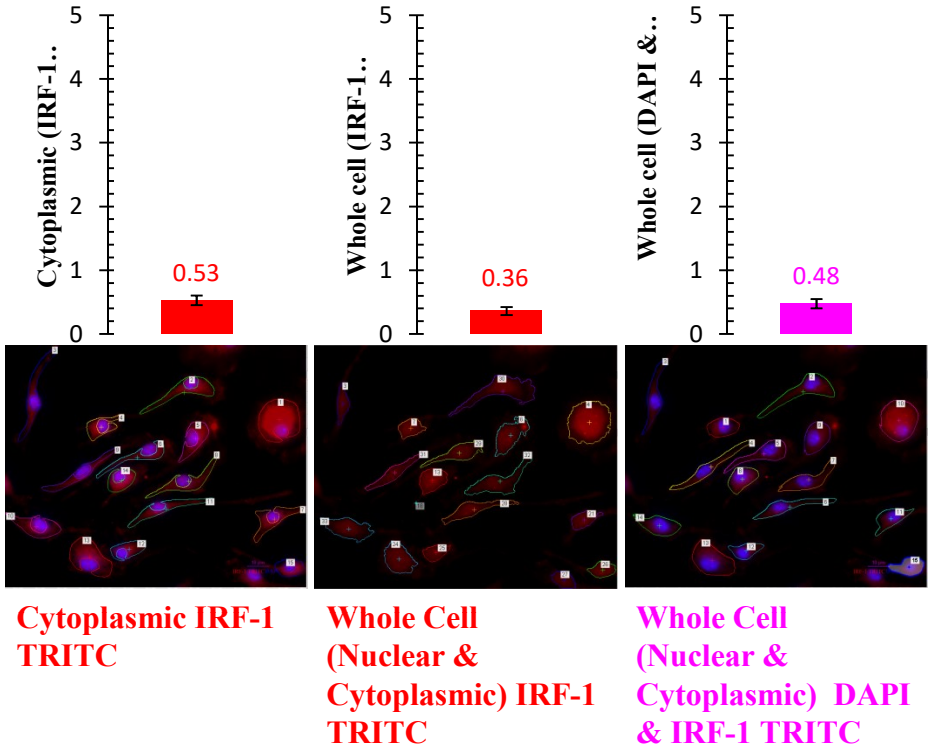

Figure 28: Expression and localization of interferon regulatory factor-1 (IRF-1) in the mesenchymal stem (Passage -1) cells (MS-P1cells) derived from the bone marrow by immunofluorescence. (A): DIC image of MS-P1cells. **(B):** DAPI stained nuclei of MS-P1cells showing the heterogeneous distribution of nuclear DNA. **(C):** Confocal immunofluorescence microscopic image illustrates the expression of IRF-1 (red) in MS-P1 cells. **(D):** Merged image showing both DAPI and IRF-1 signals in MS-P1 cells, which show both nuclear and cytoplasmic expression. **(E):** Graph showing nuclear DAPI, nuclear DAPI & IRF-1 TRITC, nuclear IRF-1 TRITC, cytoplasmic IRF-1 TRITC, Whole Cell (nuclear & cytoplasmic) IRF-1 TRITC, and whole cell (nuclear & cytoplasmic) DAPI & IRF-1 TRITC intensity respectively, as mean ± SEM level. Nuclear staining is in blue by DAPI [4, 6-diamidino-2-phenylindole]. IRF-1 staining is in the red due to TRITC [Tetramethylrhodamine] fluorescence. Scale bar: 10µm.

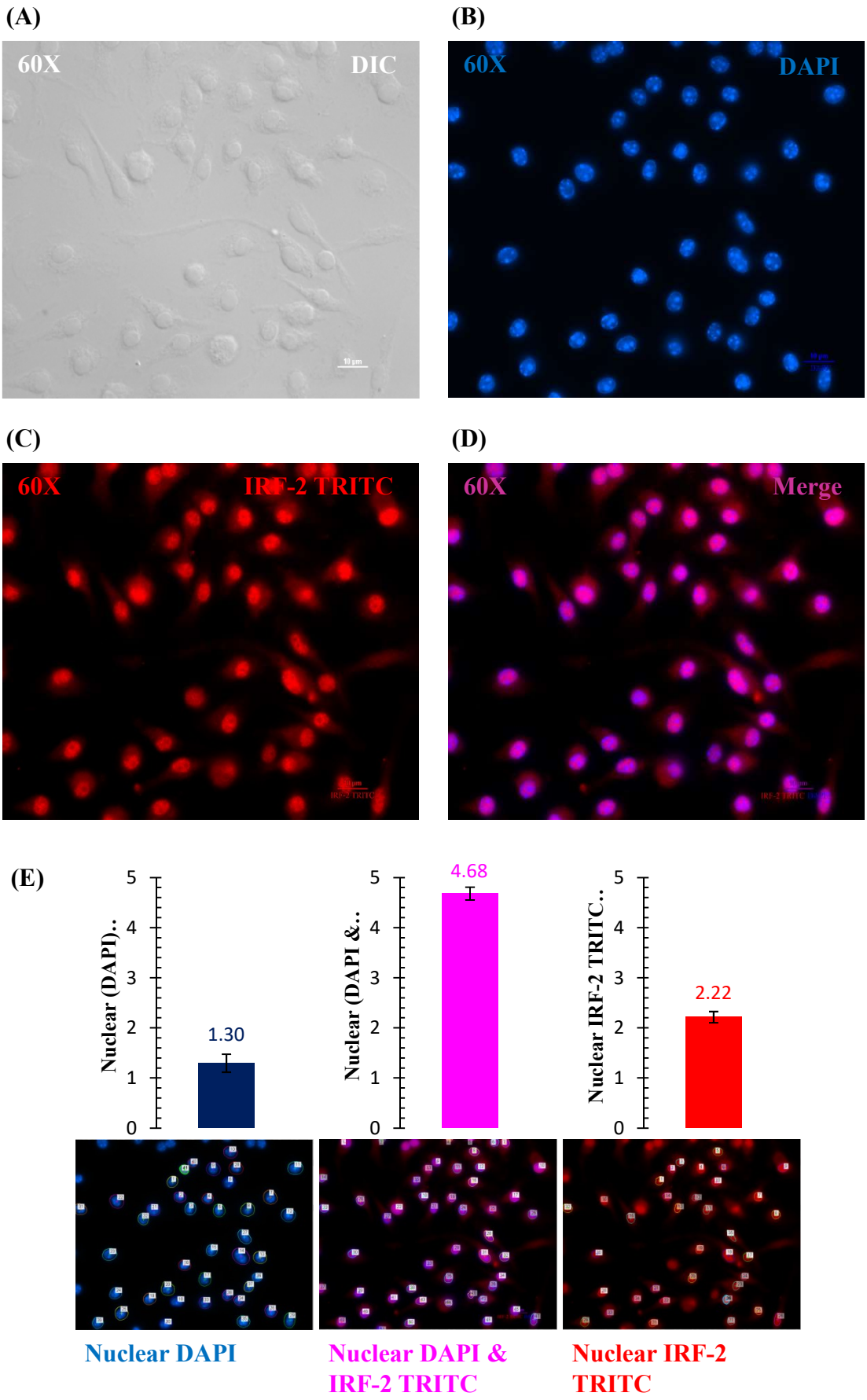

Figure 29 (continued)

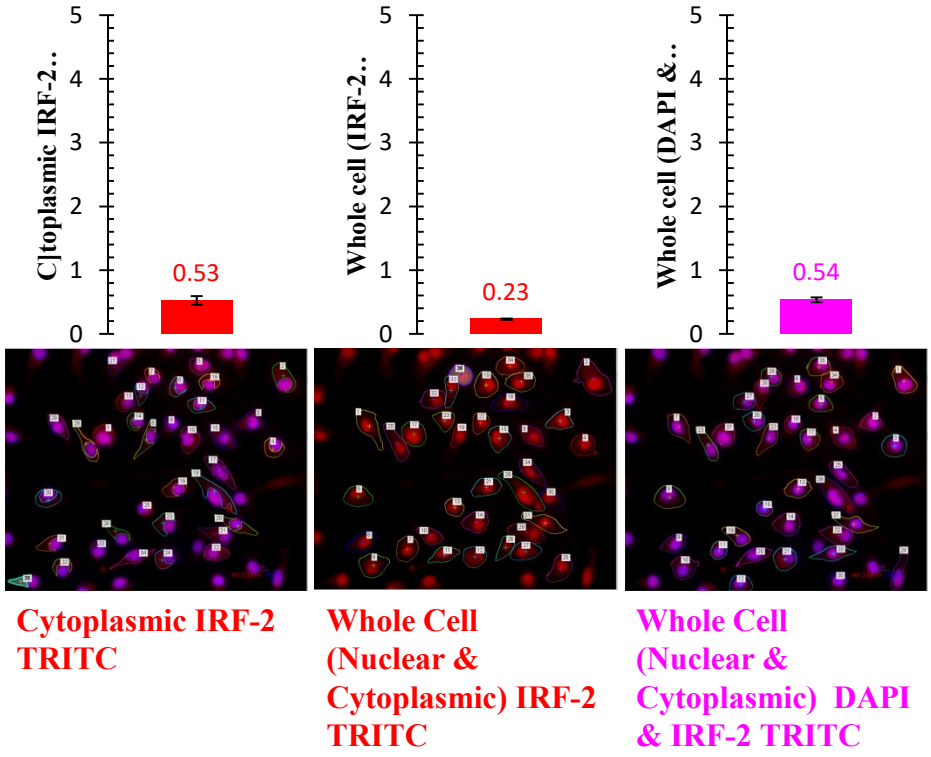

Figure 29: Expression and localization of interferon regulatory factors-2 (IRF-2) in the mesenchymal stem (Passage -1) cells (MS-P1cells) derived from bone marrow by immunofluorescence. (A): DIC image of MS-P1cells. **(B):** DAPI stained nuclei of MS-P1cells showing heterogeneous distribution of nuclear DNA. **(C):** Confocal immunofluorescence microscopic image illustrates the expression of IRF-2 (red) in MS-P1 cells. **(D):** Merged image showing both DAPI and IRF-2 signals in MS-P1 cells, which show both nuclear and cytoplasmic expression. **(E):** Graph showing nuclear DAPI, nuclear DAPI & IRF-2 TRITC, nuclear IRF-2 TRITC, cytoplasmic IRF-2 TRITC, Whole Cell (nuclear & cytoplasmic) IRF-2 TRITC, and whole cell (nuclear & cytoplasmic) DAPI & IRF-2 TRITC intensity respectively, as mean ± SEM . Nuclear staining is in blue by DAPI [4, 6-diamidino-2-phenylindole]. IRF-2 staining is in the red due to TRITC [Tetramethylrhodamine] fluorescence. Scale bar: 10µm.

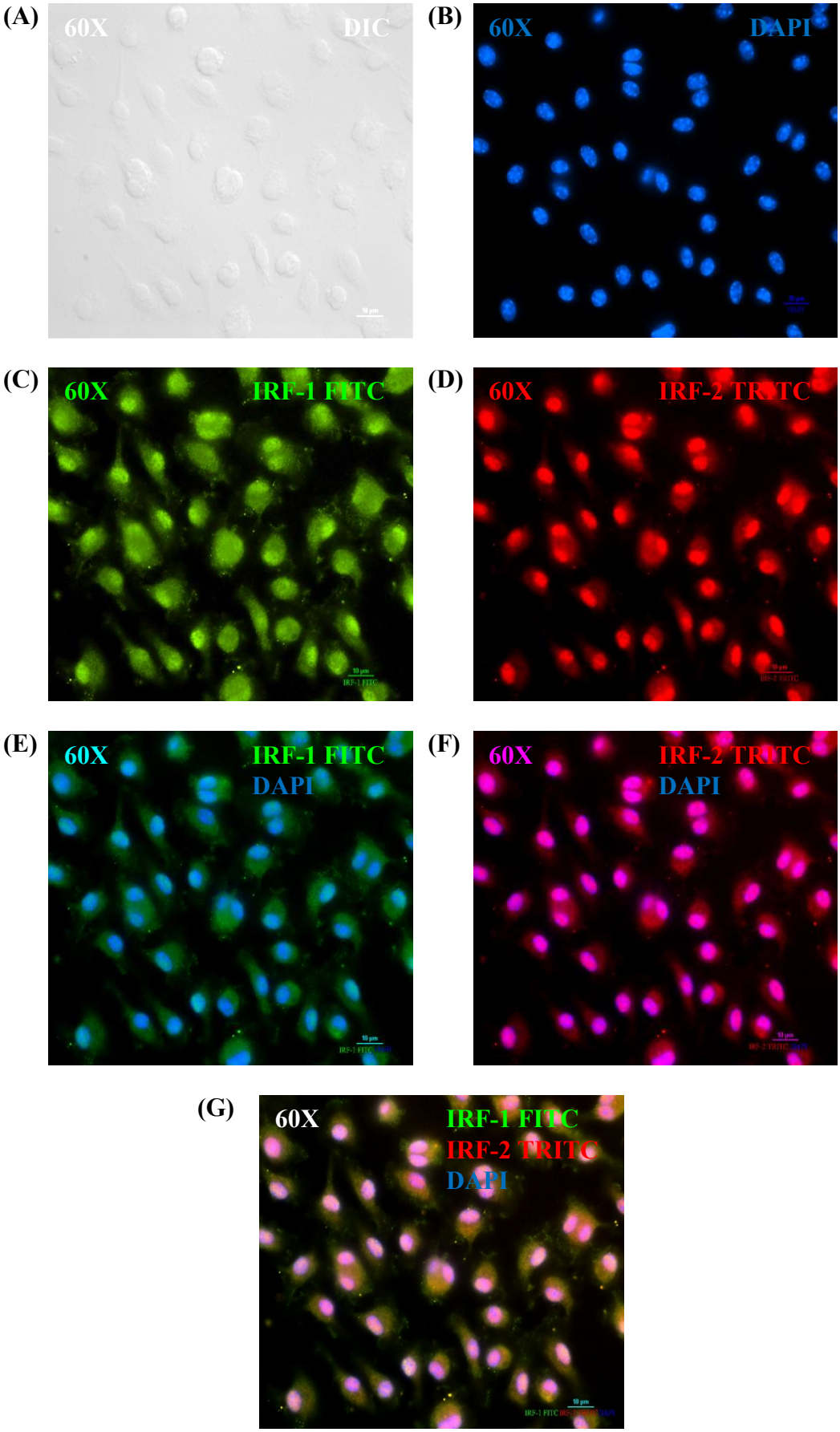

Figure 30 (continued)

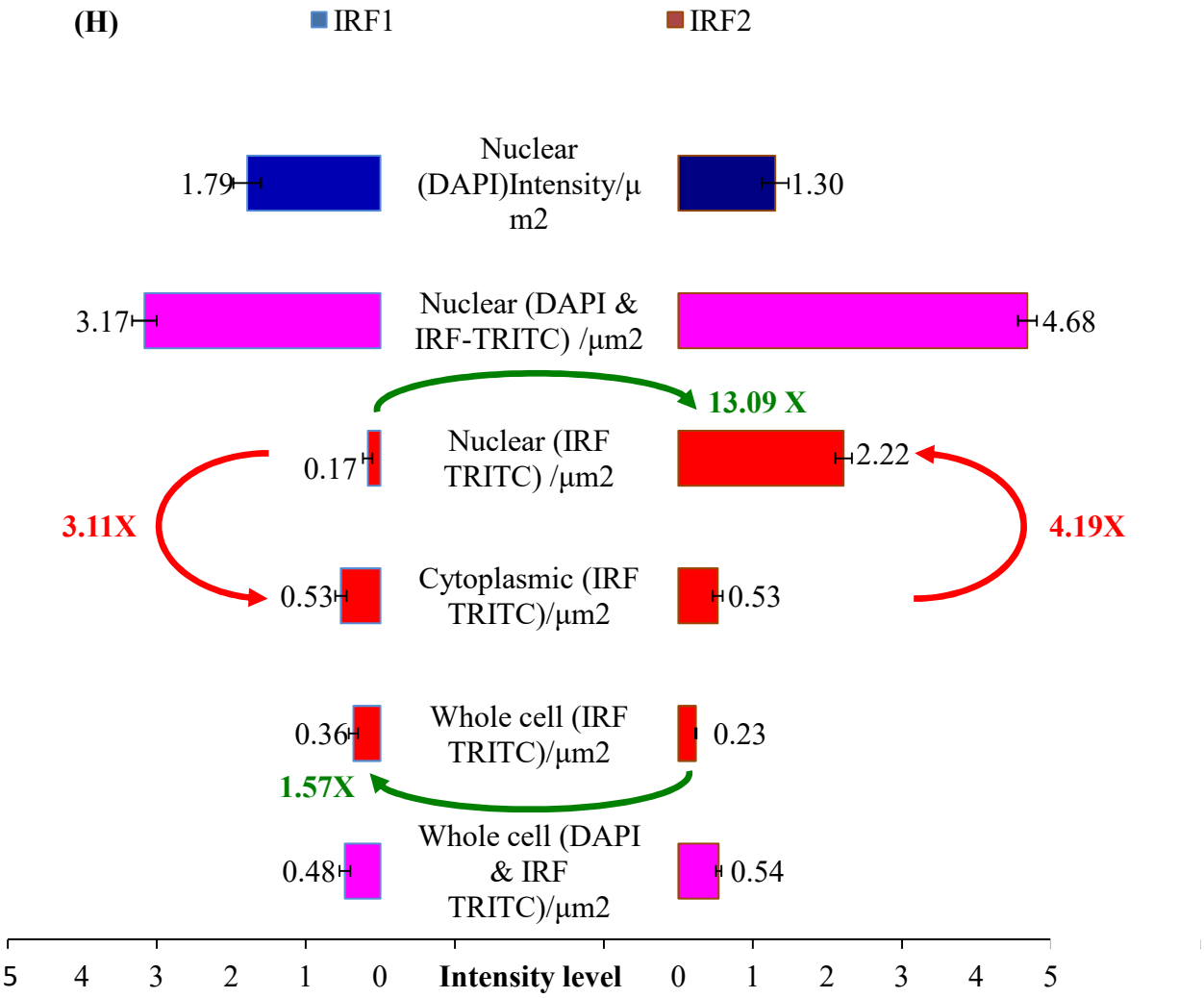

Figure 30: Expression and localization of interferon regulatory factor-1 and -2 (IRF-1 and IRF-2) in the mesenchymal stem (Passage -1) cells (MS-P1cells) derived from bone marrow after double staining by immunofluorescence. (A): DIC image of MS-P1cells showing the various sizes of MS-P1cells. **(B):** DAPI stained nuclei of MS-P1cells showing heterogeneous distribution of nuclear DNA. **(C** and **D):** Confocal immunofluorescence microscopic images showing the expression of IRF-1 (green) and IRF-2 (red) in the MS-P1cells respectively. **(E** and **F):** Merged images showing DAPI & IRF-1 and DAPI & IRF-2 signals in MS-P1cells respectively. **(G):** Merged image showing DAPI, IRF-1, and IRF-2 signals in MS-P1cells. **(H):** Comparative analysis of IRF-1 and IRF-2 intensities plotted into graph, which is showing nuclear DAPI, nuclear DAPI & IRF-2 TRITC, nuclear IRF-2 TRITC, cytoplasmic IRF-2 TRITC , Whole Cell (nuclear & cytoplasmic) IRF-2 TRITC, and whole cell (nuclear & cytoplasmic) DAPI & IRF-2 TRITC intensities of IRF-1 and IRF-2 in MS-P1 cells respectively, as mean ± SEM level. Nuclear staining is in blue by DAPI [4, 6-diamidino-2 phenylindole]. IRF-1 staining is in green due to FITC [Fluorescein isothiocyanate] fluorescence. IRF-2 staining is in red due to TRITC [Tetramethylrhodamine] fluorescence. Scale bar: 10µm.

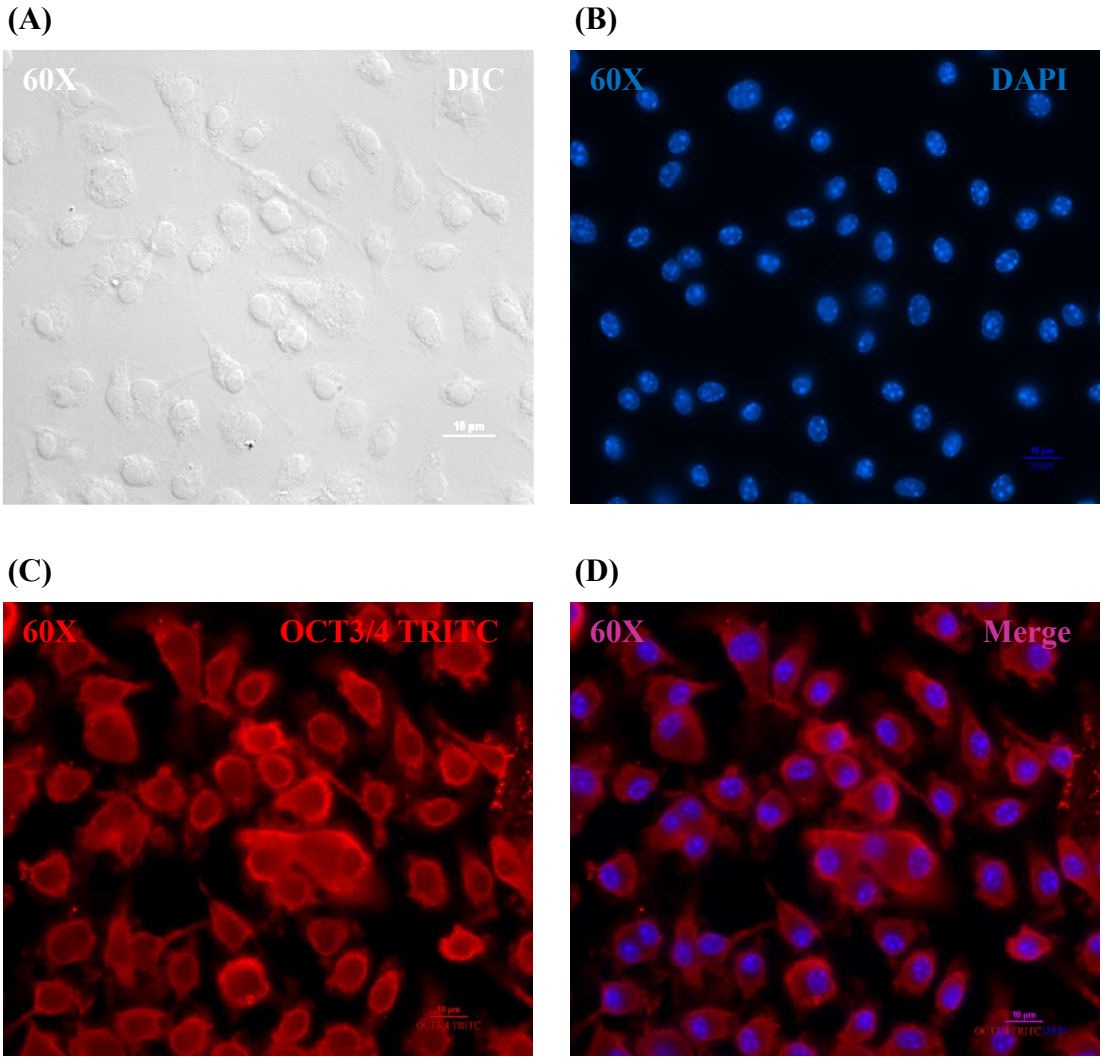

Figure 31: Mesenchymal stem (Passage-1) cells (MS-P1cells) show localization and expression of pluripotency-associated transcription factor Oct3/4 (A): DIC image of MS-P1cells. **(B):** DAPI stained nuclei of MS-P1cells showing heterogeneous distribution of nuclear DNA. **(C):** Confocal immunofluorescence microscopic image illustrates the expression of Oct3/4 (red) in MS-P1Cells. **(D):** Merged image showing both DAPI and Oct3/4 signals in MS-P1cells. Nuclear staining is in blue by DAPI [4, 6-diamidino-2-phenylindole]. Oct3/4 staining is in red due to TRITC [Tetramethylrhodamine] fluorescence. Scale bar: 10µm.

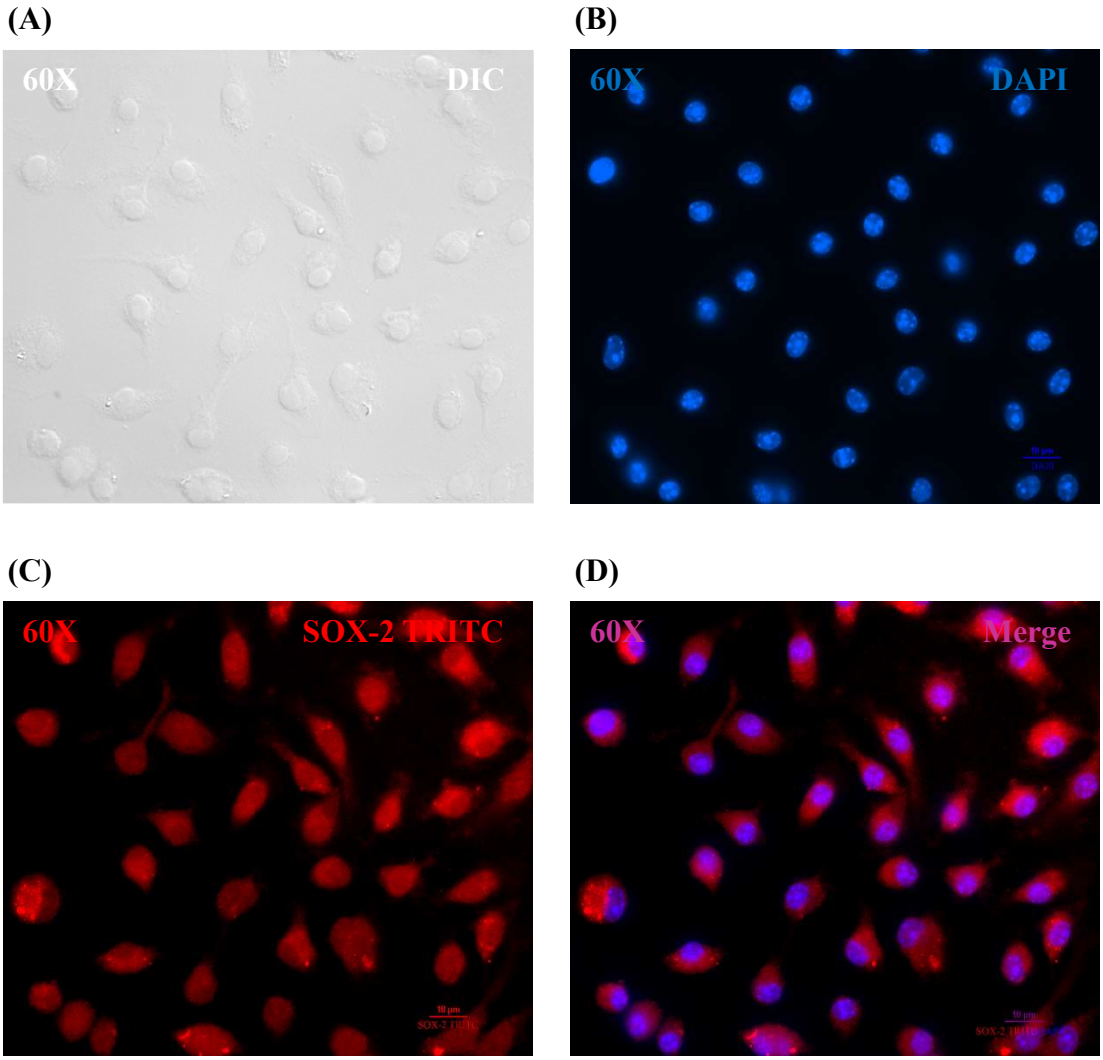

Figure 32: Mesenchymal stem (Passage-1) cells (MS-P1cells) show localization and expression pluripotency-associated transcription factor Sox-2 (A): DIC image of MS-P1cells. **(B):** DAPI stained nuclei of MS-P1cells showing heterogeneous distribution of nuclear DNA. **(C):** Confocal immunofluorescence microscopic image illustrates the expression of Sox-2 (red) in MS-P1Cells. **(D):** Merged image showing both DAPI and Sox-2 signals in MS-P1Cells. Nuclear staining is in blue by DAPI [4, 6-diamidino-2-phenylindole]. Sox-2 staining is in red due to TRITC [Tetramethylrhodamine] fluorescence. Scale bar: 10µm.